

Copyright © and Moral Rights for this thesis are retained by the author and/or other copyright owners. A copy can be downloaded for personal non-commercial research or study, without prior permission or charge. This thesis cannot be reproduced or quoted extensively from without first obtaining permission in writing from the copyright holder(s). The content must not be changed in any way or sold commercially in any format or medium without the formal permission of the copyright holders.

Note if anything has been removed from thesis.

Illustrations p6, 7, 9, 14, 20, 21, 22, 24, 28, 228

When referring to this work, the full bibliographic details must be given as follows:

Chambers, A. C. (2012). *The role of ODV structural proteins in baculovirus replication*. PhD Thesis. Oxford Brookes University.

The role of ODV structural proteins in baculovirus replication

Adam C Chambers

A thesis submitted in partial fulfilment of the requirements of Oxford Brookes University for the degree of Doctor of Philosophy

This research programme was carried out in collaboration with Oxford Expression Technologies Ltd



February 2012

Abstract

Baculoviruses are arthropod-specific viruses with a circular, double-stranded DNA genome (80-180 kb). Two structural forms are produced during virus replication, comprising budded virus (BV) and occlusion-derived virus (ODV). The BV is produced from 12 hours post infection (hpi) and spreads the infection from tissue to tissue within the host. The ODV is formed 20 hpi and enveloped within occlusion bodies (OBs).

The aim of this project was to elucidate the mechanisms involved in ODV production by deleting putative genes involved in ODV, but not BV production. A secondary aim of the project was to determine whether removing these genes improved the quantity/quality of recombinant proteins produced by baculovirus expression vectors.

Genes for ODV structural proteins were selected and individual gene deletion mutants were generated. Three of these ($\Delta orf79$, $\Delta odv-e28$, and $\Delta odv-ec43$) unexpectedly prevented virus replication in insect cell culture. *orf79* and *odv-ec43* were demonstrated to be essential genes as viability could be restored after a rescue assay with the target gene, whereas the loss of infectivity in $\Delta odv-e28$ probably resulted from an effect on *helicase*, an essential neighbouring gene.

Three deletion mutant viruses ($Ac\Delta cg30$, $Ac\Delta odv-e66$ and $Ac\Delta odv-e56$) that were viable in insect cell culture were studied for any effect on ODV production and OB formation using bioassays and electron microscopy imaging. Deletion of *odv-e66* and *odv-e56* both negatively affected oral infectivity of OBs, whereas the deletion of *cg30* increased infectivity. The electron microscopy imaging of the OBs of these deletion mutant viruses identified abnormalities for $Ac\Delta cg30^{pol+}$ and $Ac\Delta odv-e56^{pol+}$. $Ac\Delta cg30^{pol+}$ OBs seemed to be degraded due to deformities in the polyhedron envelope (PE) while $Ac\Delta odv-e56^{pol+}$ OBs were surrounded by another protein structure but had no apparent difference in structure or ODV packaging compared to the parental virus. The formation of BV by the *pif3* deletion mutant virus was reduced, although plaques were still formed in titrations of infectivity. BV production could only be restored by a rescue assay with *pif3*, suggesting PIF3 may have another function that is yet to be fully characterized.

The deletion of *orf118/pif1* and *pif2* were analysed for their effect on recombinant protein production expressed from the *polh* promoter, using activity assays. Both the deletion of *orf118/pif1* and *pif2* caused a reduction in the intracellular protein, beta-galactosidase. However, the deletion of *pif2* did not impact the expression of urokinase, an extracellular recombinant protein. This project also investigated through mutagenesis the possible role of the PIF1 RGD motifs in oral infection of larvae. The initial findings suggest that the PIF1 RGD motifs functional role is not very clear and indicate that PIF1 RGD motifs are not involved in integrin binding but could mediate other interactions during viral entry into the midgut cells.

While the mechanism involved in the production of ODV was not elucidated, a number of interesting observations have been made about the targeted structural components of the ODV that were investigated, which could aid the understanding of the major transition from BV to ODV production during the baculovirus infection

Presentations

The work described in this thesis has been presented at international conference and workshops in the form of poster and oral presentations.

Oral presentations

CHAMBERS, A. C., Hitchman, R. B., King, L. A. & Possee, R. D., (2009), High Throughput Analysis of Baculovirus Gene Function In Insect Cells. School of Life Sciences Postgraduate Research Student Symposium, Oxford Brookes University, Oxford, UK.

CHAMBERS, A. C., Hitchman, R. B., King, L. A. & Possee, R. D., (2010), High Throughput Analysis of Baculovirus Gene Function In Insect Cells. School of Life Sciences, Symposium, Oxford Brookes University, Oxford, UK.

Poster presentations

CHAMBERS, A. C., Hitchman, R. B., King, L. A. & Possee, R. D., (2010), High Throughput Analysis of Baculovirus Gene Function In Insect Cells. School of Life Sciences Postgraduate Research Student Symposium, Oxford Brookes University, Oxford, UK.

CHAMBERS, A. C., Hitchman, R. B., King, L. A. & Possee, R. D., (2010), High Throughput Analysis of Baculovirus Gene Function In Insect Cells. 43th Annual Meeting of the Society for Invertebrate Pathology, Trabzon, Turkey. **Winner of 3rd place prize for best poster presentation.**

Acknowledgments

The last four years of my life have been an amazing discovery of not just knowledge but of myself as well. It has not always been “easy sailing” and without the help and the support of others it would have been much more difficult. I like to take this opportunity to thank these people.

I'd like to personally thank my whole supervisor team, Robert Possee, Linda King and Richard Hitchman, for all their guidance and support through these last four years. I am extremely grateful to Robert Possee for giving me the opportunity to do this PhD and to Oxford Expression Technologies Ltd for their sponsorship.

I would like to thank Barry Martin for all the training and advice for Electron microscopy work contained within this thesis. A special thanks to my “mum” Kay Chambers for all the laboratory technical support and aid with contacting the “other side” when needed.

I am extremely grateful to the past and current members of the Insect Virus Research group that I've had the pleasure of meeting and making the last four years an enjoyable one; Caz, Fernanda, Evi, John, Ananya, Rahul, David, Farheen, Elisabetta and Sarah. I'd like to extend this gratitude to all members of Oxford Expression Technologies Ltd but two in particular; Richard and Olga.

I'd like to extend all my love and thanks to my family for all their emotional support during this time, without this support I would not have reached this point today. I am extremely thankful to my parents for always being there for me and believing in me even when I did not.

This last section is for one particular person, who supported me unconditionally and gave me the courage to continue on even when I thought I could not.

"Askim, sen benim herseyimsin. Bu yil boyunca gosterdigin destekten dolayi sana cok tesekkur ederim. Tum dilegim, ihtiyacin oldugunda sana ayni destegi gosterebilmektir sevgilim".

Table of contents

Abstract	i
Presentations.....	ii
Acknowledgments.....	iii
Table of contents.....	iv
List of Figures	ix
List of Tables.....	xi
List of Abbreviations.....	xii
Chapter 1 Introduction	1
1.1 Introduction to Baculoviruses	2
1.2 The <i>Baculoviridae</i> family	3
1.2.1 The discovery of baculoviruses	3
1.2.2 Baculovirus Characteristics	4
1.2.3 The Structure of Occlusion Bodies.....	5
1.2.4 The role of genome heterogeneity in baculovirus virulence.....	7
1.2.5 The classification of baculoviruses	8
1.3 The Baculovirus Life Cycle	10
1.3.1 Initial Virus Entry through the Midgut.....	10
1.3.2 Infection of the Midgut Epithelium.....	11
1.3.3 Virus entry into the nuclei	12
1.3.4 Viral exit from the nuclei.....	12
1.3.5 Midgut Epithelium bypass mechanism.....	13
1.3.6 Infection of the inner tissues.....	13
1.3.7 Cell Defence: Apoptosis	15
1.3.8 Spread of infection throughout the host tissues	16
1.3.9 The Virogenic Stroma	17
1.3.10 The Nucleocapsid.....	18
1.3.11 The Occlusion Derived Virus and Occlusion bodies	19
1.3.12 The Budded Virus.....	23
1.4 Baculovirus Expression Vector Systems	25
1.4.1 Introduction to Baculovirus Expression Vector Systems	25
1.4.2 Improvements to the Baculovirus Expression Vector Systems.....	26
1.4.2a The BacPAK6 system.....	26
1.4.2b The Bac-to-Bac™ system	27
1.4.2c The <i>flashBAC</i> ™ system	28
1.5 Aims of Thesis	30
Chapter 2 Materials & Methods	31
2.1 Materials	32
2.1.1 Chemicals	32
2.1.2 Plasmids	32
2.2 Bioinformatics.....	33
2.2.1 Baculovirus sequences	33
2.2.2 Multiple sequence alignments.....	33

2.2.3 Protein pattern search	33
2.3 Insect Larvae, Cells and Viruses.....	33
2.3.1 Insect larvae and cell lines	33
2.3.2 Virus amplification	34
2.3.3 Transfection of insect cells	34
2.3.3a Generation of Recombinant viruses.....	35
2.3.4 Titration of virus stocks	35
2.3.4a Plaque assay titration	35
2.3.4b Plaque purification of recombinant viruses	36
2.3.4c Alternative plaque purification method	36
2.3.5 Temporal analysis of virus replication.....	37
2.3.6 Purification of Baculovirus DNA	37
2.3.6a Purification of large quantities of virus DNA using Caesium Chloride	37
2.3.6b Purification of virus DNA from 35mm dishes.....	38
2.3.6c Purification of virus DNA using a Viral Nucleic Acid Kit	39
2.3.7 Virus infection of insect larvae.....	40
2.3.8 BV injection <i>in vivo</i>	40
2.3.9 Purification of OBs from virus-infected larvae.....	40
2.3.9a Purification of OBs from single infected larvae	41
2.3.10 Enumerating OBs from infected larvae	41
2.3.11 Bioassays	42
2.3.11a Statistical analysis of Bioassay data	42
2.4 Microscopy Methods	42
2.4.1 Laser scanning confocal microscopy of fixed cells	42
2.4.2 Electron microscopy of OBs	43
2.5 Bacteria methods	44
2.5.1 Preparation of chemically competent <i>E. coli</i> cells	44
2.5.2 Preparation of chemically competent <i>E. coli</i> cells – Inoue method	45
2.5.3 Transformation of competent <i>E. coli</i> cells with plasmid DNA.....	45
2.5.4 Preparation of electrocompetent <i>E. coli</i> cells containing pRedET	46
2.5.5 Electroporation of competent <i>E. coli</i> cells	46
2.5.6 Plasmid DNA purification from <i>E. coli</i> cells	47
2.5.7 Purification of large quantities of bacmid DNA using caesium chloride...	47
2.5.8 Red/ET recombination system	48
2.5.9 Bacmid transfection of insect cells	49
2.6 Molecular Biology Methods.....	49
2.6.1 Restriction enzyme digestions of DNA	49
2.6.2 Dephosphorylation of DNA.....	49
2.6.3 Ligation of DNA	49
2.6.4 Agarose gel electrophoresis	50
2.6.5 Isolation of DNA from agarose gels	50
2.6.6 Polymerase chain reaction (PCR)	50
2.6.7 TOPO and pGEM-T cloning of PCR fragments.....	51
2.6.8 DNA sequencing.....	51
2.6.9 Generation of Oligonucleotide fragments	51

2.6.10 Mutagenesis	52
2.7 Protein Analysis	52
2.7.1 SDS-PAGE analysis of protein samples	52
2.7.2 Western blot analysis of proteins	52
2.7.3 Enzyme activity assays	53
2.7.3a β -galactosidase activity assay	53
2.7.3b Urokinase activity assay	54
Chapter 3 A bioinformatic analysis of target ODV structural proteins	55
3.1 Introduction	56
3.2 Structural proteins of the occlusion derived virus	56
3.2.1 Occlusion-derived virus structural protein: ODV-E66	62
3.2.2 Occlusion-derived virus structural protein: ORF79	64
3.2.3 Occlusion-derived virus structural protein: CG30	70
3.2.4 Occlusion-derived virus structural protein: ODV-E28	73
3.2.5 Occlusion-derived virus structural protein: ODV-EC43	76
3.2.6 Occlusion-derived virus structural protein: ODV-E56	79
3.2.7 Occlusion-derived virus structural proteins: PIF2 & PIF3	80
3.3 Conclusion	92
Chapter 4 Construction of baculovirus gene deletion mutants	93
4.1 Introduction	94
4.1.1 Red/ET recombination system	97
4.2 Construction of parental bacmid (AcBacPAK5/ <i>lacZ</i> /BAC ^{pol})	100
4.3 Construction of the kanamycin gene cassette with AcMNPV flanking sequences and production of ODV deletion mutant bacmids	105
4.4 Deletion of the remaining six AcMNPV ODV genes using AcBAC Δ <i>chitinase</i> as the parental bacmid DNA	113
4.5 Recovery of virus after transfection of Sf9 cells with deletion bacmids	116
4.6 Characterization of Ac Δ <i>odv-ec43</i> , Ac Δ <i>orf79</i> and Ac Δ <i>odv-e28</i>	121
4.6.1 Ac Δ <i>odv-ec43</i>	121
4.6.2 Ac Δ <i>odv-e28</i> and Ac Δ <i>orf79</i>	125
4.5 Discussion	130
4.5.1 Construction of deletion mutant viruses	130
4.5.2 Analysis of the deletion mutant virus; Ac Δ <i>odv-ec43</i>	131
4.5.3 Analysis of the deletion mutant virus; Ac Δ <i>odv-e28</i>	132
4.5.4 Analysis of the deletion mutant virus; Ac Δ <i>orf79</i>	133
4.5.5 Conclusion	134
Chapter 5 Characterisation of AcΔ<i>odv-e66</i>, AcΔ<i>cg30</i> and AcΔ<i>odv-e56</i> ..	135
5.1 Introduction	136
5.2 Characterisation of <i>odv-e66</i> , <i>cg30</i> and <i>odv-e56</i>	136
5.2.1 <i>odv-e66</i>	136
5.2.2 <i>cg30</i>	136
5.2.3 <i>odv-e56</i>	136
5.3 Amplification of deletion mutant viruses for analysis	137

5.4 Temporal analysis of virus replication in <i>Ac</i> Δ <i>odv-e66</i> , <i>Ac</i> Δ <i>cg30</i> , <i>Ac</i> Δ <i>odv-e56</i> and <i>AcBAC</i> Δ <i>chitinase</i> -infected Sf9 cells.....	139
5.4.1 Cell Viability.....	139
5.4.2 Budded Virus Production.....	139
5.5 Western blot analysis of VP39 production in <i>Ac</i> Δ <i>cg30</i> -infected Sf9 cells.....	140
5.6 Restoration of <i>polh</i> into <i>AcBAC</i> Δ <i>chitinase</i> , <i>Ac</i> Δ <i>odv-e66</i> , <i>Ac</i> Δ <i>cg30</i> and <i>Ac</i> Δ <i>odv-e56</i>	145
5.7 Bioassays for <i>Ac</i> Δ <i>chitinase</i> ^{Pol+} , <i>Ac</i> Δ <i>odv-e66</i> ^{Pol+} , <i>Ac</i> Δ <i>cg30</i> ^{Pol+} and <i>Ac</i> Δ <i>odv-e56</i> ^{Pol+}	147
5.8 Electron microscopic analysis of <i>Ac</i> Δ <i>chitinase</i> ^{Pol+} , <i>Ac</i> Δ <i>odv-e66</i> ^{Pol+} , <i>Ac</i> Δ <i>cg30</i> ^{Pol+} and <i>Ac</i> Δ <i>odv-e56</i> ^{Pol+} OBs.....	149
5.9 Discussion.....	151
5.9.1 <i>Ac</i> Δ <i>odv-e66</i>	151
5.9.2 <i>Ac</i> Δ <i>cg30</i>	152
5.9.3 <i>Ac</i> Δ <i>odv-e56</i>	154
5.9.4 Conclusion.....	156
Chapter 6 Characterisation of <i>Ac</i>Δ<i>pif2</i> and <i>Ac</i>Δ<i>pif3</i>.....	158
6.1 Introduction.....	159
6.1.1 <i>per os</i> infectivity factor (PIF) family.....	159
6.1.2 PIF2.....	159
6.1.3 PIF3.....	160
6.2 Characterization of <i>Ac</i> Δ <i>pif2</i> and <i>Ac</i> Δ <i>pif3</i>	160
6.3 Temporal analysis of virus replication in <i>Ac</i> Δ <i>pif2</i> - and <i>AcBacPAK5lacZ/BAC</i> ^{pol} -infected Sf9 cells.....	163
6.3.1 Virus-infected cell viability.....	163
6.3.2 Budded virus production.....	163
6.3.3 β -galactosidase production.....	165
6.4 Construction of recombinant viruses for urokinase synthesis.....	167
6.5 Temporal analysis of virus replication in <i>AcBacPAK5urokinase</i> ^{pol} and <i>AcUK</i> Δ <i>pif2</i> infected Sf9 cells.....	169
6.5.1 Cell viability.....	169
6.5.2 Budded virus production.....	169
6.5.3 Urokinase production.....	171
6.6 <i>Ac</i> Δ <i>pif3</i>	173
6.6.1 Rescue of <i>pif3</i>	173
6.6.2 Infectivity of <i>Ac</i> Δ <i>pif3</i> and rescued viruses <i>Ac</i> Δ <i>pif3-Rpif3</i> ^{pol} and <i>Ac-pif3</i> ³	177
6.6.3 Construction of 6xHis-tagged <i>pif3</i> virus (<i>Ac-hispif3</i>).....	179
6.6.4 Immunoblotting analysis of <i>Ac-hispif3</i> PIF3 expression.....	181
6.6.5 Sub cellular localisation of PIF3 during baculovirus infection.....	182
6.7 Discussion.....	185
6.7.1 Analysis <i>Ac</i> Δ <i>pif2</i> -infected cell viability and BV production.....	185
6.7.1a Analysis of <i>Ac</i> Δ <i>pif2</i> β -galactosidase activity.....	186
6.7.1b Analysis of <i>AcUK</i> Δ <i>pif2</i> urokinase activity.....	187
6.7.2 Analysis of the deletion mutant virus <i>Ac</i> Δ <i>pif3</i>	188
6.7.3 Conclusion.....	189

Chapter 7 Characterisation of <i>AcΔorf118/pif1</i>	190
7.1 Introduction.....	191
7.2 Construction of a deletion mutant: <i>AcBACΔorf118/pif1</i>	194
7.2.1 PCR Analysis of <i>AcBACΔorf118/pif1</i>	196
7.2.2 Restriction Enzyme Analysis of <i>AcBACΔorf118/pif1</i>	196
7.3 Construction of <i>AclacZΔorf118/pif1</i>	199
7.4 Temporal analysis of virus replication in <i>AclacZΔorf118/pif1</i> and <i>AclacZΔchitinase/cathepsin</i> infected Sf9 cells.	201
7.4.1 Cell Viability	201
7.4.2 Budded Virus Production	202
7.4.3 β-galactosidase production.....	204
7.5 Construction of recombinant viruses with PIF1 RGD motif mutations.	206
7.5.1 <i>AcBACΔpif1</i>	210
7.6 Bioassays for <i>Ac<pif1< i="">^{Arg96AlaPol+}, <i>Ac<pif1< i="">^{Arg478AlaPol+} and <i>Ac<pif1< i="">^{Arg96/478AlaPol+}</pif1<></i></pif1<></i></pif1<></i>	216
7.7 Discussion.....	219
7.7.1 Analysis of the deletion mutant virus; <i>AclacZΔorf118/pif1</i>	219
7.7.2 Characterisation summary for <i>pif1</i> mutant viruses	221
7.7.3 Analysis of the PIF1 RGD motif mutant viruses	221
7.7.4 Conclusion	222
 Chapter 8 Final Discussion and Future work	 224
8.1 Summary of Thesis	225
8.2 Discussion of thesis results and future work	227
8.2.1 Construction of deletion mutant viruses	227
8.2.2 Construction of Synthetic virus	229
8.2.3 Construction of Insect expression vector	229
8.2.4 Analysis of <i>AcMNPV</i> to other occluded viruses.....	230
8.3 Concluding remarks	230
 References	 232

List of Figures

Figure 1.1 Electron microscopy of purified OBs.....	6
Figure 1.2 Major occlusion-derived virion forms	7
Figure 1.3 Phylogenetic tree of Baculoviridae family	9
Figure 1.4 The baculovirus replication cycle	14
Figure 1.5 Proteins of the nucleocapsid.....	20
Figure 1.6 The budded and occlusion-derived virus	21
Figure 1.7 Scanning electron microscopy of OBs.....	22
Figure 1.8 Electron microscopy of a baculovirus BV	24
Figure 1.9 Illustration of the method used to construct recombinant viruses	26
Figure 1.10 BacPAK6 method used to construct recombinant viruses.....	27
Figure 1.11 Bac-to-Bac™ method used to construct recombinant viruses	28
Figure 1.12 <i>flashBAC</i> ™ method used to construct recombinant viruses	29
Figure 3.1 Sequence alignments of Type I and Type II ODV-E66 Sequences	65
Figure 3.2 Sequence alignments of ORF79 Sequences	69
Figure 3.3 Sequence alignments of Type I and Type II CG30 Sequences	72
Figure 3.4 Sequence alignments of Type I and Type II ODV-E28 Sequences	75
Figure 3.5 Sequence alignments of Type I and Type II ODV-EC43 Sequences.....	78
Figure 3.6 Sequence alignments of Type I and Type II ODV-E56 Sequences	82
Figure 3.7 Sequence alignments of Type I and Type II PIF2 Sequences	86
Figure 3.8 Sequence alignment of PIF2 Sequence against betabaculovirus homologue	88
Figure 3.9 Sequence alignments of Type I and Type II PIF3 Sequences	90
Figure 3.10 Sequence alignment of PIF3 Sequence against betabaculovirus homologue	91
Figure 4.1 Illustration of the method used to disrupt a target gene.	96
Figure 4.2 pRedET plasmid	98
Figure 4.3 Illustration of the formation of AcBacPAK5/ <i>lacZ</i> /BAC ^{pol}	102
Figure 4.4 <i>Hind</i> III restriction enzyme analysis of AcBacPAK5/ <i>lacZ</i> /BAC ^{pol} virus	104
Figure 4.5 Schematic showing the construction of the kanamycin resistance gene cassette with AcMNPV flanking arms.	106_Toc325351681
Figure 4.6 Schematic of the construction of AcBacPAK5/ <i>lacZ</i> /BAC ^{pol} Δ <i>pif2</i> bacmid.	108
Figure 4.7 PCR analysis of AcBacPAK5/ <i>lacZ</i> /BAC ^{pol} Δ <i>cg30</i> DNA	109
Figure 4.8 PCR analysis of AcBacPAK5/ <i>lacZ</i> /BAC ^{pol} Δ <i>pif2</i> DNA	110
Figure 4.9 <i>Hind</i> III restriction enzyme analyses of AcBacPAK5/ <i>lacZ</i> /BAC ^{pol} Δ <i>pif2</i> and AcBacPAK5/ <i>lacZ</i> /BAC ^{pol} Δ <i>odv-ec43</i> bacmids.....	111
Figure 4.10 <i>Hind</i> III restriction enzyme analyses of deletion mutant bacmids.....	114
Figure 4.11 PCR analysis of deletion mutant virus DNA.....	119
Figure 4.12 Schematic of the construction of AcBacPAK5/ <i>lacZ</i> /BAC ^{pol} Δ <i>odv-ec43</i> bacmid.	121
Figure 4.13 Insertion of baculovirus genes into pOET3 and pBAC5	123
Figure 4.14 Schematic of the construction of (A) AcBACΔ <i>chitinase</i> Δ <i>odv-e28</i> and (B) AcBACΔ <i>chitinase</i> Δ <i>orf79</i>	128
Figure 5.1 Schematic of the construction of Δ <i>odv-e66</i> , Δ <i>cg30</i> and Δ <i>odv-e56</i> bacmids.	138
Figure 5.2 Cell viability of AcΔ <i>odv-e66</i> , AcΔ <i>cg30</i> or AcΔ <i>odv-e56</i> -infected Sf9 cells.	141
Figure 5.3 Kinetics of budded virus production for AcΔ <i>odv-e66</i> , AcΔ <i>cg30</i> or AcΔ <i>odv-e56</i>	142
Figure 5.4 Western blot analysis of AcMNPV, AcBACΔ <i>chitinase</i> and AcΔ <i>cg30</i> infected Sf9 cells.	143
Figure 5.5 Semi-quantification of VP39 production in AcMNPV-, AcBACΔ <i>chitinase</i> - and AcΔ <i>cg30</i> -infected Sf9 cells	144
Figure 5.6 The restoration of the polyhedrin gene in AcBACΔ <i>chitinase</i> Δ <i>odv-e66</i> , Δ <i>cg30</i> and Δ <i>odv-e56</i> bacmids.....	146
Figure 5.7 Mortality of AcMNPV, AcΔ <i>chitinase</i> ^{Pol+} , AcΔ <i>odv-e66</i> ^{Pol+} , AcΔ <i>cg30</i> ^{Pol+} and AcΔ <i>odv-e56</i> ^{Pol+} infected larvae.....	148

Figure 5.8 Electron microscopy of purified OBs from <i>Ac</i> Δ chitinase ^{Pol+} , <i>Ac</i> Δ odv-e66 ^{Pol+} , <i>Ac</i> Δ cg30 ^{Pol+} and <i>Ac</i> Δ odv-e56 ^{Pol+} infected larva.	150
Figure 6.1 Schematic of the construction of Δ <i>pif2</i> (A) and Δ <i>pif3</i> (B) bacmids	162
Figure 6.2 Cell viability of <i>AcBacPAK5/lacZ/BAC</i> ^{pol} or <i>Ac</i> Δ <i>pif2</i> -infected Sf9 cells.....	164
Figure 6.3 Kinetics of budded virus production by <i>Ac</i> Δ <i>pif2</i>	164
Figure 6.4 β -galactosidase activities in virus-infected cell cultures	166
Figure 6.5 Coomassie blue and western blot analyses of <i>AcBacPAK5</i> urokinase ^{pol} and <i>AcUK</i> Δ <i>pif2</i> -infected Sf9 cells	168
Figure 6.6 Cell viability of <i>AcBacPAK5</i> urokinase ^{pol} and <i>AcUK</i> Δ <i>pif2</i> -infected Sf9 cells.....	170
Figure 6.7 Kinetics of budded virus production by <i>AcBacPAK5</i> urokinase ^{pol} and <i>AcUK</i> Δ <i>pif2</i>	170
Figure 6.8 Graphical presentation of Urokinase expression against time for <i>AcUK</i> Δ <i>pif2</i> Time Course.....	172
Figure 6.9 Insertion of baculovirus genes into pBAC1	175
Figure 6.10 PCR analyses of <i>Ac</i> Δ <i>pif3</i> , <i>Ac-pif3'</i> and <i>Ac</i> Δ <i>pif3-Rpif3'</i> ^{pol} DNA.....	178
Figure 6.11. Schematic showing the construction of 6xHis-tagged <i>pif3</i> fragment and insertion into Topo vector.	180
Figure 6.12. Western blot analysis of <i>Ac-hispif3</i> infected Sf9 cells.....	181
Figure 6.13 Time course of PIF3 localisation in <i>Ac-hispif3</i> infected TN-368 cells	183
Figure 7.1 Sequence alignments of Type I PIF1 Sequences.....	193
Figure 7.2 Schematic of the construction of <i>AcBAC</i> Δ <i>orf118/pif1</i> bacmid.	195
Figure 7.3 PCR analysis of <i>AcBAC</i> Δ <i>orf118/pif1</i> DNA	197
Figure 7.4 <i>HindIII</i> restriction enzyme analyses of deletion mutant bacmids.....	198
Figure 7.5 Schematic showing the insertion of <i>lacZ</i> at <i>polh</i> locus for <i>AcBAC</i> Δ <i>orf118/pif1</i>	199
Figure 7.6 Virus-infected cell viabilities.	202
Figure 7.7 Kinetics of budded virus production for <i>Ac</i> <i>lacZ</i> Δ <i>orf118/pif1</i>	203
Figure 7.9 Schematic of the <i>pif1</i> mutations.....	208
Figure 7.10 Schematic of the initial method used to construct <i>pif1</i> mutant viruses	209
Figure 7.11 Schematic of the construction of <i>AcBAC</i> Δ <i>pif1</i> bacmid.....	210
Figure 7.12 Insertion of <i>pif1</i> coding regions into modified pAcUW21	213
Figure 7.13 PCR analysis of recombinant virus DNA from <i>pif1</i> mutants	215
Figure 7.14 Mortality of <i>AcMNPV</i> , <i>Ac</i> Δ chitinase ^{Pol+} , <i>Ac</i> <i>pif1</i> ^{Pol+} , <i>Ac</i> Δ <i>pif1</i> ^{Pol+} , <i>Ac</i> <i>pif1</i> ^{Arg96AlaPol+} , <i>Ac</i> <i>pif1</i> ^{Arg478AlaPol+} and <i>Ac</i> <i>pif1</i> ^{Arg96/478AlaPol+} infected larvae	218
Figure 8.1 Circular map of the <i>AcMNPV</i> genome.....	228

List of Tables

Table 2.1 Plasmids used in this thesis	32
Table 2.2 Viruses used in this thesis	34
Table 2.3 Antibodies used for Laser scanning confocal microscopy	43
Table 2.4 E. coli strains used in this thesis	44
Table 2.5 Antibiotics used in bacteria cultures	46
Table 2.6 Antibodies used for Western blotting	53
Table 3.1 Target structural proteins of the AcMNPV occlusion-derived virus	57
Table 3.2 Potential structural proteins of the occlusion-derived virus	58
Table 4.1 Sequence of ODV primers and their location on the AcMNPV genome	107
Table 4.2: The predicted alterations to the banding pattern of <i>HindIII</i> -digested parental bacmid...	115
Table 4.3: Summary of deletion mutant bacmids.	115
Table 4.4 Sequence of external and internal primers for each target gene.	118
Table 4.5: Summary of results from <i>AcΔodv-ec43</i> rescue experiments.....	125
Table 4.6: Summary of results from <i>AcΔorf79</i> and <i>AcΔodv-e28</i> rescue experiments.....	127
Table 5.1 Infectivity of <i>AcΔodv-e66^{Pol+}</i> , <i>AcΔcg30^{Pol+}</i> and <i>AcΔodv-e56^{Pol+}</i> occlusion bodies	147
Table 6.1 Budded virus titres for <i>AcΔpif3</i> , <i>Ac-pif3</i> and <i>AcΔpif3-Rpif3^{Pol}</i> stocks	177
Table 7.1: Summary of <i>pif1</i> mutant viruses.	206
Table 7.2 Infectivity of <i>Acpif1^{Arg96AlaPol+}</i> , <i>Acpif1^{Arg478AlaPol+}</i> and <i>Acpif1^{Arg96/478AlaPol+}</i> occlusion bodies	216

List of Abbreviations

β -galactosidase gene	<i>lacZ</i>
aa:	amino acid
ATP:	adenosine triphosphate
BAC:	bacterial artificial chromosome
BEVs:	baculovirus expression vectors
bp:	base pairs
BSA:	bovine serum albumin
BV:	budded virions
C-terminal:	carboxy-terminal
CMV	cytomegalovirus immediate early gene
DAPI:	4',6-diamidino-2-phenylindole
DMF	dimethylformimide
DMSO:	dimethylsulphoxide
DNA:	deoxyribonucleic acid
dNTP:	deoxynucleotide triphosphate
dpi:	days post infection
dsDNA:	double stranded deoxyribonucleic acid
<i>egt</i> :	ecdysteroid-UDP-glycosyl transferase (gene)
EB	European Bioinformatics Institute
EM:	electron microscopy
EMBL	European Molecular Biology Laboratory
F-actin:	filamentous actin
FB	<i>flashBAC</i> TM
FBG	<i>flashBACGOLD</i> TM
FBU	<i>flashBACULTRA</i> TM
FCS	foetal calf serum
GFP:	green fluorescent protein
GV:	granulovirus
hpi:	hours post infection
IAP	inhibitors of apoptosis
ICTV:	International Committee on the Taxonomy of Viruses
INM	inner nuclear membrane
LB:	luria broth
LD	lethal dose
LEF	late expression factor protein
<i>lef</i>	late expression factor gene
MNPV:	multi-capsid nucleopolyhedrovirus
MOI:	multiplicity of infection
MSA:	Multiple Sequence Alignment
NCBI:	National Centre for Biotechnology Information
NPV:	nucleopolyhedrovirus
N-terminal:	amino-terminal
OBs	occlusion bodies
ODV:	occlusion derived virions
ONPG	<i>ortho</i> -Nitrophenyl- β -galactoside
orf:	open reading frame
P10:	The baculovirus 10 kDa protein
<i>p10</i> :	The baculovirus 10 kDa protein gene
PBS:	phosphate buffered saline
PCR:	polymerase chain reaction
PE:	polyhedral envelope
pfu:	plaque forming units
<i>pif</i>	per os infectivity factor

PM	peritrophic membrane
<i>polh</i> :	polyhedrin (gene)
Polh:	polyhedrin (protein)
p.s.i.	pounds per square inch
RE	restriction enzyme
RGD motif	arginine-glycine-aspartic acid motif
RNA:	ribonucleic acid
rpm:	rotations per minute
SDS:	sodium dodecyl sulfate
SDS-PAGE:	sodium dodecyl sulfate polyacrylamide gel electrophoresis
<i>Sf</i> :	<i>Spodoptera frugiperda</i>
SNPV:	single-capsid nucleopolyhedrovirus
<i>T. ni</i>	<i>Trichoplusi ni</i>
uPA	urokinase-type plasminogen activator enzyme
X-gal	5-Bromo-4-chloro-3-indolyl β -D-galactopyranoside
wt:	wild type

Viruses

The *Baculoviridae*

AcMNPV: *Autographa californica* nucleopolyhedrovirus
 AdhoNPV: *Adoxophyes honmai* nucleopolyhedrovirus
 AgNPV: *Anticarsia gemmatalis* nucleopolyhedrovirus
 AnpeNPV: *Antheraea pernyi* nucleopolyhedrovirus
 BmNPV: *Bombyx mori* nucleopolyhedrovirus
 CfDEFNPV: *Choristoneura fumiferana* defective nucleopolyhedrovirus
 CfNPV: *Choristoneura fumiferana* nucleopolyhedrovirus
 ChocGV: *Christoneura occidentalis* granulovirus
 CpGV: *Cydia pomonella* granulovirus
 CuniNPV: *Culex nigripalpus* nucleopolyhedrovirus
 EcobNPV: *Ectropis obliqua* nucleopolyhedrovirus
 EppoNPV: *Epiphyas postvittana* nucleopolyhedrovirus
 HearNPV: *Helicoverpa armigera* nucleopolyhedrovirus
 HycuNPV: *Hyphantria cunea* nucleopolyhedrovirus
 HzNPV: *Helicoverpa zea* nucleopolyhedrovirus
 LdNPV: *Lymantria dispar* nucleopolyhedrovirus
 MacoNPV B: *Mamestra configurata* nucleopolyhedrovirus B
 OpNPV: *Orgyia psuedotsugata* nucleopolyhedrovirus
 P1xyNPV: *Plutella xylostella* nucleopolyhedrovirus
 PoGV: *Phthorimaea operculella* granulovirus
 PiraGV: *Pieris rapae* granulovirus
 PxNPV: *Plutella xylostella* nucleopolyhedrovirus
 RoNPV: *Rachiplusia ou* nucleopolyhedrovirus
 SeNPV: *Spodoptera exigua* nucleopolyhedrovirus
 SfMNPV: *Spodoptera frugiperda* nucleopolyhedrovirus

Chapter 1

Introduction

1.1 Introduction to Baculoviruses

The *Baculoviridae* family contains a wide range of arthropod-specific viruses, which are known to infect over 600 host species found in a number of different invertebrate orders (Herniou *et al.*, 2003). Many of the baculovirus species identified and characterized so far are found in the order *Lepidoptera*, leaving the non-lepidopteran isolates less well defined. Due to the high species specificity among lepidopteran baculovirus isolates, it is believed that baculoviruses coevolved with *Lepidoptera* (Zanotto *et al.*, 1993). Presently, a database of more than 4000 genes is available from around 40 completely sequenced baculovirus genomes. Thirty-one core genes have been reported to be conserved across all the sequenced genomes, which suggests it is likely they serve essential roles in the baculovirus life cycle (Hiscock and Upton, 2000; McCarthy and Theilmann, 2008).

Much research has gone into baculoviruses at the molecular level to improve their use as pesticides, expression systems and more recently for gene therapy. In the next sections I will briefly discuss each of these applications and give details on their usage.

Baculoviruses have been used for decades as biocontrol agents against forestry and agriculture pests, including the velvetbean caterpillar, cotton bollworm and gypsy moth (Zhang, 1994; Moscardi, 1999; Cook *et al.*, 2003). Baculoviruses make good biocontrol agents due to their host specificity; they have little impact on the environment and are non-hazardous to human health. In contrast, xenobiotic pesticides damage the environment by killing beneficial insects and can be hazardous to humans. Baculovirus insecticides are restricted to lepidopteran and hymenopteran pests, although developments for mosquito insecticides are under way with the characterization of mosquito-specific baculoviruses (Moser *et al.*, 2001; Andreadis *et al.*, 2003).

Since the 1980s, baculoviruses have been used as an expression vector system allowing large quantities of recombinant proteins to be produced from insect cells infected with recombinant budded virus (BV), which contains a foreign gene usually under the control of the polyhedrin gene (*polh*) promoter. More recently, baculovirus genomes have been modified to produce large quantities of heterologous proteins by removing selected non-essential genes. This reduces the viral protein load on the host cell's mechanisms allowing an increase in recombinant protein production (Hitchman *et al.*, 2010a; Hitchman *et al.*, 2010b). The development of a baculovirus expression system marketed as *flashBAC*TM (FB) (Oxford Expression Technologies Ltd, Oxford UK), has reduced the time required to produce recombinant viruses to a one step process, whereas other baculovirus expression systems require a screening process to identify recombinant virus

from a mixed population (Possee *et al.*, 2008). The key factors for most baculovirus expression systems are that they produce high levels of expression of target proteins and that the host insect cell's post-translation modification enables functionally authentic proteins to be made (Hitchman *et al.*, 2011; van Oers, 2011; Hitchman *et al.*, 2012).

Modified baculovirus genomes can be used to transduce mammalian cells for gene expression or therapy. One of the primary reasons for using baculoviruses in this way is that they cannot cause an infection in human cells (Carbonell *et al.*, 1985). The BacMam technology generally uses pFastBac transfer vectors to create recombinant baculoviruses in bacterial cells that contain genes under the cytomegalovirus immediate early gene (CMV) promoter, which is active in mammalian cells (Kost *et al.*, 2007). Once these modifications are introduced into the baculovirus genome via a normal transposition method, they are subsequently used to infect insect cells (Kost *et al.*, 2005; Condreay and Kost, 2007; Fornwald *et al.*, 2007). The resulting "BacMam" particles are generally concentrated prior to use to improve the efficiency of introducing them into mammalian cells (Hofmann *et al.*, 1995; Boyce and Bucher, 1996; Monsma *et al.*, 1996).

Research into the use of baculoviruses as gene therapy vectors has increased over the last decade. The literature contains a large number of publications showing the applications of the baculovirus vectors towards the treatment of diseases. The more recently publications show the possible treatment for myocardial infarction or ischemic skeletal muscle and several cancers. In the case of myocardial infarction or ischemic skeletal muscle, the expression of vascular endothelial growth factor or Angiopoietin-1 could be used to treat the disease by inducing angiogenesis, thereby increasing the blood supply to target area (Paul *et al.*, 2011; Heikura *et al.*, 2012). The research into the possible treatment of cancers using baculovirus vectors is more complex and normally results in vectors being constructed to target specific cancers. However, some baculovirus vectors do express proteins that could treat a wide range of cancers such as endostatin or angiostatin, which are anti-angiogenic proteins (Luo *et al.*, 2011; Rivera-Gonzalez *et al.*, 2011).

1.2 The *Baculoviridae* family

1.2.1 The discovery of baculoviruses

The production of silk from cultured silkworms has been carried out in China for over 5000 years and this industry is intimately linked with the discovery of baculoviruses. Ancient

Chinese texts dating back almost 4000 years on the rearing of silkworm give references to a disease with baculovirus characteristics (Tanada and Kaya, 1993; Miller, 1997). The culturing of silkworms had spread from Asia to Europe by about 550 C.E due to it being a major item of commerce at the time (Steinhaus, 1975). A poem by the Bishop of Alba, Marcus Hieronymus Vida (born in Cremona, 1490) describing the liquefaction of *Bombyx mori* silkworm caterpillars is believed to be the earliest description of a baculovirus infection in European literature (Granados and Federici, 1986). These descriptions date back before the germ theory of disease had even been put forward and it wasn't until the late 19th century that Dimitrii Ivanowsky discovered viruses as a causative agent of disease.

With the discovery of the light microscope in the 19th century, the cause of the disease described in Marcus Hieronymus Vida poem could be characterised by highly refractile occlusion bodies found in the cells of infected larva. Due to these refractile structures being polyhedron shaped, this led to the disease being termed “polyhedroses” by the mid-1800s (reviewed in Granados and Federici, 1986). However, it had been suggested that the infectious particle was encased within these occlusion bodies. This was not confirmed until the late 1940s by the visualisation of rod shaped virions using electron microscopy (reviewed in Harrison and Hoover, 2012). Further investigation established the crystalline polyhedral nature of the occlusion body structure located in the nuclei of infected cells and this established the group name nuclear polyhedrosis virus (Bergold, 1953), which was later renamed nucleopolyhedroviruses (NPV) (Murphy *et al.*, 1995). In the 1920s, an earlier baculovirus occlusion body was characterized that was smaller and granular shaped. This group of viruses was termed “granulosis” viruses (reviewed in Jehle, 2009) and then renamed granuloviruses in 1995 (GVs) (Murphy *et al.*, 1995). These two occlusion body morphologies have divided the baculovirus family and defined the taxonomical division. In 1973, Mauro Martignoni proposed the baculovirus family was termed *Baculoviridae*, derived from the latin word *baculum*, meaning “rod” after the rod-shape structure of the virions (Vago *et al.*, 1974).

1.2.2 Baculovirus Characteristics

Baculoviruses contain a closed, circular, double-stranded DNA genome, varying in size between 80 kb and 180 kb, in a rod-shaped virus particle between 200-400 nm in length and 36 nm wide (Funk *et al.*, 1997). This rod-shaped structure is known as the capsid and has polarity due to differences in structure at either end. Inside, the DNA is highly condensed and has several associated proteins. This structure as a whole is known as the core. The capsid and the enclosed core as a whole unit are known as the

nucleocapsid (Fraiser, 1986).

The baculovirus is found in two forms. The BV form buds from infected cells and is involved in spreading the infection from tissue to tissue in the host larvae (Volkman and Goldsmith, 1985). The initial infection and horizontal transmission of baculoviruses in host larvae is mediated by the oral route using the second form, the occlusion-derived virus (ODV). Late in infection ODVs are occluded in a protein matrix known as occlusion bodies (OBs) and it is this protein matrix that protects the ODV from environmental factors (reviewed in Adam and McClintock, 1991; Boucias and Pendland, 1998).

The evolution of an occlusion viral particle that allows delayed transmission has appeared in two other insect-infecting virus taxa: the *Entomopoxvirinae* subfamily of the *Poxviridae* and the Cypovirus genus of the *Reoviridae* family (Rohrmann, 1986; Adams and Bonami, 1991). However, the existence of two virion phenotypes in one virus makes the *Baculoviridae* family unique, compared to other insect viruses.

1.2.3 The Structure of Occlusion Bodies

The structure of the occlusion body is the key factor that divides the *Baculoviridae* family into two genera. The NPV forms polyhedral OBs that are easily observed under a light microscope due to their larger size and light refractory polyhedral structure. This allowed baculoviruses to be first described in the sixteenth century as previously discussed (reviewed in Adam and McClintock, 1991). The major protein component of the NPV OB is a ~30 kDa protein called polyhedrin, which gives the OB structure an average diameter range of 800-2000 nm (Bilimoria, 1991). The second genus GV forms granulin OBs, which are more difficult to resolve under a light microscope and appear as dark granules. The major protein component of the GV OB is a ~30 kDa protein called granulin, which gives the OBs an ovoid shape that is roughly 500 nm long and 200 nm wide. Electron microscope images of both NPV and GV OBs are shown in Figure 1.1.

The OBs of both genera become surrounded in a glycoprotein multilayered lattice during formation called the calyx or polyhedrin membrane or polyhedral envelope (PE) (Whitt and Manning, 1988; Adam and McClintock, 1991). The PE is comprised of a protein/carbohydrate matrix that forms a lattice or net, which contains hexagonal pores ranging from 6 to 15 nm in diameter. The PE is a physical barrier surrounding the OB, giving extra protection from the environment and resistance to digestion from viral and other enzymes (Adam and McClintock, 1991). Deletion of the PE results in unstable OBs that have an uneven surface and are prone to losing ODVs (Russell and Rohrmann, 1990; Russell *et al.*, 1991).

Figure 1.1 Electron microscopy of purified OBs

EM images that represent the two structural forms of OBs, (A) EM image of polyhedrin OB from *Autographa californica* nucleopolyhedrovirus and (B) EM image of granulin OBs of *Plodia interpunctella* granulovirus. (Image courtesy of R.D Possee).

Another difference between the two genera is that NPV OBs normally contain many virions whereas GV OBs contain just a single virion. NPV also seem to infect a greater range of host insects than GV, which have only been isolated from lepidopteran hosts (Herniou *et al.*, 2003). The ODV within the NPV polyhedra can contain single (SNPV) or multiple (MNPV) nucleocapsids, ranging from 1 to 15 nucleocapsids per ODV (Hughes and Addison, 1970; Ackermann and Smirnov, 1983; Funk *et al.*, 1997). Whereas the majority of granulin OBs contain ODV carrying a single nucleocapsid, there are a few rare multiple GVs (Falcon and Hess, 1985). An illustration of SNPV, MNPV and GV OBs is shown in Figure 1.2. Because of this characteristic being so distinctive for specific isolates, it was used in the early taxonomy of NPVs. However, once baculovirus sequence data accumulated phylogenetic relationships could be defined. It was discovered that the MNPV and SNPV division did not conform to the phylogeny of the viruses. For example *Bombyx mori* nucleopolyhedrovirus (BmNPV) is closely related to *Autographa californica* nucleopolyhedrovirus (AcMNPV) but is considered a SNPV (Rohrman, 2011). However, even though the content of the ODV is not considered a useful taxonomical trait, it is still continually used to name baculoviruses because of historical values.

Figure 1.2 Major occlusion-derived virion forms

Schematic representation of major occlusion-derived virion forms as described in section 1.3. The Figure shows both MNPV and SNPV virions of the NPV polyhedron OB and the smaller GV granulum OB with its single embedded virion (Slack and Arif, 2007).

1.2.4 The role of genome heterogeneity in baculovirus virulence

The infection of host larva by insect viruses containing multiple genotypes is a common occurrence (Graham *et al.*, 2004; Cory *et al.*, 2005; Hitchman *et al.*, 2007a). Both the baculovirus replication cycle within the host larva and the physical structure of the MNPV ODV allows the high prevalence of infection by multiple genotypes. The OBs can contain between 20 and 80 ODVs, which in turn can contain between 1 to 15 nucleocapsids each (Simon *et al.*, 2004; Clavijo *et al.*, 2009). It has been shown that the maintenance of virus diversity during horizontal transmission favours the occlusion of genotypically heterogeneous ODV in each OB. This allows multiple genotypes to infect individual midgut columnar epithelial cells during primary infection (Clavijo *et al.*, 2010). Secondary infection caused by BV also allows the infection of multiple genotypes, as it has been estimated that each insect cell within the larva is infected by 4 BV (Bull *et al.*, 2001; Simon *et al.*, 2006).

However, such an infection strategy causes deletion genotypes to occur and these typically contain deletions to essential genes for replication and transmission (Roux *et al.*, 1991). Therefore, these deletion genotypes become reliant on the complete genotype for gene products to complete their replication cycle and ODV particles. These multiple genotypes are probably important for virus survival and pathogenicity, due to the minority genotypes not being eliminated (Munoz *et al.*, 1999).

The genotypically diverse population isolates of the type I alphabaculovirus, *Spodoptera frugiperda* (SfMNPV) have been investigated (Escribano *et al.*, 1999; Simon *et al.*, 2011). The host of SfMNPV is the fall armyworm found throughout the Americas. The Nicaraguan SfMNPV isolate (SfNIC), was demonstrated to have nine different genotypes, eight of which contained deletions varying in length (4.8–16.4 kb) within a single region of the genome. One of these genotypes was comparable to wild type SfMNPV (SfNIC-B) and showed greater infectivity than any of the other deletion genotypes when isolated from the mixed population. Three of these deletion genotypes were not orally infectious, with genotype SfNIC-C the most abundant (Simon *et al.*, 2004). Clavijo *et al.* (2009) demonstrated that mixed population comprising a synthetic deletion genotype, which was the same as SfNIC-C, and SfNIC-B were more orally infectious than single populations of SfNIC-B. Clavijo *et al.* (2009) also concluded that most likely cause of this increased oral infectivity was the deletion of *pif1* and *pif2*, suggesting a decrease in *pif1* and *pif2* ratios in a viral population could increase the transmission of a pathogen containing mixed genotypes.

1.2.5 The classification of baculoviruses

The advance in DNA sequencing method have allowed baculovirus genome sequencing to accelerate and this increase in whole baculovirus genome sequences has greatly expanded our understanding of their diversity and evolution. It is believed that baculovirus evolution is associated with the host that they infect, suggesting that as the host becomes genetically isolated so does the virus. This process is known as host dependent evolution and is not uncommon in viruses, for example, it is seen in papilloma virus, a small DNA virus that infects mammals (Soeda *et al.*, 1980). This host association for baculoviruses is based on the N-terminal polyhedrin and granulin sequences (Rohrmann *et al.*, 1981). Therefore, the *Baculoviridae* family has been divided into four major groups; Alphabaculoviruses (Lepidopteran NPVs), Betabaculoviruses (Lepidopteran GVs), Gammabaculoviruses (Hymenopteran NPVs) and Deltabaculoviruses (Dipteran NPVs) (Jehle *et al.*, 2006). The phylogenetic tree shown in Figure 1.3 illustrates this division in the *Baculoviridae* family

Figure 1.3 Phylogenetic tree of Baculoviridae family

The phylogenetic tree was constructed using amino acid alignment of 29 baculovirus core genes from 29 sequenced baculovirus genomes. This demonstrates the clear division of four groups in the baculoviridae family (Jehle *et al.*, 2006).

The alphabaculoviruses are further split into two types due to significant differences in gene content. However, the most notable difference is the BV major fusion glycoproteins for Type I NPV this is GP64 whereas for Type II NPV it is F protein. It has been put forward that ancestral Type I NPV acquired *gp64* and this stimulated their distinct evolution from Type II (Herniou *et al.*, 2001; Jiang *et al.*, 2009).

The Type I alphabaculovirus, AcMNPV was isolated from the Alfalfa looper and is the model baculovirus for this project (Vail *et al.*, 1973). AcMNPV is genetically very similar to other baculoviruses found in *Trichoplusia ni*, *Rachiplusia ou* and *Plutella xylostella* (Bonning and Hammock, 1992). The replication times given in the following sections are based on AcMNPV and these replication times are generally shorter compared to other baculoviruses (Slack and Arif, 2007).

1.3 The Baculovirus Life Cycle

1.3.1 Initial Virus Entry through the Midgut

The OBs allow the baculovirus to remain dormant, but viable in the environment for decades, unlike a lipid bilayer enveloped virus that is susceptible to desiccation and loss of viability due to damaging factors such as UV (Bergold, 1963). The ability to remain dormant in the environment for long lengths of time is beneficial when infecting invertebrates as they can undergo population changes due to seasonal and environmental factors, in which extensive periods of time can pass before a permissive host is reintroduced into the environment allowing further viral transmission (Kukan, 1999). Initial infection occurs through the oral route when a larva inadvertently consumes OBs either through cannibalization or contaminated plant matter. The OBs travel through the foregut that is lined by part of the larva exoskeleton cuticle containing chitin and involved in uptake, storage, and physical processing of food, and through a valve into the midgut (Slack and Arif, 2007). The midgut does not contain a cuticle and the alkaline environment (pH 10-11) of the larval midgut causes the protein matrix forming the OB to dissolve (Terra and Ferreira, 1994). The PE is most likely degraded by proteinases associated with the OB or present in the midgut. This leads to the release of the ODVs into the midgut lumen (Terra and Ferreira, 1994), around 12 minutes after entry into the midgut (Adam and McClintock, 1991).

After release, ODVs come against their first obstacle, the peritrophic membrane (PM) that needs to be breached before infection of the midgut epithelium can be achieved. The PM is comprised of chitin, mucopolysaccharides and protein arranged in net or lattice formation, which occurs in two forms. In type I, the PM is produced by ring of secretory cells located at the entry of the midgut and is delaminated from the entire midgut epithelium. In some cases type I PM only form in response to feeding (Lehane, 1997). In type II, the PM is always present and produced along the whole length of the midgut. Therefore, forming a hollow tube protecting the midgut epithelium from direct contact from the content of the midgut lumen (Slack and Arif, 2007; Hegedus *et al.*, 2009). The PM is regenerated from the epithelial cells to protect them from abrasive food material that could cause damage, to restrict the passage of large particles such as bacteria, fungi and viruses and provides the larva with some defence (Barbehenn and Martin, 1995). The ODVs cannot rely on chance encounters with lesions in the PM caused by the passage of food alone; therefore PM-compromising proteases and chitinase are either co-occluded with ODVs in the OB matrix or located on the ODV surface (Wang and Granados, 1997).

Some baculoviruses encode these proteases and most are metalloproteinases as they contain divalent cations as an integral component of their structure (Lepore *et al.*, 1996; Wang and Granados, 1997; Peng *et al.*, 1999). Enhancins are one group of metalloproteinases found concentrated in the OB and are believed to digest the mucin component of the PM, thus allowing the ODV access to the midgut epithelial cells (Wang and Granados, 1997). However, many baculoviruses do not encode these proteases and are not inhibited by the PM. Alternative mechanisms could be involved using bacterial proteinases that are normally found contaminating the OB. These bacterial proteinases can function in the alkaline condition of the midgut and therefore degrade the PM, allowing the ODV access to the midgut epithelium (Rubinstein and Polson, 1983).

1.3.2 Infection of the Midgut Epithelium

The larvae midgut epithelium is primarily composed of two cell types, goblet cells that are involved in potassium ion transport into the midgut, and the columnar cells, which are involved in secreting digestive enzymes and absorbing nutrients through their brush border (Adam and McClintock, 1991). The ODV lipid envelope fuses directly to the columnar cell membrane, specifically at the apical ends of the microvilli (Haas-Stapleton *et al.*, 2004). The fusion process of the ODV membrane to the columnar cell membrane and the subsequent entry of the nucleocapsid into the cell are carried out by a group of gene products known as *per os* infectivity factors (Kikhno *et al.*, 2002). This family includes *p74* (*pif0/Ac138*; (Faulkner *et al.*, 1997)), *Ac22* (*pif2*; (Pijlman *et al.*, 2003)), *Ac96* (*pif4*; (Fang *et al.*, 2009)), *Ac115* (*pif3*; (Ohkawa *et al.*, 2005)), *Ac119* (*pif1*; (Kikhno *et al.*, 2002)), and *Ac148* (*pif5*; (Sparks *et al.*, 2011a)). All members are found conserved among all sequenced baculoviruses and deletion of any of these genes from the baculovirus genome has no effect on viral replication in cell culture. However, these deletions do cause a loss of oral infectivity.

All of this provides evidence that the baculovirus family uses a common pathway for oral infection and this could involve a proteinase-sensitive cellular receptor that has been demonstrated to bind ODV (Horton and Burand, 1993). The ODV also contains two other structural proteins, *Ac145* (Lapointe *et al.*, 2004) and *Ac150* (Zhang *et al.*, 2005) that have similar properties to PIF. They both contain chitin binding domains, however, the mechanisms of their interaction during oral infection is unknown. It has been suggested that they aid in binding of the ODV to the apical tips of the columnar cell microvilli, where the enzyme involved in chitin synthesis for the PM is located (Lapointe *et al.*, 2004; Zhang *et al.*, 2005; Wang and Zhang, 2006).

1.3.3 Virus entry into the nuclei

Once the nucleocapsids are released into the cytosol, they migrate to the nuclear membrane by actin polymerisation (Charlton and Volkman, 1991; van Loo *et al.*, 2001; Ohkawa *et al.*, 2010). Strong evidence suggests that the nucleocapsid dock with the nuclear pore before being transported into the nucleus (Summers, 1971; Granados, 1978). The baculovirus nucleocapsids have a diameter of 40-70 nm and thus are small enough to pass through the nuclear pore complex, which has been characterised to have a channel size of 38-78 nm (Alber *et al.*, 2007). In early infection, empty nucleocapsid have been observed in the nuclei of infected cells (Granados and Lawler, 1981) and more recently, the major capsid protein VP39 has been fluorescently tagged using GFP. This allowed nucleocapsids to be localised both to the nuclear pore and within nuclei using confocal microscopy (Ohkawa *et al.*, 2010). Once in the nucleus, the viral genome is released and this whole process takes roughly 30 minutes (Chisholm and Henner, 1988). This leads to a cascade of gene expression where viral genes are expressed, structural genes are synthesized, DNA replication begins and new progeny viruses are assembled and released (Slack and Arif, 2007). Figure 1.4 A provides an illustration of the primary infection process.

1.3.4 Viral exit from the nuclei

The nucleocapsids are released from the nucleus of the midgut epithelial cells by budding out of the nuclear membrane (Granados and Lawler, 1981). During this budding process the nucleocapsid obtains an envelope, which contains at least one viral protein, GP16 (Gross *et al.*, 1993). The nucleocapsids are directed through the cytoplasm towards parts of the plasma membrane modified with the viral envelope glycoprotein. During this transition process the nucleocapsids lose their nuclear-derived envelope. The nucleocapsids then bud out of the plasma membrane forming new progeny viruses (BV) to allow secondary infection. The viral envelope proteins for Type I alphabaculovirus are GP64 and the F protein (Blissard and Rohrmann, 1989; Pearson *et al.*, 2001). However, for Type II alphabaculovirus this is a homologue of the F protein as they lack a functional GP64 (Pearson *et al.*, 2000). It has been demonstrated that AcMNPV-infected columnar cells in *T. ni* larvae distribute their GP64 towards the basal and lateral regions of the cell. This directs the budding of new progeny virus away from the midgut lumen and towards susceptible tissues (Engelhard *et al.*, 1994). However, in infected cells where specific targeting is not critical for the spread of infection GP64 has a polar distribution (Keddie *et al.*, 1989).

1.3.5 Midgut Epithelium bypass mechanism

It has been suggested that there could be a mechanism for avoiding replication in midgut columnar cells that can be sloughed off into the lumen. This process involves nucleocapsids bypassing replication in the columnar cell and instead being transported directly to the basal region and budding into tracheal cells or haemolymph (Granados and Lawler, 1981; Washburn *et al.*, 1999). As previously mentioned GP64, is required to direct nucleocapsids to the plasma membrane and its gene does contains both an early and late promoter. Therefore, during early infection GP64 could be present to allow this process to occur. Evidence for this mechanism was shown by a delay in oral infection when the early promoter of *gp64* was eliminated from AcMNPV but no effect on infection time was observed when the same virus was injected into the larval hemocoel (Washburn *et al.*, 2003a; Zhang *et al.*, 2004).

However, the current model for bypassing replication in columnar cells would only apply to MNPV because it requires several nucleocapsids infecting a single cell. These nucleocapsids would split into two groups; those that enter the nucleus to begin replication and express the *gp64* to produce GP64 to allow the other nucleocapsids that remained in the cytoplasm to bypass the nucleus. Therefore, it is highly unlikely that SNPV would infect a single columnar cell with enough nucleocapsids to achieve this affect (Washburn *et al.*, 2003a; Washburn *et al.*, 2003b; Rohrmann, 2011). Figure 1.4 A provides an illustration of this bypass mechanism.

1.3.6 Infection of the inner tissues

The envelope fusion proteins GP64 or active form of F protein, described above, are not only required for exiting cells but are also involved in initiating secondary infection in other cells. GP64 has been shown to initiate the uptake of the BV via clathrin-mediated endocytosis in insect cells (Long *et al.*, 2006). Once this process is stimulated clathrin becomes concentrated on the inside of the plasma membrane at the point of entry allowing the uptake of the BV within a vesicle. Clathrin-mediated endocytosis is normally involved in the selective uptake of proteins. The uptake is stimulated by binding to a receptor on the surface of the cell with internalisation signals, which cause the pit to invaginate into the cytoplasm of the cell that results in an endocytic vesicle containing the protein (Long *et al.*, 2006). This mechanism is commonly used by many viruses (Rohrmann, 2011). However, the receptor that GP64 interacts with has not been defined nor has a common molecule, such as a phospholipid, due to the ability of the baculovirus BV to enter a number of different cell types (Tani *et al.*, 2001).

Figure 1.4 The baculovirus replication cycle

Schematic representation of the Baculovirus replication cycle (Friesen and Miller, 2001).

A: Infection of a midgut epithelial cell by ODV (primary phase of infection). The polyhedrin matrix dissolves in the midgut lumen (step 1), releasing ODVs. These cross the peritrophic membrane (step 2) and enter columnar cells through direct membrane fusion to the microvillus (step 3). Released nucleocapsids migrate to the nucleus (step 4) and enter through nuclear pores (step 5). The viral genome is released (step 6) and this results in a cascade of gene expression where viral genes are expressed, structural genes are synthesized, DNA replication begins and new progeny viruses are assembled and released (step 7-11). Alternatively nucleocapsids bypass replication stage and instead transported to the basal region then released (step 12) .

B: Infection of a cultured or secondary site of infection by BV. The BV enter the cell through receptor mediated endocytosis (Step 1-2). As the endosome acidifies, virus and endosomal envelopes fuse (step 3), releasing nucleocapsids into the cytoplasm. Released nucleocapsids migrate to the nucleus (step 4) and enter through a nuclear pore (step 5). The viral genome is released (step 6) and the virus replication cycle is initiated as described above (step 7-11). During the very late phase, nucleocapsids are retained in the nucleus, acquire envelopes (step 12), and are embedded within a crystalline matrix of polyhedrin (step 13) to form OBs. Mature OBs are released by cell lysis.

The internalised vesicle is then transported using the cytoskeleton network of the cell to the endosome, where they merge together releasing the content of the vesicle into the endosome. The environment of the endosome is slightly acidic (pH 5.9-6.0) that causes a conformational change in the GP64 allowing the viral envelope to merge with the endosome membrane. This results in the release of the naked nucleocapsid into the cytoplasm of the cell, where it is transported to the nucleus and the viral replication begins (Rohrmann, 2011). Interestingly, it has been demonstrated that this conformational change of GP64 at low pH has the ability to fuse directly with the insect cell plasma membrane independent of endocytosis. However, it is highly unlikely that the virus would encounter these low pH conditions outside of the cells within the larva (Dong *et al.*, 2010).

1.3.7 Cell Defence: Apoptosis

Programmed cell death or apoptosis is a self-destructive response evolved in multicellular organisms to allow the safe elimination of cells that have either become damaged or malfunctioning, or to facilitate the development of the organism (Ashida *et al.*, 2011; Fuchs and Steller, 2011). Two classic examples of apoptosis used during development are in human embryogenesis to remove webbing between fingers and toes (Fuchs and Steller, 2011) or metamorphosis of larva into adult insect (Rohrmann, 2011). In the case of baculovirus infected larva, apoptosis is one of the primary strategies used by a cell to avoid virus infection spreading throughout the organism (Engelhard and Volkman, 1995). Apoptosis involves a series of specific events including loss of attachment to adjacent cells, cell shrinkage, nuclear fragmentation, chromatin condensation, DNA fragmentation and subsequent disintegration of the cell into apoptotic bodies, which are then eliminated by phagocytosis (Clem *et al.*, 1991; Hershberger *et al.*, 1992; Clem and Miller, 1994; Manji and Friesen, 2001; Schultz and Friesen, 2009). All these events of apoptosis are caused by the activation of a family of cysteine proteases known as caspases, which are separated into two groups; initiator and effector caspases (Thornberry *et al.*, 1992). When a cell is stimulated to undergo apoptosis, initiator caspases are activated, which in turn activate the effector caspases by proteolytic processing. These effector caspases cleave cellular proteins resulting in the observed effects of apoptosis.

To prevent cellular apoptosis, baculoviruses produce two groups of proteins, P35 and inhibitors of apoptosis (IAP). *p35* is found in a limited number of Type I alphabaculoviruses, which are all closely related to AcMNPV. However, most baculoviruses encode multiple copies of *iap* genes (Clem *et al.*, 1991; Thiem and

Chejanovsky, 2004). Both P35 and IAP proteins affect caspases. In insect Sf21 cells, P35 has been shown to directly block the activity of mature SF-caspase-1, whereas some IAP proteins block SF-caspase-1 at the processing and activation level (Prikhod'ko *et al.*, 1999). P35 has also been shown to block other caspases during baculovirus infection (Clem, 2007), whereas IAPs function more widely blocking caspases, degradation of caspases via targeting for ubiquitination and have been shown to interfere with other pro-apoptotic proteins (Vaux and Silke, 2005; Eckelman *et al.*, 2006). It has been demonstrated that the deletion of *p35* can reduce BV yield by 15,000-fold during infection of insect cells in culture and also reduces the mortality rate of infected larva (Hershberger *et al.*, 1992; Clem and Miller, 1994).

Because to the midgut cells are prone to apoptosis, it might be beneficial for baculoviruses to encode anti-apoptotic proteins that were located to ODV. Neither P35 nor IAP proteins are located to the ODV, but this isn't surprising due to their location in the cytoplasm of the infected cell and the assembly of nucleocapsids in the nucleus (Slack and Arif, 2007). P33 is a nucleocapsid associated protein that could be involved in preventing apoptosis as it binds to p53, which itself is a human protein that is involved in apoptosis and cell cycle regulation (Prikhod'ko *et al.*, 1999; Collot-Teixeira *et al.*, 2004). The existence of an insect homologue to p53 further supports this theory, but research on P33 so far has shown no signs of preventing p53-induced apoptosis and has in fact shown the opposite effect causing p53-mediated apoptosis to increase two-fold when co-expressed (Prikhod'ko *et al.*, 1999). However, this co-expression experiment was done using plasmids that expressed only p53 or P33. Therefore P33 could require other viral proteins to inhibit p53 mediated apoptosis.

1.3.8 Spread of infection throughout the host tissues

The midgut cells undergo constant turn over, where old cells are sloughed off into the lumen and replaced by new ones from regenerative cells at the base of the epithelium. This combined with the fact that they are prone to apoptosis and cell cycle arrest, means that the midgut is a poor tissue for virus infection (Engelhard and Volkman, 1995; Uwo *et al.*, 2002). The tissues beyond the midgut contain actively dividing cells, but ODV are highly specific for the midgut epithelial cells in an alkaline environment (Slack and Arif, 2007). This suggests that it was advantageous for the baculovirus to evolve the BV phenotype, which can operate in the slightly acidic environment (pH 6.4 to 6.8) of the host internal tissues such as the tracheoblasts, haemocytes and fat body (Haas-Stapleton *et al.*, 2004). The formation of two distinct phenotypes at different

times during the infection cycle is known as a bi-phasic replication cycle, shown in Figure 1.4.

It is not surprising therefore that the midgut epithelium is not the major tissue for viral replication, but is instead an initial staging ground where BV can be produced to infect other susceptible cells and tissues in the larvae. Allowing the midgut epithelium to recover is beneficial to the baculovirus as this allows the larvae to continue to feed and grow, in turn maximizing production of progeny virus (Slack and Arif, 2007). Interestingly, *Culex nigripalpus* nucleopolyhedrovirus (CuniNPV) (Moser *et al.*, 2001) and certain types of GVs (Federici and Stern, 1990) appear to only replicate in the midgut epithelium but the development of infection in these viruses is not fully understood.

The tracheal system is an insect's respiratory system, which branches out and penetrates nearly every tissue including the midgut epithelium (Washburn *et al.*, 1995). Therefore, progeny BVs derived from midgut epithelium that infect a tracheolar cell, will use the tracheal system as a major conduit to allow access to deeper tissues, including the haemocoel. The haemocoel is another important target for the baculovirus, as it allows the infection of haemocytes. Haemocytes circulate throughout the open circulatory system and are involved in immune response, therefore this increases the spread of infection in the larvae by allowing greater access to tissues and reducing the host defences (Slack and Arif, 2007). The last tissue of importance is the fat body that acts as an insect "liver", and therefore its energy rich cells are ideal for the production of viral progeny (Figure 1.4)

1.3.9 The Virogenic Stroma

The baculovirus infection cycle can be broken into distinct stages. The length of these stages is virus species specific (Slack and Arif, 2007). The baculovirus replication cycle begins soon after the delivery of the genome into the host cell nucleus from the nucleocapsid. The host cell begins to be manipulated into a "viral factory" by virion-associated proteins along with viral immediate early proteins, whose genes are expressed within 30 minutes post-infection (Chisholm and Henner, 1988). The virogenic stroma is one of these manipulations, and is the site for viral RNA transcription, DNA replication and nucleocapsid assembly.

The virogenic stroma begins as an electron dense, irregular-shaped, granular region in the centre of the nucleus and can be observed in the first 6 hours of AcMNPV infection.

The composition of the virogenic stroma is mainly RNA and DNA, along with proteins that form support for RNA and DNA complexes (Young *et al.*, 1993). Heterochromatin is highly condensed, histone-associated host genomic DNA that is relocated to the edges of the nucleus during this time, which gradually disappears as the virogenic stroma expands (Williams and Faulkner, 1997). This re-arrangement of the nucleus is carried out by viral interaction with tubulin (Volkman and Zaal, 1990).

The virogenic stroma expands until 12 hours post-infection (hpi) at which point it fills most of the nucleus and, during this expansion, cavities form inside it. The edges of these cavities are the sites of nucleocapsid assembly. The nucleocapsids assembled between 12 and 20 hpi are destined to become the BV virion phenotype (Slack and Arif, 2007). These nucleocapsids leave the virogenic stroma and cross the nuclear ring zone, another major partition of the nucleus that surrounds the virogenic stroma, and the nucleocapsids reach the nuclear membrane. Once at the nuclear membrane, the nucleocapsids are transported through and across the cytosol to the cell membrane, where they bud out acquiring an envelope from the host membrane that contains virus encoded proteins. Presently, the process of translocation of the nucleocapsids across the cell is not well defined and although early studies indicated a role for cellular actin (Braunagel *et al.*, 2001; Lu *et al.*, 2004), a more recent study suggest a role also for microtubules (Danquah *et al.*, 2012).

The virogenic stroma composition has been resolved, but the structure is still not well understood due to it being essential for viral replication. Two viral proteins have been shown to be associated with the virogenic stroma; single-stranded DNA binding protein (dbp) (Ac25) and PP31 (Ac36) (Guarino *et al.*, 1992; Mikhailov *et al.*, 2008). The deletion of *dbp* from the virus genome caused the loss of the virogenic stroma that resulted in the production of abnormal nucleocapsids (Vanarsdall *et al.*, 2007), whereas the deletion of *pp31* resulted in an overall decrease in transcription of late genes (Gomi *et al.*, 1997; Yamagishi *et al.*, 2007).

1.3.10 The Nucleocapsid

The ODV and BV nucleocapsids are structurally similar; they both contain complete viral genomes and have several major proteins in common (Figure 1.5). The nucleocapsid length is determined by the size of viral genome packaged. This gives the baculovirus nucleocapsids a length ranging from 250-400 nm and a diameter of 40-70 nm (Boucias and Pendland, 1998). The nucleocapsids are polar with a base on one end and an apical cap on the other end. During nucleocapsid assembly the apical cap

is oriented towards the virogenic stroma, which is also oriented to the peplomer end of BV (Fraiser, 1986) and found associated with the nascent envelopes of the ODV (Adam and McClintock, 1991). VP39 is the most abundant structural protein of the nucleocapsid and is arranged into stacked rings around the nucleoprotein core. VP39 is the major capsid protein but there are a number of other minor but important capsid-associated proteins (Slack and Arif, 2007). An illustration of the nucleocapsid is shown in Figure 1.5, indicating that the nucleocapsid is a complex structure of multiple protein types rather than a simple protein sheath of VP39.

Contained within the nucleocapsid are super-coiled virus DNA and virus proteins known as the nucleoprotein core. The most abundant protein of the nucleoprotein core is basic protein (P6.9), which interacts with the negatively-charged DNA backbone through positively-charged arginine residues. This interaction allows the viral genome to condense into the nucleocapsid and is controlled through Zn^{2+} levels within the nucleoprotein core (Wilson and Consigli, 1985; Funk and Consigli, 1993).

1.3.11 The Occlusion Derived Virus and Occlusion bodies

At ~20 hpi, the virogenic stroma changes to ODV production, which causes it to recede and become more condensed. The nucleocapsids produced during this time are transported into the nuclear ring zone, which expands to accommodate the accumulating nucleocapsids (Slack and Arif, 2007). During this retention in the nuclear ring zone, the nucleocapsids become enveloped in a lipid bilayer that resembles the inner nuclear membrane (INM) in composition (Braunagel and Summers, 1994). The ODV envelope contains more saturated fatty acid phospholipids than the BV envelope, which causes the ODV envelope to be more rigid. Another difference between the two virion envelopes is that the ODV envelope contains phosphatidylcholine instead of phosphatidylserine found in the BV envelope (Slack and Arif, 2007). An illustration of ODV compared to BV is shown in Figure 1.6.

Figure 1.5 Proteins of the nucleocapsid

Schematic representation of nucleocapsid described in section 1.3.10. Some of the AcMNPV nucleocapsid proteins are illustrated and proteins marked with * have not had their location confirmed to the nucleocapsid (Slack and Arif, 2007).

Figure 1.6 The budded and occlusion-derived virus

Schematic representation of the BV and ODV, showing the location of virally encoded proteins in BV and ODV, and the composition of their lipid membrane (Federici, 1997).

The mechanism involving this major transition from BV to ODV production during the baculovirus infection is still unresolved; however, several theories have been suggested. It could simply be a result of the deletion of a viral component essential for the transit of nucleocapsid through the cytoplasm or the reorganisation of the virogenic stroma that prevents the nucleocapsids from leaving the nucleus (Rohrmann, 2011). During the later stages of viral infection, the ODV envelope proteins accumulate causing the nucleocapsids to become enveloped within the nucleus. This envelope could prevent the nucleocapsids from leaving the nucleus, suggesting that only the earlier naked nucleocapsids have the ability to leave the nucleus and transit through the plasma membrane (Rohrmann, 2011).

The origin of the ODV envelope is still under debate. It maybe synthesized *de novo* or be acquired from the inner nuclear membrane (INM). There is considerably more evidence available for the latter. Late in infection, the INM modified with ODV envelope proteins invaginates as microvesicles into the nuclear ring zone. If this mechanism is used then the virus must induce “de novo” INM synthesis during infection to produce enough material to envelope all nucleocapsids destined to be ODV (Braunagel *et al.*, 1996).

The ODV envelope contains a wide range of viral proteins and is more diverse than the BV envelope proteins. These proteins are transported to the ODV envelope by unique

mechanisms and are mostly non-glycosylated. Prior to envelopment, the ODV nucleocapsid is packaged in a proteinaceous virus derived tegument, which becomes more condensed around the nucleocapsids after occlusion. Occlusion begins shortly after ODVs begin to appear in the nuclear ring zone and the fully formed OBs are present by 24 hpi (Slack and Arif, 2007). The OB is composed of polyhedrin that is hyperexpressed during the late stages of infection and accumulates within the nucleus of an infected cell, before crystallising into a lattice that surrounds ODV (Jarvis *et al.*, 1991; Carstens *et al.*, 1992). The mechanisms that causes this occlusion process are unclear and could be dependent on the concentration of polyhedrin or the ODV themselves could cause the formation of OBs. However, in BmNPV at least one protein has been shown to be essential for the occlusion process, Bm56. The deletion of *Bm56* caused ODV not to be incorporated into the OB (Xu *et al.*, 2008). Another protein known as P10 is also hyperexpressed during late stages of infection, this protein forms tubule-like structures with the cell cytoskeleton that penetrate both the nucleus and the cytoplasm (Patmanidi *et al.*, 2003; Carpentier *et al.*, 2008; Carpentier and King, 2009). P10 has been demonstrated to be involved in assembly of the PE on mature OB during the late stages of infection (Lee *et al.*, 1996).

The OBs are released from the nuclei of an infected cell by a lytic process from 48 hpi (Figure 1.7). The viral protein cathepsin plays a role in releasing the OBs from infected cells as well liquefaction of the host. This was demonstrated by an AcMNPV cathepsin-deletion mutant, in which OBs were not released from infected cells in cell culture (Slack *et al.*, 1995). P10 is another protein which has been shown to be involved in cell lysis and interacts with host cell microtubules (Patmanidi *et al.*, 2003).

Figure 1.7 Scanning electron microscopy of OBs

Scanning EM images that represent the packaging (A, 48hpi) and release of OBs (B, 72hpi) from AcMNPV-infected cell (King and Possee, 1992)

The larval exoskeleton is comprised of chitin that makes it rigid and strong and this obstacle has to be overcome to allow the OBs from the lysed cells to be released into the environment. Therefore it is not surprising that some baculoviruses encode enzymes (viral chitinase and cathepsin) that breakdown the larval exoskeleton facilitating the liquefaction of the host allowing the OBs to be widely dispersed (Slack *et al.*, 1995; Hawtin *et al.*, 1997). It has been suggested that viral chitinase is retained in the endoplasmic reticulum in infected cells to prevent its early release, therefore allowing virus replication to continue before the host is liquefied (Hawtin *et al.*, 1995). Deletion of either viral chitinase or cathepsin causes infected larva to remain intact for several days after death (Hawtin *et al.*, 1997).

Predators will also ingest the baculovirus-infected larvae due to them being weakened from the infection and disperse OBs in their faeces. The OBs can survive passage through the predators digestive system (Abbas and Boucias, 1984). Baculoviruses have also been shown to change the wandering behaviour of the host larvae to increase the chance of horizontal transmission by moving up the host plant to increase OB coverage or moving into less UV exposed areas to increase chances of OB survival (Raymond *et al.*, 2005). The RNA processing enzyme encoded by *Ac1* is believed to be involved in this change in behaviour because larva infected with BmNPV containing a deletion of this gene did not present any signs in terminal movement during late infection, which was seen in those larva infected with complete BmNPV. However, it is unclear how this RNA processing enzyme could account for this behaviour change (Kamita *et al.*, 2005). More recently, Hoover *et al.* (2011) demonstrated using deletion mutant viruses that the expression of the viral gene ecdysteroid uridine 5'-diphosphate (UDP)-glucosyltransferase (*egt*) was required for inducing climbing behaviour of *Lymantria dispar* nucleopolyhedrovirus (LdMNPV) infected gypsy moth.

1.3.12 The Budded Virus

The BV is a single nucleocapsid encased in a loosely fitted envelope. This could be due to cytoplasmic proteins being present in the space between the nucleocapsid and the envelope (Figure 1.6). The BV envelope proteins are transported to the cell membrane from the endoplasmic reticulum after being sorted and N-glycosylated (Whitford *et al.*, 1989). The BV envelope is bulbous at one end and the surface is serrated when viewed by transmission EM (Figure 1.8). These serrations are known as peplomers and are believed to contain GP64 and Fusion protein (Volkman *et al.*, 1984). The GP64 major viral glycoprotein and the F protein are involved in mediating budding,

attachment and entry of BVs in to cells. This leads to the two proteins often being referred to as ENV proteins (Hefferon *et al.*, 1999). The F protein requires proteolytic cleavage to become active unlike GP64, which does not require any further modification after incorporation into the envelope (Westenberg *et al.*, 2002). In Type I NPVs, both ENV proteins are present but the F protein seems to have lost its ENV functions, whereas Type II NPV just contain a functional F protein (Herniou *et al.*, 2001).

Figure 1.8 Electron microscopy of a baculovirus BV

An EM image that represents the AcMNPV BV showing the characteristic rod-shape of the virion with a bulbous serrated surface at one end. Taken from “The Big Picturebook of Viruses” at www.virology.net. Attributed to Eric B. Carstens (Queen’s University, Kingston, Ontario, Canada, 1996)

1.4 Baculovirus Expression Vector Systems

1.4.1 Introduction to Baculovirus Expression Vector Systems

The baculovirus expression vector system (BEVS) was first developed in the mid 1980's and is now widely used for the production of recombinant proteins in insect cells (Smith *et al.*, 1983a; Pennock *et al.*, 1984; Summers, 2006; van Oers, 2011). Recombinant BV containing a foreign gene, usually under the control of the *polh* promoter, is used to infect cells and during the later stages of viral infection large quantities of recombinant protein are normally produced. The host insect cells have the ability to process signal peptides, assemble oligomeric proteins and enable proper post-translational modifications such as glycosylation, phosphorylation and disulfide bond formation to allow authentically processed proteins to be produced.

The earliest BEVS were based on polyhedra-negative viruses, which had their polyhedrin coding region replaced with a foreign gene to produce a recombinant baculovirus. The foreign gene expression was driven by the strong polyhedrin promoter. Since the development of the BEVS, it has been widely used and is often the first choice for the production of certain classes of proteins e.g. kinases (Hitchman *et al.*, 2011; van Oers, 2011; Hitchman *et al.*, 2012).

The baculovirus genome is too large to insert the foreign gene directly; instead transfer vectors are used containing sequences that flank the polyhedrin gene. Using insect cell homologous recombination proteins, the foreign gene is inserted into the virus genome resulting in recombinant virus. The viral replication cycle produces BV containing the recombinant virus genome, which can be harvested from the culture medium (Smith *et al.*, 1983a; Pennock *et al.*, 1984).

Using the baculovirus expression system as described above, both a mixture of recombinant and original parental viruses are produced after the initial round of replication (Figure 1.9). Before the recombinant virus can be used as the expression vector, it has to be separated from the parental virus. This separation is traditionally achieved by plaque-purification, however this process is labour-intensive, technically demanding and time-consuming (Kitts *et al.*, 1990).

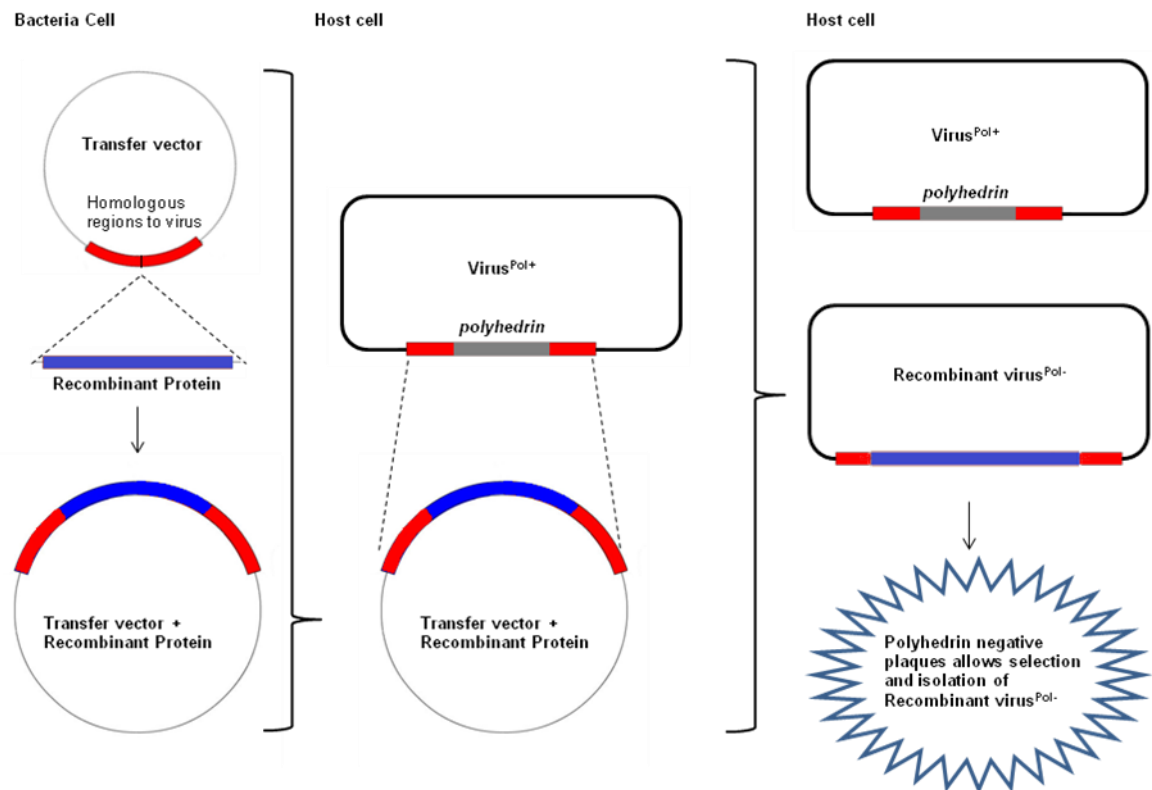


Figure 1.9 Illustration of the method used to construct recombinant viruses

The transfer vector containing homologous regions to polyhedrin gene is modified by the direct insertion of recombinant protein into the transfer vector. Viral DNA and modified transfer vector are introduced into the host cells to allow homologous recombination to occur and finally the recombinant virus is selected for using the OBs as a negative marker.

1.4.2 Improvements to the Baculovirus Expression Vector Systems

1.4.2a The BacPAK6 system

The BacPAK6 system replaces polyhedrin with *lacZ*, which contains a *Bsu361* restriction site, as well as two extra *Bsu361* sites in the two genes flanking *lacZ* (Kitts and Possee, 1993). Digestion with *Bsu361* removes the *lacZ* gene and a fragment of an essential gene (*orf1629*) producing linear virus DNA that is unable to replicate within insect cells (Figure 1.10). Co-transfection with a transfer vector restores infectivity of the now circular virus DNA by replacing *orf1629*, as well as inserting the foreign gene into the virus genome. This resulted in ~90% recovery of recombinant virus plaques. However, *Bsu361* digestion is never 100% efficient and the final virus population will always contain a mixture of recombinant and parental virus that requires purification by plaque-assay (Kitts and Possee, 1993).

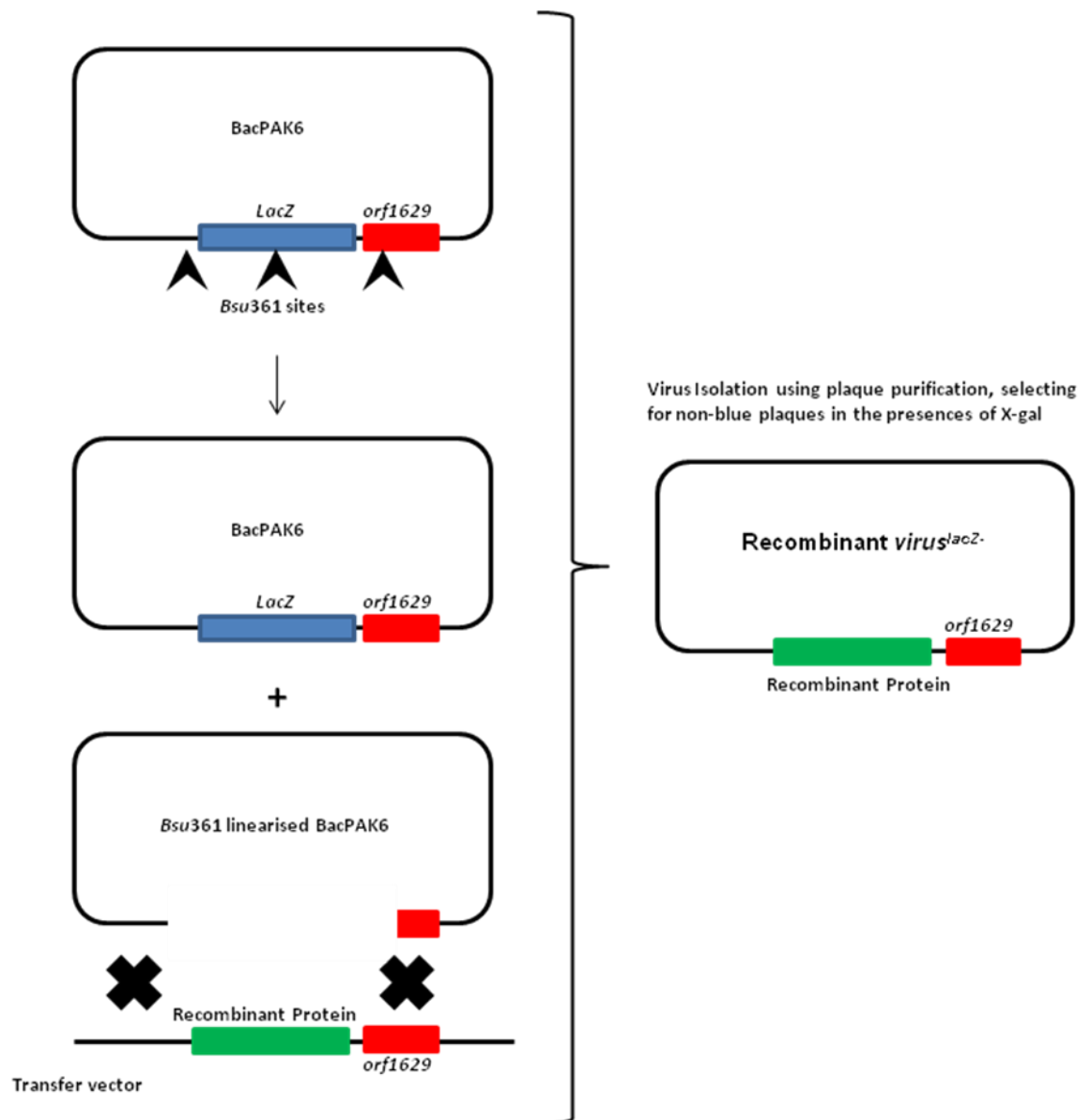


Figure 1.10 BacPAK6 method used to construct recombinant viruses

Sf9 Cells co-transfected with transfer vector and *Bsu361* linearised BacPAK6 DNA, to form recombinant virus^{*lacZ*-}. Recombinant virus^{*lacZ*-} was isolated from parental background using plaque purification, selecting for *lacZ* negative plaques.

1.4.2b The Bac-to-Bac™ system

A significant step forward was taken in 1997 with the development of the Bac-to-Bac™ system, which allows the production of recombinant baculoviruses without the need for plaque purification and is marketed by Invitrogen (Figure 1.11). The baculovirus genome is maintained in bacteria by a mini-F replicon. A selectable marker gene (*lacZ*) and Tn7 transposition sites are also inserted into the baculovirus genome. The transfer

vector encodes Tn7 transposase functions and a foreign gene. Transposition is carried out in *E. coli*, which results in the foreign gene being inserted at the polyhedrin locus between left and right arms of Tn7, resulting in the disruption of *lacZ*. The recombinant clones are then selected on agar plates containing appropriate antibiotics and X-gal. Non-blue colonies are selected and amplified. The recombinant virus DNA is recovered via a simplified alkaline lysis method, and is transfected into insect cells to produce BV (Kost *et al.*, 2005; Possee *et al.*, 2008).

Figure 1.11 Bac-to-Bac™ method used to construct recombinant viruses

Illustration of the generation of recombinant virus using the Bac-to-Bac™ system (From the Invitrogen Bac-to-Bac™ system manual), insertion of target gene into the bacmid disrupts *lacZ* allowing selection of non-blue colonies in the presence of X-gal. The recombinant bacmid DNA is then isolated and used to transfect insect cells to produce recombinant viruses.

1.4.2c The *flashBAC*™ system

The *flashBAC*™ system was developed by Oxford Brookes University and NERC CEH oxford (Possee *et al.*, 2008) and is sold by Oxford Expression Technologies. At the heart of *flashBAC*™ technology is an AcMNPV genome that lacks part of an essential

gene (*orf1629*) and contains a bacterial artificial chromosome (BAC) at the polyhedrin gene locus, replacing the polyhedrin coding region. The BAC allows the viral DNA to be maintained and propagated, as a circular genome, within bacterial cells (Ho Je *et al.*, 2001; Possee *et al.*, 2008).

flashBAC[™] uses the same principles as BacPAK6 but is maintained in bacterial cells and doesn't require linearization prior to use. The *flashBAC*[™] DNA is co-transfected into insect cells with a transfer vector that restores the function of ORF 1629 and inserts the foreign gene allowing the virus DNA to replicate and produce virus particles. The foreign gene replaces the BAC sequence (Figure 1.12). The key difference between *flashBAC*[™] and BacPAK6, is that no plaque assay selection is required as non-recombinant virus are unable to replicate (Ho Je *et al.*, 2001; Possee *et al.*, 2008). *flashBACGOLD*[™] (FBG) is an enhanced version of *flashBAC*[™], in which both chitinase and cathepsin have been deleted to improve protein yield and quality due to them being deleterious to recombinant protein production, intracellular transport and stability (Hitchman *et al.*, 2010b). Recently *flashBACULTRA*[™] (FBU) was developed, which contains further deletions of *p10*, *p74* and *p26* and this resulted in a further increase in protein yield (Hitchman *et al.*, 2010a). The development of FBU strongly suggests that further deletions of non-essential genes from the baculovirus genome could increase recombinant protein yield by freeing up cellular resources.

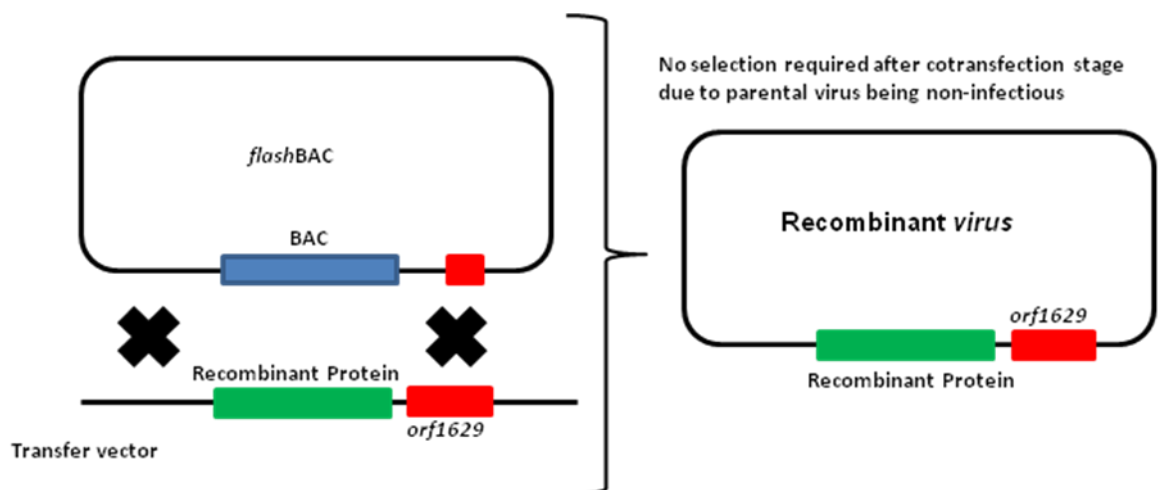


Figure 1.12 *flashBAC*[™] method used to construct recombinant viruses

Sf9 Cells co-transfected with transfer vector and *flashBAC*[™] DNA, to form a recombinant virus. The *flashBAC*[™] virus is non-infectious due to missing part of the essential gene *orf1629*. Therefore, the recombinant virus does not require isolation from parental virus after the co-transfection stage.

1.5 Aims of Thesis

The overall aim of this thesis is to elucidate the mechanisms involved in the production of occlusion-derived virus (ODV) by using the Red/ET recombination system to remove auxiliary genes involved in ODV production, which are non-essential for replication in insect cell culture. A secondary aim of the thesis is to determine whether deletion of ODV-specific genes, and preventing ODV production, will improve the BEVs by producing greater levels of high quality recombinant proteins. Chapter 3 describes the literature review undertaken to identify structural components of the ODV, which are not found in the BV and can be deleted from the AcMNPV genome without affecting infectivity. Chapter 4 describes the use of the Red/ET recombination system in deleting the target genes from the AcMNPV genome and characterises those deletions that prevented replication of the virus in insect cell culture. Chapter 5 characterises those deletion mutant viruses that remained viable in insect cell culture, specifically considering their effects on ODV production and occlusion into the OBs using bioassays and electron microscopy. The thesis also investigates the deletion of *orf118/pif1*, *pif2* and *pif3* on recombinant protein production (Chapter 6 and Chapter 7). In addition, Chapter 7 investigates the RGD motifs of PIF1 and the possible role they could have on the function of PIF1 during oral infection of larva with OBs.



Chapter 2

Materials & Methods

2.1 Materials

2.1.1 Chemicals

General chemicals were purchased from the following companies unless stated otherwise: BDH Chemicals Ltd, Fisher Scientific and Sigma-Aldrich. Molecular biology reagents were purchased from Invitrogen, New England Biolabs, Fermentas or Promega. Cell culture media was supplied by GIBCO (Invitrogen) or PPA.

All solutions made were sterilised by either autoclaving (15 pounds per square inch (p.s.i.) for 15 minutes or 10 p.s.i. for 20 minutes) or by filtration through 0.45 or 0.2 µm filters.

2.1.2 Plasmids

The plasmids used within thesis are shown in Table 2.1

Table 2.1 Plasmids used in this thesis

Plasmids	Reference	Source
pAcEI-I	(Possee, 1986)	R. D. Possee
pAcUW21	(Lopez-Ferber <i>et al.</i> , 1995)	
pBluescript-BAC		
pCH110	(Hall <i>et al.</i> , 1983)	
pBAC5		Novagen
pBacPAK8		Clontech
pBacPAK8-urokinase		R. B. Hitchman
pBluescript ^{pif1}		Advantagen
pBluescript ^{Arg96Ala}		
pBluescript ^{Arg478Ala}		
pBluescript ^{Arg96/478Ala}		
pGEM-T		Promega
pOET3		Oxford Expression Technologies, Ltd
pRedET plasmid	(Muyrers <i>et al.</i> , 2000)	Gene Bridge
TOPO vector		Invitrogen

2.2 Bioinformatics

2.2.1 Baculovirus sequences

The AcMNPV sequence was retrieved from the Viral Genome Project database (Bao *et al.*, 2004), hosted by the National Centre for Biotechnology Information (NCBI, <http://www.ncbi.nlm.nih.gov/>). The target open reading frames amino acid sequences were obtained from the AcMNPV sequence and used in a BLAST search (NCBI, <http://blast.ncbi.nlm.nih.gov/Blast.cgi>). This allowed amino acid sequences that were homologous to the target proteins to be found and used in multiple sequence alignments.

2.2.2 Multiple sequence alignments

Sequences were aligned by multiple sequence alignment using the ClustalW2 software hosted by the European Bioinformatics Institute (EBI, <http://www.ebi.ac.uk/Tools/msa/clustalw2/>). The ClustalW2 software default settings were used to calculate and generate all the alignments within this thesis. Alignments were then shaded according to amino acid similarity using the GenDoc software package, downloaded from <http://en.bio-soft.net/format/GeneDoc.html> (Nicholas *et al.*, 1997) and run locally.

2.2.3 Protein pattern search

The TMPRED software tool, hosted by EXPASY (<http://expasy.org/tools/>) was used to scan the target sequence for any transmembrane regions (Hofmann and Stoffel, 1993). The NetNGlyc 1.0 and NetOGlyc 3.1 Server tools, hosted by Center for Biological Sequence Analysis (CBS, <http://www.cbs.dtu.dk/services/>) were used to identify any potential N- or O- linked glycosylation sites within the target sequence.

2.3 Insect Larvae, Cells and Viruses

2.3.1 Insect larvae and cell lines

All *Trichoplusia ni* (*T. ni*) larvae were provided by T. Carty, from continuous cultures reared at the Centre for Ecology & Hydrology, Wallingford. The larvae were maintained on a modified Hoffmans Tobacco Hornworm diet at 24°C (Hunter *et al.*, 1984). Healthy

first-third instar larvae were provided for experiments. Fresh gloves were used for handling different virus and insect stocks and all exposed surfaces were covered in sheets of Whatman paper, which were regularly changed.

The cell lines used for propagating virus were *T. ni* (Tn368) and *Spodoptera frugiperda* (Sf21 and Sf9). Tn368 cells and Sf21 cells were maintained in TC100 medium supplemented with 10% foetal calf serum (FCS) and Sf9 cells were maintained in serum-free insect express Sf9-s2 as described in King & Possee (1992)

2.3.2 Virus amplification

Virus stocks (Table 2.2) were amplified in Sf9 cells using the method described by King & Possee (1992). Cells were seeded at a density of 1.2×10^6 cells/ml in a shaker culture and monitored until they had reached a density of 2×10^6 cells/ml. Then they were infected with virus at a multiplicity of infection (MOI) of 0.1 pfu/cell. The cell suspension was harvested when all the cells showed cytopathic effect, approximately 4-6 days post infection (dpi). The cell suspension was centrifuged at 4,000 rpm for 15 minutes at 4°C (TY-JS 4.2 rotor, J6-MI Beckman centrifuge) to remove any cells. The supernatant fraction containing the virus was aliquoted into sterile tubes and stored in the dark at 4°C.

Table 2.2 Viruses used in this thesis¹

Virus	Reference	Source
AcMNPV strain C6	(Ayres <i>et al.</i> , 1994)	R. D. Possee
BacPAK5	(Kitts and Possee, 1993)	
AcBAC Δ chitinase,	(Hawtin <i>et al.</i> , 1997)	
<i>Ac</i> Δ <i>pif1lacZ</i>		
BacPAK6	(Kitts and Possee, 1993)	R. B. Hitchman
AcBAC Δ chitinase/cathepsin	(Hitchman <i>et al.</i> , 2010b)	

¹Viruses constructed within this thesis not included

2.3.3 Transfection of insect cells

Sf9 cells were transfected with virus DNA (100 ng) alone or virus DNA (100 ng) plus plasmid DNA (500 ng) using the liposome-mediated transfection method (Lipofectin™, Invitrogen) as described by King & Possee (1992). In duplicate, TC100 (0.5 ml) was added to 7ml tubes containing the virus and plasmid DNA, which was then mixed with 0.5 ml TC100, containing 10 μ l lipofectin (1mg/ml). The sample was then left at room

temperature for 30 minutes, before being adding to a 35 mm dish containing 1×10^6 cells. Dishes were incubated overnight at 28°C before adding 1 ml of insect express Sf9-s2 containing Penicillin/Streptomycin (20 µl/ml) to each dish. The virus sample was then harvested after the dishes had been incubated for 5 days at 28°C.

2.3.3a Generation of Recombinant viruses

Recombinant viruses were generated using the standard method described by King & Possee (1992) or *flashBAC*TM system, which was carried out using the supplier's instructions (Oxford Expression Technologies Ltd) (Possee *et al.*, 2008). The standard method used the same technique as described in section 2.3.3. However, Sf9 cells were transfected with restriction enzyme linearised virus DNA and plasmid DNA; all subsequent steps followed section 2.3.3. Recombinant viruses generated using this method were purified from the background parental virus using the method described in section 2.3.4b and 2.3.4c.

2.3.4 Titration of virus stocks

Virus stocks were either titrated using the standard plaque assay technique described by King & Possee (1992) or a qPCR-based titration system, *baculoQUANT*TM, which was carried out using the supplier's instructions (Oxford Expression Technologies Ltd) (Hitchman *et al.*, 2007b).

2.3.4a Plaque assay titration

Sf21 or Sf9 cells were seeded in at a density of 1.4×10^6 or 1×10^6 cells/35mm dish, respectively. The dishes were left at 28°C for 1 hour, to allow the attachment of the cells. Serial ten-fold dilutions were set up for each virus stock to be titrated in relevant media. The media overlay was then removed from the dishes and replaced with 100 µl of the relevant virus dilution for 1 hour at room temperature. After the incubation, the virus overlay was removed and replaced with 2 ml 1% low gelling temperature agarose (1 ml relevant media: 1ml 2% low gelling temperature agarose). The agarose overlay was left to set at room temperature (approximately 15 minutes). An additional 1 ml of relevant media was then added to each dish, which were then incubated at 28°C.

Once the monolayer was at confluence, the plaques were stained (normally 3-5 dpi). If visualisation of *lacZ* expression was required, the liquid overlay was removed and

replaced with 1 ml phosphate buffered saline (PBS) containing 10 μ l 5% X-gal (5-Bromo-4-chloro-3-indolyl β -D-galactopyranoside) in dimethylformimide (DMF). Dishes were then incubated for 3-4 hours at 28°C, before staining with neutral red.

All dishes were stained with neutral red that allows the visualisation of plaques, by staining live cells. 1 ml of 0.33% neutral red solution (Sigma-Aldrich) diluted 15-fold in PBS was added to the liquid overlay. Dishes were then incubated at 28°C for 4 or more hours to allow the staining of the monolayer. After this incubation, the overlay was decanted into disinfectant and dishes briefly dried on tissue paper. The dishes were then stored overnight at room temperature in the dark and the next day, plaques were manually counted on a light box.

2.3.4b Plaque purification of recombinant viruses

The plaque assay method described in section 2.3.4a, was also used to isolate recombinant viruses from their parental background. This involved using X-gal staining to visualise recombinant viruses from parental background using blue/white selection (as described above). Agar plugs were taken from the centre of plaques and dispersed in 500 μ l of relevant media. This process was repeated until only plaques containing recombinant viruses were present. The final plaque picks were amplified by using the dispersed agar plug to infect a T25 tissue culture flask containing 1×10^6 Sf9 cells. Once these virus passage P1 stocks were harvested at 3-5 dpi, the remaining monolayers were stained with 2 ml PBS containing 20 μ l 5% X-gal to ensure no parental background (*lacZ*) was present. The P1 stocks were titrated and used to generate P2 working stocks as described under section 2.3.2.

2.3.4c Alternative plaque purification method

An alternative method was also used to isolate recombinant viruses. Agar plugs were taken from the centre of plaques and used to infect cells (5×10^5 Sf9 cells) within a single well of a 24 well plate containing in 400 μ l insect express Sf9-s2. After 72hpi, DNA from the BV was extracted using the High Pure Viral Nucleic Acid Kit (Roche Applied Science) as described by the manufacturer and used in PCR to identify the virus types present.

2.3.5 Temporal analysis of virus replication

Time course studies were carried out by infecting Sf9 cells using the method described by King & Possee (1992). The required volume of cells were seeded at a density of 1.5×10^6 cells/ml in a shaker culture and monitored until they had reached a density of 2.5×10^6 cells/ml. The Sf9 cell culture was then subdivided into 16 ml shaker cultures and infected with virus at a multiplicity of infection (MOI) of 5 pfu/cell. However, infections were carried out with virus diluted in the relevant culture medium, in a final volume of 4 ml, which causes the total volume of the culture to reach 20 ml and 2.0×10^6 cells/ml. Triplicate shaker cultures were set up for each virus and cells mock infected with medium were also included.

During the time course study, 1 ml samples from each shaker culture was harvested (0, 6, 12, 24, 48, 72, 96 and 120 hpi) into 1.5 ml microcentrifuge tube and cells pelleted by centrifugation at 13,000 rpm for 5 minutes. The supernatant was carefully removed into 1.5 ml microcentrifuge tube and stored at 4°C, whereas the pellet was stored at -20°C. Once the time course was completed samples were titrated (section 2.3.4) and processed for protein activity assays (section 2.7.3).

A second 10 µl sample was also taken from each culture during the harvesting, to allow cell viability to be determined using 2% (w/v) trypan blue (Sigma-Aldrich). For each sample 1 µl 2% (w/v) trypan blue and 9 µl PBS was added, before placing into the wells of a glass haemocytometer and left to settle for 1 minute. Blue (dead) and non-blue (alive) cells were counted under light microscope and cells were only counted if they lay within one of the five squares or touched the left-hand or top boundary lines.

2.3.6 Purification of Baculovirus DNA

2.3.6a Purification of large quantities of virus DNA using Caesium Chloride

A 400 ml culture of Sf9 cells was seeded at a density of 5×10^5 cells/ml in a shaker culture and monitored until they had reach a density of 2×10^6 cells/ml. At this density, the culture was infected with virus at an MOI of 0.1 pfu/cell by direct addition of the virus to the culture. The cell suspension was harvested when all the cells showed cytopathic effect, approximately 4-6 days dpi. The cell suspension was centrifuged at 4,000 rpm for 15 minutes at 4°C (TY-JS 4.2 rotor, J6-MI Beckman centrifuge) to

remove any cells. The supernatant containing the virus was centrifuged at 24,000 rpm for 1 hour at 4°C (SW40 Ti rotor, Optima LE-80K Beckman Ultracentrifuge) to pellet the BV. Two ml of 1x TE buffer (10mM Tris.Cl; pH 8.0; 1 mM EDTA) was added to the pellet and incubated overnight at 4°C to aid resuspension of the pellet.

The pellet was resuspended and loaded onto a 30/50% (w/v) sucrose step gradient in ultraclear tubes (25 x 89 mm Beckman). An overlay of liquid paraffin was added and samples were centrifuged at 24,000 rpm, 4°C for 1 hour (SW40 Ti rotor, Optima LE-80K Beckman Ultracentrifuge). After centrifugation, the BV-containing band was retrieved from the sucrose interface. The BVs were diluted with 10 volumes of 1x TE buffer, and centrifuged for 24,000 rpm for 1 hour at 4°C (SW40 Ti rotor, Optima LE-80K Beckman Ultracentrifuge). The supernatant fraction was carefully removed and discarded and the pellet containing BV was re-suspended in 1 ml 1x TE buffer.

The BV sample was incubated at 60°C for 30 minutes with the addition of sarkosyl (final concentration 4% (w/v)) to release the DNA. The sample was then layered onto a 5 ml cushion of 50% (w/w) caesium chloride containing 0.5 µg/ml ethidium bromide. An overlay of liquid paraffin was added and samples were centrifuged at 35,000 rpm, 20°C for 1 hour (SW40 Ti rotor, Optima LE-80K Beckman Ultracentrifuge). The virus DNA band was harvested and ethidium bromide was extracted from the sample with water-saturated butanol. The virus DNA was then dialysed against 500 ml TE stirred at 4°C in the dark for 2-4 days. The TE was replaced every 24 hours and once the DNA was harvested, it was stored at 4°C. The concentration and quality of the virus DNA was then determined by spectrophotometric measurements and restriction enzyme analysis (section 2.6.1).

2.3.6b Purification of virus DNA from 35mm dishes

Sf9 cells were seeded in 35mm tissue culture dishes at a density of 1×10^6 cells/dish and were incubated to attach at 28°C for 1 hour. Cells were infected at an MOI of 5 pfu/cell using 100 µl diluted in the relevant culture medium. After 1 hour incubation at room temperature, the inoculum was replaced with 2 ml of the relevant medium and the dishes were incubated at 28°C for 2-3 days. Cells mock infected with medium were also included. The virus DNA purification technique used was described by King & Possee (1992).

Purification of virus DNA from BV

After 2-3 dpi, the supernatant was harvested and cells removed by centrifugation at 4,000 rpm for 5 minutes. The supernatant was transferred to a fresh 2 ml microcentrifuge tube and BV was pelleted by centrifugation at 13,000 rpm for 15 minutes. The supernatant was carefully removed and the BV pellet was resuspended in 100 μ l 1x TE buffer. Two and half μ l of both 10% (w/v) SDS and 20 mg/ml Proteinase K were added and the sample was incubated at 37°C for 1 hour. The DNA was extracted twice by gently mixing with equal volumes of phenol/chloroform and once with chloroform. 0.1 volumes of 3M Sodium acetate and 2 volumes of 100% ethanol were added to the sample to precipitate the DNA overnight at -20°C. The DNA was pelleted by centrifugation (13,000 rpm for 10 minutes) and the supernatant was carefully removed. The pellet was air-dried for 5 minutes before the addition of 20 μ l 1x TE buffer. The sample was either placed overnight at 4°C or heated at 65°C for 15 minutes to aid resuspension of the DNA pellet. The sample was stored at 4°C and used for restriction digest or PCR analyses.

Purification of Intracellular virus DNA

Using the same dish of infected cells, after 2-3 dpi, the cell monolayer was harvested and the cells were pelleted by centrifugation (3,000 rpm for 5 minutes). The supernatant was carefully removed and the pellet resuspended in 0.5 ml PBS. The cells were repelleted and resuspended in 250 μ l TE buffer and 250 μ l insect cell pellet lysis buffer (50 mM Tris pH 8.0, 5% (v/v) β -mercaptoethanol, 0.4% (w/v) SDS, 10 mM EDTA). After the addition of 12.5 μ l 20 mg/ml Proteinase K and 2.5 μ l RNaseA, the sample was incubated at 37°C for 30 minutes. After this incubation, the DNA was subsequently extracted and precipitated using the method described above

2.3.6c Purification of virus DNA using a Viral Nucleic Acid Kit

An alternative method using the High Pure Viral Nucleic Acid Kit (Roche Applied Science) was also used to purify viral DNA from BV, which was carried out using the supplier's instructions.

2.3.7 Virus infection of insect larvae

The methodology described by King & Possee (1992) was used to propagate viruses and purify their occlusion bodies (OBs). Viral infection of the larvae was carried out in plastic tubs (8 cm diameter, 6 cm height) containing 22 ml of semi-artificial diet (modified Hoffmans Tobacco Hornworm diet; Hunter *et al.*, 1984). A Gilson pipette was used to apply 200 μ l purified OBs (concentrations between 10^3 and 10^6 OBs/ μ l) to the surface of the diet and evenly spread out across the diet using a plastic disposable spreader. After the inoculum had air dried at room temperature, 10 late-third or early fourth instar *T. ni* larvae were placed into each tub and approximately 2 cm slit placed in the lid to allow ventilation. The infected larvae were kept at room temperature in normal illumination.

The diet plug method described by King & Possee (1992), was also used to infect larvae. Diet plugs approximately 1 mm² were placed into 96-well micro titre plate, which had been inoculated with 1 μ l dilution of OBs (concentrations between 10^0 and 10^3 OBs/ μ l). An early third instar larvae was placed in each well and tissue paper spread with MilliQ water was placed over the wells before replacing the lid. The insects were incubated overnight at room temperature and those larvae that had consumed the contaminated diet were transferred to small individual plastic containers (poly-pots) using soft, blunt forceps. These poly-pots contained sufficient diet to support the larvae for the remainder of their feeding period. A control group of larvae that were treated identically but had 1 μ l of MilliQ water applied to each diet plug in place of the OB suspension

2.3.8 BV injection *in vivo*

Early fourth instar *T. ni* larvae were injected with 1 μ l BV (10^5 and 10^6 BV/ μ l) in their haemocoels using a micro-applicator fitted with a syringe and a BD Microfine u100 8mm/30G 0.3 ml needle (Westons Internet). Injected larvae were then incubated at room temperature in individual poly-pots and checked daily for signs of infection.

2.3.9 Purification of OBs from virus-infected larvae

The virus-infected larvae were stored at -20°C and thawed at room temperature on the day of purification before purifying OBs using the method described by Harrap *et al.*

(1977). The larvae were placed into a stomacher bag with 5 ml 0.1% (w/v) SDS and macerated into a smooth paste using a p1000 Gilson tip to disrupt the insect. This extract was filtered into a 50ml conical flask through two layers of muslin and 0.5 ml of 0.1% (w/v) SDS was used to wash any remaining extract through the muslin. The extract was then centrifuged at 4500 rpm, 20°C for 30 minutes (TY-JS 4.2 rotor, J6-MI Beckman centrifuge). After the supernatant fraction had been carefully removed, the pellet was re-suspended in a small volume of 1x TE buffer.

The extract was loaded onto a 50/60% (w/v) sucrose step gradient in ultraclear tubes (25 x 89 mm Beckman). An overlay of liquid paraffin was added and samples were centrifuged at 24,000 rpm, 4°C for 1 hour (SW40 Ti rotor, Optima LE-80K Beckman Ultracentrifuge). After centrifugation, the purified OBs were retrieved from the sucrose interface. The OBs were diluted with 10 volumes of 1x TE buffer, and centrifuged for 10,000 rpm for 30 minutes at 4°C (SW40 Ti rotor, Optima LE-80K Beckman Ultracentrifuge). The pellet was re-suspended in 1-2 ml TE buffer, depending on size of pellet, and stored at 4°C.

2.3.9a Purification of OBs from single infected larvae

The OBs from a single virus-infected larva were also purified using the following method. The 'V-shaped' base was removed from a 0.5 ml microcentrifuge tube using a heated scalpel and melted onto two layers of muslim to form a filter. This modified microcentrifuge tube was placed into a 2 ml microcentrifuge tube and loaded with extract from a single larva, which had been vortexed in 500 µl 1x TE buffer for 1 minute. The filter was centrifuged in a bench-top centrifuge at 13,000 rpm, 20°C for 1 minute. The filtrate was layered onto 300 µl of 30% (w/v) sucrose, in a 1.5 ml microcentrifuge tube and centrifuged at 13,000 rpm for 5 minutes. The supernatant was removed and the pellet re-suspended in 150-300 µl dH₂O.

2.3.10 Enumerating OBs from infected larvae

A diluted sub-sample of the OB suspension was placed into the wells of a C-chip haemocytometer (Labtech) and left to settle for 10 minutes. OBs were counted under light microscope phase-contrast objective at X400 magnification, and the concentration of the original suspension was then calculated.

2.3.11 Bioassays

Bioassays were carried out using third instar larvae inoculated with a range of OB doses. Individual larvae were incubated overnight with a diet plug inoculated with a defined number of OBs (10^0 , 10^1 , 10^2 or 10^3 OBs). If the diet-plug had been eaten by the larvae after 24hpi, then they were transferred to fresh diet, incubated at room temperature and monitored four times a day for viral death. The highest OB dose (10^4 OBs) was droplet fed to the larvae within a disposable plastic petri dish. Once the larva had finished feeding it was transferred to fresh diet, incubated at room temperature and also monitored four times a day.

2.3.11a Statistical analysis of Bioassay data

Bioassay data was analysed using chi-square analysis (Microsoft Office Excel 2007) and Probit analysis (PoloPlus, LeOra Software), which were used to compare oral infectivity between viruses. The values for lethal dose (LD_{50} and LD_{90}) were determined by linear regression and two-tailed student t-test was used to analysis the survival times between viruses.

2.4 Microscopy Methods

2.4.1 Laser scanning confocal microscopy of fixed cells

For confocal microscopy, TN368 cells were seeded at 2.5×10^6 cells per 35mm tissue culture dish, which contained a glass coverslip (No. 0 thickness 22 mm diameter, Scientific Laboratory Supplies Ltd). The cells were allowed to settle for 1 hour at 28°C , before being infected at a MOI of 5 pfu/cell. Infections were carried out with virus diluted in the relevant culture medium, in a final volume of 100 μl . After 1 hour incubation at room temperature, the virus inoculum was replaced with 2 ml of the relevant medium and the dishes were incubated at 28°C for the required time. Mock infected samples comprised cells treated identically with 100 μl of medium containing no virus.

The TN368 cells growing on the coverslips were chemically fixed using paraformaldehyde (Thermo-Scientific) at the required time post-infection. This was carried out by first washing the cells once or twice with 2 ml of PBS before treating

them with 1 ml 4% (v/v) paraformaldehyde for 1 hour. The fixed samples were then washed with 1 ml PBS and stored at 4°C in 2 ml PBS.

Immunofluorescence staining was performed on the fixed samples by first washing them with 1 ml PBS, before permeabilising the cells with a 10 minutes treatment of PBS-BSA (PBS containing 1% (w/v) bovine serum albumin (Sigma-Aldrich)) containing 0.1% (v/v) Triton X-100. The samples were then washed twice with 2 ml PBS and followed by two washes with 2 mls of PBS-BSA blocking solution. The samples were then incubated at room temperature with the primary antibody (Table 2.3) at the relevant dilution in 100 µl of PBS-BSA. After this incubation the samples were then washed three times with 2 ml of PBS-BSA, before treatment with the diluted secondary antibody (Table 2.3) in 100 µl of PBS-BSA for 45 minutes. Samples were then finally washed five times with 2 ml of PBS-BSA and mounted onto microscopy slides with Vectashield (Vector Laboratories), a glycerol-based mounting media containing the DNA stain 4',6-diamidino-2-phenylindole (DAPI). The slides were then sealed with clear nail-varnish and stored protected from light at 4°C.

Table 2.3 Antibodies used for Laser scanning confocal microscopy

Antibody target	Antibody source species	Working Dilution (Immuno-fluorescence)
anit-6xHis-tag	Mouse	1:1000
anti-mouse IgG conjugated to TRITC	Goat	1:64

The samples were visualised within a month of staining on a confocal laser scanning microscopy (Zeiss LSM 510 META confocal system mounted on an Axio Imager-Z1 upright microscope). The Zeiss LSM 510 image acquisition software was used to acquire the images and Zeiss LSM Image browser was used to label the images.

2.4.2 Electron microscopy of OBs

The OBs purified from a single virus-infected larva (section 2.3.9a), were used in the electron microscopy (EM) studies carried out in this thesis. The dH₂O was removed from the OB pellets and replaced with the primary fixative (2% (w/v) paraformaldehyde, 2% (v/v) glutaraldehyde solution in cacodylate buffer (0.1 M NaCl, 0.05 M cacodylate pH 7.5)). The samples were incubated at room temperature for 1.5 hour. The samples were washed four times for 10 minutes at room temperature in 1 ml cacodylate buffer. The secondary fixative (1% (w/v) aqueous Osmium Tetroxide) was then added and

samples incubated for 1 hour at room temperature. The samples were washed four times for 10 minutes at room temperature in 1 ml ultra-pure water. Samples were stained overnight at 4°C in 500 µl 0.5% (w/v) aqueous uranyl acetate and following the incubation washed two times for 10 minutes at room temperature in 1 ml ultra-pure water. The samples were then dehydrated through a series of 20-100% ethanol washes, before being embedded in Spur resin (Taab Laboratories). Ultra thin sections were obtained using PT-PC PowerTome Ultramicrotomes (RMC) and subsequently stained with filtered 0.5% (w/v) aqueous uranyl acetate and lead citrate. The sections were then washed in ultra-pure water and dried, before images were obtained using a Hitachi H7650 electron microscope.

2.5 Bacteria methods

The *Escherichia coli* (*E. coli*) strains used within thesis are shown in Table 2.4

Table 2.4 *E. coli* strains used in this thesis¹

Bacteria Name	Strain
DH5α	F- φ80 <i>lacZ</i> ΔM15 Δ(<i>lacZYA-argF</i>) U169 <i>recA1 endA1 hsdR17</i> (<i>r_k</i> ⁻ , <i>m_k</i> ⁺) <i>phoA supE44 λ- thi-1 gyrA96 relA1</i>
DH10B	F- <i>mcrA</i> Δ(<i>mrr-hsdRMS-mcrBC</i>) φ80 <i>lacZ</i> ΔM15 Δ <i>lacX74 recA1 endA1 araD139</i> Δ (<i>ara, leu</i>)7697 <i>galU galK λ-rpsL nupG</i> /pMON14272 / pMON7124
Top 10	F- <i>mcrA</i> Δ(<i>mrr-hsdRMS-mcrBC</i>) φ80 <i>lacZ</i> ΔM15 Δ <i>lacX74 recA1 araD139</i> Δ(<i>ara-leu</i>) 7697 <i>galU galK rpsL</i> (Str ^R) <i>endA1 nupG λ-</i>

¹*E. coli* strains used in this study were purchased from Invitrogen

2.5.1 Preparation of chemically competent *E. coli* cells

A 10 ml Luria Broth (LB, 10g bactotryptone, 5g NaCl and 5g yeast extract in 1 litre of deionised water, sterilised by autoclaving) culture was set up by picking a single colony from a fresh plate of *E. coli* cells. This culture was incubated overnight at 37°C with shaking (200 rpm). 1ml of this overnight culture was then used to inoculate 100 ml of LB, which was grown at 37°C with shaking until it reached a cell density corresponding to 0.4-0.5 spectrophotometer reading at OD₆₅₀. The culture was then chilled on ice for 30 minutes, before the cells were pelleted by centrifugation in a pre-chilled rotor at 4000 *g* for 15 minutes (TY-JS 4.2 rotor, J6-MI Beckman centrifuge). The cell pellet was

then resuspended in ice-cold 0.1 M CaCl₂ and chilled on ice for 1 hour. The cells were then re-pelleted by centrifugation at 4000 *g* for 30 minutes (TY-JS 4.2 rotor, J6-MI Beckman centrifuge). This final pellet was resuspended in a small volume of ice-cold 0.1 M CaCl₂, 15% glycerol, to allow aliquots of 500 µl into 0.2 ml microcentrifuge tube to be dispensed and stored at -70°C.

2.5.2 Preparation of chemically competent *E. coli* cells – Inoue method

A 5 ml LB culture was set up by picking a single colony from a fresh plate of *E. coli* cells and this culture was incubated for 6-8 hours at 37°C with shaking (200 rpm). Varying volumes of this culture was then used to inoculate three flasks containing 250 ml of SOB media (20 g tryptone, 5 g yeast extract and 0.5 g NaCl in 1 litre of deionised water after pH adjusted to 7.0; sterilised by autoclaving). These starter cultures were then grown overnight at 18°C with shaking. When one of the cultures had reached a cell density corresponding to 0.55 spectrophotometer reading at OD₆₀₀, it was then chilled on ice for 30 minutes. Before the cells were pelleted by centrifugation in a pre-chilled rotor at 2500 *g* for 10 minutes (TY-JS 4.2 rotor, J6-MI Beckman centrifuge). The cell pellet was then resuspended in 80 ml ice-cold Inoue buffer (55 mM MnCl₂, 15 mM CaCl₂, 250 mM KCl, 10 mM PIPES (pH 6.7)) and the cells were then re-pelleted by centrifugation. The final pellet was resuspended in 10 ml Inoue buffer and 750 µl DMSO. Aliquots of 500 µl were dispensed into 0.2 ml microcentrifuge tube and flash frozen in either liquid nitrogen or ethanol dry-ice bath. These aliquots were then stored at -70°C.

2.5.3 Transformation of competent *E. coli* cells with plasmid DNA

Competent *E. coli* cells (sections 2.5.1/2.5.2) were thawed on ice and 50 µl mixed with 2-3 µl of a ligation reaction or 10 ng of vector DNA. This mixture was cooled on ice for 15 minutes before being heat shocked for 45 seconds at 42°C. One ml SOC media was then added to the mixture and incubated at 37°C for 1 hour. Cell aliquots of 100 µl were dispensed across separate plates of LB-agar containing the appropriate antibiotic(s) (Table 2.5) and spread across the surface using plastic disposable spreaders. The plates incubated at 37°C overnight.

Table 2.5 Antibiotics used in bacteria cultures

Antibiotic	Stock	Working solution (Plasmids)	Working solution (Bacmids)
Ampicillin	50 mg/ml in dH ₂ O	50 µg/ml	N/A
Kanamycin	30 mg/ml in dH ₂ O	50 µg/ml	15 µg/ml
Tetracycline	10 mg/ml in 75% (v/v) ethanol	3 µg/ml	N/A
Chloramphenicol	30 mg/ml in ethanol	N/A	15 µg/ml

2.5.4 Preparation of electrocompetent *E. coli* cells containing pRedET

A 10 ml LB culture containing Tetracycline (3 µg/ml; LB-Tet) was established by picking a single colony from a fresh plate of *E. coli* cells containing the pRedET plasmid (Gene Bridge). This culture was incubated overnight at 30°C with shaking (200 rpm). Five ml of this overnight culture was used to inoculate 400 ml of LB-Tet, which was grown at 30°C with shaking until it reached a cell density corresponding to 0.3 spectrophotometer reading at OD₆₀₀. Once at this density, 15 ml 10% (w/v) L-arabinose was added to the culture and placed at 37°C with shaking for 1 hour. This induced the expression of recombination proteins from the pRedET vector. The cells were pelleted by centrifugation in a pre-chilled rotor at 4000 rpm for 15 minutes (TY-JS 4.2 rotor, J6-MI Beckman centrifuge). The cell pellet was resuspended in 200 ml of ice-cold dH₂O and the cells were re-pelleted. After this the cell pellet was resuspended in 100 ml of ice-cold dH₂O and re-pelleted, this stage was repeated. The cell pellet was resuspended in 15 ml ice-cold 10% (v/v) glycerol and re-pelleted. This final pellet was resuspended in a small volume of ice-cold 10% (v/v) glycerol, to allow aliquots of 500 µl to be dispensed into 0.2 ml microcentrifuge tube and stored at -70°C.

The preparation of electrocompetent *E. coli* cells that did not harbour the pRedET vector was also carried out. In these preparations, the appropriate antibiotic was used and the cultures were grown at 37°C with shaking until they reached a cell density corresponding to 0.4-0.5 spectrophotometer reading at OD₆₀₀. Subsequent pelleting and washes with ice-cold dH₂O were performed as described above.

2.5.5 Electroporation of competent *E. coli* cells

The competent *E. coli* cells (section 2.5.4) were thawed on ice and 40 µl mixed with 3-5 µl PCR product or 1 ng of vector DNA. This mixture was added to a 1 mm cuvette

(Geneflow) and chilled on ice for 10 minutes prior to electroporation. Transformation was achieved using a Bio-Rad Gene Pulser II (BIO-RAD) or Electroporator 2510 (Eppendorf) according to the manufacturers' protocols. Immediately after transformation 1 ml SOC medium was added to the cuvette, to allow transfer of the cells from the cuvette to 15 ml tube. The cells were then incubated at 37°C for 1 hour, after which 100 µl cell aliquots were dispensed into separate plates of LB-agar containing the appropriate antibiotic(s) and spread across the surface using plastic disposable spreaders. The plates were incubated at 37°C overnight.

2.5.6 Plasmid DNA purification from *E. coli* cells

Depending on the quantity of plasmid DNA required a QIAprep Spin Miniprep Kit, QIAGEN Plasmid Midi Kit or QIAGEN Plasmid Maxi Kit was used and the procedure carried out as described in the supplier's instructions (QIAGEN).

For bacmid DNA an adapted version of the Miniprep Kit QIAGEN protocol was used. Briefly, the bacterial culture was treated as described in the QIAGEN protocol but at step five the clear supernatant was transferred to a fresh tube containing 0.7 vol isopropanol, to precipitate the DNA. The sample was inverted to mix and centrifuged at 13,000 rpm for 30 minutes at 4°C (J-25.5 rotor, Avanti J-25i Beckman centrifuge). Immediately the supernatant was removed and 500 µl 70% (v/v) ethanol was added to the pellet before being centrifuged at 13,000 rpm for 5 minutes at 4°C (J-25.5 rotor, Avanti J-25i Beckman centrifuge). This wash was repeated and the final pellet was left to air dry for 15 minutes. The bacmid DNA pellet was re-suspended in 30 µl TE buffer.

2.5.7 Purification of large quantities of bacmid DNA using caesium chloride

For bacmid DNA, an adapted version of the Miniprep Kit QIAGEN protocol by R. D. Possee was used.

A 5 ml LB culture containing chloramphenicol at 25 µg/ml (LB-Cm) was set up by picking a single colony from a fresh plate of *E. coli* cells. This culture was incubated overnight at 37°C with shaking (200 rpm). 0.2 ml of this overnight culture was then used to inoculate 200 ml of LB-Cm, which was grown at 37°C with shaking overnight. The cells were pelleted at 4200 rpm for 20 minutes at 4°C (TY-JS 4.2 rotor, J6-MI

Beckman centrifuge). The supernatant was removed and the cell pellet resuspended in 20 ml Qiagen buffer P1 (containing RNase A 100 µg/ml). 40 ml Qiagen Buffer P2 was added and the tube was inverted several times to gently mix the samples. Finally, 30 ml chilled Qiagen Buffer P3 was added, the tube was mixed as before and incubated on ice for 20 minutes. The sample was then centrifuged at 4200 rpm for 30 minutes at 4°C (TY-JS 4.2 rotor, J6-MI Beckman centrifuge). The supernatant was filtered through Whatman paper to remove any remaining precipitate. The DNA was precipitated by the addition of 100 ml isopropanol. The sample was then centrifuged at 4200 rpm for 60 minutes at 4°C (TY-JS 4.2 rotor, J6-MI Beckman centrifuge). The supernatant was carefully removed and the pellet was gently resuspended in 5 ml 70% (v/v) ethanol. The sample was transferred to a 15 ml Oakridge tubes and centrifuged at 12,000 rpm for 10 minutes at 4°C (J-25.5 rotor, Avanti J-25i Beckman centrifuge). The supernatant was carefully removed and the pellet allowed to air-dry for 5-10 minutes. 0.7 ml 1x TE buffer was added to the pellet and stored overnight at 4°C to aid resuspension of the DNA pellet.

The DNA pellet was re-suspended and layered onto a 5 ml cushion of 50 % (w/w) caesium chloride containing 0.5 µg/ml ethidium bromide. An overlay of liquid paraffin was added and samples were centrifuged at 35,000 rpm, 20°C for 1 hour (SW40 Ti rotor, Optima LE-80K Beckman Ultracentrifuge). The bacmid DNA was harvested, loaded onto a second gradient and centrifuged again. The bacmid DNA was harvested and ethidium bromide was extracted from the sample with water saturated butanol. The bacmid DNA was dialysed against 500 ml TE stirring at 4°C in the dark for 2-4 days. The TE was replaced every 24 hours and once the DNA was harvested, it was stored at 4°C. The concentration and quality of the bacmid DNA was then determined by spectrophotometric measurements and restriction enzyme analysis (section 2.6.1).

2.5.8 Red/ET recombination system

The Red/ET recombination system (Gene Bridge) was used to generate deletion mutant bacmids. The supplier's instructions were carried out with alterations given in sections 2.5.4 and 2.5.5.

2.5.9 Bacmid transfection of insect cells

Sf9 cells were transfected with bacmid DNA (100 ng) alone or bacmid DNA (100 ng) plus plasmid DNA (500 ng) using the liposome-mediated transfection method (Lipofectin™, Invitrogen) as described by King & Possee (1992). Subsequent steps were performed as described in sections 2.3.3 and 2.3.3a.

2.6 Molecular Biology Methods

2.6.1 Restriction enzyme digestions of DNA

Restriction endonucleases (RE) were purchased from New England Biolabs, apart from *SrfI*, which was purchased from Stratagene. The DNA (plasmid, bacmid and virus) concentration was determined spectrophotometrically and was digested using a variety of standard restriction enzymes methods as described in the supplier's instructions. Digests were performed in 1.5 ml microcentrifuge tubes in a total volume of 25-50 µl and incubated at 37°C for 1-4 hours.

2.6.2 Dephosphorylation of DNA

Following the purification of restriction enzyme digested vector DNA (section 2.6.1), Shrimp Alkaline Phosphatase (SAP, Promega) was added to the sample (1 U/µg DNA) along with Shrimp Alkaline Phosphatase buffer and incubated at 37°C for 15-30 minutes. After this incubation, the SAP was heat-inactivated at 65°C for 15 minutes.

2.6.3 Ligation of DNA

Ligation reactions were carried out using 50 ng of plasmid vector DNA (SAP and non-SAP treated) with varying concentrations of inserts, using molar ratios of vector DNA: insert DNA of 1:1, 1:3 and 3:1. Reactions were carried out using T4 DNA ligase (New England Biolabs) as described in the supplier's instructions, at room temperature for 1 hour.

2.6.4 Agarose gel electrophoresis

Horizontal agarose gels were routinely carried out to allow the estimation of DNA concentrations and visualisation of restriction enzyme profiles. The concentration of High gelling temperature agarose (Lonza) varied from 0.6% to 1% (w/v) depending upon the sizes of the DNA fragments to be separated. Submerged gel electrophoresis was performed in 1x TAE buffer (Tris-Acetate 40 mM, EDTA 1 mM) containing 0.5 μ g/ml ethidium bromide. Prior to electrophoresis, samples were mixed with 1:5 volumes of 5x loading buffer (40% sucrose, 5x TAE, 2.5% SDS, 0.1% bromophenol blue dye). Electrophoresis separations were performed at 25-100 volts (V) for 1 to 18 hours as required. Following electrophoresis, DNA was both visualised and documented using a UV transilluminator (Ingeneous system supplied by Syngene Bio imaging Ltd).

2.6.5 Isolation of DNA from agarose gels

The 1% (w/v) low gelling temperature agarose (Lonza) gels containing ethidium bromide (0.5 μ g/ml) were used to separate DNA fragments during electrophoresis in 1 x TAE buffer at 50V. The DNA was visualised under UV light and the required fragments excised from the gel, using a sterile scalpel. The DNA was purified from the gel using a QIAquick™ Gel Extraction Kit (QIAGEN), as described by the supplier.

2.6.6 Polymerase chain reaction (PCR)

Synthetic oligonucleotides were designed by the author and synthesised by Eurofins MWG Operon. They were supplied as freeze-dried pellets, which were re-suspended in dH₂O to give a stock concentration of 100 pmol/ μ l and stored at -20°C.

Reactions were performed using a RoboCycler gradient 96 (Stratagene) PCR machine. The 50 μ l reaction mixture consisted of 0.8 pmol each of the forward and reverse primers, with approximately 10 ng of DNA, 100 nM dNTPs, 2.5 mM MgCl₂ and 2.5 Units DNA polymerase. Taq DNA polymerase and supplied buffer purchased from New England Biolabs was used for general PCR purposes. Expand DNA polymerase and supplied buffer purchased from Roche Applied Science was used when greater fidelity was required. All PCR amplifications included a negative control that contained MilliQ water in place of template DNA in the reaction mix. 5 μ l of each reaction was then

analysed by agarose gel electrophoresis (section 2.6.4), to identify a successful reaction.

2.6.7 TOPO and pGEM-T cloning of PCR fragments.

The PCR generated fragments with either Taq or Expand DNA polymerase were cloned into either the TOPO-TA vector (Invitrogen) or pGEM-T (Promega). The ligation reactions were carried out as described in the supplier's instructions.

2.6.8 DNA sequencing

All DNA sequencing was outsourced to Geneservice, Oxford or CEH, Wallingford. The free software developed by Geospiza Inc, Finch TV (<http://www.geospiza.Com/index.shtml>) was used to visualise and analyze sequence data.

2.6.9 Generation of Oligonucleotide fragments

Reactions were performed using a RoboCycler gradient 96 (Stratagene) PCR machine. The 100 μ l reaction mixture consisted of 10 μ l 10x T4 DNA ligase buffer (NEB), 70 μ l dH₂O and 10 μ l each of the forward and reverse primers to give a final concentration of 0.1 μ g/ μ l:

The reaction was placed at 95°C for 3 minutes to denature the DNA. After 3 minutes, the heat block is switched off and allowed to cool to room temperature. This allows the primers to anneal and form the oligonucleotide fragment.

After this the DNA was extracted twice by gently mixing with equal volumes of phenol/chloroform and once with chloroform. Ten μ l 3M Sodium acetate and 200 μ l 100% ethanol were added to the sample to precipitate the DNA. The DNA was pelleted by centrifugation in bench centrifuge at 13,000 rpm for 5 minutes and washed twice in 75% (v/v) ethanol. The pellet was air-dried for 5 minutes before being resuspended in 40 μ l 1x TE buffer and stored at -20°C. The DNA concentration was determined spectrophotometrically and used in ligation reactions (section 2.6.3).

2.6.10 Mutagenesis

Mutations were introduced into the AcMNPV *pif1* sequence that resulted in either or both amino acids 96 (cgt to gcg) and 478 (cgc to gcg) to be changed from arginine to alanine. These mutations were synthesized by Advantagen Ltd and provided in pBluescript.

2.7 Protein Analysis

2.7.1 SDS-PAGE analysis of protein samples

Protein samples were analysed by standard sodium dodecyl sulphate polyacrylamide gel electrophoresis (SDS-PAGE) as described in Sambrook and Russell (2001). Samples to be run on a SDS-PAGE were first quantified using the Qubit system (Invitrogen) as described in the supplier's instructions. After the quantification, 1/5th volume of 6X Laemmli SDS-PAGE loading buffer (250mM Tris-HCl pH 6.8, 10% (w/v) sodium dodecyl sulphate (SDS), 50% (v/v) glycerol, 0.05-0.5% (w/v) bromophenol blue and 25% (v/v) β -mercaptoethanol, which was added just before use) was added to the sample. The samples were boiled in a waterbath for 5 minutes and centrifuged to remove any insoluble matter (13,000 rpm, 5 minutes). Samples were run on 12% SDS-PAGE gels using the mini-PROTEAN vertical gel electrophoresis system (Bio-Rad). The SDS-PAGE gels were either Coomassie stained or blotted onto nitrocellulose membranes (Section 2.7.2).

For Coomassie staining, the gels were placed in 0.25% (w/v) Coomassie Brilliant Blue R-250 dissolved in; 50% (v/v) methanol, 10% (v/v) glacial acetic acid, for 4 or more hours. The gels were destained for 2 or more hours using 30% (v/v) methanol, 10% (v/v) glacial acetic acid. Images of the gels were taken using a digital camera, before they were dried between two sheets of cellophane using small amount of gel drying buffer (40% (v/v) methanol, 10% (v/v) glycerol, 7.5% glacial acetic acid) and plastic frame system (Promega).

2.7.2 Western blot analysis of proteins

Proteins were transferred from the SDS-PAGE (section 2.7.1) onto nitrocellulose membrane using the Trans-Blot SD semi-dry transfer cell system (Bio-Rad) as instructed by the manufacturer. Once the proteins had been transferred, the membrane

was washed in blocking buffer (PBS-T (PBS, 0.1% (v/v) Tween 20) with 5% (w/v) skimmed milk powder) for 1 hour at room temperature with rotation. The membranes were incubated for another hour rotating in 5-10 ml blocking buffer containing the primary antibody (Table 2.6) at the desired concentration. Membranes were washed four times for 15 minutes at room temperature with rotation in 10 ml PBS-T. The membranes were subsequently incubated for 1 hour, rotating in 10 ml blocking buffer containing the alkaline phosphatase conjugated secondary antibody (Table 2.6) at the desired concentration. Membranes were washed four times for 15 minutes at room temperature, with rotation in 10 ml PBS-T. 10 ml alkaline phosphatase buffer (100mM Tris-HCl pH 9.5, 100 mM NaCl, 5mM MgCl₂) containing 66 µl Nitro blue tetrazolium (stock concentration at 50 mg/ml in 70% (v/v) DMF) and 33 µl 5-Bromo-4-chloro-3-indolyl phosphate p-toluidine salt (stock concentration at 50 mg/ml in dH₂O) was added to the membranes to visualise any bound alkaline phosphatase conjugated antibody. The development was stopped by washing the membrane with dH₂O three times and leaving it to air-dry.

Table 2.6 Antibodies used for Western blotting

Antibody target	Antibody source species	Working Dilution (Western blotting)
anit-6xHis-tag	Mouse	1:1000
Anti-VP39 (AcMNPV)	Mouse	1:500
Anti-uPA (Urokinase)	Mouse	1:1000
anti-mouse IgG conjugated to alkaline phosphatase	Goat	1:30,000

2.7.3 Enzyme activity assays

Samples from the time course studies (section 2.3.5) were harvested from shaker cultures and the cells were pelleted by centrifugation in a bench centrifuge at 6,000 rpm for 5 minutes. The supernatant fractions were carefully removed to 1 ml microcentrifuge tubes and stored at 4°C, whereas the cell pellets were stored at -20°C until used in the activity assays.

2.7.3a β-galactosidase activity assay

The cell pellets and 2x assay buffer (200 mM sodium phosphate buffer (pH 7.3), 2 mM MgCl₂, 100 mM β-mercaptoethanol, 1.33 mg/ml ONPG) were thawed at room temperature on the day of the assay. The cell pellets were resuspended in 100µl of

Reporter Lysis Buffer (RLB, Promega) and incubated at room temperature for 15 minutes. The samples were then vortexed briefly and cell debris was pelleted by centrifugation in bench centrifuge at 13,000 rpm for 2 minutes. Supernatants were carefully transferred to new 0.5 ml microcentrifuge tubes and serial log dilutions (10^{-3} to 10^{-5}) were set up for each sample to be tested in RLB. Triplicate 90 μ l of each dilution were then added to separate wells in a 96 well plate along with 90 μ l of 2x assay buffer. A negative control 90 μ l RLB and known standards were also performed. The reaction was incubated at 37°C for 30 minutes and stopped after this incubation by the addition of 300 μ l 1M Sodium carbonate. The absorbance of each well at 420 nm was then read using an ELx808 ultra microplate reader (Biotek). The standards were used to plot a standard curve to allow the conversion of the samples from wavelength readings into β -galactosidase activity after the removal of the negative control value.

2.7.3b Urokinase activity assay

Urokinase activity assay was performed on time course study samples using uPA activity assay kit, which was carried out using the supplier's instructions (Millipore).

Chapter 3

A bioinformatic analysis of target ODV structural proteins

3.1 Introduction

Baculoviruses are found in two forms. The budded virus (BV) form buds from infected cells and is involved in spreading the infection between cells and tissues in the host larvae. The initial infection of larvae and subsequent horizontal transmission of baculoviruses between hosts is mediated by the oral route using the second form, the occlusion-derived viruses (ODVs), which are found embedded in polyhedra. Both the BV and ODV forms contain nucleocapsids (NC) that are comprised of many similar proteins, however, the genome within these nucleocapsids is identical for both forms. The differences between the BV and ODV become apparent when the membrane envelopes are examined, showing variation in both protein and lipid content as described in Chapter 1 (section 1.3.12). In the exploitation of baculoviruses (largely AcMNPV) as expression vectors (section 1.4), only the BV form of the virus is required for propagation of recombinant viruses in cell culture. It could be considered that production of ODV in recombinant virus-infected cells is a waste of limited cellular resources that might otherwise be directed into either BV or recombinant protein synthesis. One of the longer term aims of this project is to identify and delete ODV-specific genes to abrogate or at least limit ODV production and determine, if in doing so, the yield of recombinant protein can be increased.

The first stage, however, was to identify putative ODV genes that could be deleted from the virus genome without affecting the ability of the virus to replicate in cell culture.

3.2 Structural proteins of the occlusion derived virus

The ODV envelope contains a wide range of viral proteins and is more diverse than the BV envelope. These proteins are transported to the ODV envelope by unique mechanisms and are mostly non-glycosylated. Eight putative gene deletion targets were selected for further study (Table 3.1) from the data collected on ODV proteins (Table 3.2). Recent proteomic investigations and reviews of the baculovirus ODV have been published (Braunagel *et al.*, 2003; Slack and Arif, 2007; Rohrmann, 2011) and together with information from publications on specific ODV proteins, Table 3.2 was compiled showing all known structural proteins of the ODV.

The target genes were selected because they encoded structural components of the ODV that were not found in the BV (using the literature available at the start of this thesis) and thus were predicted to have no effect on BV production in cell culture. The targeted genes have been listed in Table 3.1 and are individually reviewed in the following sections.

Table 3.1 Target structural proteins of the AcMNPV occlusion-derived virus

orf	Name	Predicted mass(kDa)	aa	Proposed ODV localization	Comments
46	ODV-E66	79	704	Envelope	Interacts with ODV-E25 and possibly involved in ODV capsid envelopment – Deletion mutant had no effect on BV production.
79	12.1 kDa	12.2	104	Nucleocapsid	Very similar to UvrC intron encoded nucleases, bacterial protein involved in DNA repair after UV damage
88	CG30	30.1	264	Nucleosome	Possibly a ubiquitin ligase due to it being a ring finger protein which could catalyze the ubiquitination and destruction of p53 – but experimental work was inconclusive for CG30 ubiquitin ligase activity. Deletion mutants produced more BV and were more infectious orally.
96	ODV-E28	19.8	173	Envelope	One of the 31 core baculovirus genes, Located to the ODV envelope and essential for oral infection
109	ODV-EC43	44.8	390	Nucleocapsid	Located both to the ODV nucleocapsid and envelope.
148	ODV-E56	40.9	376	Envelope	Essential for oral infection and Over expression causes a major decrease in envelopment of ODV.
22	PIF2	43.8	382	Envelope	Essential for oral infection – binding to the midgut cells
115	PIF3	23	204	Envelope	Essential for oral infection – not involved in binding/fusion to the midgut cells – possibly plays a role in translocation of ODV capsid along the microvillus

Notes: The table was constructed from four sources (Ayres *et al.*, 1994; Braunagel *et al.*, 2003; Slack & Arif, 2007; Rohrmann, 2011).

Chapter 3

Table 3.2 Potential structural proteins of the occlusion-derived virus

orf	Name	Alt Name	Left	Dir	Right	Predicted MW (kDa)	aa	pI	Motifs	Proposed ODV localization	Comments	References
14	<i>Jef-1</i>		10513	<-	11311	30.8	266	8.8	DNA Bind	Nucleosome	One of the six core baculovirus replication proteins – functions as a primase, allowing DNA replication of the lagging strand	(Slack & Arif, 2007)
49	PCNA	ETL	39643	<-	40498	28.6	285	5.2	DNA Bind	Nucleosome	DNA replication factor/involved in repair of UV damaged DNA/promote cell cycle shifts into S phase – Non-essential but enhances infectivity.	(Slack & Arif, 2007)
58	6.8 kDa		47574	<-	47745	6.8	57	9.8	Nuclear	Nucleosome		
65	DNA pol		52329	<-	55281	114.3	984	8.6	DNA Bind	Nucleosome	DNA polymerase - One of the six core baculovirus replication proteins	(Slack & Arif, 2007)
66	Desmoplakin	93 kDa	55292	->	57716	93.9	808	5.3	Topoisomerase	Nucleosome	possibly involved in mediating supercoiling of viral DNA and shows some homology to Type I topoisomerases.	(Slack & Arif, 2007)
67	<i>Jef-3</i>		57721	<-	58876	44.6	385	5.1	DNA Bind	Nucleosome	One of the six core baculovirus replication proteins, binds to single stranded DNA, P143 and IE-1	(Slack & Arif, 2007)
70	HCF-1		60110	->	60980	34.4	290	9.2	Zincfing	Nucleosome	Required for DNA replication in <i>T. ni</i> and allows oral infection of <i>T. ni</i> larvae.	(Slack & Arif, 2007)
77	VLF-1		63813	<-	64950	44.4	379	9.2	Nuclear	Nucleosome	essential for virus replication, also associated with BV nucleocapsid, during nucleocapsid assembly may possibly play a role in processing of the viral genome.	(Slack & Arif, 2007)
86	PNK/PNL		72131	<-	74213	80.8	694	8.8	NTPBind	Nucleosome	Non-essential - Possibly involved in RNA splicing IE-0, which effects host specificity through ratio of IE-0/IE-1	(Slack & Arif, 2007)
88	cg30		74737	<-	75529	30.1	264	8.8	LeucineZip	Nucleosome	Possibly a ubiquitin ligase due to it being a ring finger protein which could catalyze the ubiquitination and destruction of p53 – but experimental work was inconclusive for CG30 ubiquitin ligase activity. Deletion mutants produced more BV and were more orally infectious.	(Thiem and Miller, 1989)
92	p33		78699	<-	79476	30.9	259	8.2	p53 binding	Nucleosome	Possibly involved in preventing apoptosis/cell cycle progression due to binding to p53 which is involved in apoptosis and cell cycle regulation.	(Slack & Arif, 2007)
95	helicase	p143	80694	<-	84357	143.2	1221	8.4	DNA Bind	Nucleosome	One of the six core baculovirus replication proteins, involved in separating viral DNA during DNA replication.	(Slack & Arif, 2007)
100	p6.9	basic protein, VP12	86712	<-	86877	6.9	55	12.3	Nuclear	Nucleosome	Interacts with DNA through positively charged arginine residues, enabling condensation of DNA into nucleocapsid. Interaction believed to be control through phosphorylation.	(Slack & Arif, 2007)
133	Alk-exo	AN	112560	->	113817	48.3	419	8.9	DNA Bind	Nucleosome	Alkaline exonuclease – possibly involved in removing aberrant DNA structures from condensing DNA, also shown to bind to complex with LEF-3	(Slack & Arif, 2007)

Chapter 3

orf	Name	Alt Name	Left	Dir	Right	Predicted MW (kDa)	aa	pI	Motifs	Proposed ODV localization	Comments	References
147	IE-1		127198	->	128944	66.9	582	6.1	DNA Bind	Nucleosome	One of the six core baculovirus replication proteins and transcriptional activator of viral genes, could possibly be the main reason why IE-1 is found in ODVs to begin transcription of early viral genes after unpackaging of the viral genome in the nucleus	(Kawasaki <i>et al.</i> , 2004)
89	vp39	capsid	75534	<-	76575	38.9	347	6.2		Capsid	Main Structural Protein of Nucleocapsid	(Slack & Arif, 2007)
129	p24	capsid protein	109900	->	110494	22.1	198	5.8		Capsid	Found also in the BV capsid, <i>SpitNPV</i> 's P24 believed to be homodimer in ODV	(Slack & Arif, 2007)
9	p78/83	ORF1629, 83/87	5287	<-	6916	60.7	543	5.8	LeucineZip	Capsid Base	Phosphoprotein, nucleates actin polymerisation – possibly involved in translocation into nucleus after infection	(Slack & Arif, 2007)
5	12.4 kDa	ORF 4	2779	->	3106	12.4	109	9.1		Nucleocapsid		
30	54.6 kDa	ORF 15	24315	<-	25704	54.7	463	7.6		Nucleocapsid		
39	p43		31078	<-	32167	43.5	363	9.8		Nucleocapsid		
54	vp1054		45222	->	46317	42.1	365	8.2		Nucleocapsid	Essential protein which is required for capsid assembly through arrangement of VP39 monomers	(Slack & Arif, 2007)
59	8.2 kDa		47882	<-	48089	8.2	69	9.4		Nucleocapsid	strong homology to ChaB, an <i>E. Coli</i> protein involved in divalent cation transport – possibly role for orf59 is Zn ²⁺ transport into capsid which inhibits phosphorylation of p6.9	(Slack & Arif, 2007)
74	30.5 kDa		62311	<-	63106	30.6	265	5		Nucleocapsid		
79	12.1 kDa		65290	<-	65602	12.2	104	10.3		Nucleocapsid	Very similar to UvrC intronencoded nucleases, bacterial protein involved in DNA repair after UV damage	
101	BV/ODV-C42	p40	86921	<-	88004	41.5	361	8.2		Nucleocapsid	Yeast two-hybrid experiments show interactions with p78/83 and ODV-EC27	(Braunagel <i>et al.</i> , 2001)
102	13.1 kDa		88026	<-	88392	13.3	122	5.3		Nucleocapsid	Possibly involved in shifting the cell cycle – shows some similarities to Never In Mitosis gene A which is a protein involved in cell cycle regulation.	(Slack & Arif, 2007)
104	vp80	p87	89564	->	91637	79.9	691	5.4		Nucleocapsid	Structural protein only found in NPVs	(Slack & Arif, 2007)

Chapter 3

orf	Name	Alt Name	Left	Dir	Right	Predicted MW (kDa)	aa	pl	Motifs	Proposed ODV localization	Comments	References
109	ODV-EC43	44.8 kDa	94721	<-	95891	44.8	390	8.5		Nucleocapsid	Located both to the nucleocapsid and envelope of ODVs	(Fang <i>et al.</i> , 2003)
114	49 kDa		97886	<-	99158	49.3	424	6.9		Nucleocapsid		
132	25 kDa		111873	->	112530	25.1	219	8.5		Nucleocapsid		
142	49 kDa		123632	->	125063	55.4	477	8.7		Nucleocapsid	Essential for BV production - Required for ODV envelopment and subsequent	(McCarthy <i>et al.</i> , 2008)
80	gp41		65607	<-	66834	45.4	409	8.2	O-glyc	Tegument	Temperature sensitive mutant – prevented nucleocapsids exit from the nucleus therefore effected BV production	(Braunagel and Summers, 2007)
144	ODV-EC27		125357	->	126227	33.5	290	6	Cyclin	Tegument	Effects cell cycle, by binding to cyclin dependent kinases – binds to cycle kinase 2 which causes G2/M phase arrest.	(Belyavskiy <i>et al.</i> , 1998)
16	BV/ODV-E26	ORF 1, DA26	13092	->	13767	25.9	225	10.1		Envelope	Lacks transmembrane domain - associates with FP25K which possibly gives them a role in BV/ODV envelope proteins trafficking	(Burks <i>et al.</i> , 2007)
22	Pif2	ORF 6/8	17301	->	18447	43.8	382	5.1	Transmembrane	Envelope	ORFs 6/8 joined as a larger coding region - Essential for oral infection – binding to the midgut cells	(Pijlman <i>et al.</i> , 2003)
23	F-protein	ORF 9, ENV	18513	->	20583	79.9	690	5.3	Transmembrane	Envelope	Fusion protein - BV envelope with host endosomal membranes releasing nucleocapsids for initial infection - Accelerates mortality of host	(Braunagel & Summers, 2007)
46	ODV-E66		36718	->	38830	79	704	6.3	Transmembrane	Envelope	Interacts with ODV-E25 and possibly involved in ODV capsid envelopment – Deletion mutant had no effect on BV production.	(Hong <i>et al.</i> , 1997)
61	FP25K	FP protein	48513	<-	49155	22.2	214	9.1		Envelope	Also found in BV – associates with BV/ODV-E26 which possibly gives them a role in BV/ODV envelope proteins trafficking.	(Wu <i>et al.</i> , 2005)
83	VP91	p95, p91, p96	67884	->	70425	96.2	847	4.6	Transmembrane	Envelope	Possibly involved in cross linking virion envelope with nucleocapsid through covalent bonds to unknown nucleocapsid protein(s). Also found in BV.	(Braunagel & Summers, 2007)
94	ODV-E25	p25	79971	->	80655	25.5	228	5.9	Transmembrane	Envelope	Found also in BV, but more abundant in ODVs – Interacts with ODV-E66 and possibly involved in ODV capsid envelopment	(Hong <i>et al.</i> , 1997; Li <i>et al.</i> , 2006)
96	ODV-E28	Pif4	84346	->	84865	19.8	173	4.8	Transmembrane	Envelope	One of the 31 core baculovirus genes, Located to the ODV envelope and essential for oral infection	(Fang <i>et al.</i> , 2009)

Chapter 3

orf	Name	Alt Name	Left	Dir	Right	Predicted MW (kDa)	aa	pI	Motifs	Proposed ODV localization	Comments	References
115	Pif3		99182	<-	99794	23	204	4.9	Transmembrane	Envelope	Essential for oral infection – not involved in binding/fusion to the midgut cells – possibly plays around in translocation of ODV capsid along the microvillus	(Ohkawa <i>et al.</i> , 2005)
119	Pif1		100699	->	102289	59.8	530	5.6	Transmembrane	Envelope	Essential for oral infection – binding to the midgut cells	(Kikhno <i>et al.</i> , 2002)
138	p74	Pif-0	119135	<-	121070	73.9	645	4.9	Transmembrane	Envelope	Essential for oral infection, binds to 30kDa insect midgut receptor protein and the central transmembrane domain possibly involved in membrane fusion after trypsin cleavage.	(Faulkner <i>et al.</i> , 1997; Haas-Stapleton <i>et al.</i> , 2004)
143	ODV-E18		125153	->	125339	6.6	62	12	Transmembrane	Envelope	Shown to be strongly associated homodimer – produces a chimeric fusion protein or a heterodimer called ODV-E35 with ODV-EC27 – Essential for BV production.	(McCarthy and Theilmann, 2008)
145	11k protein		126299	->	126530	8.9	77	4.6	Transmembrane	Envelope	Enhances oral infectivity – associated to ORF150 another 11k protein – Also incorporated into BV	(Lapointe <i>et al.</i> , 2004)
148	ODV-E56		129008	<-	130136	40.9	376	5.1	Transmembrane	Envelope	Essential for oral infection and Over expression causes a major decrease in envelopment of ODV.	(Braunagel <i>et al.</i> , 1996; Theilmann <i>et al.</i> , 1996; Rashidan <i>et al.</i> , 2002)
150	11k protein		130456	->	130753	11.2	99	4.6	Transmembrane	Envelope	Enhances oral infectivity – sometimes associated to ORF145 another 11k protein – Possibly involved in release of ODVs from OB protein matrix. - Also incorporated into BV	(Lapointe <i>et al.</i> , 2004)

The table was constructed from four key sources (Ayres *et al.*, 1994; Braunagel *et al.*, 2003; Slack & Arif, 2007; Rohmann, 2011) to create a list of 48 ODV-associated proteins. The putative functions of many of these proteins has been analysed in the literature and the results summarised in the comments column. The left and right columns define the end positions of the ORF on AcMNPV genome, Dir column indicates the direction of the transcript(s) from that ORF, aa column is the number of amino acids encoded by the ORF from the first ATG codon and 'pI' column is the isoelectric point of the protein expressed from the ORF.

3.2.1 Occlusion-derived virus structural protein: ODV-E66

The *odv-e66* is located in the *Hind*III E fragment of AcMNPV genome at 36718-38830bp (Ayres *et al.*, 1994). Sequence analysis indicated that *odv-e66* is 2112 bp and encodes a protein of 704 aa with a predicted molecular mass of 79kDa. Alignment of the ODV-E66 peptide sequence with its homologues in other Type I and II alphabaculovirus shows that it is highly conserved among Type I and shares 29% amino acid sequence identity with Type II. From the alignments in Figure 3.1, it can be seen that both the C- and N-termini of ODV-E66 Type I and Type II demonstrated large variation, as shown by the shift in the transmembrane domain between these homologues. However, the central domain of ODV-E66 shows more conservation with the Type II alphabaculovirus showing ~45% amino acid sequence identity compared to an overall ~29% amino acid sequence identity. AcMNPV ODV-E66 also shares ~47% amino acid sequence identity when aligned with homologues from the betabaculoviruses. In all three alignments, the N-termini of ODV-E66 homologues show large variation compared to the rest of the peptide sequence. This could suggest that the active part of ODV-E66 is either within the central domain or C-terminus of ODV-E66 with the N-terminus important in anchoring ODV-E66. A transmembrane region was identified by TMPRED at the EXPASY server and ODV-E66 also contains an inner nuclear membrane sorting motif (INM-SM) (Braunagel and Summers, 2007). The protein has 13 potential N-linked glycosylation consensus sequences (Asn-Xaa-Ser/Thr), however, only eight of them were predicted to be glycosylated by NetNGlyc 1.0 Server at CBS (Center for biological sequence analysis).

The N-terminal amino acid sequence is highly hydrophobic and it has been demonstrated that the protein is membrane bound at this terminus to the ODV envelope (Hong *et al.*, 1997). It was demonstrated that 23 amino acids at the N-terminus of ODV-E66 were sufficient to transport and localise fusion proteins to discrete locations within the nucleus. The results from this study also suggested that ODV envelope proteins could be transported back from the endoplasmic reticulum to the nucleus through the outer and inner nuclear membrane (Hong *et al.*, 1997). The transportation of ODV-E66 is believed to be mediated by another viral protein FP25K, due to deletion mutants of FP25K failing to translocate ODV-E66 to inner nuclear membrane vesicles (Rosas-Acosta *et al.*, 2001).

Internal transmembrane motifs, which are not conserved in position and do not have high transmembrane probability scores, are found in some ODV-E66 homologues. ODV-E66 is found in all lepidopteran baculoviruses, along with another envelope protein ODV-E25. It has been demonstrated by yeast two hybrid and immunoprecipitation experiments that these two proteins interact at the exposed C-terminal regions (Braunagel *et al.*, 1999).

The same study using the previous technique also showed that ODV-E66 binds to the major capsid protein VP39; suggesting strongly that both ODV-E66 and ODV-E25 are closely oriented on the inner side of the ODV envelope (Braunagel *et al.*, 1999). Further support for this was shown when ODV-E25 remained associated with the nucleocapsid and was not completely released from the ODV by NP-40 detergent (Russell and Rohrmann, 1997). This could suggest that ODV-E66 and ODV-E25 are involved in ODV capsid envelopment. Therefore, if ODV-E66 is oriented inside then no effect on ODV attachment or fusion to the midgut would be expected (Russell and Rohrmann, 1997). However, evidence against this role has been shown because ODV-E66 can be cleaved by trypsins in ODV preparations, and this would indicate that ODV-E66 is exposed at the surface (Hong *et al.*, 1994).

Interestingly, however, yeast two hybrid and immunoprecipitation experiments carried out on samples from mutant virus infections that expressed ODV-E66 lacking its N-terminus (Δ NE66), demonstrated that Δ NE66 interacted with α -adaptin. In *Drosophila melanogaster* midgut plasma membrane, α -adaptin is a marker for endocytosis (Dornan *et al.*, 1997), therefore, if this interaction is functionally important, ODV-E66 could function during primary infection as a recognition factor for ODV and midgut cells (Braunagel and Summers, 2007). During a random screening for peptides that bound to brush border membrane vesicles derived from the midgut of *Heliothis virescens*, two peptides that have similarity to ODV-E66 were identified. It was then shown that ODV-E66 could bind to whole midgut tissues of *H. virescens* and during competitive assays between one of these peptides identified HV1 and purified AcMNPV ODV a decrease in mortality of the larva was seen at lower doses and increased in survival times at the highest doses. Therefore this result suggests that ODV-E66 is located on the surface of the ODV envelope and may play a role in larva midgut epithelium infection (Sparks *et al.*, 2011b).






Recently Xiang *et al.* (2011) constructed deletion mutant virus that did not express the N-terminal of ODV-E66 and demonstrated that this deletion mutant virus had no affect on BV production. However, the LD₅₀ for this deletion mutant virus was 10 times higher than the rescued or parental viruses when larva were infected orally, suggesting that ODV-E66 is not essential for viral replication but plays an important role in the oral infectivity of AcMNPV. A truncated form of ODV-E66 has recently been shown to have enzyme activity to catalyze the breakdown of chondroitin sulphate. This linear polysaccharide molecule influences development, organ morphogenesis, inflammation and infection by interacting with and regulating cytokines and growth signal transductions (Sugiura *et al.*, 2011). However, further study is required to understand the role of this enzyme activity in the baculovirus replication cycle.

3.3.2 Occlusion-derived virus structural protein: ORF79

The *orf79* is located between 65290-65602bp on the AcMNPV genome and produces a protein of 104 amino acids with a predicted molecular mass of 12.2 kDa, which is believed to be associated with the ODV nucleocapsid (Braunagel *et al.*, 2003). However, analysis of the promoter sequence of *orf79* showed no transcriptional start site motif that is normally associated with baculovirus genes upstream of the predicted translational start codon. This could suggest that *orf79* is expressed from the *gp41* promoter by read through. The function of *orf79* is unknown but it shares strong homology to a bacterial UvrC intron-encoded endonuclease, which is involved in DNA repair after UV damage (Aravind *et al.*, 1999). The UvrC intron-encoded endonucleases make incisions on either side of the DNA lesion enabling repair of the damaged DNA (Aravind *et al.*, 1999). In the bacterial system, the nucleases form part of a complex with ABC-type UvrA ATPases and UvrB helicases (Lin *et al.*, 1992; Lin and Sancar, 1992). Therefore this suggests that *orf79* could be a member of the UvrC superfamily of endonucleases and could play a role in UV damage repair of the baculovirus genome. It is possible that AcMNPV could have acquired *orf79* from a bacteria or another insect virus, as there is an *orf79* homologue in the insect iridovirus type 6 (Rohrmann, 2011).

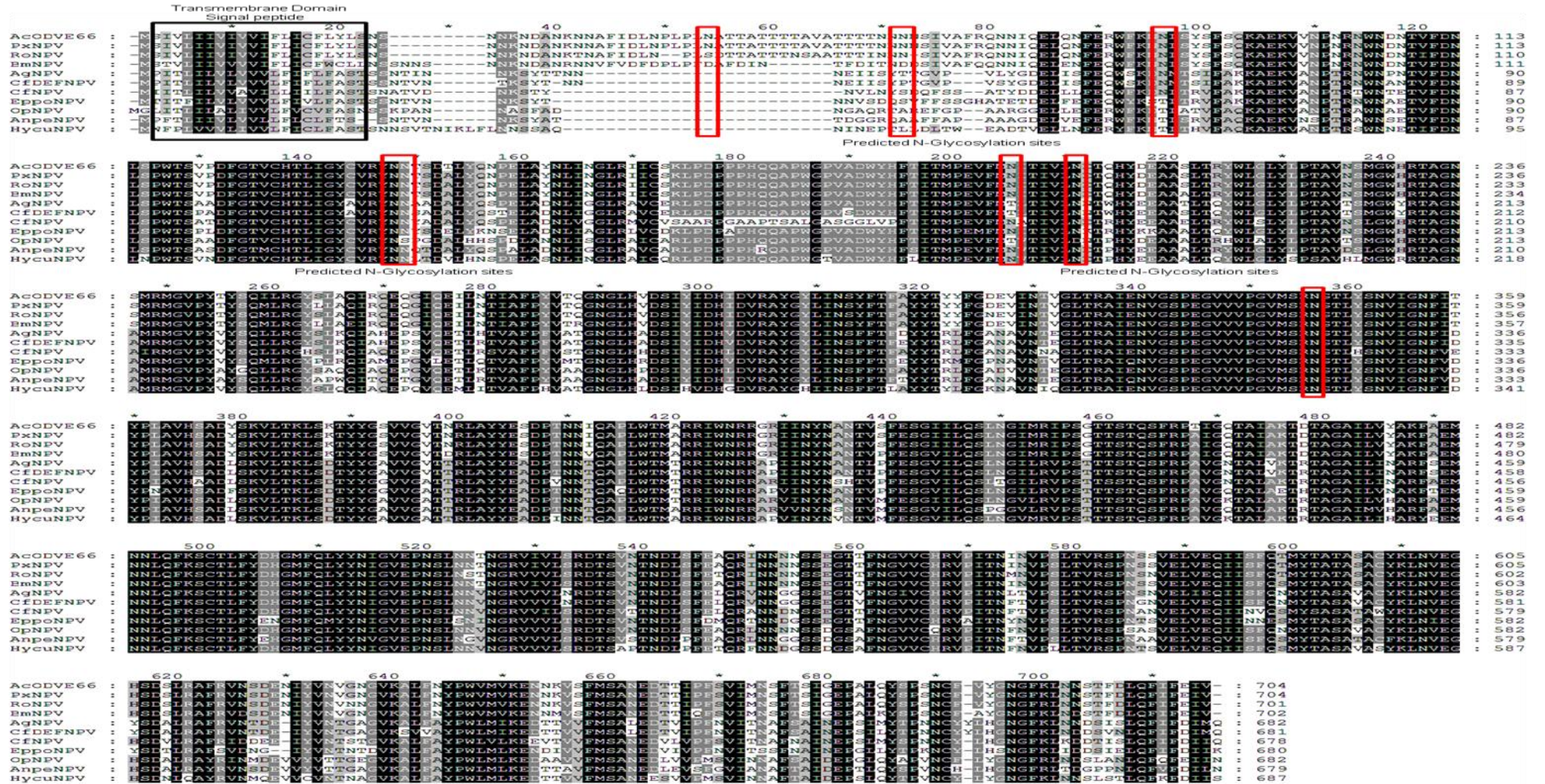
Figure 3.2 presents alignments of the ORF79 peptide sequence with its homologues in alphabaculovirus Type I, which show that ORF79 is highly conserved. ORF79 has also been aligned with homologues from two enterobacteria, *Yersinia pseudotuberculosis* and *Dickeya zeae*, and another invertebrate virus, *Trichoplusia ni* ascovirus. This alignment demonstrated the high similarity between these proteins, which supports the theory that ORF79 may have been acquired from bacteria (Rohrmann, 2011). No signal peptide sequence was predicted from the ORF79 amino acid sequence using SIGNALP and no transmembrane region was identified by TMPRED at the EXPASY server. ORF79 has no potential N-linked glycosylation consensus sequences (Asn-Xaa-Ser/Thr) and none were predicted to be glycosylated by NetNGlyc 1.0 Server at CBS, thus further supporting the theory that *orf79* was gained from bacteria, as glycosylation does not occur in bacteria.

Figure 3.1 Sequence alignments of Type I and Type II ODV-E66 Sequences

The sequence alignments of type I and type II alphabaculoviruses ODV-E66 sequences were shaded using the GeneDoc software package to highlight the conserved amino acid sequences; (Conserved mode: , 100%, 80% , 60% ). Potential transmembrane domains and a signal peptide have been indicated by  and possible N-glycosylated sites have been indicated with . AcMNPV ODVE66 sequence was also aligned against betabaculovirus ODV-E66 homologues to demonstrate the conserved amino acids between ODV-E66 alphabaculovirus and betabaculovirus.

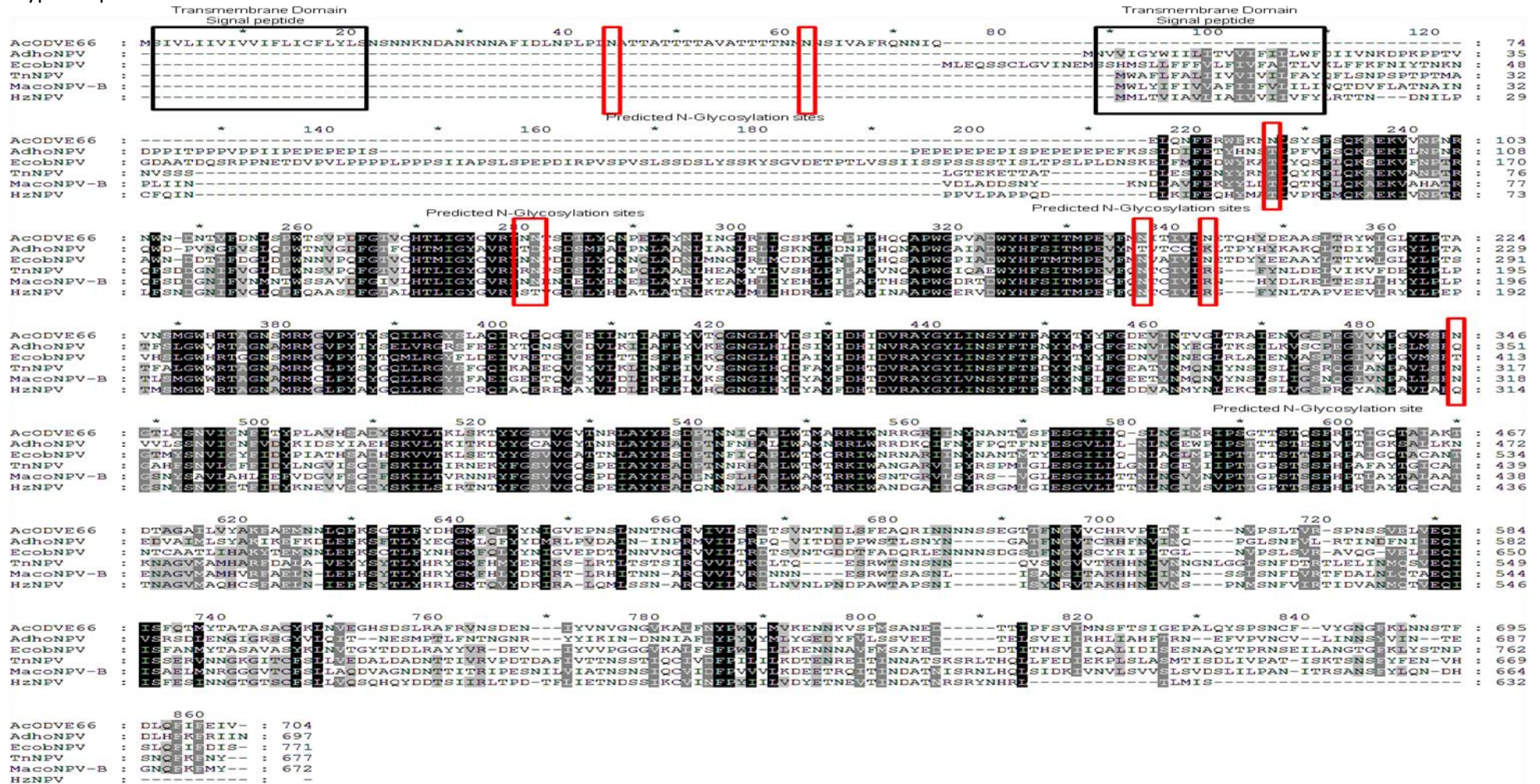
Chapter 3

Type I alphabaculovirus



Chapter 3

Type II alphabaculovirus



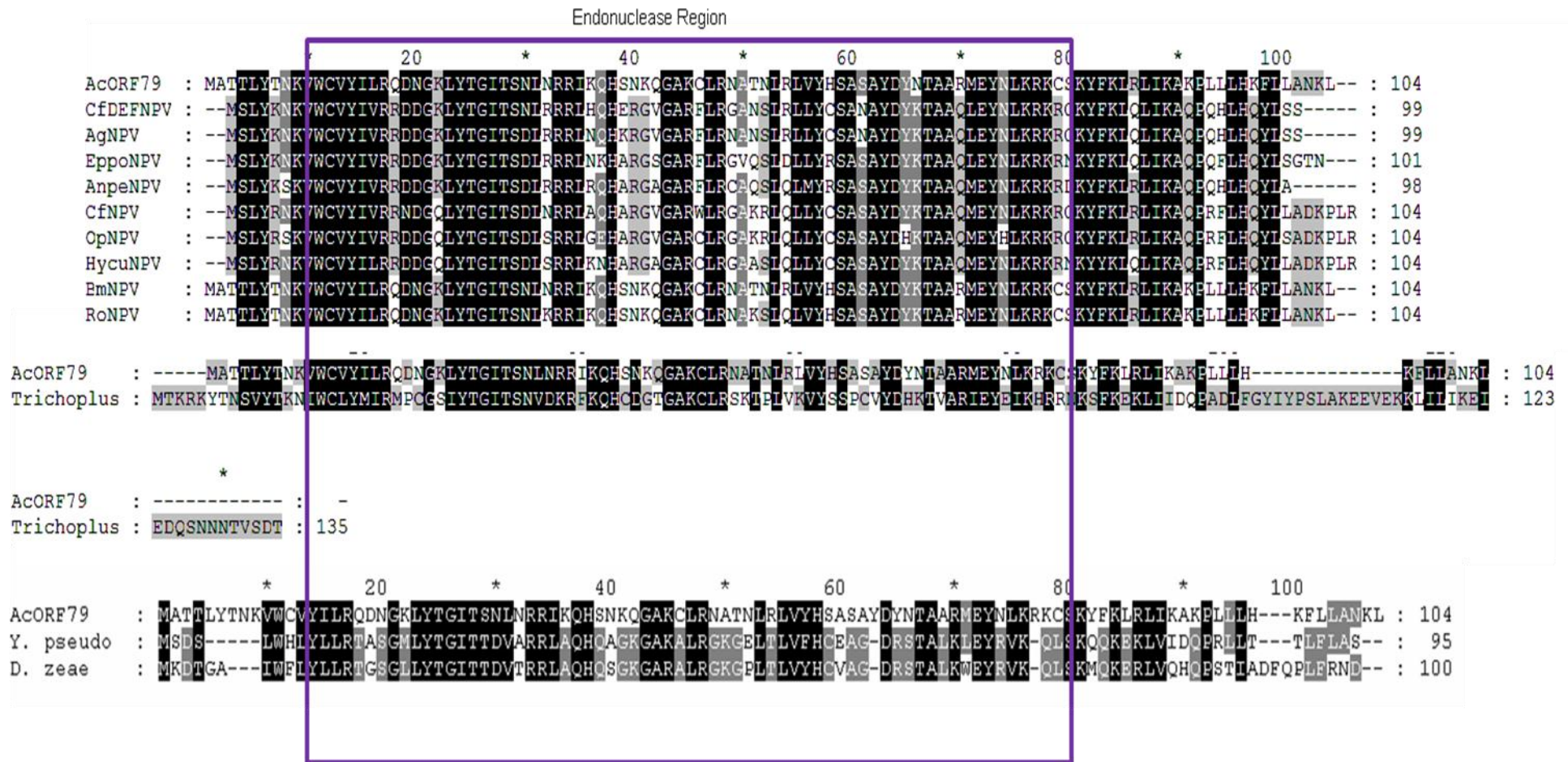


Figure 3.2 Sequence alignments of ORF79 Sequences

The sequence alignments of type I alphabaculoviruses ORF79 sequences were shaded using the GeneDoc software package to highlight the conserved amino acid sequences; (Conserved mode: 100%, 80%, 60%). ORF79 was also aligned against enterobacteria; *Yersinia pseudotuberculosis* and *Dickeya zeae* and another invertebrate infecting virus; *Trichoplusia ni* ascovirus to show the conserved sequences between these species. The Endonuclease region is highlighted by .

3.2.3 Occlusion-derived virus structural protein: CG30

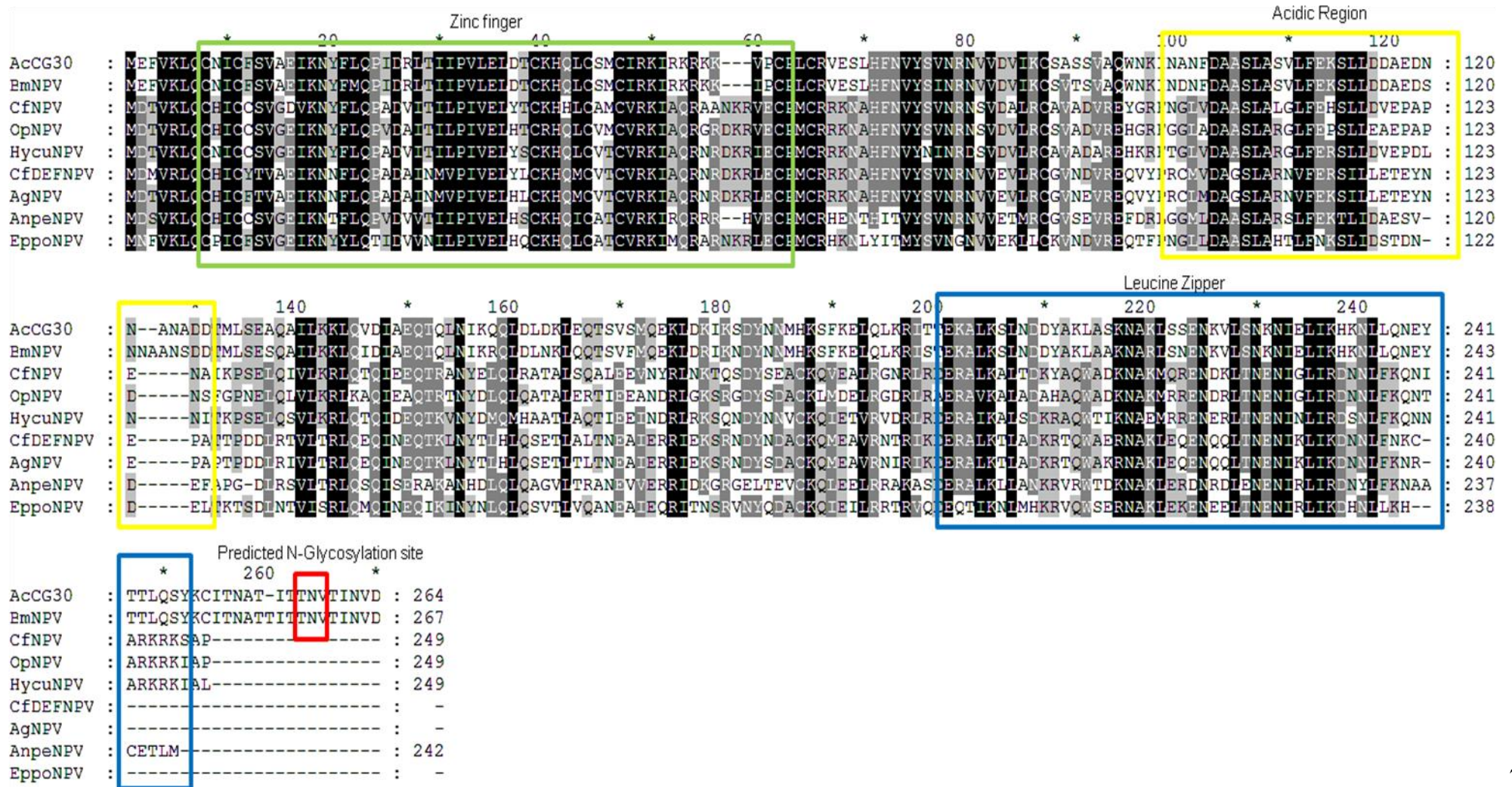
The *cg30* is located in the *HindIII* C fragment of AcMNPV genome at coordinates 74737-75529bp (Ayres *et al.*, 1994). Sequence analysis indicated that *cg30* is 792 bp and encodes a protein of 264 aa with a predicted molecular mass of 30.1 kDa. Figure 3.3 shows the alignments of the CG30 peptide sequence with its homologues in other type I and II alphabaculovirus, showing it shares ~34% amino acid sequence identity with Type I and only ~14% with Type II. No signal peptide sequence was predicted from the CG30 amino acid sequence using SIGNALP and no transmembrane region was identified by TMPRED at the EXPASY server either. CG30 has two potential N-linked glycosylation consensus sequences (Asn-Xaa-Ser/Thr), however, only one of them was predicted to be glycosylated by NetNGlyc 1.0 Server at CBS.

The location of CG30 is most likely to be inside the nucleocapsid bound to the viral genome because CG30 contains two DNA binding motifs, comprising a zinc ring finger motif (C3HC4) and a leucine zipper motif at the C-terminus and N-terminus, respectively (Thiem and Miller, 1989). The *cg30* is only found in NPV and all homologues of *cg30* are located downstream of, and in the same direction as, *vp39*, which encodes the major capsid protein VP39. It has been suggested that *cg30* may be transcribed from the *vp39* late promoter and that the bicistronic mRNA produced can translate both CG30 and VP39 (Blissard *et al.*, 1989; Thiem and Miller, 1989; Lu and Iatrou, 1996). However, *cg30* contains its own early promoter and there is no evidence currently available that any bicistronic mRNA is produced. However, from the available information on baculovirus bicistronic translation and the fact that only 2bp separate the end of *vp39* and the beginning of *cg30*, it is highly likely that CG30 is expressed at the same time as VP39 but in smaller amounts (Chang and Blissard, 1997).

The AcMNPV genome expresses a number of viral proteins that contain ring finger motifs, however, CG30 is the only one located to the ODV. Imai *et al.* (2003) hypothesized that these ring finger motif proteins were ubiquitin ligases that could possibly be involved in the ubiquitination and destruction of cellular p53. The targeting and degradation of p53 to shift the cell cycle into the DNA replication phase using virus encoded ubiquitin ligases has already been described for other viruses such as herpesviruses and adeno-associated viruses (Weger *et al.*, 2002; Boutell and Everett, 2003). However, tests for ubiquitin ligase activity for CG30 were inconclusive (Imai *et al.*, 2003).

Chapter 3

Type I alphabaculovirus



Chapter 3

Type II alphabaculovirus

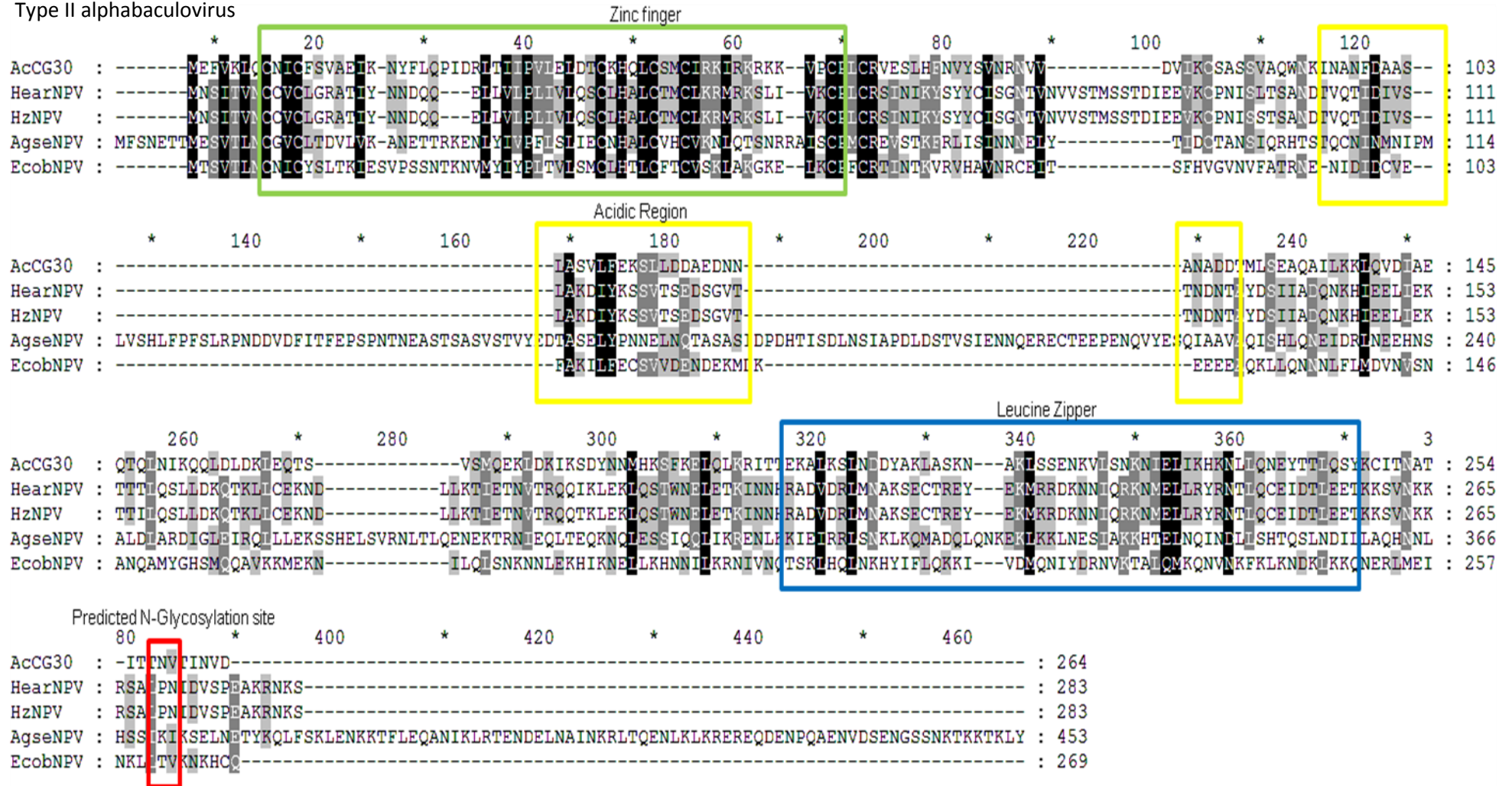


Figure 3.3 Sequence alignments of Type I and Type II CG30 Sequences

The sequence alignments of type I and type II alphabaculoviruses CG30 sequences were shaded using the GeneDoc software package to highlight the conserved amino acid sequences; (Conserved mode: 100%, 80%, 60%). Zinc finger region is indicated by , Acidic region is indicated by and Leucine Zipper region is indicated by .

A *cg30* deletion mutant virus was shown to be slightly more infectious orally and produced more BV than the parental virus. This showed that CG30 was nonessential for viral infection and, in fact, seemed to be limiting the production of BV and OB, permitting the authors to conclude that CG30 might have some long term evolutionary benefit (Passarelli and Miller, 1994). The CG30 contains a central acidic domain that suggests it could play a role in transcriptional activation; however, there is no evidence to date to support this theory (Thiem and Miller, 1989; Passarelli and Miller, 1994).

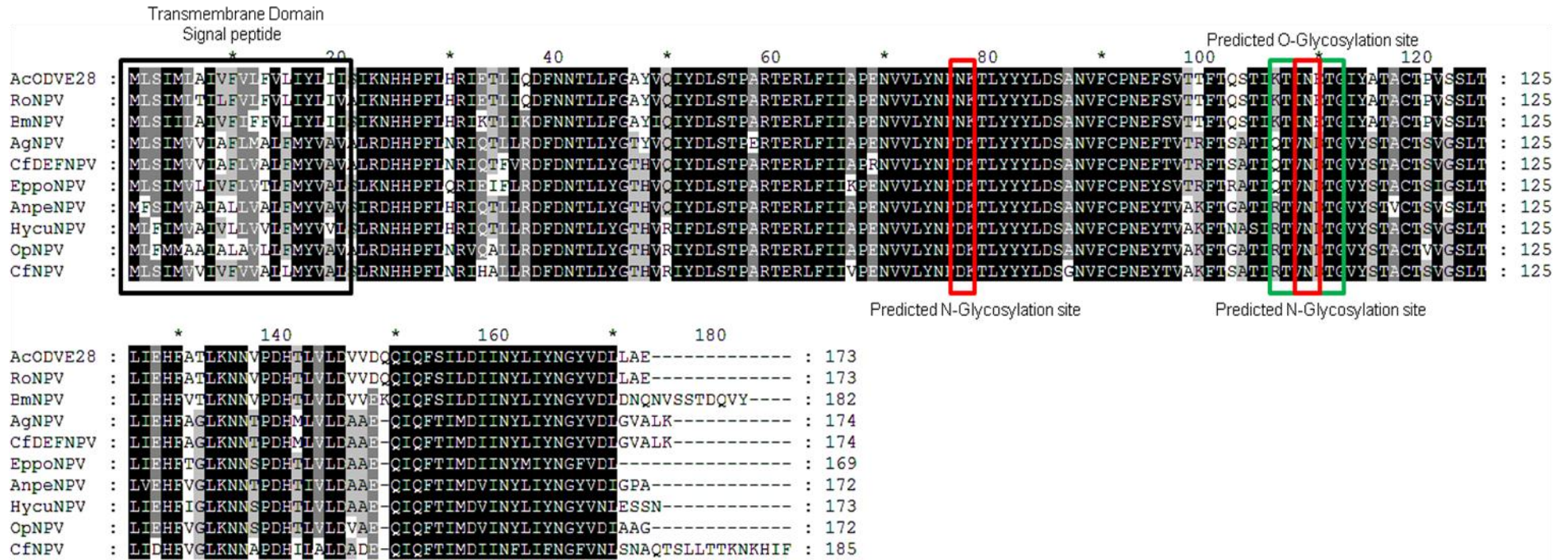
3.3.4 Occlusion-derived virus structural protein: ODV-E28

The *odv-e28* is located in the *Hind*III H fragment of AcMNPV genome at coordinates 84346-84867bp (Ayres *et al.*, 1994). Sequence analysis indicated that *odv-e28* is 519 bp and encodes a protein of 173 aa with a predicted molecular mass of 19.8 kDa. Figure 3.4 shows the alignments of the ODV-E28 peptide sequence with its homologues in other Type I and II alphabaculovirus, showing it is highly conserved among Type I and shares ~53% amino acid sequence identity with Type II. A transmembrane region was identified by TMPRED at the EXPASY server and the protein was predicted to contain an INM-SM (Braunagel and Summers, 2007). ODV-E28 has three potential N-linked glycosylation consensus sequences (Asn-Xaa-Ser/Thr) with only two of them being indicated by NetNGlyc 1.0 Server at CBS to be glycosylated. ODV-E28 could also contain two potential O-linked glycosylation sites as predicted by NetOGlyc 3.1 Server at CBS and as indicated in Figure 3.4. However, it should be noted that the scores for these O-linked glycosylation sites were only just over the threshold of 0.5 at 0.510 and 0.526.

The *odv-e28* is one of the 31 core genes conserved among all baculoviruses sequenced to date. The ODV-E28 demonstrates similarities with other ODV envelope proteins at the N-terminal region. Most of the core genes have been assigned roles related to DNA replication, gene expression, packaging and assembly or *per os* infection. The ODV-E28 homologue in *Bombyx mori* nucleopolyhedrovirus (BmNPV) is ORF79, encoding Bm79 a 28 kDa protein that was located to the ODV envelope, and represented the first characterization of ODV-E28 (Xu *et al.*, 2006). Recently, ODV-E28 has been shown to be involved in *per os* infection and it has been suggested to be part of the *per os* infectivity factor family; *pif4* (Fang *et al.*, 2009). The ODV-E28 is transcribed from a late promoter located 141 nucleotides upstream of a start codon within *helicase* and produces a protein with predicted molecular mass of 19.8 kDa. The ODV-E28 has a highly hydrophobic transmembrane signal peptide, which strongly supports its proposed location in the ODV envelope (Fang *et al.*, 2009).

Chapter 3

Type I alphabaculovirus



Chapter 3

Type II alphabaculovirus



Figure 3.4 Sequence alignments of Type I and Type II ODV-E28 Sequences

The sequence alignments of type I and type II alphabaculoviruses ODV-E28 sequences were shaded using the GeneDoc software package to highlight the conserved amino acid sequences; (Conserved mode: \blacksquare , 100%, \square , 80%, \square , 60%). Potential transmembrane domains and a signal peptide have been indicated by \square and possible N-glycosylated sites have been indicated with \square and possible O-glycosylated sites have been indicated with \square .

3.3.5 Occlusion-derived virus structural protein: ODV-EC43

The *odv-ec43* is located in the *HindIII* A1 fragment of AcMNPV genome at coordinates 94721-95891bp (Ayres *et al.*, 1994). Sequence analysis indicated that *odv-ec43* is 1170 bp and encodes a protein of 390 aa with a predicted molecular mass of 44.8 kDa. Figure 3.5 illustrates the alignments of the ODV-EC43 peptide sequence with its homologues in other Type I and II alphabaculovirus, showing it is highly conserved among Type I and shares about 50% amino acid sequence identity with Type II. The region between 310 and 324 amino acids of ODV-EC43, that is not highly conserved among Type I alphabaculovirus, is missing in Type II alphabaculovirus, suggesting that this sequence may be redundant and not necessary for ODV-EC43 function. No signal peptide sequence was predicted using SIGNALP and no transmembrane region was identified by TMPRED at the EXPASY server. ODV-EC43 has three potential N-linked glycosylation consensus sequences (Asn-Xaa-Ser/Thr) as indicated by NetNGlyc 1.0 Server at CBS, however only one of them was predicted to actually be glycosylated.

The ODV-EC43 is another one of the 30 conserved genes among baculoviruses, but its function is unknown. Some ODV-EC43 homologues contain transmembrane domain motifs. The ODV-EC43 homologue in *Helicoverpa armigera* single nucleocapsid nucleopolyhedrovirus (HaSNPV) is ORF94, encoding Ha94 that was located to both the ODV envelope and the nucleocapsid (Fang *et al.*, 2003). The ODV-EC43 has been detected in the AcMNPV ODV; but was not specifically located to any fraction of the ODV in the study (Braunagel *et al.*, 2003). However, the fact that ha94 is located to both the envelope and nucleocapsid of ODV, does suggest that AcMNPV ODV-EC43 is located to both these locations. Interestingly ODV-EC43 appears to be under the control of both an early and late promoter, whereas Ha94 is only under control of a late promoter and was expressed from 24hpi (Fang *et al.*, 2003). If the early promoter is active in AcMNPV, this could suggest that ODV-EC43 plays an earlier role in AcMNPV infection that has not been observed in HaSNPV. More recently, Lin *et al.* (2009) demonstrated, using electron microscopy, that deletion of *odv-ec43* from AcMNPV blocked nucleocapsid formation that resulted in the abrogation of BV and ODV production but had no affect on viral DNA replication, as shown by qPCR analysis.

Chapter 3

Tyve I alphabaculovirus

```

AcODVEC43 : MECPFQICVGISDRFFAFPHNLVEPQSDVGNKLIENLIVYVPTEDRLYIDKKCFPKENSVLVYRHEEDVNIIDSRSPKKTASATIVYWNPLVPITEIGAGETRVFVSVLLTNNLFCYNTMIVE : 122
RoNPV : MECPFQICVGISDRFFAFPHNLVEPQSDVGNKLIENLIVYVPTEDRLYIDKKCFPKENSVLVYRHEEDVNIIDSRSPKKTASATIVYWNPLVPITEIGAGETRVFVSVLLTNNLFCYNTMIVE : 122
BmNPV : MECPFQICVGISDRFFAFPHNLVEPQSDVGNKLIENLIVYVPTEDRLYIDKKCFPKENSVLVYRHEEDVNIIDSRSPKKTASATIVYWNPLVPITEIGAGETRVFVSVLLTNNLFCYNTMIVE : 122
CfNPV : MECPFQIKVGVSDRFFAFPPYSLVEPQSDVGNRPTEENLVVYVPTADVLYVEKRNFRFRSVLVYKHEQDYNGNSQAPKKTGAATVYWNPLVPITEIGAGETRVFVSVLLTNNLFCYNTMIVE : 122
OpNPV : MECPFQIKVGVSDRFFAFPPYSLVEPQSDVGNRPTEENLVVYVPTADVLYVEKRNFRFRSVLVYKHEQDYNGNSQAPKKTGAATVYWNPLVPITEIGAGETRVFVSVLLTNNLFCYNTMIVE : 122
HycuNPV : MECPFQIKVGVSDRFFAFPPYSLVEPQSDVGNKPTENLIVYVPTADVLYVEKRNFRFRSVLVYKHEQDYNGNSQAPKKTGAATVYWNPLVPITEIGAGETRVFVSVLLTNNLFCYNTMIVE : 122
AgNPV : MECPFQIKVGVSDRFFAFPPYSLVEPQSDVGNRPTEENLVVYVPTADVLYVEKRNFRFRSVLVYKHEQDYNGNSQAPKKTGAATVYWNPLVPITEIGAGETRVFVSVLLTNNLFCYNTMIVE : 122
CfDEFNPV : MECPFQIKVGVSDRFFAFPPYSLVEPQSDVGNRPTEENLVVYVPTADVLYVEKRNFRFRSVLVYKHEQDYNGNSQAPKKTGAATVYWNPLVPITEIGAGETRVFVSVLLTNNLFCYNTMIVE : 122
EppoNPV : MECPFQIKVGVSDRFFAFPPYSLVEPQSDVGNRPTEENLVVYVPTADVLYVEKRNFRFRSVLVYKHEQDYNGNSQAPKKTGAATVYWNPLVPITEIGAGETRVFVSVLLTNNLFCYNTMIVE : 122

```

```

AcODVEC43 : HENPKCPIEFYFETDMQSAQSALLKNR---NGQSVFPPIK-SNLRPIACEIPLSHFKELVESNDFLLCFNLETSTMVKILSLKRIFCFIQYRKPARYVINLPHEEIDNLYNKLNWERTRR : 240
RoNPV : HENPKCPIEFYFETDMQSAQSALLKNR---NGQSVFPPIK-SNLRPIACEIPLSHFKELVESNDFLLCFNLETSTMVKILSLKRIFCFIQYRKPARYVINLPHEEIDNLYNKLNWERTRR : 240
BmNPV : HENPKCPIEFYFETDMQSAQSALLKNR---NGQSVFPPIK-SNLRPIACEIPLSHFKELVESNDFLLCFNLETSTMVKILSLKRIFCFIQYRKPARYVINLPHEEIDNLYNKLNWERTRR : 240
CfNPV : HENPKCPIEFYFGLMCPACKLIMNPKKLVDMRAHALPLNYNELRPINCELPLAHFKELTESDKFLLCFNLETSTMVKILSLKRIFCFIQYRKPARYVINLPHEEIDNLYNKLNWERTRR : 244
OpNPV : HENPKCPIEFYFGLMCPACKLIMNPKKLVDMRAHALPLNYNELRPINCELPLAHFKELTESDKFLLCFNLETSTMVKILSLKRIFCFIQYRKPARYVINLPHEEIDNLYNKLNWERTRR : 244
HycuNPV : HENPKCPIEFYFGLMCPACKLIMNPKKLVDMRAHALPLNYNELRPINCELPLAHFKELTESDKFLLCFNLETSTMVKILSLKRIFCFIQYRKPARYVINLPHEEIDNLYNKLNWERTRR : 244
AgNPV : HENPKCPIEFYFGLMCPACKLIMNPKKLVDMRAHALPLNYNELRPINCELPLAHFKELTESDKFLLCFNLETSTMVKILSLKRIFCFIQYRKPARYVINLPHEEIDNLYNKLNWERTRR : 244
CfDEFNPV : HENPKCPIEFYFGLMCPACKLIMNPKKLVDMRAHALPLNYNELRPINCELPLAHFKELTESDKFLLCFNLETSTMVKILSLKRIFCFIQYRKPARYVINLPHEEIDNLYNKLNWERTRR : 244
EppoNPV : HENPKCPIEFYFGLMCPACKLIMNPKKLVDMRAHALPLNYNELRPINCELPLAHFKELTESDKFLLCFNLETSTMVKILSLKRIFCFIQYRKPARYVINLPHEEIDNLYNKLNWERTRR : 244

```

```

AcODVEC43 : LMKGDVPSNCATVNRSSLKYIKCAQSLLCIPDYSQTVVDFVKMFQKIIFPYQLVENVIIKLNNEIQMVSSAPNKAEPYKIRLFCKNDSIAISSGIVPINMPDFSEPN-TFDYSDYANRIN : 361
RoNPV : LMKGDVPSNCATVNRSSLKYIKCAQSLLCIPDYSQTVVDFVKMFQKIIFPYQLVENVIIKLNNEIQMVLSAPNKAEPYKIRLFCKNDSIAISSGIVPINMPDFSEPN-TFDYSDYANRIN : 361
BmNPV : LMKGDVPSNCATVNRSSLKYIKCAQSLLCIPDYSQTVVDFVKMFQKIIFPYQLVENVIIKLNNEIQMISVAPNKAESYRKRIRLFCKNDSIAISSGIVPINMPDFSEPN-TFDYSDYANRIN : 362
CfNPV : LLRGDIPSNCAATVNRSSLQYVKAQTLLEIAKCSQTVVDFVRIQQLIFPYQIVPIVIVKLNSTNTST----GQIADVNRVRFVCKNDSVAITAGCVPVNMPDVAEIVN-TFDNADFDDEH : 361
OpNPV : LLRGDIPSNCAATVNRSSLQYVKAQTLLEIAKCSQTVVDFVRIQQLIFPYQIVPIVIVKLNSTNLAKS----GQTAHENRVRVFCNDSVAITAGCVPVNMPDVAEIVN-TFDNADFDDEH : 361
HycuNPV : LLRGDIPSNCAATVNRSSLQYVKAQTLLEIAKCSQTVVDFVRIQQLIFPYQIVPIVIVKLNSTNTN----GRVANVERMRVFCNDSVAITAGCVPVNMPDVAEIVN-TFDNADFDDEH : 360
AgNPV : LLRGDIPSNCAATVNRSSLQYVKAQTLLEIAKCSQTVVDFVRIQQLIFPYQIVPIVIVKLNSTNLKS---SMDTMRNCRVRFVCKNDSVAITLRGSPVNMPDVAEIVN-TFDNADFDDEH : 363
CfDEFNPV : LLRGDIPSNCAATVNRSSLQYVKAQTLLEIAKCSQTVVDFVRIQQLIFPYQIVPIVIVKLNSTNLKS---STDAIRNCRVRFVCKNDSVAITLRGSPVNMPDVAEIVN-TFDNADFDDEH : 363
EppoNPV : LLRGDIPSNCAATVNRSSLQYVKAQTLLEIAKCSQTVVDFVRIQQLIFPYQIVPIVIVKLNSTLVHTG-QYMETNKNCRVRFVCKNDSVAITLRGSPVNMPDVAEIVN-TFDNADFDDEH : 365

```

Predicted N-Glycosylation site

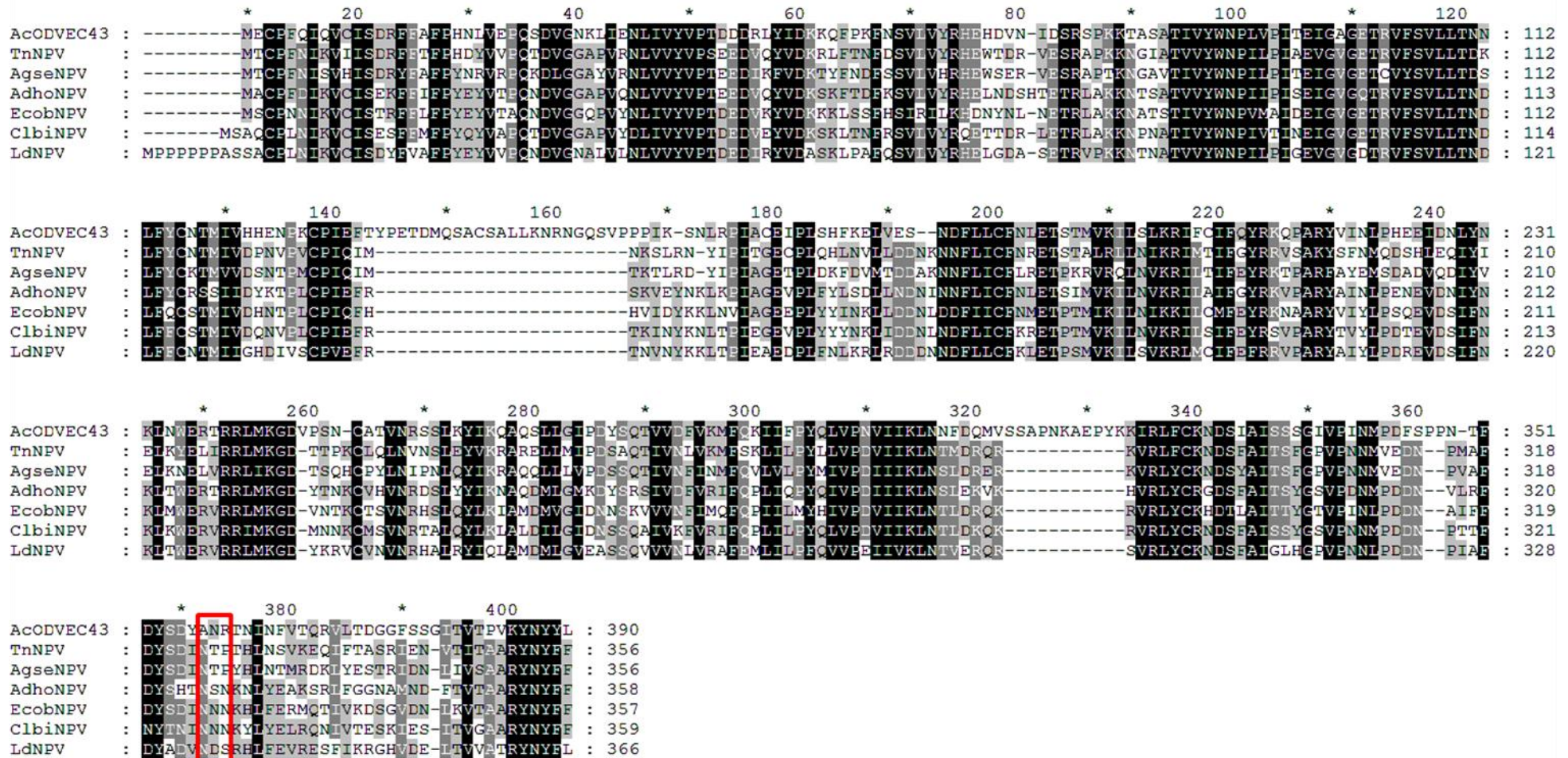
```

AcODVEC43 : INFVTRQVRLTEGGFSSGIVTVFVKYNYFL : 390
RoNPV : INFVTRQVRLTEGGFSSGIVTVFVKYNYFL : 390
BmNPV : INFVTRQVRLTEGGFSSGIVTVFVKYNYFL : 391
CfNPV : LKRAANRVAVDGVFTSGVTVHAVKYNFYFL : 390
OpNPV : LKQVANRVAVDGVFTSGVTVHAVKYNFYFL : 390
HycuNPV : LKRIANRVAVDGVFTSGVTVHAVKYNFYFL : 389
AgNPV : LKKIADRVSVDGVFTSGVAVHVMKYNFYFL : 392
CfDEFNPV : LKKIADRVSVDGVFTSGVAVHVMKYNFYFL : 392
EppoNPV : LKQVMNRVAVDGVFTSGVAVHVMKYNFYFL : 394

```

Chapter 3

Type II alphabaculovirus



Predicted N-Glycosylation site

Figure 3.5 Sequence alignments of Type I and Type II ODV-EC43 Sequences

The sequence alignments of type I and type II alphabaculoviruses ODV-EC43 sequences were shaded using the GeneDoc software package to highlight the conserved amino acid sequences; (Conserved mode: X, 100%, 80%, 60%). Possible N-glycosylated sites have been indicated with .

3.3.6 Occlusion-derived virus structural protein: ODV-E56

The ODV-E56 was characterised simultaneously in two baculoviruses: OpMNPV (Theilmann *et al.*, 1996) and AcMNPV (Braunagel *et al.*, 1996). The OpMNPV ODV-E56 migrated in SDS-PAGE as 46 and 43 kDa proteins (Theilmann *et al.*, 1996), whereas the AcMNPV ODV-E56 migrated as 67 and 56 kDa proteins (Braunagel *et al.*, 1996). The genome sequence predicts that the size of these proteins, for both OpMNPV and AcMNPV, is around 41 kDa, suggesting that both homologues are post-translationally modified. However, Braunagel *et al.* (1996) showed that N-glycosylation did not account for the differences and Theilmann *et al.* (1996) put forward the idea that the multiple forms observed may be due to proteolytic cleavage. Both studies demonstrated that ODV-E56 was exclusively associated with the ODV envelope (Braunagel *et al.*, 1996; Theilmann *et al.*, 1996).

Figure 3.6 depicts the alignments of the ODV-E56 peptide sequence with its homologues in other Type I and II alphabaculovirus, showing it is highly conserved among Type I examples and shares ~35% amino acid sequence identity with Type II. AcMNPV ODV-E56 also shares ~42% amino acid sequence identity when aligned with homologues from betabaculoviruses. A transmembrane region was identified by TMPRED at the EXPASY server but no signal peptide sequence was predicted using SIGNALP. ODV-E56 has four potential N-linked glycosylation consensus sequences (Asn-Xaa-Ser/Thr), although only two of them were predicted to be glycosylated by NetNGlyc 1.0 Server at CBS. ODVE56 could also contain potential O-linked glycosylation sites predicted by NetOGlyc 3.1 Server at CBS, interestingly all these O-linked glycosylation sites are predicted at the C-terminal of ODV-E56 shown in Figure 3.6.

Unlike the other ODV envelope proteins, ODV-E56 shows a strong transmembrane motif at its C-terminus that has been proven to be required for the translocation of ODVE56 into the nucleus and localization into the ODV envelope (Braunagel *et al.*, 1996). The ODV-E56 transmembrane domain prediction is similar to P74, suggesting that ODV-E56 is exposed on the surface of ODV. Additionally, ODVE56 contains transmembrane domain in its central region.

An ODV-E56 deletion mutant virus was used to demonstrate that ODV-E56 has no effect on BV production, ODV assembly or occlusion; although no bioassay data was presented (Braunagel *et al.*, 1996). However, this study used a virus with a disrupted, rather than deleted, *odv-e56* and attempts to generate a complete *odv-e56* deletion mutant virus were unsuccessful. It was demonstrated in the same study that over expression of ODV-E56,

under control of the *polh* promoter, had a major effect on ODV maturation, decreasing envelopment of ODV to near undetectable levels. But there was no effect on either ODV envelope protein transport to microvesicles, the quantity of microvesicles or their association with nucleocapsids. This suggests that ODV-E56 plays a role in ODV morphogenesis (Braunagel and Summers 2007). However, more recently it has been shown that ODV-E56 is essential for oral infection of *Heliothis virescens* larva, supporting the suggestion that ODV-E56 is exposed on the surface of ODV (Sparks *et al.*, 2011a). The results from this study suggest that ODV-E56 does not play a role in binding or fusion of the ODV to the midgut but instead at a critical point before or after this event, prompting the authors to recommend that ODV-E56 should be renamed PIF5 (Sparks *et al.*, 2011a).

3.2.7 Occlusion-derived virus structural proteins: PIF2 & PIF3

The *per os* infectivity factor (PIF) family contains proteins that are essential for oral infection of lepidopteran larval hosts by AcMNPV. To date, the PIF family consists of P74, PIF1, PIF2, PIF3 and PIF4 that are all core genes conserved among all sequenced baculoviruses. The two of interest in this study are PIF2 and PIF3 that have already been demonstrated to be members of the *per os* infectivity factor family (Pijlman *et al.*, 2003; Ohkawa *et al.*, 2005).

PIF2 was first characterized in *Spodoptera exigua* multiple nucleopolyhedrovirus (SeMNPV) as ORF35 (Pijlman *et al.*, 2003) using a *per os* bioassay functional genomics approach that identified proteins that were non-essential for replication of the virus in insect cell culture but essential for oral infection. The AcMNPV homologue for PIF2 is ORF22 that produces a 44 kDa protein, which contains a highly conserved hydrophobic N-terminal transmembrane motif. This serves to anchor PIF2 to the ODV envelope and is similar to the inner nuclear membrane sorting motif of ODV-E66 and ODV-E25 (Hong *et al.*, 1997; Braunagel *et al.*, 2004). The AcMNPV PIF2 has been located to the ODV, whereas SeMNPV PIF2 has yet to be established as part of the ODV (Braunagel *et al.*, 2003).

Figure 3.7 shows the alignments of the PIF2 peptide sequence with its homologues in other Type I and II alphabaculovirus, showing it is highly conserved among both Type I and Type II. AcMNPV PIF2 is also highly conserved among homologues from betabaculoviruses, as shown in Figure 3.8. A transmembrane region was identified by TMPRED at the EXPASY server and it contains an INM-SM (Braunagel and Summers,








2007). PIF2 has seven potential N-linked glycosylation consensus sequences (Asn-Xaa-Ser/Thr), all of which are predicted by NetNGlyc 1.0 Server at CBS to be glycosylated.

PIF3 was more recently described by Ohkawa *et al.* (2005) as a 23 kDa protein encoded by AcMNPV ORF115 that is essential for oral infection. Like PIF2, PIF3 contains an N-terminal transmembrane domain that most likely anchors the protein to the ODV envelope. However, unlike PIF2, PIF3 was not identified as a component of the AcMNPV ODV during protein composition analysis that could suggest the relative levels of each of these PIF proteins differs (Braunagel *et al.*, 2003).

The alignments of PIF3 peptide sequence with its homologues in other Type I and II alphabaculovirus can be seen in Figure 3.9 PIF3 is shown to be highly conserved among Type I but only shares ~30% amino acid sequence identity with Type II. From the alignments in Figure 3.10 it can be seen that the region after the transmembrane domain in both Type I and II alphabaculovirus shows variation compared to the rest of the peptide sequence. AcMNPV PIF3 also shares ~31% amino acid sequence identity when aligned with homologues from betabaculoviruses, as shown in Figure 3.10. A transmembrane region was identified by TMPRED at the EXPASY and PIF3 contains an INM-SM (Braunagel and Summers 2007). PIF3 has two potential N-linked glycosylation consensus sequences (Asn-Xaa-Ser/Thr), all of which are predicted by NetNGlyc 1.0 Server at CBS to be glycosylated.

It has been shown that PIF2 and PIF3 along with two other conserved PIF proteins; PIF1 and P74 form a stable complex on the surface of the ODV, which is essential for the early stages of baculovirus oral infection (Peng *et al.*, 2010). However, the roles of PIF2 and PIF3 in oral infection differ because the former is involved in mediating specific binding to primary midgut cells. Whereas PIF3 deletion mutants showed similar ODV binding levels as wild type virus, during binding and fusion assays, so this protein must be involved in a critical event in early primary infection; deletion mutants being unable to infect larva through the oral route (Ohkawa *et al.*, 2005). It was suggested by Ohkawa *et al.* (2005) that PIF3 may be involved in the translocation of the ODV capsids along the microvillus of the midgut cells. Alternatively it could interact with cytoskeletal elements aiding transport of the ODV, if it is located on the inside of the ODV envelope (Slack and Arif, 2007).

Figure 3.6 Sequence alignments of Type I and Type II ODV-E56 Sequences

The sequence alignments of type I and type II alphabaculoviruses ODV-E56 sequences were shaded using the GeneDoc software package to highlight the conserved amino acid sequences; (Conserved mode: , 100%, , 80%, , 60% ). Potential transmembrane domain and signal peptide have been indicated by  and possible N-glycosylated sites have been indicated with  and possible O-glycosylated sites have been indicated with . AcMNPV ODV-E56 sequence was also aligned against betabaculovirus ODV-E56 homologues to demonstrate the conserved amino acids between ODV-E56 alphabaculovirus and betabaculovirus.

Chapter 3

Type I alphabaculovirus

```

AcODVE56 : MS FFSNLRVAVNKLYPN CASFLIDNTR LLSTPAGFTNVLNAPS VRNIGNRRFQPGYCLSNQC FVSTSDINRITRNNDVPIRNV FQGISDPQINSISQLRRVDNVPDFNYHTKCTRNAVK : 121
PxNPV : MS FFSNLRVAVNKLYPN CASFLIDNTR LLSTPAGFTNVLNAPS VRNIGNRRFQPGYCLSNQC FVSTSDINRITRNNDVPIRNV FQGISDPQINSISQLRRVDNVPDFNYHTKCTRNAVK : 121
RoNPV : MS FFSNLRVAVNKLYPN CASFLIDNTR LLSTPAGFTNVLNAPS VRNIGNRRFQPGYCLSNQC FVSTSDINRITRNNDVPIRNV FQGISDPQINSISQLRRVDNVPDFNYHTKCTRNAVK : 121
EmNPV : MS FFTNLRFVAVNKLYPN CASFLADNTR LLSTPAGFTNVLNAPS VRNIGNRRYQPGYCLSNRRFVSTSDINRITRNNDVPIRNV FQGISDPQINSISQLRRVDNVPDFNYHTKCTRNAVK : 121
AgNPV : MS FFTNLRFVAVNKLYPN CASFLADNTR LLSTPAGFTNVLS TSPSRNLGNCRYPGYNLSNQC FVSAGDINRITRSDNVPRI RNV FQGISDPQINSISQLRRVDNVPDAGLHVKKTRCDAVK : 121
CfDEFNPV : MS FFTNLRFVAVNKLYPN CASFLADNTR LLSTPAGFTNVLS TSPSRNLGNCRYPGYNLSNQC FVSAGDINRITRSDNVPRI RNV FQGISDPQINSISQLRRVDNVPDAGLHVKKTRCDAVK : 121
CfNPV : MS FFTNLRFVAVNKLYPN CASFLIDNTR LLSTPAGFTNVLRAPS SRNLGNCRFEPGYNLSNQC FVSAGDINRITRSDNVPRI RNV FQGISDPQINSISQLRRVDNVPDAGLHVKKTRCDAVK : 122
OpNPV : MS FFTNLRFVAVNKLYPN CASFLIDNTR LLSTPAGFTNVLRAPS SRNLGNCRFEPGYNLSNQC FVSAGDINRITRSDNVPRI RNV FQGISDPQINSISQLRRVDNVPDAGLHVKKTRCDAVK : 121
EppoNPV : MS FFTNLRFVAVNKLYPN CASFLADNTR LLSTPAGFTNVLS TSPSRNLGNCRYPGYNLSNQC FVSAGDINRITRSDNVPRI RNV FQGISDPQINSISQLRRVDNVPDAGLHVKKTRCDAVK : 122
AnpeNPV : MS FFTNLRFVAVNKLYPN CASFLADNTR LLSTPAGFTNVLS TSPSRNLGNCRYPGYNLSNQC FVSAGDINRITRSDNVPRI RNV FQGISDPQINSISQLRRVDNVPDAGLHVKKTRCDAVK : 122
HycuNPV : MS FFSNLRVAVNRVYVSNASEVTDNSR LLSTPAGFTNVLNAPS VRNIGNRRYQPGYCLSNQC FISAGDINRITRSDNVPRI RNV FQGISDPQINSISQLRRVDNVPDAGLHVKKTRCDAVK : 121
  
```

Transmembrane Domain

Predicted N-Glycosylation site

```

AcODVE56 : QNFPETNVRTPEGVQNALQQNPRHHSYMCSSRVGGTGILLATGGYFLFSAATI VQDIINA INNTGGSYVVCCKDAGEI AEA CLLLQRTCRQDENINCSIVTICPEPDLIPNPPPELTNMQGGF : 244
PxNPV : QNFPETNVRTPEGVQNALQQNPRHHSYMCSSRVGGTGILLATGGYFLFSAATI VQDIINA INNTGGSYVVCCKDAGEI AEA CLLLQRTCRQDENINCSIVTICPEPDLIPNPPPELTNMQGGF : 244
RoNPV : QNFPETNVRTPEGVQNALQQNPRHHSYMCSSRVGGTGILLATGGYFLFSAATI VQDIINA INNTGGSYVVCCKDAGEI AEA CLLLQRTCRQDENINCSIVTICPEPDLIPNPPPELTNMQGGF : 244
EmNPV : QNFPETNVRTPEGVQNALQQNPRHHSYMCSSRVGGTGILLATGGYFLFSAATI VQDIINA INNTGGSYVVCCKDAGEI AEA CLLLQRTCRQDENINCSIVTICPEPDLIPNPPPELTNMQGGF : 244
AgNPV : QNFPETNVRSDGVDRALQQNPRINTYLGGARTAGVGVLLAGGAYLTFSAATI VQDIIRALNNTGGSYVVRGSSCGETA DACLLLGRTCCQDENINCSIVSICERDPLINETAACLQICSGF : 243
CfDEFNPV : QNFPETNVRSDGVDRALQQNPRINTYLGGARTAGVGVLLAGGAYLTFSAATI VQDIIRALNNTGGSYVVRGSSCGETA DACLLLGRTCCQDENINCSIVSICERDPLINETAACLQICSGF : 243
CfNPV : QNFPETNVRSDGVDRALQQNPRINTYLGGARTAGVGVLLAGGAYLTFSAATI VQDIIRALNNTGGSYVVRGSSCGETA DACLLLGRTCCQDENINCSIVSICERDPLINETAACLQICSGF : 243
OpNPV : QNFPETNVRSDGVDRALQQNPRINTYLGGARTAGVGVLLAGGAYLTFSAATI VQDIIRALNNTGGSYVVRGSSCGETA DACLLLGRTCCQDENINCSIVSICERDPLINETAACLQICSGF : 243
EppoNPV : QNFPETNVRSDGVDRALQQNPRINTYLGGARTAGVGVLLAGGAYLTFSAATI VQDIIRALNNTGGSYVVRGSSCGETA DACLLLGRTCCQDENINCSIVSICERDPLINETAACLQICSGF : 244
AnpeNPV : QNFPETNVRSDGVDRALQQNPRINTYLGGARTAGVGVLLAGGAYLTFSAATI VQDIIRALNNTGGSYVVRGSSCGETA DACLLLGRTCCQDENINCSIVSICERDPLINETAACLQICSGF : 244
HycuNPV : QNFPETNVRSDGVDRALQQNPRINNHLCNRTAGVGVLLAGGAYLTFSAATI VQDIIRALNNTGGSYVVRGSSCGETA DACLLLGRTCCQDENINCSIVSICERDPLINETAACLQICSGF : 243
  
```

Transmembrane Domain

Predicted O-Glycosylation sites

```

AcODVE56 : NYEVEKTVCRGSDPFAADPDSQYVDISDLLEGQTIMCIEPYNLDLIGDLGLLELLGDDGLVGSNSNSDSVSKLMPILLIGAVLFLGLLIFYIYRYMMKGGGGG--VGAATSTPTPIVVS : 365
PxNPV : NYEVEKTVCRGSDPFAADPDSQYVDISDLLEGQTIMCIEPYNLDLIGDLGLLELLGDDGLVGSNSNSDSVSKLMPILLIGAVLFLGLLIFYIYRYMMKGGGGG--VGAATSTPTPIVVS : 366
RoNPV : NYEVEKTVCRGSDPFAADPDSQYVDISDLLEGQTIMCIEPYNLDLIGDLGLLELLGDDGLVGSNSNSDSVSKLMPILLIGAVLFLGLLIFYIYRYMMKGGGGG--VGAATSTPTPIVVS : 367
EmNPV : NYEVEKTVCRGSDPFAADPDSQYVDISDLLEGQTIMCIEPYNLDLIGDLGLLELLGDDGLVGSNSNSDSVSKLMPILLIGAVLFLGLLIFYIYRYMMKGGGGG--VGAATSTPTPIVVS : 363
AgNPV : NYEVEKTVCRGSDPFAADPDSQYVDISDLLEGQTIMCIEPYNLDLIGDLGLLELLGDDGLVGSNSNSDSVSKLMPILLIGAVLFLGLLIFYIYRYMMKGGGGG--VGAATSTPTPIVVS : 361
CfDEFNPV : NYEVEKTVCRGSDPFAADPDSQYVDISDLLEGQTIMCIEPYNLDLIGDLGLLELLGDDGLVGSNSNSDSVSKLMPILLIGAVLFLGLLIFYIYRYMMKGGGGG--VGAATSTPTPIVVS : 351
CfNPV : NYEVEKTVCRGSDPFAADPDSQYVDISDLLEGQTIMCIEPYNLDLIGDLGLLELLGDDGLVGSNSNSDSVSKLMPILLIGAVLFLGLLIFYIYRYMMKGGGGG--VGAATSTPTPIVVS : 364
OpNPV : NYEVEKTVCRGSDPFAADPDSQYVDISDLLEGQTIMCIEPYNLDLIGDLGLLELLGDDGLVGSNSNSDSVSKLMPILLIGAVLFLGLLIFYIYRYMMKGGGGG--VGAATSTPTPIVVS : 361
EppoNPV : NYEVEKTVCRGSDPFAADPDSQYVDISDLLEGQTIMCIEPYNLDLIGDLGLLELLGDDGLVGSNSNSDSVSKLMPILLIGAVLFLGLLIFYIYRYMMKGGGGG--VGAATSTPTPIVVS : 366
AnpeNPV : NYEVEKTVCRGSDPFAADPDSQYVDISDLLEGQTIMCIEPYNLDLIGDLGLLELLGDDGLVGSNSNSDSVSKLMPILLIGAVLFLGLLIFYIYRYMMKGGGGG--VGAATSTPTPIVVS : 367
HycuNPV : NYEVEKTVCRGSDPFAADPDSQYVDISDLLEGQTIMCIEPYNLDLIGDLGLLELLGDDGLVGSNSNSDSVSKLMPILLIGAVLFLGLLIFYIYRYMMKGGGGG--VGAATSTPTPIVVS : 366
  
```

Predicted O-Glycosylation sites

Predicted N-Glycosylation site

```

AcODVE56 : MQNLTPTTAPR---- : 376
PxNPV : MQNLTPTTASR---- : 377
RoNPV : MQNLTSTTAPR---- : 378
EmNPV : MQHIASTTAPRR--- : 375
AgNPV : PPPIAQNRI----- : 370
CfDEFNPV : ----- : -
CfNPV : PPPTQQTYNSTKQQI : 379
OpNPV : PPATNLNE---QQQI : 374
EppoNPV : TPTTRA----- : 372
AnpeNPV : PPPARRE----- : 374
HycuNPV : PQPIPLQTRG----- : 376
  
```

Chapter 3

Type II alphabaculovirus

```

AcODVE56 : --MSFFSNLRAVVKLYP--NQASFITDNR--LLTSTFAGFTNVLNAPSVRNIGNRRFPGYQLSNNQFVSTSDINRTRRNDVPNIRGVFQG-ISDPOINSLSQIRRVVNDVPEFNYHTKQTR : 116
LdNPV : --MSFFSLRRVNVKYP--NPNQFLAVDNLRVLNSIFNGFQNVFSAPSTRQIGTNRVPGYNLENNRFVPSDDINRVMRNDTACMRNIFTS-ADNSQLNSIGQLRRVVDNIIPDAGLHAAELR : 117
AdhoNPV : --MSFFSLRRVNVRYT--NPNQFVNVQDNLVQLSSPFGFQNVFSAPTIRVIG-DSVYVPGYSLSNNQFISTADMNRIRMRNDTPNIRNIFPS-ANDAQINSVGTIRRADNVDPANLHSLDIR : 116
EcobNPV : --MSFFSLRRVNVKYP--NPNQFTNVQDNLVQLSSPFGFQNVFSAPTIRVIG-DSVYVPGYSLSNNQFVPSDDINRVMRNDVTCIRNIFTS-ANNQINSINQIRRIDNIPDANLHSSAMR : 115
TnNPV : --MSFENELRKINKLY--PNTTQFN-LDNLAVVNNAPNGEKNVLSSTSIQNAGNRRFIPGYNIGNNFISADMNRIRMRNDVTSIRNVEGNTPTQTDLNLGLSLRRADNVDPANLHSAAMR : 117
AgseNPV : MTSNFFRELRLNVNKTY--LNPSTFV-ADNNTIFSIENGFQNVFNNPTVNIIGNRRFPGYNIENNNFVGAEMNSVMRTNDTVGLRRIFGNTPPTQNDYTGILNRYRFSANVPDANMHSKQIR : 119
SeNPV : ---MREFLRSVNRTEPTNNIASET-NQNLNVINNSPQGFERNVLSNPTVDIGNGQVREPGYALENNQMISSAEMNSIMRNDTSAGMRRVFGNNLSNNDYNGLSQLRRAANIIPDANMHSRQIR : 117
MacoNPV-B : -MSNIFRELRLRVNVKYPNPNVNTL-LDNLAVVNSSEGQFVLSNPTVNIIGNRRFPGYNIENNNFISADMNSVMRNDTSCIRRTFGNNTVDNDITGLSRMRQSENIPDARFNSAEIR : 120

```

Transmembrane Domain

```

AcODVE56 : SNAVKQNFETNVRTFEGVQNALQQNPRTHSYMQSIRVGGTGLLITATGCFYLFSAATI VQDIIEAINNIGGSYYVVGKTAGETAEACLLLRQTRQDPNINQSDVITICPEPDLIFNNPPEIT : 238
LdNPV : RQGVKSNYPSTNTRTEGGVEGVLATNPRTHARLNGIKSVGTALLIGGGVYLVFSAATI VQDLVSAIENRVGGSYVVGNGGSSSVCLLITHTRCQLD-TNINSDVSVQCFDPLIFDPAGQR : 238
AdhoNPV : KTAVKDNPSTNTRSCQGVENVLEQQPRIRTYLENKIAAGVITLVGAGVYLAFAASI VQDIISALNIGGSYYYVVGNGGDIRACILRDRTCQLN-VNINNVVILCFDPLITSSEI-IA : 236
EcobNPV : RNAVKQNFENTVRTFEDGIQVNLQNFSTNTYLTNKTAGVAVLLGAGVYLIIFTSATI IQDIIIEALNRRVGGSYFICGRNGGDESDTCLLVDRTPCRLENPNE-NVNECFLEDPLIINNVEAIR : 236
TnNPV : RNAVKQNFSTNTRTEAGVGNVLEQNPRITNHLQTKTAGVVSLLIGVGVYLVFSAATI IQDIIIEAINRRTGGSFYRGSDDGDNITACLLVDRTPCRLQHPFANSDVIRKCFDPLISNPTI-IQ : 238
AgseNPV : RDAVKNNPSTRTRTEEGVENSI SANPRIDAYLNNKTAGYVCLLGVGVYLVFSAATI VQDIIEAINRRTGGSYHTRGISGGDEVSVCLLIRFTRCLRP-ELDSN-VTVCVNDPLLENGPE-IE : 238
SeNPV : RDAVKNNPSTRTRTEAGIENSINRNFAINNRILQGLKAGVAALLGTGAVLVFQYASI VQDIIEAIRRRTGGSYHTTGIINGGDELRTCLLMNRTPCVKPDLYDSN-VTVCVNDPLLADQSE-IS : 237
MacoNPV-B : KDSVKTSNPSTNTRTEEGVQVNLNPNPQNRHLSNKTAGYICLLTGVGVYLAFASAATI VQDIIEAINRRTGGSYVVGNGGEEAATTCLLIRHTCHNT-HLGED-VNICTRDPLITDASQ-IN : 239

```

Transmembrane Domain

```

AcODVE56 : NMCQGFNYEVEKTVCRGSDPSALPDSPOQYVDISDLPAGQTIIMCIEPYSFGDLVGDLDGLDGLLWLLGDEGLVGRSINVSDFVSGKLMPIILLICAVLFLGLIFRYIYRYNMKGGGGG--VGAATP : 358
LdNPV : AICNGFNYEREQSVCRASDEYALPDSPOQYVDISDLPAGHTIIMCLEPYNIGDLIGDLGLDHLGEEGLVGRSINNSKILLSKLLWELLVALIGFAVVLILVFEKRI MNKQTVDIRANA--- : 356
AdhoNPV : NICRGFNYAVEQTVCRASDEPTALVNSPOQYVDISDLPAGQTIICVEPYLLIGDLIGDLGLDHLGEEGLVGRSINDFSKLIGQKLLPILILLEGFIIVMIGIIEKRI MSTPITATADNVKPI- : 357
EcobNPV : AICNNDYETEQTVCRADEYAHPSLQYVDISDLPAGQTIIMCIEPYNGDLIGDLGLDHLGEEGLISNSINDFSKLISDILLPILVLCGILLVVVAEPIIKRYMNSNSVTSATNAPS : 358
TnNPV : NICQGFNYEREKSVCRASDENANINTEQYVDISDLPSPQTIICVEPYNMGDLIGDLGLDHLGEEGLVGRSINFSQISDSLLPFIIVMIGIIFAFIILIGYIIEKRI F--NRQTVS--VEPNR : 356
AgseNPV : NICNFDYETECSVCRSDENANEDTPQYLDISNIGEDQMSICIEPYDFGDLVADLGLDHLGEEGLVGRSINFSKLSDSLLPFIIVMIGIIFAFIIVVLCYIEKRI S--NKQTVN--IEPV : 356
SeNPV : RICDGFNYEVEKTVCRASDENAYEFSPOQYVDISELSTQMLHCIEPYDFGDLIADLGLDGLLGENGSITQSINFSKLSDSLLPFIIVMIGIIFAFIIVVLCYIEKRI NS--NRQTVQFQPMVP : 358
MacoNPV-B : AICHGFNYEVEKTVCRASDENAVATPQYVDISELPHQTIIMCIEPYNMGDLIGDLIGGLLGEEGLVGRSINFSQISDSLLPVLIIIGVILLIVVFIQYMEKRI GS-GSGGN--LQPI : 358

```

Predicted O-Glycosylation sites

```

AcODVE56 : PTHIVISMQNPTTAPR : 376
LdNPV : ----- : -
AdhoNPV : ----- : -
EcobNPV : INVRT----- : 363
TnNPV : IR----- : 358
AgseNPV : TAMPMTAVPIQVE----- : 369
SeNPV : TAVPVTPLPIQVE----- : 371
MacoNPV-B : TQVAPITVPIRTVAA--- : 373

```

Predicted N-Glycosylation site

Chapter 3

```

                *      20      *      40      *      60      *      80      *      100     *      120
AcODVE56 : -MSFFNLRVAVNKLYPNQASFTIDNTRILTS-TEAGFTNVLLNAPSVRNIGNNRFQPGYQLSNNQFVSTSDINRITRNNDVPIRGVVFQGISDFEQINSLSQLRRVDNVPLFNYHTKQTRSNVAVKQN : 123
ChocGV   : MASEFTGLRRINKVYPNTNSFLSDHALFIRNQTIVGFN--LNNPTTNGIAGCNVTPGYNING-TFVSNANVNSVLRNNDVVGMRQIFFEASNNQMNGLTNLRRADNIPDSTIHSIKTRKNNVQKS : 122
CpGV     : -MSFFRGLRRINKVYNDPSGFTTDHAQLIRNQTIVGFN--LNNPTTNGLANGTYVPGYNING-AFISNTNVNTVLRNNDVVGMRQLFFDASNNQMNGLTNLRRADNIPDSTLHGLQTRKNGVKTS : 121
PoGV     : -MSFFSGLRRINKVYPNPDSFLFDHTQLIRNQTIVGFN--LNNPLTVSAPNGQQIPGYNVNG-SFVSTANINYLVRNNDVVGMRQIFFTANNSQMNGLGGLRRADNIPDSTLHSLERKREIKNA : 121
PiraGV   : MASLFSGLRRINKVYPMVNSFAIDHSTFIRNKSEFGN--LNNPSTLTGPNQVPIPGYTIIN-RFVSNADVNSVLRNNDVVGMRDIFENVINNMNGLTNLRRADNIPDSSLNSLQTKKNNVKS : 122

```

```

                *      140     *      160     *      180     *      200     *      220     *      240     *
AcODVE56 : EPETNVRTPEGVQNALQQNPRIHSYMQSLKVGCTGILLATGTYFLFSAATLVQDIINAINNTGGSYYVQCKDAG---EIAEACLLLQRTGRQDPNLNQSDVITGPFDELELNNPP-----ELTN : 239
ChocGV   : EPETVVRDRAGVENALAQNPRIGDYLRG---AGYVILFGVGVYLVINVADLVGSIVDAINRTGGSWYFRGNGADNENNIQSCILRYRTCGVP--FTDIQDSVQVLDPHATNVDPMLTLEASD : 242
CpGV     : EPETAVRDRVGVENALAQNPRIADYLRG---AGYVILFGVGVYLVINVADLVSSIVEALNRTGGSWYFRGNGGDNESNIDACVLRYSRSGMS--LADIDEFVCELDPHDNNVDPLL SFDEARN : 241
PoGV     : EPETAVRDRSGVERALAQNPRIADYLRG---AGYVILFGVGVYLVINVADLVGSIVDALNRTGGSWYFRGNGCATSEDQIEACILRYRSCGMP--FSDIQNDVQVLDPELVINVDPLLKFDFAIR : 241
PiraGV   : EPETVVRDRDGVVYVLLKKNPRISTYLRG---AGYVILVAGVYLVINVADLVGSIVDAINRTGGSWYFRGHNGADNEDNTTACVLRYSRSGMK--FEDIEESLCVLDPHDNNVDPLMSIEEARV : 242

```

```

                260      *      280      *      300      *      320      *      340      *      360      *
AcODVE56 : MCQGFNYEVEKTVCRGSDPSADPDSFQYVDISDI PAGQTILMCIPEPYSFGDLVGDLDGLDWLLGDEGLV GKSSNVSDSVSGKLMETILLIGAVLFI GLIFFYFTYRYMMKGGGGGGVGAATSPTPIVI : 364
ChocGV   : FCNNYNHATEQSVCRGSDPNANPTSIQYLDISLHASNQTIECIPEPYDFGLIGDLGLDWLLGDNQIVTASSNSTL SVSDNELLTILLVIGGILVILFIFGFIIYKVTITKRSI----- : 353
CpGV     : FCNGYSLAAEGSVCRGSDTNADPSTIQYLDISETEPNQTVQCVPEPYDFGLIGDLGLDWLLGDNQVFTASSNSTL SVSNNEFTILLVIGGILLITFIFGFVIFKVVNRSSNNNTS----- : 355
PoGV     : LCEGYNYETEKSVCRAADPNADVLSIQYLDISGLSTNQTICVPEPYDFGLIGDLGLDWLLGDRCAITTSNSTL SVSDNELLTIVLAIGGLLIFIFFAFIVFKVLMKKRE----- : 351
PiraGV   : FCNGYSYVREKSVCRGSDTKADPTSIQYLDISLHATNQTICVPEPYDFGLIGDLGLDWLLGDSVFAASSNSICGFSNNEFTILLIGGVILLIFIGFIVYKVVTTKRSTT----- : 354

```

```

                380
AcODVE56 : SMQNPTPTTAPR : 376
ChocGV   : ----- : -
CpGV     : ----- : -
PoGV     : ----- : -
PiraGV   : ----- : -

```

Type I alphabaculovirus

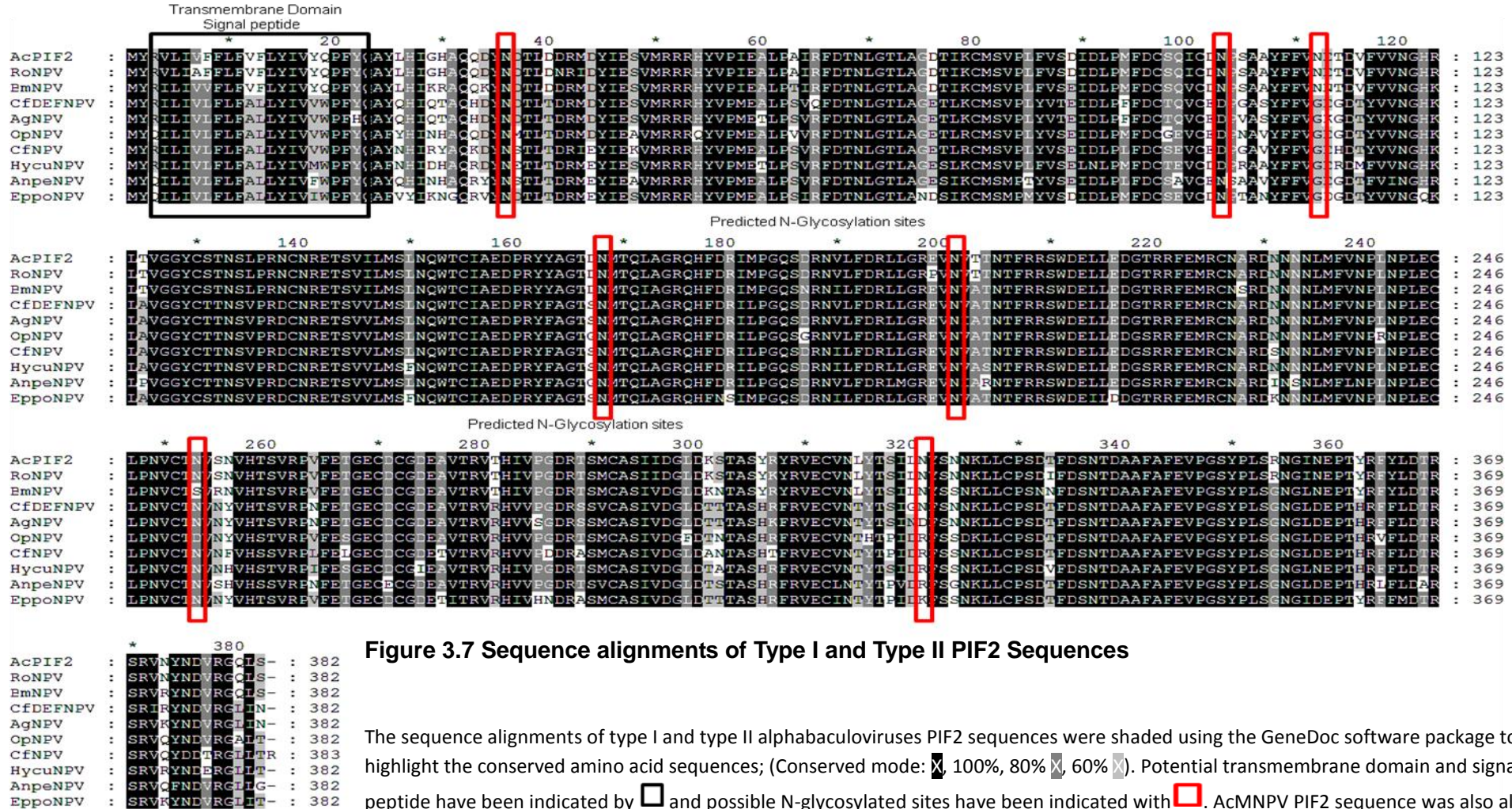
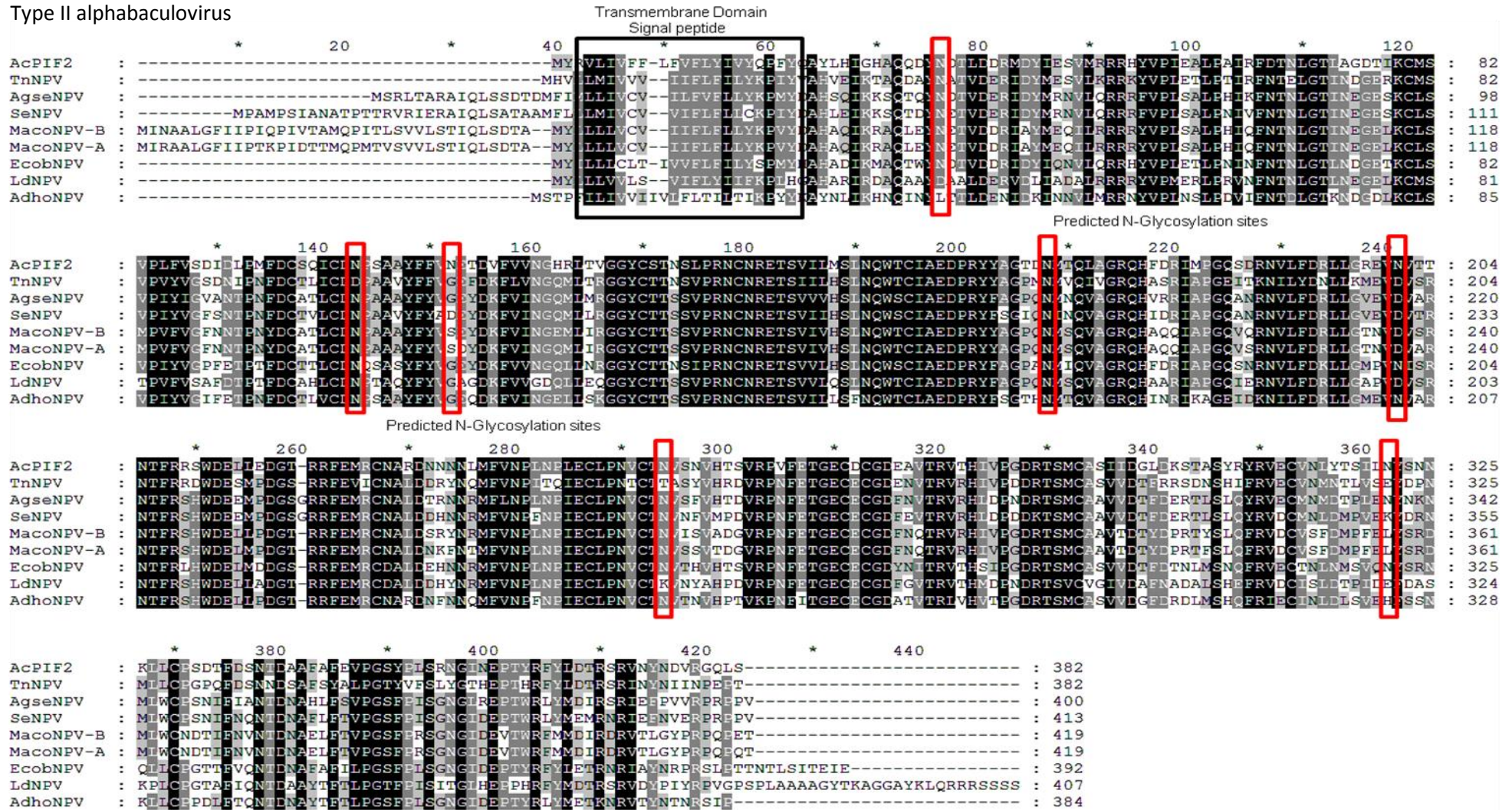


Figure 3.7 Sequence alignments of Type I and Type II PIF2 Sequences

The sequence alignments of type I and type II alphabaculoviruses PIF2 sequences were shaded using the GeneDoc software package to highlight the conserved amino acid sequences; (Conserved mode: \blacksquare , 100%, 80% \square , 60% \square). Potential transmembrane domain and signal peptide have been indicated by \square and possible N-glycosylated sites have been indicated with \square . AcMNPV PIF2 sequence was also aligned against betabaculovirus PIF2 homologues to demonstrate the conserved amino acids between PIF2 alphabaculovirus and betabaculovirus 86 see Figure 3.8.

Chapter 3

Type II alphabaculovirus



Chapter 3

```

AcPIF2 : MNRVLIIVFFLEVLVYQFFVQAYLHGHAQQDYNDTLDLRMYIESVNRRRHYVPIEALFAIRFDNLGCTIAGDTIKMSVLELVSDIILPMFDSCICDNPSSAYFFVNETDV FVNVNGHRLTVG : 127
CpGV   : ML-ILTVILFVLELFLFYLYPLHYHQCHYETVARNQLDD--DFFRESMQRRRYAPLHLLPVRWHSNFDITIGC---SCFSVPTLVTTSTNGTFDCTAVCNDERAVYFFVNPDKFIVNGARLVSG : 121
PiraGV : MY-FLFVILSVLFIFFLYVPHLTYTCIYQEKTRRIILND--DILRKSQNRRYAPLHLLPVRWHSNFDITIGS--SSCFSPVPTLVTTSTNGTFDCAVAVCNERAVYFFVNPDMYIVNGERLSSG : 123
ChocGV : ML-ILVILFVLELFIFFLYPLHYHQCTFDANYRQELLEDD--EDFKDSMQRRRYAPLHLLPVRWHTNFDITIGS--SNCFSPVPTLVTTSTNGTFDCTAVCNDERAVYFFVNPDMYIVNGERLMSG : 123
PoGV   : MY-IVLVIIVFVLELFIFFLYPLHRYTNMYEDAVERNLFLEE--N--RE--FFRRYAPLHLLPVRWHSNFDITIGS----CFSPVPTLVTTSTNGTFDCTAVCNDERAVYFFVNHEDMYIVNGERLPSG : 115




AcPIF2 : GYCSTNSLPRNCNRETSVILMSLNQWTCIAEDPRYYAGTDNMTQLAGRQHFDRIMPQSDRNVLFDRLIGREVNVTNTNFRRSWDELLEDGTRRFEMRCN-ARLNNNNLMFVNPINLECLPNVCTN : 253
CpGV   : GYCTVNSVPRHCNSETSLIMESVNQWTCIAEDPRFYAGECNLIQVAGRQHSDEVLPPEEMDKIVLWDNVTGAFVNEVNTFRYSWDDRMEDGSRRFVRCG-ATLQRNEMFIPNYNEIECLPNVCTS : 247
PiraGV : GYCTMNSVPRNCNSETSLILYSVNQWTCIAEDPRYFAGECNLIQVAGRQHSDEILSSDINKIVLWDNRLNRCVNEAVNTFRNSWDERLEDGRRRFVRCG-ALPKNENQMFIPNYNEIECLPNVCTS : 249
ChocGV : GYCSMNSIPRNCNSETSLILESVNQWTCIAEDPRYFAGECNLIQVAGRQHSDDLILPEDINKIVLWDNLLNRCVNEAVNTFRYSWDDKLENGNRRFEIKCD-ALDMRENQMFIPNINIECLPNVCTS : 249
PoGV   : GYCTLNSVPRNCNSETSIILYSVNQWTCIAEDPRYFAGEANLIQIAGRQHSCTIISSELDKIVLYDKLLNRFVNEISNTFRCSWDETMENGSRRFQVWCDCAELIHYNQLFIPNINIECLPNVCTN : 242

AcPIF2 : VSNVHTSVRFVFEIETCEDCGDEAVTRVTHIVPGRITSMCASIIIGLIDKSTASYRYRVECVNLYTSLILNYSNKKLLCFSDTFLENTDAFAFAEVVPGSYPLSRNGINEPTYRFLYLDTRSRVNYNDVRGQ : 380
CpGV   : VQNAHRDVKRFVFDGGVDCGDMNMTRVEHIIVNDRSSKCAAIIVNRLDGVRSYSFRVLCISLDTPIITFEABNKKLLCPFEIFNQNTDFAYEFTLHGTVPLSGNGIDEPTTIGWRDTRNRVWNSVN-- : 372
PiraGV : TQWIHRDVKRFVFEKGTCECCASNVTRVEHVDQNDPSSKCAGVNRLNKEEREFNRFVECLSLDTFVSEFNKLLCPESLFNQNTDFAYEFTLKGVIPLSGNGIDEPTTISLWKDTRNRVAVYTASR- : 375
ChocGV : VQVNVNRNRFVFEIETGDCGDMNMTRVQHIDENDTSKCAAIINRDTNRRAYSFRVECLSLDTFVNEVYRVNKKLLCPEDIFNQNTDFAYEFTLDGIIPLSGNGIDEPTTRLWEDTRSRTEWKNER-- : 374
PoGV   : VNEVHRDVKRFVFERGICDCGSANITRVEHIIINDPSSKCASTNRRNG--HDYNERVECLSLSEITEYTHDKLMCPESIFNQNTDFAYEFTLRGVVPLSGNGIDEPTTRLYRETRNRINWNDLNR- : 366

AcPIF2 : LS : 382
CpGV   : -- : -
PiraGV : -- : -
ChocGV : -- : -
PoGV   : -- : -

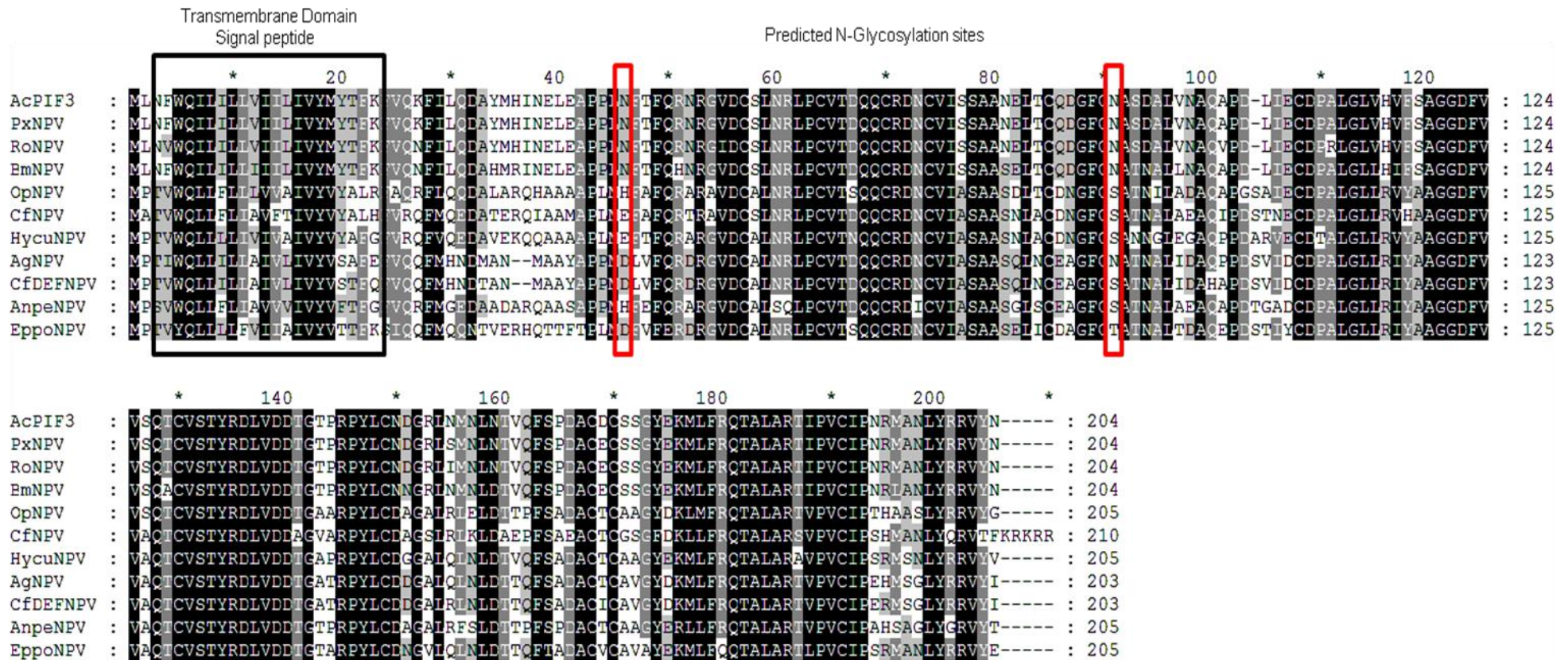
```

Figure 3.8 Sequence alignment of PIF2 Sequence against betabaculovirus homologue

The sequence alignment for AcMNPV PIF2 was carried out against betabaculovirus homologues and shaded using the GeneDoc software package to highlight the conserved amino acid sequences; (Conserved mode: , 100%, , 80%, , 60%).

Chapter 3

Type I alphabaculovirus



Chapter 3

Type II alphabaculovirus

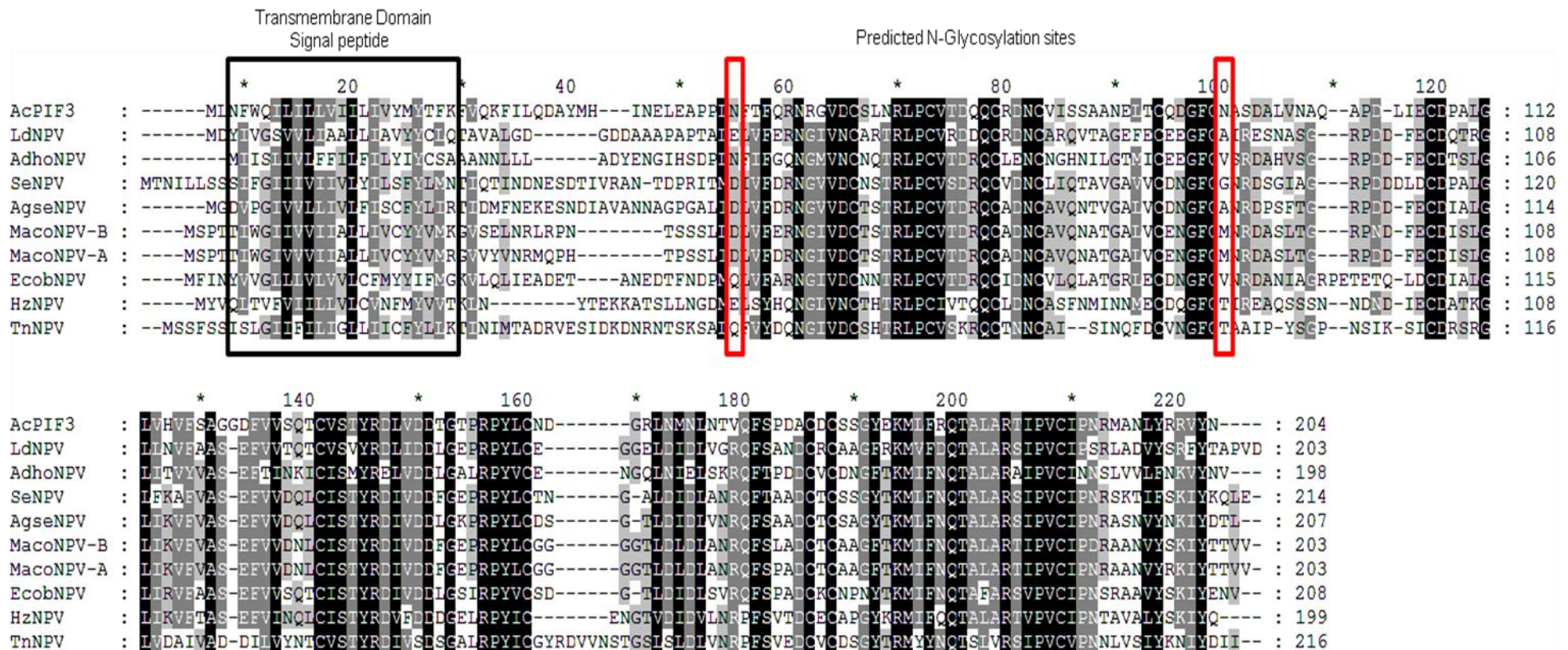


Figure 3.9 Sequence alignments of Type I and Type II PIF3 Sequences

The sequence alignments of type I and type II alphabaculoviruses PIF3 sequences were shaded using the GeneDoc software package to highlight the conserved amino acid sequences; (Conserved mode: \blacksquare , 100%, 80% \square , 60% \square). Potential transmembrane domain and signal peptide have been indicated by \square and possible N-glycosylated sites have been indicated with \square . AcMNPV PIF3 sequence was also aligned against betabaculovirus PIF3 homologues to demonstrate the conserved amino acids between PIF3 alphabaculovirus and betabaculovirus see Figure 3.10.

Chapter 3




```

      *      20      *      40      *      60      *      80      *      100      *      120
AcPIF3 : M*N*FWQIL*IL*LV*II*LV*II*LV*II*LV*MY*TFK*FV*Q*K*FI*LQ*AY*M*HINELEAP*PLNFT*FOR*NRG*V*DG*SLN*R*L*FC*V*TE*Q*CRD*NC*VI*SSA*AN*EL*T*Q*DG*-*FN*AS*DAL*V*NA*Q*AP*DL*IE*CI*PAL*GL*VH*V*FS*GG*DF*V*VS : 126
PiraGV : -M*W*N*IF*FI*LV*EV*FI*LT*II*RR*WL*RQE*Q*IMS*N*K*RV*K*IF*-----*FE*K*ENV*LD*CS*V*N*VL*CV*AN*D*Q*CRD*NC*ING*---*LI*M*HC*N*EG*GF*CS*RG*V*GV*YV*---*ADD*IE*K*CI*AN*R*GL*IV*VL*NA*IGN*L*AAE : 110
CpGV : -M*W*AV*FL*II*LV*IV*GV*V*LV*NG*WL*RT*DL*AN*M*RR*V*N*IA*-----*FE*R*H*NI*LD*CA*V*N*V*FC*V*TE*Q*CRD*NC*RG*---*LV*M*HC*N*AG*GF*CA*RG*AR*-*V*---*D*SS*VE*D*CI*AS*R*GL*V*V*VL*NA*VE*GI*V*VE : 109
ChocGV : -M*W*---*IG*IN*V*V*II*LI*A*IF*W*IA*Q*Q*NT*Y*-*N*K*RV*NI*L*-----*FE*K*ENV*LD*CS*V*N*V*FC*V*TE*Q*CRD*NC*ID*G*---*M*VM*RC*Q*GF*FC*N*K*GP*R*---*IE*N*IN*D*CI*AN*R*GL*IV*VL*NA*IN*EL*V*VE : 103
PoGV : -----*MI*IV*LL*LV*IN*TI*II*ML*ST*KK*RT*NI*EH*M*V*NI*AP*-----*FE*K*ENV*LD*CS*V*N*V*FC*V*TE*Q*CRD*NC*IG*---*MM*RC*N*D*AG*FC*GP*ENT*-*F*---*V*VR*P*ET*CI*IER*GL*IT*V*Y*TD*VG*----- : 97

      *      140      *      160      *      180      *      200      *
AcPIF3 : Q*TC*V*SI*Y*RD*LV*DI*T*GT*EP*YL*C*ND*G*-*RI*N*M*NI*NT*V*Q*FS*PD*AC*DC*SS*GY*E*ML*FR*QT*AL*ART*IP*VC*IP*NR*ME*LY*RR*V*YN*----- : 204
PiraGV : K*LC*V*SI*Y*RD*AV*DD*NG*DL*RP*Y*VC*Q*NG*-*K*M*QL*N*LE*K*DP*FN*V*DD*CT*ON*AG*FT*K*FS*YL*SG*AF*S*RT*IP*VC*IP*NA*SA*AL*YS*RI*YY*K*S*----- : 190
CpGV : R*MC*V*SI*Y*RD*V*VE*DD*G*KL*RE*Y*VC*G*SG*SM*W*LD*LE*TD*MF*SE*ED*CV*CA*AG*Y*TR*FS*Y*SS*GA*FR*TI*IP*VC*IP*NA*SA*AL*Y*CR*V*Y*V*GR*IS*CE*I*WT*W*-- : 199
ChocGV : T*M*CL*SI*Y*RD*V*IN*DD*GS*L*K*SY*VC*Q*NG*-*N*VE*L*CL*CE*NP*FE*VR*CC*Q*AS*GY*TL*FS*FS*PA*FR*TI*IP*VC*IP*N*RL*TK*LY*SR*V*Y*N*K*PV*PL*AV*V*SL*DS*R : 194
PoGV : L*LC*IS*LY*RD*V*IL*DS*GL*RE*Y*IC*SG*-*TM*IN*LE*D*GE*FS*TE*LC*VC*PP*NH*TK*FS*ET*SG*AF*TR*AI*IP*VC*VP*NI*MA*AL*Y*RR*V*Y*GEN*----- : 177

```

Figure 3.10 Sequence alignment of PIF3 Sequence against betabaculovirus homologue

The sequence alignment for AcMNPV PIF3 was carried out against betabaculovirus homologues and shaded using the GeneDoc software package to highlight the conserved amino acid sequences; (Conserved mode:  100%,  80%,  60%).

3.3 Conclusion

The first stage of this thesis was to select genes based on the literature that were structural components of the ODV, which were not found in BV and possibly would have no effect on BV production in cell culture. From this bioinformatic review conducted at the time Table 3.2 was compiled showing all known structural proteins of the ODV, eight genes were selected for further study; *odv-ec43*, *orf79*, *odv-e28*, *pif2*, *pif3*, *odv-e66*, *cg30* and *odv-e56*. This chapter goes on to individually review each of these selected genes using the current literature and this information was used to inform the interpretation of the results found in later chapters of this thesis.

The alignments undertaken in this chapter showed that all of these selected genes were highly conserved among Type I alphabaculovirus, however the percentage of amino acid sequence identity varied from 14% (*cg30*) to 53% (*odv-e28*) when aligned with homologues from Type II alphabaculovirus. Several of the selected genes; *pif2*, *pif3*, *odv-e66* and *odv-e56* had homologues in betabaculoviruses and the variation in amino acid sequence identity varied from 51% (*pif2*) to 31% (*pif3*). The alignments have also shown highly conserved regions or regions showing high variation, these could indicate either the functional region of the protein or regions that are not essential for function, respectively. For example, in all three alignments performed on ODV-E66 homologues the N-termini showed large variation when compared to the rest of the peptide sequence.

The initial research allowed the target sequence to be selected for each gene that would be deleted using the Red/ET recombination system, so that no neighbouring genes' transcription would be disrupted from the deletions carried out in Chapter 4. Further chapters of this thesis go on to explain the results gained from these deletion mutant viruses and how they compare with the literature as presented within this chapter.

Chapter 4

Construction of baculovirus gene deletion mutants

4.1 Introduction

Baculovirus ODV is comprised of a nucleocapsid wrapped in a membrane envelope that contains a number of viral proteins. A bioinformatic approach (Chapter 3) was undertaken to identify proteins that were ODV specific and had no direct association with BV structure or production according to the literature. Therefore, in principle the genes for these proteins could be deleted from the virus genome without affecting its ability to replicate in cell culture. The immediate aim of this research was to elucidate the roles of these selected proteins on the baculovirus replication cycle with specific regard to ODV production and packaging into the OB. The long term goal was to identify specific ODV gene deletions that could be used to abrogate ODV production in recombinant baculovirus-infected insect cells and reduce the wasted cellular resources that produce unnecessary ODV. To investigate the immediate aim, a system for deleting baculovirus genes was required to allow the rapid construction of virus mutants that could be characterized for any defects in ODV production.

Some methods utilized in the 1970's for studying virus gene function involved the use of chemicals such as N-methyl-N'-nitro-N-nitrosoguanidine or 5-bromodeoxyuridine to mutate randomly viral DNA and produce temperature sensitive mutants (Timbury, 1971; Brown *et al.*, 1979). This proved to be a very successful approach, especially for herpes simplex virus (HSV) where marker rescue allowed temperature sensitive mutations to be physically mapped (Stow *et al.*, 1978; Chartrand *et al.*, 1981). This permitted physical maps of HSV-coded proteins and functions to be constructed along with analysis from polypeptide profile and restriction enzyme generated fragments from the marker rescue (Stow *et al.*, 1978). Therefore this approach was a powerful tool enabling the understanding of the functional organization of viral genomes and the role of certain products in virus replication. In the case of baculovirus, this approach allowed the functional discovery of a number of gene products such as late expression factors (lef) 4 and 8, which were both shown to play a role in late and very late gene expression (Carstens *et al.*, 1994; Shikata *et al.*, 1998). However, this approach relies on random mutagenesis that requires large amounts of screening and isolation of temperature sensitive mutants.

The production of random mutations in virus genomes was suited to an era in which full virus genome sequences were unavailable. The sequencing of many virus genomes from the 1980's onwards opened the way to conduct more targeted mutations to virus genomes, rather than relying on the production of random mutants. Methods were developed that allowed the direct insertion of a marker into the viral DNA resulting in the

complete deletion or simple disruption of the target gene. Mackett *et al.* (1982) demonstrated a method that allowed the selection of thymidine kinase-negative recombinants from a wild-type Vaccinia virus background after the disruption of the thymidine kinase gene by insertion of foreign DNA from a plasmid transfer vector (Mackett *et al.*, 1982). This discovery permitted vaccines to be constructed by the insertion of sequences encoding antigens from other viruses into infectious Vaccinia virus. For example, candidate vaccines for hepatitis B virus (Smith *et al.*, 1983b) and influenza virus (Smith *et al.*, 1983c). The most common approach involved the construction of a plasmid transfer vector containing the gene under study, which could be manipulated *in vitro* and in bacteria. The target gene was then modified by insertion of a marker sequence (e.g. β -galactosidase), which could be selected subsequently in the host cell of the virus. The parental virus and transfer vector were then introduced into the host to permit homologous recombination between the two molecules (Figure 4.1).

For baculoviruses, the first examples of the use of this system were the independent studies conducted by Smith *et al.* (1983a) and Pennock *et al.* (1984) to derive expression vectors. Smith *et al.* (1983a) used a transfer vector containing beta interferon to delete the AcMNPV polyhedrin gene (*polh*) and thus produce a virus lacking the ability to make polyhedra. This polyhedrin-negative phenotype could then be selected by observing plaques with a microscope. Pennock *et al.* (1984) used the β -galactosidase gene (*lacZ*) as a selectable marker so that blue plaques formed in the presence of X-gal could be isolated. This method was also used by Ohkawa (1997) to construct 150 *Bombyx mori* NPV mutants. Each mutant had a large fragment of DNA removed from each ORF and replaced with a *lacZ* reporter cassette. These viral mutants were then screened for those that were viable in cell culture but unable to infect larvae orally and lead to the identification of a third pif gene, *pif3* (Ohkawa *et al.*, 2005).

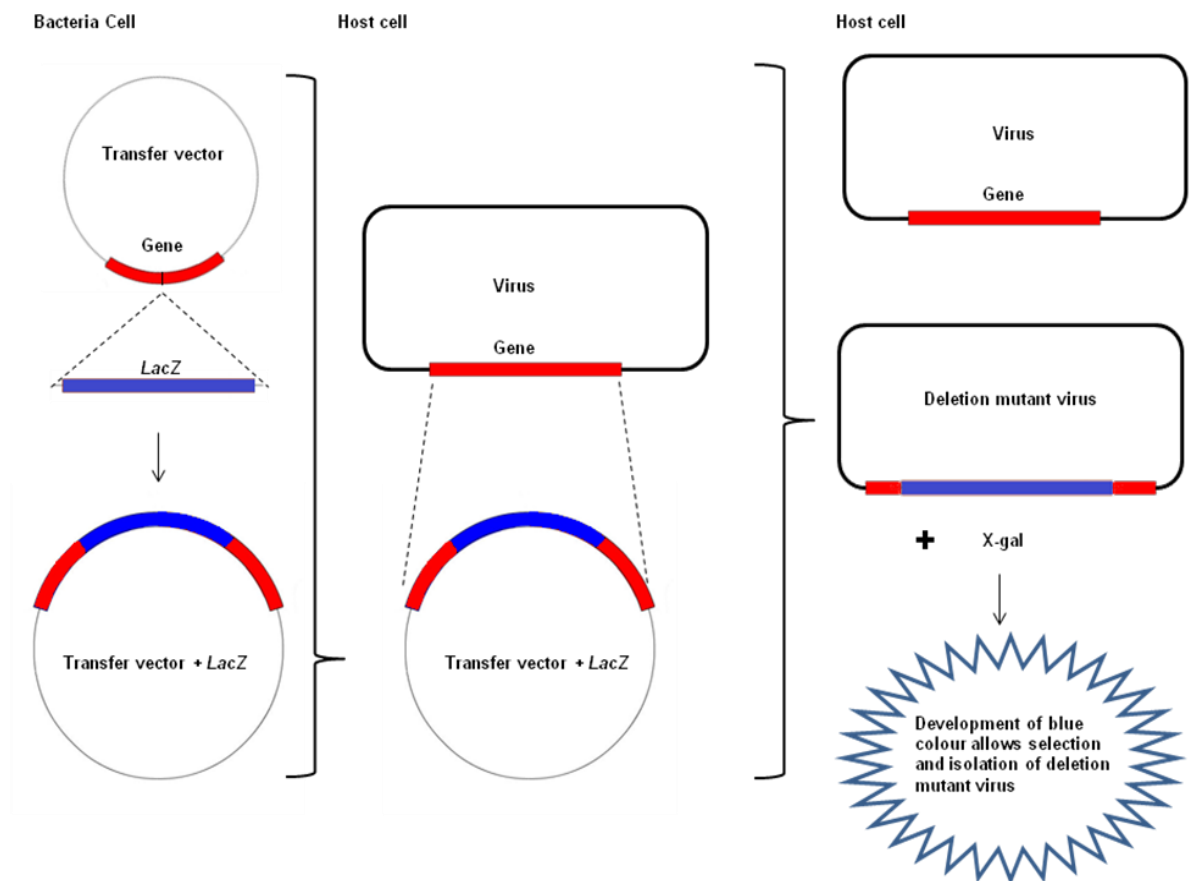


Figure 4.1 Illustration of the method used to disrupt a target gene.

The transfer vector carrying the target gene is modified by the direct insertion of *lacZ* (marker) into the transfer vector causing disruption of the target gene. Viral DNA and modified transfer vector are introduced into the host cells to allow homologous recombination to occur and finally the deletion mutant virus is selected for using the marker.

Although directed mutation of virus sequences in the host cell has proved an efficient way to generate mutants to study protein function, it is impossible to produce deletions in essential genes and recover viable virus for investigation. It is also necessary to construct a plasmid transfer vector with each modified virus gene prior to making the virus mutant via homologous recombination in insect cells. Finally, the process of recombination between a virus genome and a plasmid transfer vector is not 100% efficient, so a mixed population of viruses must be purified further by subsequent rounds of plaque purification. With some genes it was necessary to undertake 15-20 sequential plaque assays to obtain a genetically homogeneous recombinant virus (R.D. Possee, personal communication). The recovery of recombinant viruses can be enhanced if the baculovirus DNA is linearised with a restriction enzyme at the point of marker gene insertion but this is rarely possible due to the size of these genomes. For example, AcMNPV is about 134 kbp and has two

restriction enzyme sites *AvrII* and *FseI* that only digest it once. Kitts *et al.* (1990) introduced a *Bsu361* site into the *polh* locus of AcMNPV so that the virus genome could be linearized, which improved the recovery of recombinant viruses in subsequent tests to 30%. However, while this approach was useful as a tool for making recombinant viruses as expression vectors, it has little application in deriving virus mutants to study gene function.

The introduction of yeast and bacterial vectors for maintaining large circular plasmids in these hosts has enabled the development of new approaches for generating baculovirus gene mutants (Patel *et al.*, 1992; Luckow *et al.*, 1993). The yeast system has not progressed beyond an experimental technique for making recombinant viruses, although it was used to generate *lef2* and *lef8* deletion mutants (R.D. Possee, personal communication). The yeast system can also cause chimerism, rearrangements and deletions in the viral genome during the manipulation (Luckow *et al.*, 1993; Kim *et al.*, 1996). Therefore the yeast system is mainly used for inserting genes encoding recombinant proteins into the baculovirus genome at either the *p10* or *polh* locus to allow expression of these sequences in either insect cell culture or larvae.

The bacterial system is based on a low copy number plasmid or bacterial artificial chromosomes (BAC), which was originally developed for cloning large sections of human genome to aid in mapping and sequencing of the human genome (Shizuya *et al.*, 1992). The BAC is based on the *E. coli* F factor, which means the replication of the BAC is strictly controlled, resulting in only one copy per bacteria cell (Kim *et al.*, 1996). Baculovirus genomes were first maintained in bacteria by Luckow *et al.* (1993) who developed a transposition system for inserting foreign genes into AcMNPV that avoided the need to do plaque purification of recombinant viruses. While this system is of little direct use in making modifications to other regions of the AcMNPV genome, it established the principle that infectious baculovirus genomes could be recovered from bacteria and used subsequently to transfect insect cells. When this is allied with the Red/ET recombination BAC-based system used for manipulation of large DNA molecules (Zhang *et al.*, 1998), it provided an extremely convenient method for modifying any target sequence in the baculovirus genome.

4.1.1 Red/ET recombination system

The Red/ET recombination system uses homologous recombination in *E. coli*, which allows specific and accurate exchange of genetic material between two DNA molecules. This exchange occurs through homologous regions that are stretches of DNA shared by the two DNA molecules, which allows this system to specifically alter any location on the

selected DNA molecule. The core of the Red/ET recombination system comprises two phage encoded proteins; RecE and RecT, which function via a double-strand, break-repair mechanism. They were first shown in 1998 to mediate homologous recombination between the antibiotic marker kanamycin that contained homologous arms and circular DNA maintained within *E. coli*. Using this method it was shown that homologous arms as short as 42bp could successfully be used to integrate the kanamycin resistance gene into the circular DNA (Zhang *et al.*, 1998). However, the efficiency of the homologous recombination in the Red/ET system has been increased three-fold by replacing the *recE* and *recT* with their respective functional counterparts of phage lambda *red α* and *red β* . Using these coupled proteins allows this system to directly insert linear double-stranded DNA into high copy number plasmids, large episomes, BACs and the *E. coli* chromosome itself (Muyrers *et al.*, 2000).

The RecE/RecT or Red α /Red β proteins naturally function as double-stranded repair proteins during DNA breakage caused by damaging reagents. The RecE and Red α are 5'-3' exonucleases that digest one of the 5' ends of the linear double-stranded DNA, leaving a single-stranded 3' extension, which is then bound and coated by RecT or Red β . This protein-nucleic acid filament aligns with homologous DNA and allows recombination to occur between the two DNA molecules (Zhang *et al.*, 1998; Muyrers *et al.*, 1999). In the Red/ET recombination system these proteins are expressed from a single plasmid; pRedET, which was developed in A. Francis Stewart's laboratory at the European Molecular Biology Laboratory (EMBL). The Red α /Red β proteins play the key role in homologous recombination in the Red/ET recombination system, however, several other proteins are produced from the pRedET that optimize the system allowing more controlled and efficient homologous recombination.

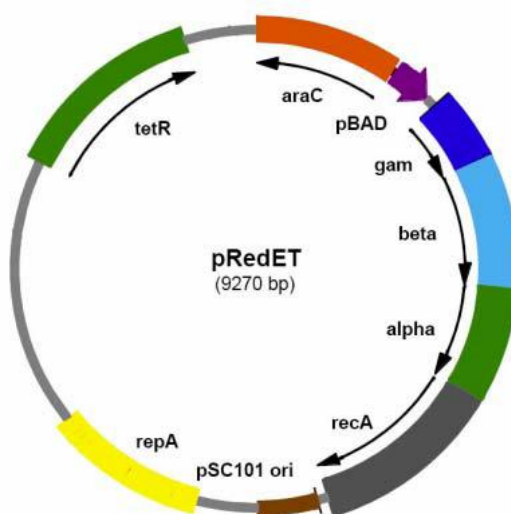


Figure 4.2 pRedET plasmid

Map of the Red/ET expression plasmid pRedET showing all the genes involved in the Red/ET recombination system (From the Gene Bridge BAC Modification Kit manual).

The pRedET contains both *red α* and *red β* along with a third λ phage gene; *gam* (Figure 4.2). The Gam protein assists the recombination by inhibiting RecBCD exonuclease activity of the *E. coli*, which prevents digestion of the linear double-stranded DNA fragment. All of the λ phage genes along with *recA* are under the control of the pBAD promoter, forming an operon that is arabinose inducible. The *E. coli* RecA protein is involved in the recombination process by aiding the protein-nucleic acid filaments binding to the homologous DNA. The *araC* produces a protein that is involved in transcriptional regulation of the pBAD promoter and forms a complex with L-arabinose which allows transcription to begin. The AraC forms a dimer in the absence of L-arabinose or presence of glucose that blocks the transcription from the pBAD promoter. The temperature sensitive RepA is required for plasmid DNA replication and the partitioning of plasmids to daughter cells at division. Therefore the plasmid is maintained at 30°C in liquid culture but due to the heat sensitive nature of RepA the plasmid copy number drops at temperatures above 37°C. This regulation of pRedET copy number along with the controlling elements of key homologous recombination genes allows the timing of the recombination event to be selectable, thereby decreasing the risk of unwanted intra-molecular rearrangement (Muyrers *et al.*, 1999).

For baculovirus, homologous recombination in *E. coli* has proven a most useful tool enabling the deletion mutants to be rapidly created and tested. McCarthy and Theilmann (2008) used homologous recombination in *E. coli* to replace *odv-e18* with a zeocin gene resistance cassette. Using this knockout they demonstrated that *odv-e18* is essential for mediating budded virus production (McCarthy and Theilmann, 2008). McCarthy *et al.* (2008) used a similar method to replaced ORF 142 a structural component of AcMNPV BV and ODV nucleocapsids with a zeocin gene resistance cassette. Using this knockout demonstrated that ORF 142 is required for budded virus production, nucleocapsid envelopment to form ODV and their subsequent occlusion (McCarthy *et al.*, 2008). Recently, Xiang *et al.* (2011) used homologous recombination in *E. coli* to construct an *odve66* deletion mutant virus and showed that this virus had no affect on viral replication but oral infectivity of this deletion mutant virus was 10 times lower than either a rescued or parental virus. This strongly indicates that ODVE66 plays an important role in oral infectivity of AcMNPV.

In this chapter, the aim was to use the Red/ET system to delete the eight ODV genes identified in Chapter 3, to produce eight mutant viruses for further characterisation in later chapters.

4.2 Construction of parental bacmid (AcBacPAK5/*lacZ*/BAC^{pol})

The AcBacPAK5/*lacZ*/BAC^{pol} was constructed to provide a virus for this research that included a complete baculovirus genome containing a BAC replicon allowing the virus genome to be maintained in *E. coli* along with a *lacZ* reporter gene. The *lacZ* would allow expression tests to be carried out in insect cells to observe any effects subsequent gene deletions could have on recombinant protein expression under the control of the *polh* promoter. The deletion mutant viruses could also be linearised due to a unique *Bsu361* site within *lacZ* allowing insertion of the *polh* or other recombinant genes at the *polh* locus. Also during the isolation of recombinant baculoviruses, the beta-galactosidase produced could serve as a selective maker for the parental virus.

The parental virus for the construction of AcBacPAK5/*lacZ*/BAC^{pol} was BacPAK5 (Kitts and Possee, 1993). A transfer plasmid was constructed using the commercially available pBacPAK8 (Clontech) into which the *lacZ* gene and BAC replicon were sub-cloned (Figure 4.3, panel A) and as described in methods (section 2.6).

Insect Sf9 cells were co-tranfected with pBacPAK8-*lacZ*/BAC and *Bsu361* linearised BacPAK5 DNA, which had been purified from BacPAK5 BVs as described in methods (section 2.3.6a), to derive the bacmid AcBacPAK5/*lacZ*/BAC^{pol} (Figure 4.3, panel B). BacPAK5 DNA contains two *Bsu361* sites that flank the *polh*; one of these sites is located in the essential gene *orf1629*. This produces a selection marker in which only those viruses that are rescued with a transfer plasmid that restores the whole of *orf1629* will be viable in insect cells. Recombination between BacPAK5 and pBacPAK8-*lacZ*/BAC should knock-out the *polh* and result in a virus (AcBacPAK5/*lacZ*/BAC^{pol}) whose only difference from AcMNPV is the presence of *lacZ* and BAC in place of the *polh*.

The resulting recombinant virus was plaque-purified for three rounds, which were required to generate polyhedrin-negative and *lacZ*-positive plaques (plaques that turned blue when stained with X-gal) (data not shown). The virus amplified to titres of 8.9×10^7 pfu/ml and infected cells turned blue in the presence of X-gal (data not shown) suggesting that the virus was replicating normally in insect cells. No polyhedra were visible under the microscope (data not shown). Virus DNA was isolated from BV and restriction digest profiles were used to first confirm the successful recombination event with insertion of *lacZ* and BAC at the *polh* locus and, second, to ensure that the rest of the virus genome restriction profile was unaffected by the recombination process (Figure 4.4). The *HindIII* restriction fragment pattern of the new AcBacPAK5/*lacZ*/BAC^{pol} virus (Figure 4.4, lane 3) was compared to the pattern of the parental BacPAK5 (Figure 4.4, lane 2). The insertion of the *lacZ* fragment and BAC replicon into the *polh* locus to produce

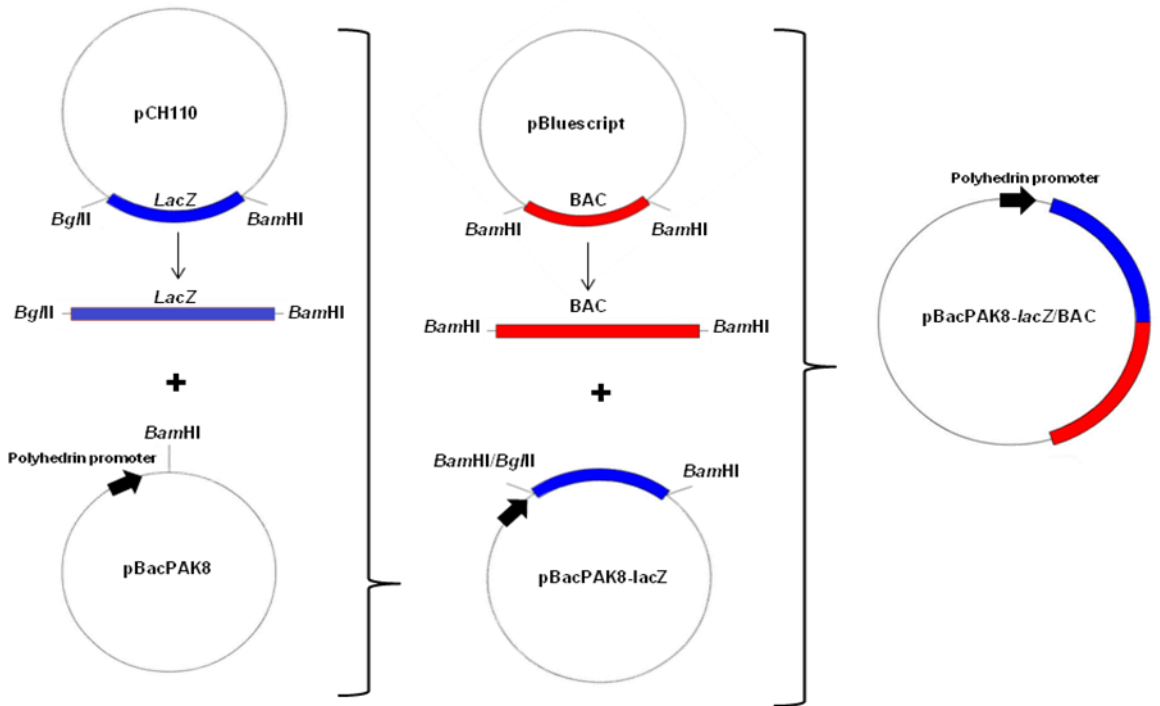
AcBacPAK5/*lacZ*/BAC^{pol} resulted in a 150bp size decrease to fragment F due to the loss of the *Hind*III site in the *polh* and the small addition from *lacZ* fragment, producing a new fragment of 8829bp (Figure 4.4, panel A, lane 3). A second new fragment with an approximate size of 9400bp appeared due to the *Hind*III site located in both the *lacZ* fragment and BAC replicon (Figure 4.4, panel B). These results confirmed that both the *lacZ* and BAC had been correctly inserted into the *polh* locus of AcBacPAK5/*lacZ*/BAC^{pol}.

Figure 4.3 Illustration of the formation of AcBacPAK5/*lacZ*/BAC^{pol}

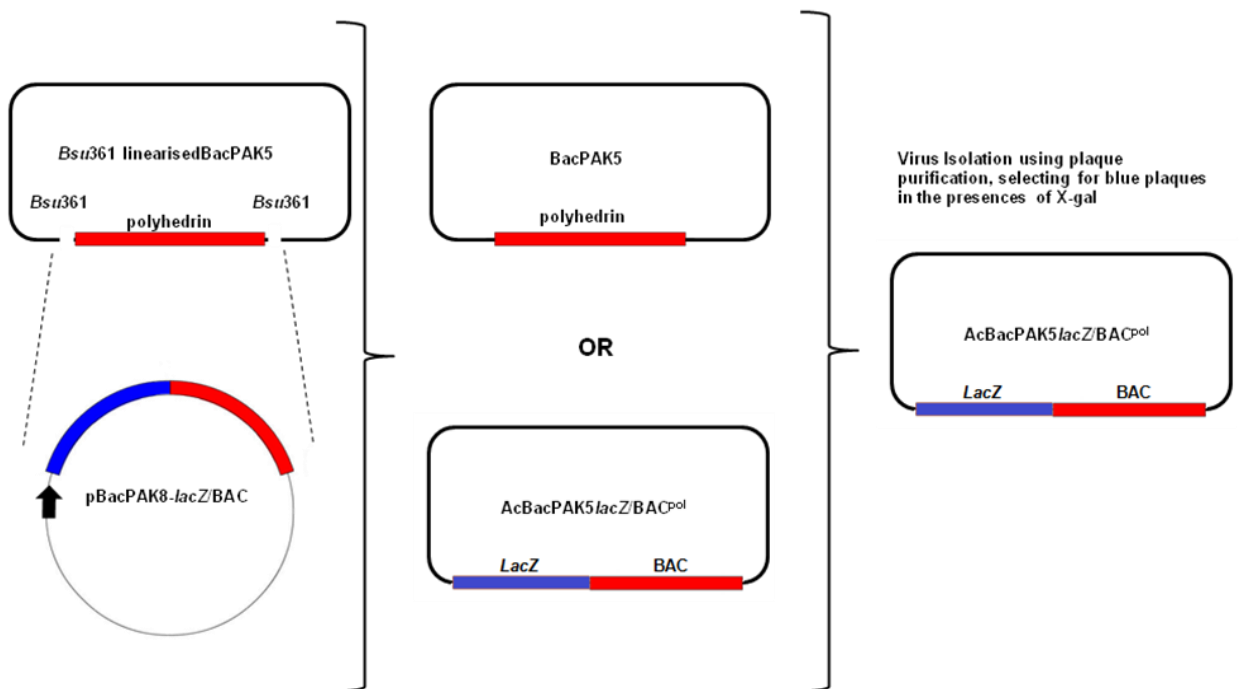
(A) The *lacZ* fragment was subcloned from pCH110 into the *Bam*HI site of pBacPAK8. This insertion resulted in a fusion of *Bam*HI and *Bgl*II sites at the 5' end of *lacZ* but left the *Bam*HI site at the 3' end intact and available for subsequent insertion of the BAC replicon from pBluescript-BAC to form pBacPAK8-*lacZ*/BAC.

(B) Sf9 Cells co-transfected with pBacPAK8-*lacZ*/BAC and *Bsu*361 linearised BacPAK5 DNA, to form AcBacPAK5/*lacZ*/BAC^{pol}. AcBacPAK5/*lacZ*/BAC^{pol} was isolated from parental background using plaque purification, polyhedrin negative and *lacZ* positive plaques were selected for further study.

A



B



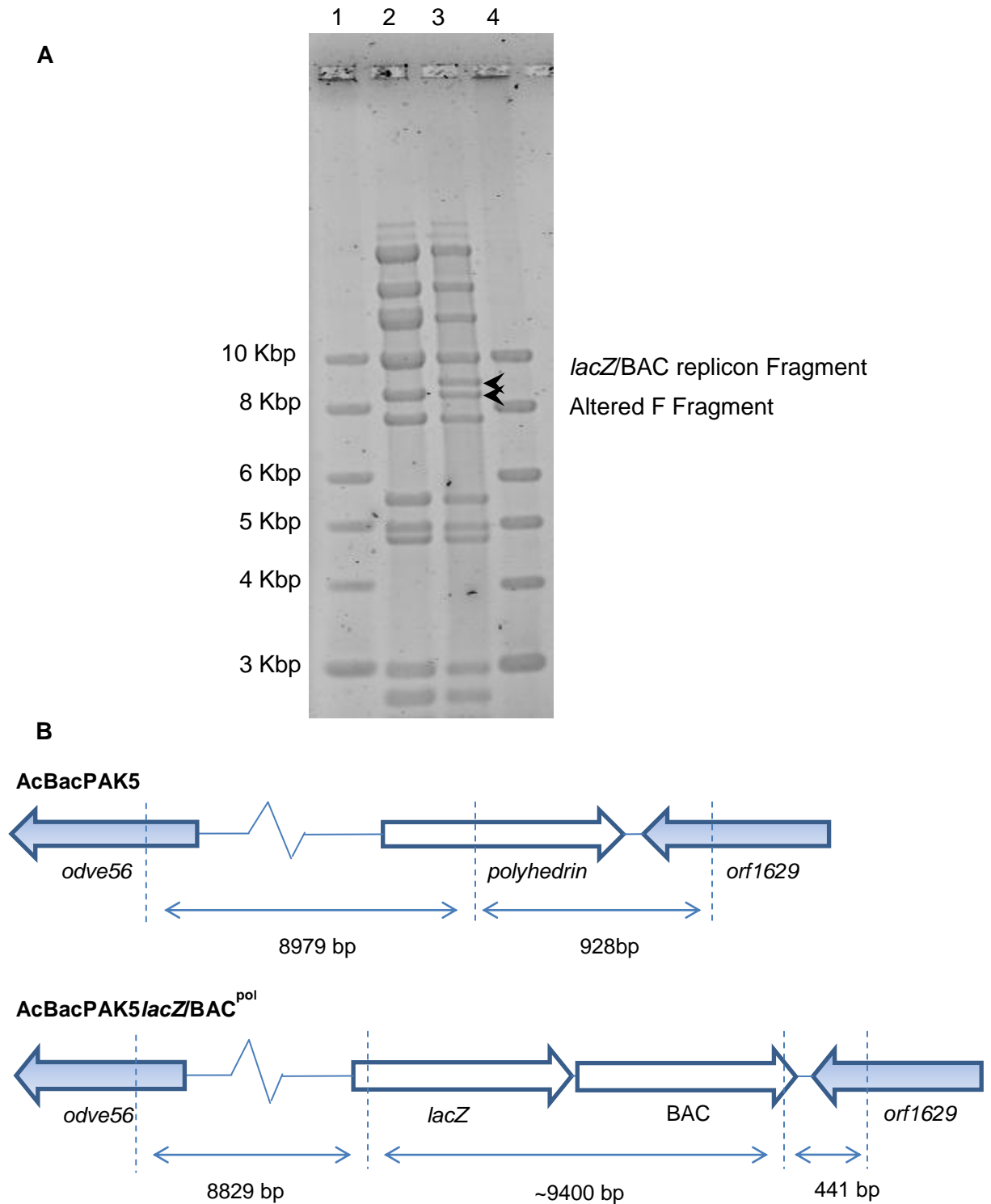


Figure 4.4 *HindIII* restriction enzyme analysis of AcBacPAK5/*lacZ/BAC*^{pol} virus

Sf9 cells were cotransfected with pBacPAK8-*lacZ/BAC* and *Bsu361*-linearised BacPAK5 virus DNA. The resulting BV was used to isolate virus DNA that was validated by restriction enzyme (*HindIII*) analysis in a 0.6% agarose gel (A). Lanes 1 and 4, NEB log2 marker in Kbp; lane 2, BacPAK5 DNA; lane 3, AcBacPAK5/*lacZ/BAC*^{pol} DNA. (B) Alternations to the *HindIII* F fragment of AcBacPAK5/*lacZ/BAC*^{pol} shown due to the replacement of polyhedrin with *lacZ/BAC* replicon.

Viral DNA purified from AcBacPAK5/*lacZ*/BAC^{pol} BV was electroporated into DH5 α *E. coli*, as described in Methods (section 2.5.5) to facilitate the use of the Red/ET recombination system to delete ODV genes from AcBacPAK5/*lacZ*/BAC^{pol}.

Thus all the experimental data indicated that pBacPAK8-*lacZ*/BAC and BacPAK5 had been used successfully to generate AcBacPAK5/*lacZ*/BAC^{pol}. (1) The restriction profile matched the expected shift in restriction fragment sizes resulting from the introduction of two *Hind*III sites flanking the inserted *lacZ* and BAC. (2) The virus could replicate in cell culture and successfully produce β -galactosidase, but not polyhedra. (3) The viral DNA could be maintained in *E. coli*, which grew in the presence of chloramphenicol due to the BAC located in the viral DNA.

4.3 Construction of the kanamycin gene cassette with AcMNPV flanking sequences and production of ODV deletion mutant bacmids

In order to delete the required AcMNPV ODV genes from the bacmid AcBacPAK5/*lacZ*/BAC^{pol}, it was necessary to construct a neomycin selection cassette (Neo cassette) flanked by relevant ODV sequences that would allow kanamycin selection. The kanamycin resistance gene fragment supplied with the Red/ET recombination system was amplified using primers with regions flanking the selected ODV genes (Figure 4.5). The flanking regions were designed to remove as much coding region from the selected ODV gene without disrupting neighbouring gene expression using the bioinformatics data (Chapter 3). In most cases portions of the ODV coding region remain because of the overlapping nature of the genes within the AcMNPV genome (Ayres *et al.*, 1994). The primers used and their locations on the AcMNPV genome are shown in Table 4.1, for specific information on each of the individual deletions refer to their own sections within this thesis.

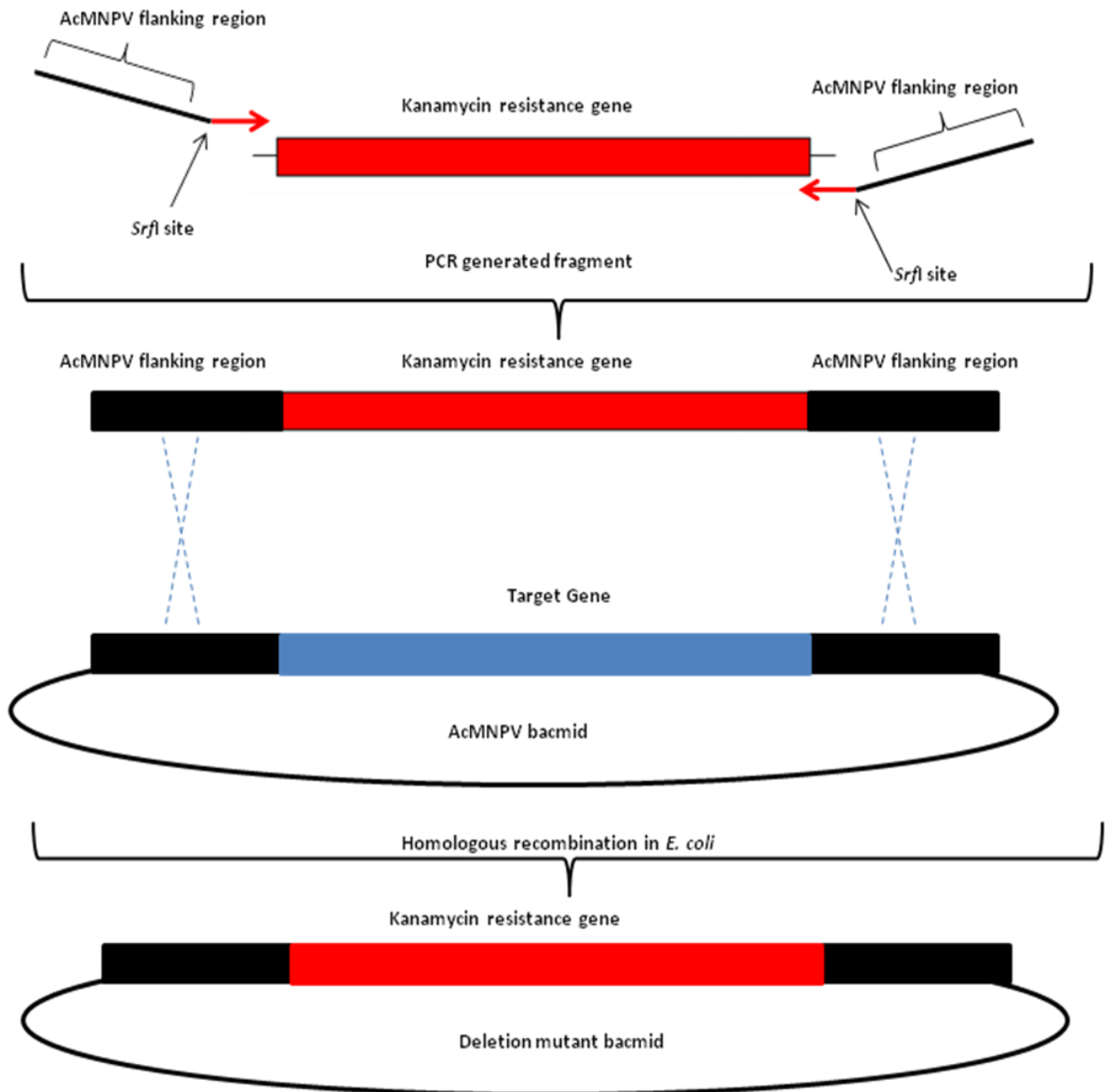


Figure 4.5 Schematic showing the construction of the kanamycin resistance gene cassette with AcMNPV flanking arms.

Primers were designed with flanking regions to the selected target ODV genes and kanamycin binding sites to allow PCR to amplify a modified kanamycin cassette with homologous arms, which could be used with the Red/ET recombination system to remove the target sequence from the AcMNPV bacmid AcBacPAK5/*acZ*/BAC^{pol}.

Chapter 4

Table 4.1 Sequence of ODV primers and their location on the AcMNPV genome

orf	Name	Primer	5' - 3' Primer Sequence	5' end
22	PIF2	ACC1	ACATTTTGAATATTTAATTCAACAATAAGTAATGGCAAT*GCCCCGGGC*neo-F	17311
		ACC2	GACGTAACATTTAAATGACTTATTGTTTGTGTTATCACAA*GCCCCGGGC*neo-R	18489
46	ODV-E66	ACC5	TATTAATAATAAGCAACATTCGACATGTCTATCGTATTGA*GCCCCGGGC*neo-F	36684
		ACC6	ACAGTCAGTCTTTTGAATATCACATTCTCCCTAAATATAA*GCCCCGGGC*neo-R	38882
96	ODV-E28	ACC9	GCACGTTTTTCAAAAAAATTGTAAAATGTTGTCAATCAT*GCCCCGGGC*neo-F	84524
		ACC10	CTATATACGCGTTATTCGGCCAACAAATCCACGTAGCCAT*GCCCCGGGC*neo-R	84742
115	PIF3	ACC13	AAAGCGCGTACTTGCTCATGTTGACAGAATCTCTTACATT*GCCCCGGGC*neo-F	99301
		ACC14	GTGCGTCACACCACGCTTTTTCACACTCAGTTAAGACGATC*GCCCCGGGC*neo-R	99836
148	ODV-E56	ACC17	AATTAATTATACATATATTTTATATTATTTTGTCTTTTA*GCCCCGGGC*neo-F	128958
		ACC18	CCTTTACTGTGATATATTTATTAATAAGTTTGTCTTTAAA*GCCCCGGGC*neo-R	130188
88	CG30	ACC21	ATATTATTACATTAAAGTAGAATGTTATGTAAACAGTTAA*GCCCCGGGC*neo-F	74687
		ACC22	GTGTTGCAGGCGAAGCAGGTGGAGGAATAGCCGTCTAAAA*GCCCCGGGC*neo-R	75581
79	12.1 kDa	ACC25	TGGTTGCCCAACCGATAGTAGGGCACGTCCAAATTCATGT*GCCCCGGGC*neo-F	65392
		ACC26	ACGCCACTCGGCCGAACACGAAAGGGCGCACTGCATAATC*GCCCCGGGC*neo-R	65644
109	ODV-EC43	ACC29	GATATAATGTCGGCCCGCGTTCGGTTTCATGATGTGCTTAA*GCCCCGGGC*neo-F	94731
		ACC30	AATAATCTAAAGTCTAATGAAGTAAGACATATACATCACG*GCCCCGGGC*neo-R	95943

Notes: The orf column contains the orf number for the corresponding gene indicated in the name column. The Primer columns show the label given to each primer along with the sequence for each primer; the black text is the region selected for homologues recombination, *SrfI* restriction site is shown by *GCCCCGGGC* and the neo-F (TGGACAGCAAGCGAACCGGAATTGC) or neo-R (TCAGAAGAACTCGTCAAGAAGGCG) indicates where the primer will bind to the kanamycin fragment (Gene Bridge) to allow amplification. The 5' end column displays the 5' end position on AcMNPV genome for each of the primers.

The eight modified kanamycin resistance gene fragments were then used to electroporate Red/ET recombination competent *E. coli* containing the AcMNPV bacmid AcBacPAK5/*lacZ*/BAC^{pol}. Kanamycin-resistant colonies were picked and the deletion mutant bacmids were analysed by PCR and restriction digests to verify that the required gene had been deleted. As an example, Figure 4.6 illustrates how the Red/ET recombination system was used to delete *pif2* from AcBacPAK5/*lacZ*/BAC^{pol}.

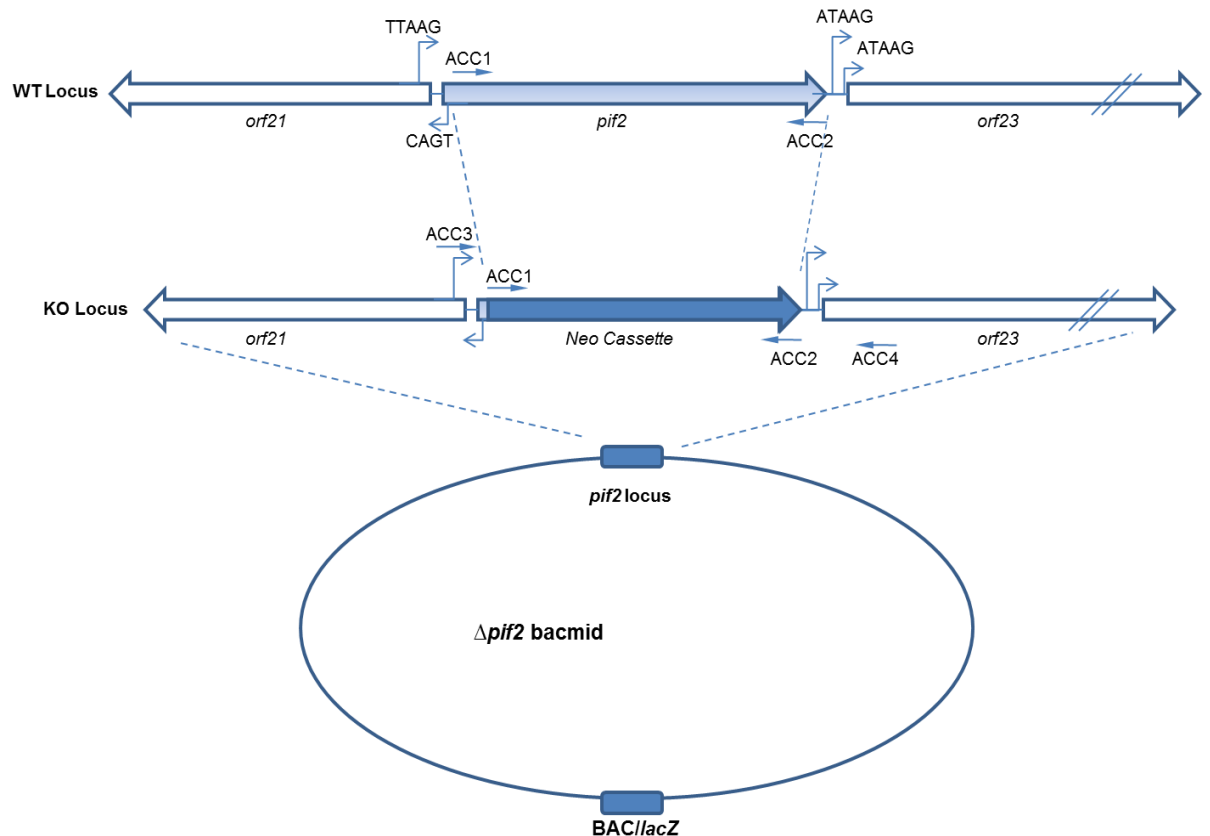


Figure 4.6 Schematic of the construction of AcBacPAK5/*lacZ*/BAC^{pol}Δ*pif2* bacmid.

Most of the *pif2* ORF was deleted by the insertion of the kanamycin resistance gene between positions 17351 and 18449 bp in the AcMNPV genome via homologous recombination in *E. coli* using the Red/ET recombination system.

However, the PCR and RE digest data indicated that the initial attempts to delete the target ODV genes from AcBacPAK5/*lacZ*/BAC^{pol} using the Red/ET recombination were unsuccessful. PCR showed the continued presence of the target ODV gene within the bacmid DNA after the selection process. As an example, *E. coli* colonies that should have contained AcBacPAK5/*lacZ*/BAC^{pol} genomes with a deletion in *cg30* ($\Delta cg30$) appeared to show both the presence of AcBacPAK5/*lacZ*/BAC^{pol}Δ*cg30* and AcBacPAK5/*lacZ*/BAC^{pol}, as evidenced by the clear amplification of both kanamycin/*cg30* (1210 bp) and *cg30* (1058 bp) fragments (Figure 4.7, lanes 3-9). This result was supported by lack of DNA

amplification in the negative control (H₂O) (Figure 4.7, lane 2) and only amplification of the 1058bp *cg30* fragment in the positive control (AcBacPAK5/*lacZ*/BAC^{pol}) (Figure 4.7, lane 2).

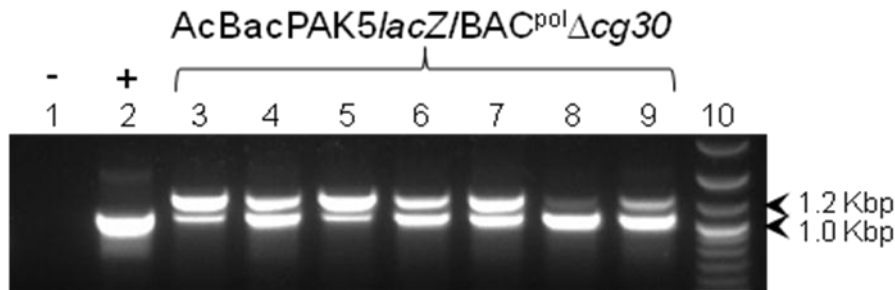


Figure 4.7 PCR analysis of AcBacPAK5/*lacZ*/BAC^{pol}Δ*cg30* DNA

DNA was isolated from putative colonies containing AcBacPAK5/*lacZ*/BAC^{pol}Δ*cg30* and analysed by PCR using primers 121 bp upstream and 110 bp downstream of the *cg30* locus and Taq DNA polymerase (lanes 3-9). A negative (water-only) control is shown in lane 1 and the parental bacmid AcBacPAK5/*lacZ*/BAC^{pol} as a positive control (lane 2). NEB log₂ Marker (Kbp) shown in lane 10 with arrows indicating 1.2 Kbp and 1.0 Kbp sizes.

Similar results were observed when screening the other seven targeted ODV genes, indicating that the Red/ET recombination system wasn't working correctly; something that had not occurred previously when constructing deletion mutant viruses (R.D. Possee, personal communication).

Further attempts to delete the target ODV genes from AcBacPAK5/*lacZ*/BAC^{pol} using the Red/ET recombination system described above were undertaken. After several attempts two of the target genes (*pif2* and *odv-ec43*) were successfully deleted from AcBacPAK5/*lacZ*/BAC^{pol}. The resultant deletion bacmids were designated AcBacPAK5/*lacZ*/BAC^{pol}Δ*pif2* (Δ*pif2*) and AcBacPAK5/*lacZ*/BAC^{pol}Δ*odv-ec43* (Δ*odv-ec43*). Figure 4.8 shows that for Δ*pif2* most clones showed only one DNA fragment with the correct size (1210 bp) amplified using primers flanking *pif2* (lanes 4-7, 9-13 and 15). Similar PCR results were obtain for Δ*odv-ec43* clones (data not shown). The integrity of these two deletion mutants was further characterised by RE digestion, as described in Figure 4.9.

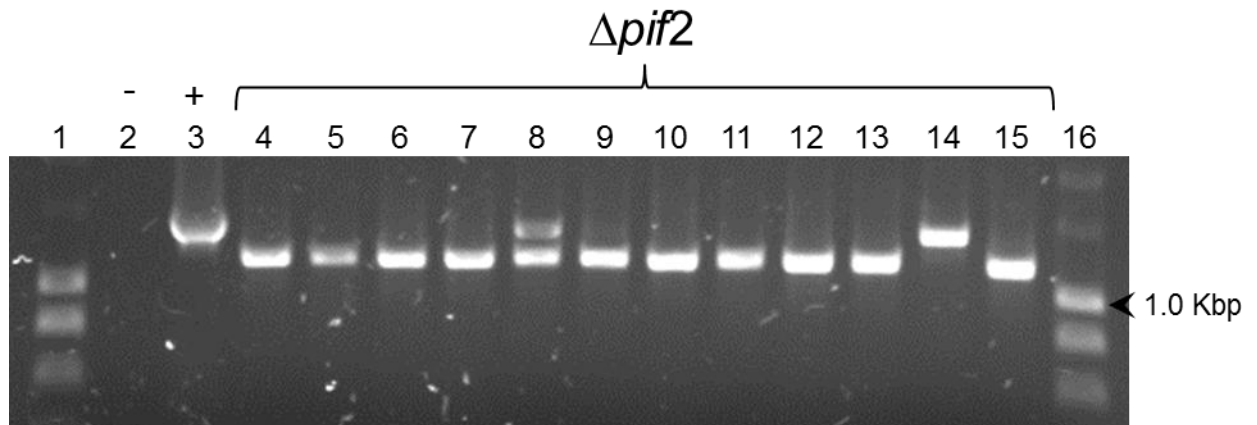


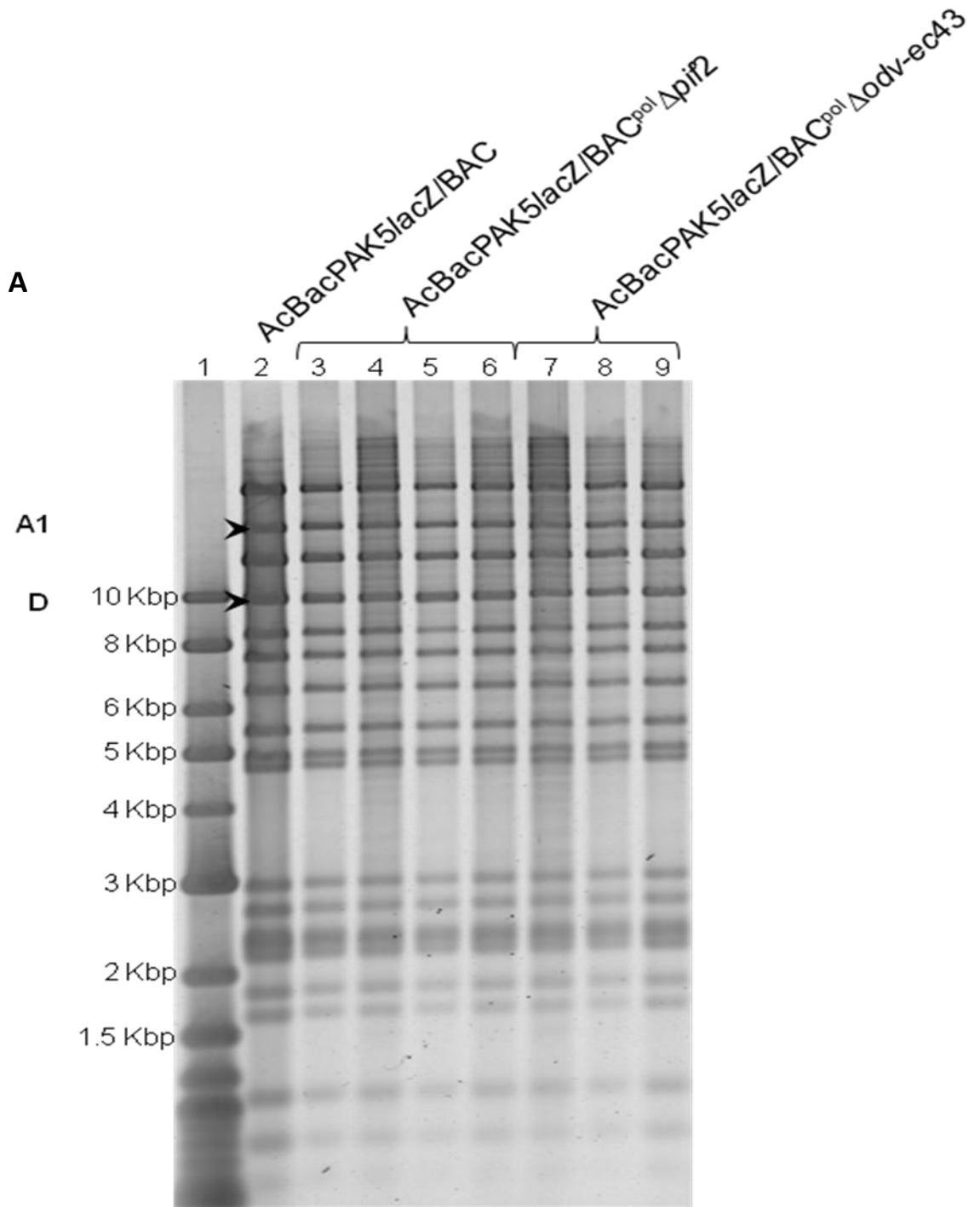
Figure 4.8 PCR analysis of AcBacPAK5/lacZ/BAC^{pol} $\Delta pif2$ DNA

DNA was isolated from putative colonies containing AcBacPAK5/lacZ/BAC^{pol} $\Delta pif2$ and analysed by PCR using primers 82 bp upstream and 120 bp downstream of the *pif2* locus (lanes 4-15). A negative (water-only) control is shown in lane 2 and the parental bacmid AcBacPAK5/lacZ/BAC^{pol} as a positive control (lane 3, 1348bp). NEB log2 Marker (Kbp) shown in lane 1 and 16.

Restriction enzyme digest profiles of $\Delta pif2$ and $\Delta odv-ec43$ (Figure 4.9 A) were used to confirm that the rest of the virus genome was unaffected by the recombination process. The *HindIII* restriction fragment pattern of the deletion mutant bacmids $\Delta pif2$ and $\Delta odv-ec43$ were compared to the pattern of the parental virus. The predicted alteration in the fragment pattern for each deletion can be seen in Figure 4.9 B and these alterations matched the profiles obtained for each of the deletion mutant bacmids in Figure 4.9 A. The gel electrophoresis image in Figure 4.9 A also showed that the rest of the deletion mutant bacmid profile fit the parental bacmid genome as expected, and that no random mutations had occurred that could be detected using this restriction enzyme.

Figure 4.9 *Hind*III restriction enzyme analyses of AcBacPAK5*lacZ*/BAC^{pol} Δ *pif2* and AcBacPAK5*lacZ*/BAC^{pol} Δ *odv-ec43* bacmids.

DNA was isolated from *E. coli* containing either AcBacPAK5*lacZ*/BAC^{pol} Δ *pif2* or AcBacPAK5*lacZ*/BAC^{pol} Δ *odv-ec43* and validated by restriction enzyme (*Hind*III) analysis in a 0.6% agarose gel. Panel A, Lane 1 NEB log2 marker in Kbp; lane 2, AcBacPAK5*lacZ*/BAC^{pol}; lanes 3-6, AcBacPAK5*lacZ*/BAC^{pol} Δ *pif2* and lanes 7-9; AcBacPAK5*lacZ*/BAC^{pol} Δ *odv-ec43*. Panel B contains a table displaying the alterations predicted in the *Hind*III restriction profile caused by the deletion of the target gene and insertion of the kanamycin fragment.



B

orf	Name	Gene size (bp)	Fragment Location	Original Fragment Size (bp)	Expected Fragment Size (bp)	Lane(s)
22	PIF2	1149	D	10001	9803	3-6
109	ODV-EC43	1173	A1	15293	15515	7-9

4.4 Deletion of the remaining six AcMNPV ODV genes using AcBAC Δ chitinase as the parental bacmid DNA

In order to try and overcome the unresolved problems with AcBacPAK5/*lacZ*/BAC^{pol} and Red/ET system (4.3), an alternative bacmid (AcBAC Δ chitinase) was used to delete the remaining six AcMNPV ODV genes; *odv-e66*, *orf79*, *cg30*, *odv-e28*, *pif3* and *odv-e56*. This bacmid contains a copy of the AcMNPV genome minus the chitinase gene (R.D Possee, personal communication). The chitinase gene is non-essential for virus replication in cell culture and plays a role in host liquefaction (Hawtin *et al.*, 1997). Importantly, it did not contain a copy of the *lacZ*, which may have compromised the original Red/ET experimental design. The changing of the bacmid proved successful and all the six remaining deletion mutant viruses were successfully constructed, using essentially the same methodology as previously described (4.3; data not shown).

The integrity of these six deletion mutants was further characterised by RE digestion, as described in section 4.3. The *Hind*III restriction fragment pattern of the deletion mutant bacmids were compared with the pattern of the parental bacmid (Figure 4.10). The expected alteration in the fragment pattern for each deletion can be seen in Table 4.2 and these alterations matched the profiles obtained for each of the deletion mutant bacmids in Figure 4.10. The gel electrophoresis image in Figure 4.10 also shows that the rest of the deletion mutant bacmid profile fit the parental bacmid genome as expected, and that no random mutations had occurred that could be detected using this restriction enzyme. A summary list of the deletion mutant bacmids constructed in 4.3 and this section, along with their abbreviations used further in this thesis, is shown in Table 4.3.

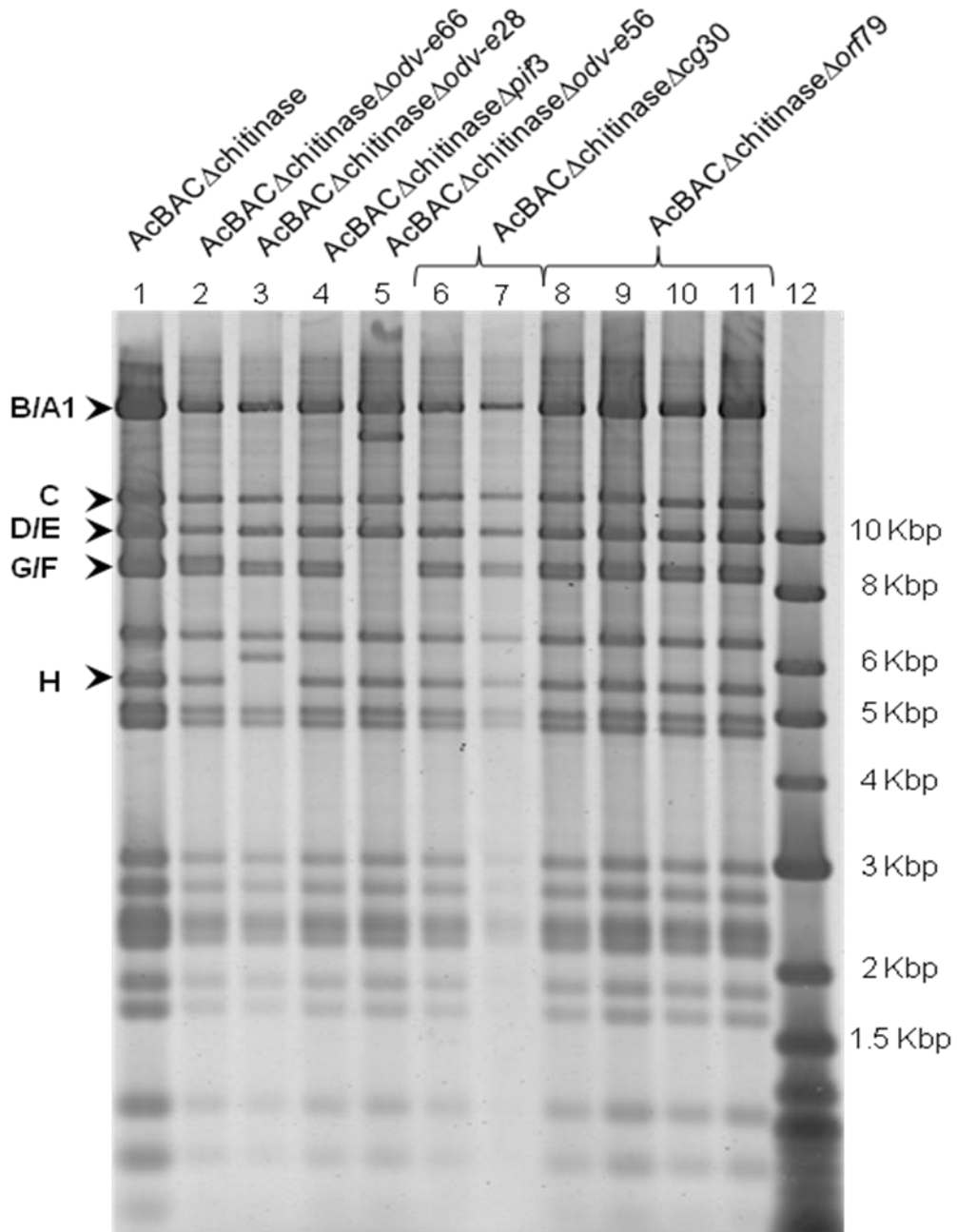


Figure 4.10 HindIII restriction enzyme analyses of deletion mutant bacmids.

DNA was isolated from *E. coli* for each of the six deletion mutant bacmids and validated by restriction enzyme (*Hind*III) analysis in a 0.6% agarose gel. Lanes 12 NEB log2 marker in Kbp; lane 1, AcBAC Δ chitinase; lane 2, AcBAC Δ chitinase Δ odv-e66; lane 3, AcBAC Δ chitinase Δ odv-e28; lane 4, AcBAC Δ chitinase Δ pi β 3; lane 5, AcBAC Δ chitinase Δ odv-e56; lanes 6-7, AcBAC Δ chitinase Δ cg30 and lanes 8-11, AcBAC Δ chitinase Δ orf79.

Table 4.2: The predicted alterations to the banding pattern of *HindIII*-digested parental bacmid.

orf	Name	Gene size (bp)	Fragment Location	Original Fragment Size (bp)	Expected Fragment Size (bp)	Lane(s)
46	ODV-E66	2099	E	9916	8768	2
96	ODV-E28	479	H	5502	5974	3
115	PIF3	615	A1	15293	15629	4
148	ODV-E56	1131	G/F	8397/8979	17196	5
88	CG30	795	C	11704	11860	6-7
79	12.1 kDa	315	B	21769	22405	8-11

Table 4.3: Summary of deletion mutant bacmids.

orf	Gene	Name	Short form bacmid name	Short form virus name ¹
22	PIF2	AcBacPAK5/lacZ/BAC ^{pol} Δ <i>pif2</i>	Δ <i>pif2</i>	AcΔ <i>pif2</i>
109	ODV-EC43	AcBacPAK5/lacZ/BAC ^{pol} Δ <i>odv-ec43</i>	Δ <i>odv-ec43</i>	AcΔ <i>odv-ec43</i>
46	ODV-E66	AcBACΔchitinaseΔ <i>odv-e66</i>	Δ <i>odv-e66</i>	AcΔ <i>odv-e66</i>
79	12.1 kDa	AcBACΔchitinaseΔ <i>orf79</i>	Δ <i>orf79</i>	AcΔ <i>orf79</i>
88	CG30	AcBACΔchitinaseΔ <i>cg30</i>	Δ <i>cg30</i>	AcΔ <i>cg30</i>
96	ODV-E28	AcBACΔchitinaseΔ <i>odv-e28</i>	Δ <i>odv-e28</i>	AcΔ <i>odv-e28</i>
115	PIF3	AcBACΔchitinaseΔ <i>pif3</i>	Δ <i>pif3</i>	AcΔ <i>pif3</i>
148	ODV-E56	AcBACΔchitinaseΔ <i>odv-e56</i>	Δ <i>odv-e56</i>	AcΔ <i>odv-e56</i>

¹This name is used for virus recovered after transfection of Sf9 cells with bacmid DNA.

4.5 Recovery of virus after transfection of Sf9 cells with deletion bacmids

Having confirmed that the eight deletion bacmids were genetically correct, the next stage was to test whether viable virus could be recovered when insect cells were transfected with the deletion mutant bacmid DNA. Bacmid DNA was purified from multiple *E. coli* colonies of each of the eight deletion bacmids (referred to as clones) and Sf9 cells were transfected as described in methods (section 2.3.3). Five of the deletion mutant viruses; *AcΔpif2*, *AcΔodv-e66*, *AcΔcg30*, *AcΔpif3* and *AcΔodv-e56* were able to successfully replicate in the Sf9 cells and produce visible virus cytopathic effects as determined from microscopic observations during virus amplification (data not shown). The viruses recovered from transfected Sf9 cells were designated “Ac” to distinguish them from the bacmid DNA isolated from *E. coli* (Table 4.3). However, cells transfected with *Δorf79*, *Δodv-e28* or *Δodv-ec43* showed no obvious signs of viral infection (data not shown). Virus DNA was purified from the BV harvested from these infections and the modified gene locus in each of the deletion mutant viruses was amplified using primers specific for each gene (Table 4.4). For each virus clone, PCR was used to (1) confirm the deletion of the target ODV gene, (2) confirm the absence of parental virus (*AcBacPAK5/acZ/BAC^{pol}* or *AcBACΔchitinase*) and (3) make the final selection of deletion mutant virus clone where multiple clones had been analysed (Figure 4.10).

Primers designed to ~110 bp upstream and ~120 bp downstream for each of the target gene loci were used in a PCR using Taq DNA polymerase to amplify the locus to allow the determination of the kanamycin insert. The insertion of kanamycin into the target locus would result in the amplification of a 1210bp fragment with any difference in this product size indicating the presence of the original gene. Primers were also designed internally for each of the target loci and these would produce a product of about ~200 bp if the gene was still present.

Figure 4.11 shows the results of the PCR; all the gels were set up with negative (H₂O) and positive (parental viral DNA) controls and as expected these showed either no amplification (negative control) or amplification of bands suggesting the target gene was present (positive control). The target gene was not detected in any of the samples tested for the *AcΔcg30*, *AcΔodv-e66*, *AcΔpif3* and *AcΔodv-e56* viruses (Figure 4.11 B, E, and D respectively). One of the *AcΔpif2* viruses does indicate the presence of *pif2* (Figure 4.11 A, lane 13). There were no products generated for the *AcΔorf79* virus samples with either internal or external primers (Figure 4.11 B). The *AcΔodv-e28* results suggested the presence of both *AcBACΔchitinaseΔodv-e28* and *AcBACΔchitinase*, as evidenced by the clear amplification of both kanamycin/*odv-e28* (1210 bp) and *odv-e28* (715bp) fragments

(Figure 4.11 A, lane 18). The presence of *odv-e28* was confirmed by the amplification of a 214 bp internal fragment (Figure 4.11 A, lane 21).

For *AcΔodv-ec43*, two lanes both contain a single band of 1365 bp indicating that *odv-ec43* is present in those samples (Figure 4.11 C, lanes 4 and 7). Two other lanes contain fragment sizes indicating that both *odv-ec43* and the kanamycin resistance fragment (1143 bp) are present in these samples of *AcΔodv-ec43* (Figure 4.11 C, lanes 15 and 16). The presence of *odv-ec43* was confirmed further using the internal primers giving the correct size band of 273 bp in three of the samples (Figure 4.11 C, lanes 22, 30 and 31). All other lanes indicated that neither *odv-ec43* nor the kanamycin resistance fragment was present in those samples.

The selection of a single deletion mutant virus clone for further study was only necessary for *AcΔpif2* and *AcΔcg30*, due to these two deletion mutant viruses having more than one cloned analysed in this section. For both of these deletion mutant viruses, the first clone was chosen; *AcΔpif2* (Figure 4.11 A, lanes 4 and 11) and *AcΔcg30* (Figure 4.11 B, lanes 4 and 10).

Following this initial characterisation, it was possible to divide the eight deletion mutant viruses into three clusters for further study:

1. The three mutant viruses that did not appear to replicate in insect cells (*AcΔodv-ec43*, *AcΔorf79* and *AcΔodv-e28*). These are further characterised in 4.6
2. The mutant viruses that contain deletions in non *pif* genes (*AcΔodv-e66*, *AcΔcg30* and *AcΔodv-e56*). These will be further characterised in Chapter 5.
3. The mutant viruses that contain deletions in *pif* genes (*AcΔpif2* and *AcΔpif3*). These are further characterised in Chapter 6.

Table 4.4 Sequence of external and internal primers for each target gene.

orf	Name	Primer	5' - 3' Primer Sequence	
22	<i>pif2</i>	External	ACC3	AGGCATTAAGCCCGAATTGT
			ACC4	CAGCTTTACACCGTCCATGA
		Internal	ACC37	ATATGCGATAACCCGTCTGC
			ACC38	AGGGGATTAAGCGGATTAACA
46	<i>odv-e66</i>	External	ACC7	GAATCGGTGTTGGCGTCTAT
			ACC8	CGTGATTTGTACGCGTTAGC
		Internal	ACC35	CCGATTGGTACCATTTCACA
			ACC36	CCTTGAGTCACGTACGGAAA
96	<i>odv-e28</i>	External	ACC11	TCCTGTTGCGGTGTTTCTAA
			ACC12	AGTGACTCTTTCACCCATTGC
		Internal	ACC33	TTTGGCGCGTATGTACAGATT
			ACC34	TGGCATATATTCCCGTCTCG
115	<i>pif3</i>	External	ACC15	AGCGTAATTCACGTTGTTCGTT
			ACC16	TCAGATGCATGACGGTAAAAA
		Internal	ACC39	GTACGTGCTCACGCATGTTT
			ACC40	GCACATTAACGAGTTGGAAGC
148	<i>odv-e56</i>	External	ACC19	ACGTTTGCGGAACAAAAACT
			ACC20	TCTCGCCCAGAATCTAAAGC
		Internal	ACC41	GACCCAAGTCGCCAACTAAA
			ACC42	CACCGGCGGAAGTTATTATG
88	<i>cg30</i>	External	ACC23	CGACACAAATAATTGGCATCA
			ACC24	ACTTTTTGCGCAACGACTTTA
		Internal	ACC45	TTGCGTAATCGTCATTGAGC
			ACC46	GCAGAAGACAACAACGCAAA
79	12.1 kDa	External	ACC27	TCGCTAAATTGTTGCGGTTTC
			ACC28	TTACAACAAGGACGCCAACG
		Internal	ACC43	AGTGGTTTGGCTTTGATGAGA
			ACC44	TGTACATTCTGCGGCAAGAC
109	<i>odv-ec43</i>	External	ACC31	GTTGTGGGCTTGGATGATGT
			ACC32	ATTACAATTACGTGCCCGACA
		Internal	ACC47	GTCCACAACCGTTTGGCTAT
			ACC48	AATCTGGAAACGTCCACCAT

Notes: The orf column contains the orf number for the corresponding gene indicated in the name column. The Primer columns indicates whether the primer is external or internal to the target gene and the label given to each primer along with the sequence for each primer.

Figure 4.11 PCR analysis of deletion mutant virus DNA

DNA was isolated from BV for each of the eight deletion mutant viruses and analysed by PCR using both external and internal primers. Marker used NEB Log2 Marker, Negative (water-only) and Positive control (AcBAC Δ chitinase or AcBacPAK5/*acZ*/BAC^{pol}) found in first two lanes in each primer set followed by samples using either external primers (external) or internal primers (internal).

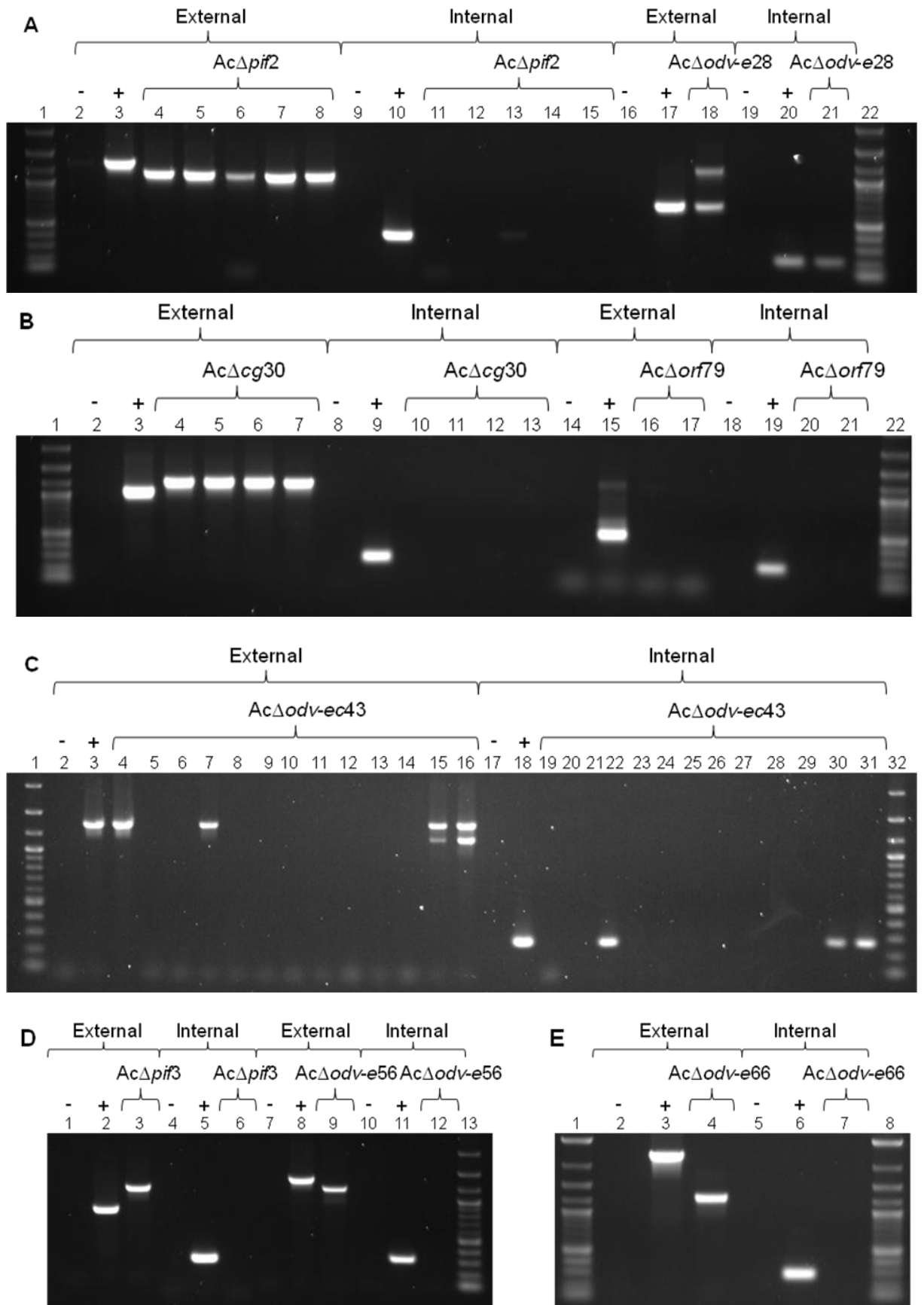
(A) PCR results from *Ac Δ pif2* clones using ACC3/ACC4 external primers and ACC37/ ACC38 internal primers and from *Ac Δ odv-e28* clone using ACC11/ACC12 external primers and ACC33/ACC34 internal primers.

(B) PCR results from *Ac Δ cg30* clones using ACC23/ACC24 external primers and ACC45/ACC46 internal primers and from *Ac Δ orf79* clone using ACC27/ACC28 external primers and ACC43/ACC44 internal primers.

(C) PCR results from *Ac Δ odv-ec43* clones using ACC31/ACC32 external primers and ACC47/ACC48 internal primers.

(D) PCR results from *Ac Δ pif3* clone using ACC15/ACC16 external primers and ACC39/ACC40 internal primers and from *Ac Δ odv-e56* clone using ACC19/ACC20 external primers and ACC40/ACC41 internal primers.

(E) PCR results from *Ac Δ odv-e66* clone using ACC7/ACC8 external primers and ACC35/ACC36 internal primers.



4.6 Characterization of *Ac* Δ *odv-ec43*, *Ac* Δ *orf79* and *Ac* Δ *odv-e28*

4.6.1 *Ac* Δ *odv-ec43*

As described in Chapter 3, *odv-ec43* is one of the 31 conserved baculovirus genes and although it has not been characterized, its homologue in HaSNPV, ORF94, encodes a protein that has been localized to the ODV envelope and nucleocapsids. The Red/ET system was successfully used to produce a deletion mutant bacmid (Δ *odv-ec43*) in which the majority of the coding region of *odv-ec43* was removed and replaced with a kanamycin resistance gene, leaving ~50bp of *odv-ec43* at the 5' end to ensure that the *orf108* promoter was unaffected by the deletion as summarized in Figure 4.12.

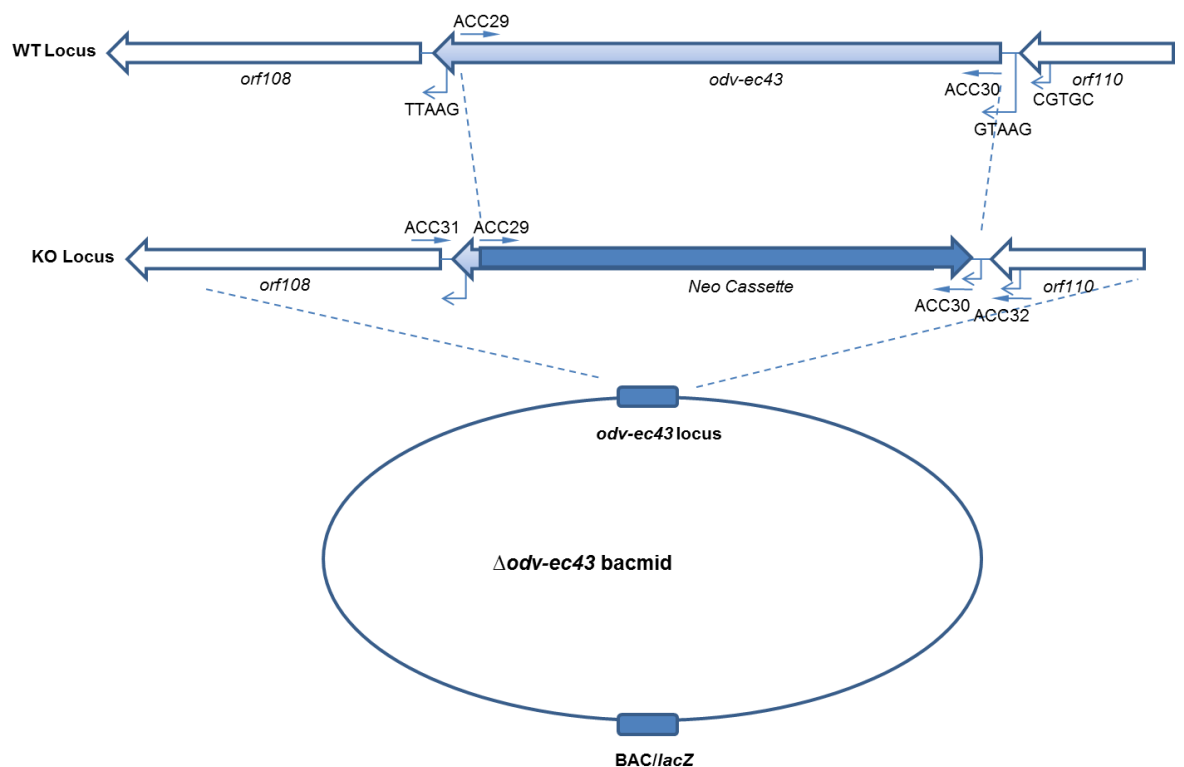


Figure 4.12 Schematic of the construction of *Ac*BacPAK5/*lacZ*/BAC^{pol} Δ *odv-ec43* bacmid.

The *odv-ec43* ORF was mostly deleted by the insertion of kanamycin resistance gene between 94771 and 95893 bp on the *Ac*MNPV genome via homologous recombination in *E. coli* using the Red/ET recombination system.

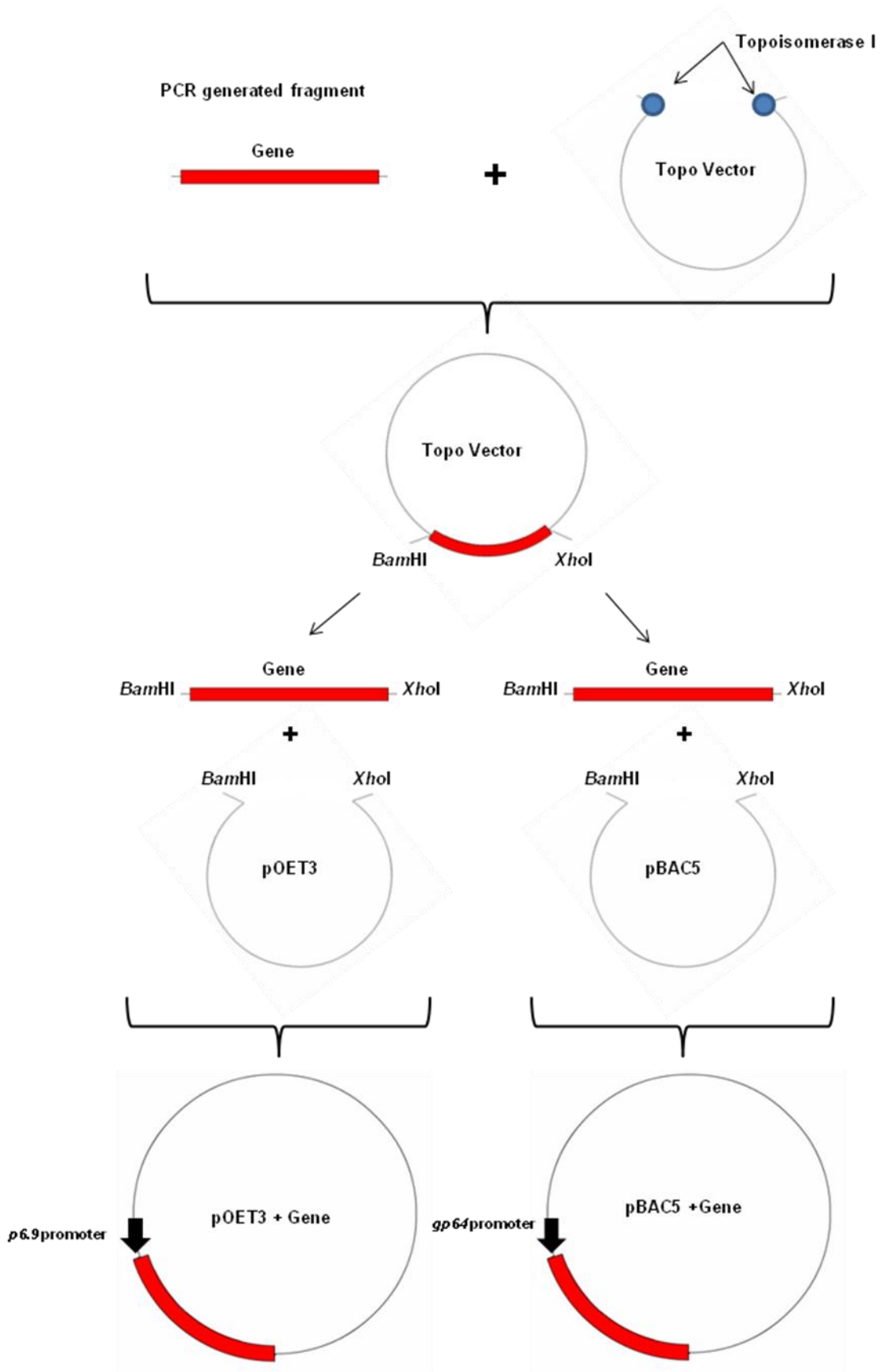
However, initial attempts to amplify the virus (*Ac* Δ *odv-ec43*) following transfection of Sf9 cells with Δ *odv-ec43* proved unsuccessful with no signs of viral infection detected as determined by microscopic observation. However, on further investigation of Δ *odv-ec43*-transfected insect cells stained with X-gal at 72 hours post-transfection, it became apparent

that the primary transfected cells were showing a blue coloration suggesting that β -galactosidase was being produced from the viral genome. Only individual cells turned blue further suggesting that the virus was not able to spread to neighboring cells. This indicated that ODV-EC43 may be essential for BV production but not for DNA replication or gene expression. Another possibility was that the deletion in *odv-ec43* had affected neighboring genes despite the precautions taken to avoid this (Chapter 3), preventing the recovery of a fully replication-competent virus. Therefore the next stage of this study was to investigate whether the deletion of *odv-ec43* could be rescued by the deleted gene at its native locus or at the *polh* locus. Rescue at the native locus would indicate whether the observed phenotype was attributable to the *odv-ec43* gene and rescue at the *polh* locus would indicate whether any of the neighboring genes had been affected by the deletion; if the rescue at the *polh* locus failed to restore virus infectivity it would indicate that neighboring genes may have been affected by the deletion and a new strategy will be required.

The *odv-ec43* coding region was amplified using specific primers and AcMNPV DNA as template with proof reading polymerase (Expand, Roche). The amplified gene fragment was then inserted into a Topo vector and sequenced. The gene fragment was then removed from the Topo vector and inserted into either pOET3 (Oxford Expression Technologies Ltd) or pBAC5 (Novagen) to allow rescue of this gene at the *polh* locus under the control of two different promoters; the late *p6.9* promoter (pOET3) and early and late *gp64* promoter (pBAC5). Figure 4.13 details the cloning strategy using protocols described in methods (section 2.6). These promoters were chosen to reflect the natural expression of this gene at its own locus as *odv-ec43* is under control of both early and late promoters (Lin *et al.*, 2009). Both constructs were confirmed by RE mapping (data not shown).

Figure 4.13 Insertion of baculovirus genes into pOET3 and pBAC5

The baculovirus transfer vectors were constructed using standard classical cloning techniques. The target gene was amplified by PCR using Expand DNA polymerase and inserted into the invitrogen Topo vector, where its sequence was confirmed by DNA sequencing. The target gene was subcloned from the Topo vector into the *Bam*HI and *Xho*I sites of both pOET3 and pBAC5, and this insertion resulted in a recirculation of both pOET3 and pBAC5. These baculovirus transfer vectors would allow insertion of the target gene under the control of either *p6.9* promoter (pOET3) or *gp64* promoter (pBAC5) into the baculovirus genome at the *polh* locus through homologues recombination in insect cells.



Insect Sf9 cells were cotransfected with pOET3-*odv-ec43* or pBAC5-*odv-ec43* and Δ *odv-ec43* bacmid DNA purified from *E. coli* and linearised by restriction enzyme digestion with *Bsu361*. The Δ *odv-ec43* contains a single *Bsu361* site located within the *lacZ* at the *polh* locus. These cotransfections rescue the target gene at the *polh* locus.

For the rescue to occur at the *odv-ec43* locus, the Δ *odv-ec43* bacmid DNA purified from *E. coli* was linearised by restriction enzyme digestion with *SrfI* and Sf9 cells were cotransfected with the Topo vector containing the target gene, *odv-ec43*. The Δ *odv-ec43* bacmid contain two *SrfI* sites flanking the kanamycin insert. Due to the *Ac* Δ *odv-ec43* virus being unable to replicate in cell culture, only those viruses that are rescued with a transfer plasmid that restores infectivity will be viable in insect cells.

The resulting rescue viruses were harvested from the culture media of transfected Sf9 cells. Viability was assessed by the formation of plaques caused by cell death due to viral infection in a standard plaque assay (Table 4.5). The viability results demonstrated that rescue of *odv-ec43* at either its own locus or the *polh* locus restored infectivity of *Ac* Δ *odv-ec43*, suggesting the deletion of *odv-ec43* caused *Ac* Δ *odv-ec43* to be non-infectious.

Table 4.5: Summary of results from *Ac* Δ *odv-ec43* rescue experiments.

Plasmids	Bacmids	
	<i>AcBacPAK5lacZ/BAC^{pol}</i>	Δ <i>odv-ec43</i>
Rescue with pOET3- <i>odv-ec43</i>	Infectious	Infectious
Rescue with pBAC5- <i>odv-ec43</i>	Infectious	Infectious
Rescue with pOET3	Infectious	Non-infectious
Rescue with pBAC5	Infectious	Non-infectious
Rescue at own locus - <i>odv-ec43</i>	N/A	Infectious

4.4.2 *Ac* Δ *odv-e28* and *Ac* Δ *orf79*

The *odv-e28* is one of the 31 core genes conserved among all baculoviruses sequenced. Most of these core genes have been related to DNA replication, gene expression, packaging and assembly or *per os* infection. Recently *odv-e28* has been shown to be involved in *per os* infection and has been suggested to be part of the *per os* infectivity factor family; *pif4* (Fang *et al.*, 2009). The *odv-e28* is transcribed from a late promoter

located 141 nucleotides upstream of a start codon within *helicase* and produces protein with a predicted molecular weight of 19.8 kDa. The *odv-e28* has a highly hydrophobic transmembrane signal peptide which strongly supports its proposed location in the ODV envelope.

The *orf79* produces a protein of 104 amino acid with a predicted molecular weight of 12.2 kDa and is believed to be associated with the ODV nucleocapsid (Braunagel *et al.*, 2003). However, analysis of the promoter sequence of *orf79* showed no transcriptional start site motif normally associated with baculovirus genes upstream of the predicted start codon. This could suggest that *orf79* is expressed from *gp41* promoter by read through. The function of *orf79* is unknown but it shares strong homology to an endonuclease in a number of bacteria; UvrC intron-encoded nucleases which are involved in DNA repair after UV damage (Aravind *et al.*, 1999). Therefore, this suggests that *orf79* could be a member of the UvrC superfamily of endonucleases and might play a role in UV damage repair of the baculovirus genome.

The Red/ET system was successfully used to produce both these individual deletion mutant bacmids ($\Delta odv-e28$ and $\Delta orf79$). In $\Delta odv-e28$ part of the *odv-e28* coding region was removed and replaced with a kanamycin resistance gene, leaving 218bp of *odv-e28* at the 5' end to ensure that *helicase* promoter was unaffected and 165bp at the 3' end to ensure *orf97* promoter was also unaffected by the deletion as summarized in Figure 4.14 A. In the case $\Delta orf79$, the majority of the *orf79* coding region was removed and replaced with a kanamycin resistance gene, leaving 142bp of *orf79* at the 5' end to ensure that *orf78* promoter was unaffected by the deletion as summarized in Figure 4.14 B.

Attempts to recover $Ac\Delta orf79$ and $Ac\Delta odv-e28$ after transfection of insect Sf9 cells with bacmid DNA had proved unsuccessful (section 4.5) and no signs of virus infection were observed. Therefore the same procedure that was used to investigate whether the deletion of *odv-ec43* was the cause of its observed effects on virus replication was undertaken here for both $\Delta orf79$ and $\Delta odv-e28$. Briefly, this involved constructing transfer vectors to allow the rescue of the deleted gene at either its own locus or the *polh* locus (Figure 4.13), as this would indicate whether any of the neighboring genes had been affected by the deletion. However, at the cotransfection stage the deletion mutant virus DNA was linearised with *AvrII* instead of *Bsu361* due to the differences in the parental genome, both $\Delta orf79$ and $\Delta odv-e28$ contain a single *AvrII* site in the essential gene *orf1629*. The resulting rescue viruses were recovered from transfected Sf9 cells. Viability was assessed by the formation of plaques due to viral infection. The results demonstrated for both $Ac\Delta orf79$ and $Ac\Delta odv-e28$ that only rescuing the target gene at its own locus

could restore the infectivity of these deletion mutant viruses (Table 4.6). No plaques were obtained with attempts to rescue the viruses at the *polh* gene locus.

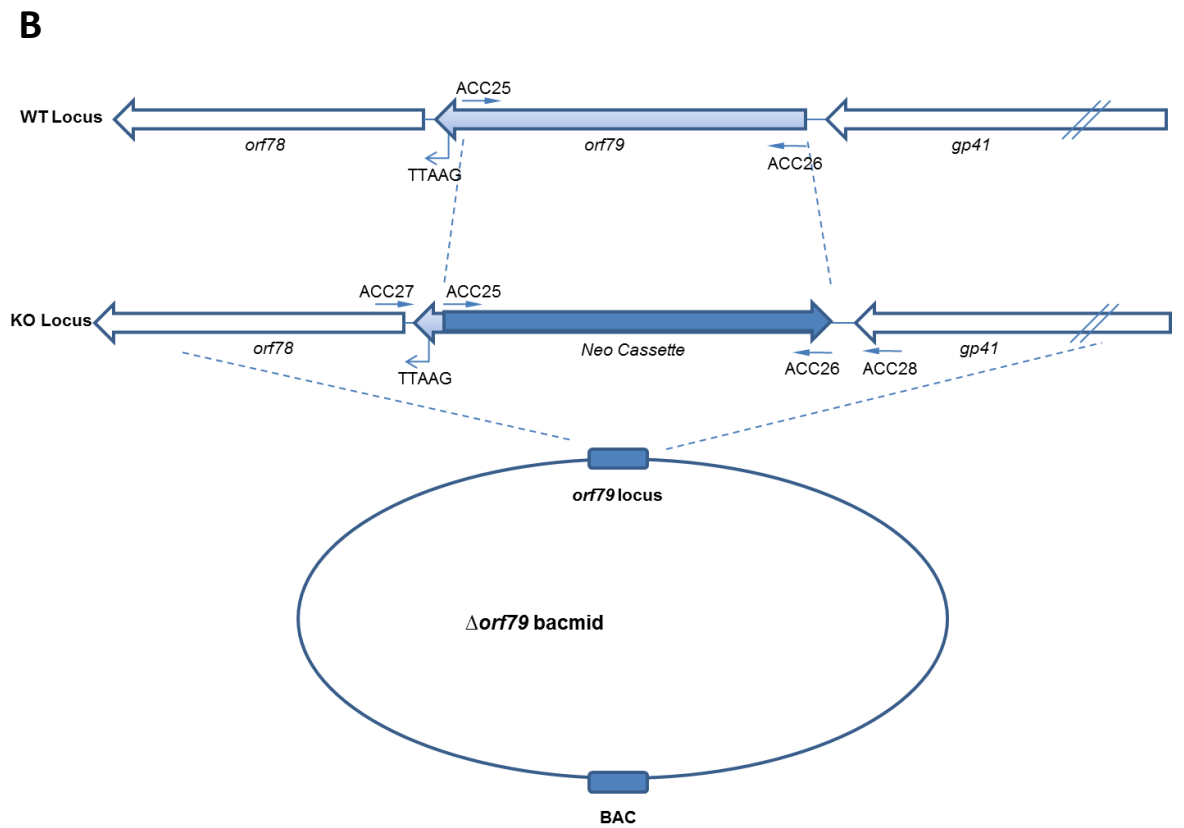
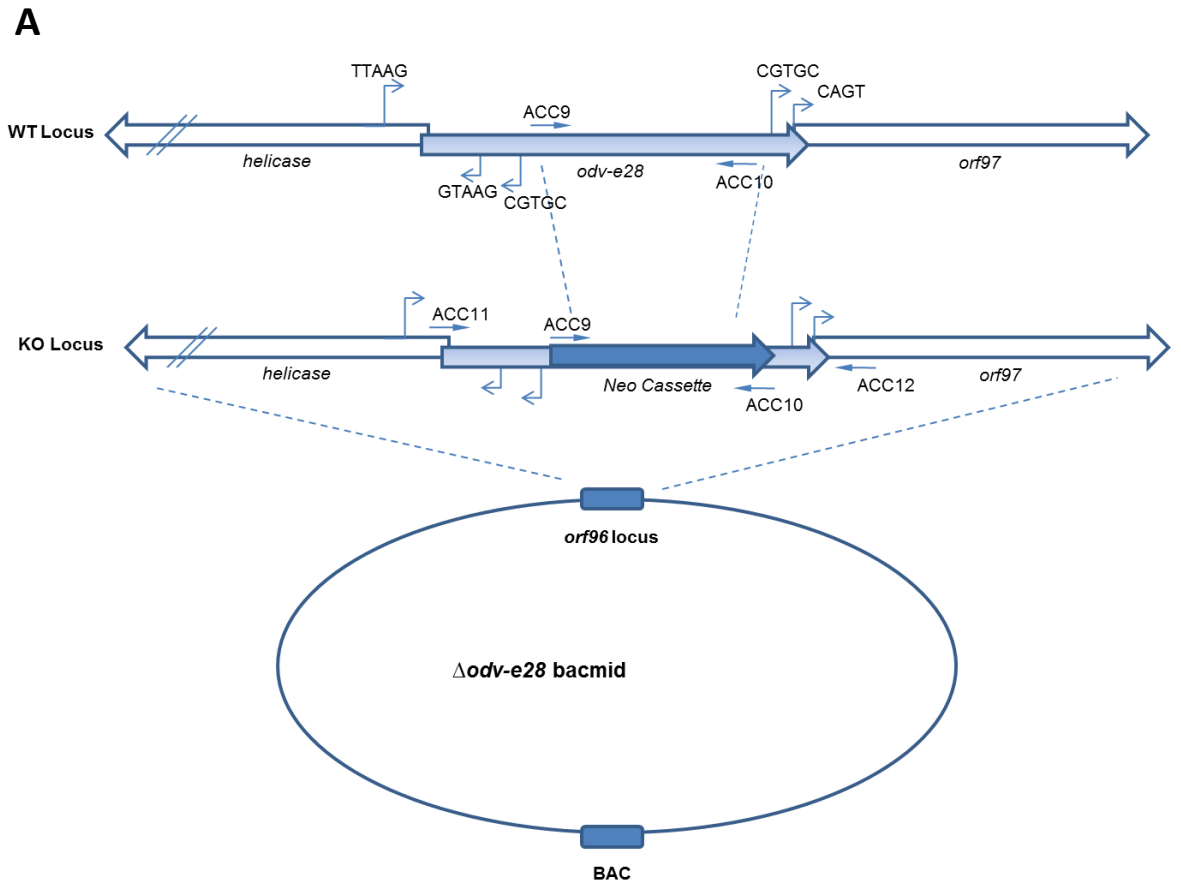
To investigate whether the deletion of *orf79* had affected the late promoter of *orf78* (Figure 4.14), *orf78* was cloned into pOET3 using the same method shown in Figure 4.13. This would allow the placement of *orf78* at the *polh* locus of *AcΔorf79* under control of the *p6.9* promoter and the resulting virus was tested for viability by plaque assay. The results showed that the placement of *orf78* at the *polh* locus was unable to rescue the infectivity of the Δ *orf79* virus suggesting that both *orf78* and *orf79* could be essential for viral replication (Table 4.6).

Table 4.6: Summary of results from *AcΔorf79* and *AcΔodv-e28* rescue experiments.

Plasmids	Bacmids		
	AcBACΔchitinase	Δ<i>orf79</i>	Δ<i>odv-e28</i>
Rescue with pOET3-<i>orf79</i>	Infectious	Non-Infectious	N/A
Rescue with pBAC5-<i>orf79</i>	Infectious	Non-Infectious	N/A
Rescue at own locus – <i>orf79</i>	N/A	Infectious	N/A
Rescue with pOET3- <i>odv-e28</i>	Infectious	N/A	Non-Infectious
Rescue with pBAC5- <i>odv-e28</i>	Infectious	N/A	Non-Infectious
Rescue at own locus - <i>odv-e28</i>	N/A	N/A	Infectious
Rescue with pOET3	Infectious	Non-Infectious	Non-Infectious
Rescue with pBAC5	Infectious	Non-Infectious	Non-Infectious
Rescue with pOET3-<i>orf78</i>	Infectious	Non-Infectious	N/A

Figure 4.14 Schematic of the construction of (A) AcBAC Δ chitinase Δ odv-e28 and (B) AcBAC Δ chitinase Δ orf79

The ORFs *odv-e28* and *orf79* were mostly deleted by the insertion of kanamycin resistance gene between 84564-84702 bp and 65432-65604 bp positions respectively on AcMNPV genome via homologous recombination in *E. coli* using the Red/ET recombination system.



4.5 Discussion

In this chapter the Red/ET recombination system was successfully used to create several viruses with mutations of specific genes. These deletion mutants were classified into three groups; those that did not appear to replicate in insect cells (*AcΔodv-ec43*, *AcΔorf79* and *AcΔodv-e28*), those containing deletions in known *pif* genes (*AcΔpif2* and *AcΔpif3*) and those that replicated in insect cells and were not part of the *pif* family (*AcΔodv-e66*, *AcΔcg30* and *AcΔodv-e56*). In spite of earlier experiences in our laboratory with the Red/ET recombination system where it was used to modify the AcMNPV genome, in this study some initial problems were encountered deleting the coding regions of interest. These difficulties necessitated the use of two different parental bacmids.

4.5.1 Construction of deletion mutant viruses

The first AcMNPV bacmid (*AcBacPAK5/lacZ/BAC^{pol}*) used as a target for gene modification contained a low copy number bac replicon at the *polh* locus. It also had a copy of the *lacZ* coding region under *polh* promoter control in tandem with this bacterial element. All other genes in the virus were left unchanged prior to the attempts with Red/ET recombination to modify the gene targets. Several experiments to insert a kanamycin gene resistance cassette into *AcBacPAK5/lacZ/BAC^{pol}* only yielded two mutants (*AcΔpif2* and *AcΔodv-ec43*). A key reason for using *AcBacPAK5/lacZ/BAC^{pol}* was the addition of *lacZ* to the virus genome so that subsequent experiments on viable virus mutants could analyse any effect on *polh* promoter activity and accompanying protein production.

However, other AcMNPV bacmids have been used with Red/ET recombination to modify virus genes without reported problems (McCarthy *et al.*, 2008; McCarthy and Theilmann, 2008; Fang *et al.*, 2009). The only significant difference between the bacmid used in this study and others was the *lacZ* coding region incorporated as a reporter. This suggested that *AcBacPAK5/lacZ/BAC^{pol}* might produce beta-galactosidase protein in the bacterial host that could inhibit the Red/ET recombination process. There is evidence that the *polh* promoter is active in *E. coli* (Lewin *et al.*, 2005), which might result in low levels of active enzyme. Furthermore, the original source of the *lacZ* cassette inserted into *AcBacPAK5/lacZ/BAC^{pol}* was pCH110. This was originally constructed as an expression vector for both prokaryotic and eukaryotic cells with *E. coli* *gpt* and SV40 early promoters. Although it has never been tested in our laboratory, it is very likely that the *gpt* promoter remains active in the *lacZ* gene cassette to facilitate beta-galactosidase production in the host cell of the bacmid. However, it is unclear how the presence of the beta-galactosidase

could affect the homologous recombination process. In experiments to investigate the feedback of L-arabinose on AraC novel activation of its native operon *lacZ* was used in a fusion with *araC* (Cass and Wilcox, 1988). This suggests that the presence of β -galactosidase in the current studies on AcMNPV gene modification wouldn't affect the expression of the proteins required for homologous recombination or directly affect the homologous recombination process between the bacmid and kanamycin cassette.

Another possibility could be that the *E. coli* containing AcBacPAK5/*lacZ*/BAC^{pol} is in fact harboring two copies of the bacmid or a single bacmid that has two copies of BacPAK5/*lacZ*. The latter is more likely due to the BAC being based on the *E. coli* F factor which means its replication is strictly controlled resulting in only one copy per bacterial cell (Kim *et al.*, 1996). The BAC is capable of maintaining DNA fragments of > 300 kb (Shizuya *et al.*, 1992), which would easily accept a duplicated AcMNPV genome (ca. 134 kbp; Ayres *et al.*, 1994). The results from the PCR analysis of DNA samples believed to be AcBacPAK5/*lacZ*/BAC^{pol} $\Delta cg30$ clearly showed two bands after amplification of the *cg30* locus, which was consistent with the presence of the native virus gene and the insertion of the kanamycin gene (Figure 4.7). This does provide some supporting evidence for the idea of two *cg30* loci in the bacterial cell. Possibly quantitative PCR could be used to determine relative gene copy numbers in the bacterial cells. If all genes encoded by the baculoviruses were equimolar then this would suggest that both *cg30* and the locus with the kanamycin cassette were contained within a single genome. If other virus genes, such as *lef-8* or *dnapol* were found to be twice the copy number of the kanamycin cassette this would suggest two copies of the bacmid in the bacterial host cell.

At this point in the study, given the uncertainties of using AcBacPAK5/*lacZ*/BAC^{pol} for construction of AcMNPV gene deletion mutants, it was decided to use an alternative bacmid, AcBAC Δ chitinase. While this did not have the *lacZ* coding region, it had been used previously in other experiments to construct AcMNPV gene deletion mutants (R.D. Possee, personal communication) and was used successfully in this study also. The problems encountered with AcBacPAK5/*lacZ*/BAC^{pol} are still to be resolved, but were eventually considered to be outside the scope of the current project.

4.5.2 Analysis of the deletion mutant virus; Ac $\Delta odv-ec43$

The deletion of *odv-ec43* in $\Delta odv-ec43$ abolished the infectivity of BV in cell culture. However, transfection of $\Delta odv-ec43$ DNA into cell cultures demonstrated that transcription and translation of viral factors was occurring in transfected cells, demonstrated by staining

of the cell monolayer with X-gal that turns the infected cells blue due to the presence of β -galactosidase produced from the viral genome. The β -galactosidase is under the control of the very late *polh* promoter and this would require all the earlier viral expression factors to be successfully expressed. This strongly suggested that the deletion of *odv-ec43* did not affect viral transcription and translation of the genome but instead maybe essential for BV assembly. This evidence is preliminary, but could be supported by further studies to measure virus DNA replication and gene expression using quantitative PCR and qRT-PCR respectively. A good control virus to use for these studies would be AcMNPV where *gp64* has been deleted, which would limit virus replication to cells initially transfected with bacmid DNA. The lack of virus encoded GP64, the major BV envelope protein, would prevent infectious virus production.

The infectivity of the Δ *odv-ec43* was rescued by insertion of *odv-ec43* at either its own locus or the *polh* locus; this confirmed that the deletion of *odv-ec43* was the cause of the observed effects and not due to bystander effects on neighboring genes. These results are consistent with other studies reported recently. Lin *et al.*, 2009 demonstrated using electron microscopy that deletion of *odv-ec43* blocked nucleocapsid formation, which subsequently inhibited synthesis of BV and ODV but had no affect on viral DNA replication as measured by qPCR (Lin *et al.*, 2009). The conclusion that *odv-ec43* is an essential virus gene product required for both BV and ODV particle formation lead to the conclusion that it was not a suitable gene to be deleted from the AcMNPV genome to enhance its attributes as an expression vector. It was therefore not considered further in work plans in this project.

4.5.3 Analysis of the deletion mutant virus; Ac Δ *odv-e28*

The deletion of *odv-e28* in Δ *odv-e28* abolished the infectivity of BV in cell culture; however rescue of *odv-e28* at the *polh* locus did not restore the infectivity of Δ *odv-e28* suggesting the cause of this loss of infectivity was not due to the deletion of *odv-e28*. The infectivity of Δ *odv-e28* could be restored if the gene was rescued at its own locus, which suggests that one or both the neighboring genes had been affected by the deletion. Figure 4.14 shows a schematic representation of the deleted region in the Δ *odv-e28* and it can be seen that the deletion could affect both of the neighboring gene promoters. The neighboring genes of *odv-e28* are *helicase* and *orf97*. It is most likely that the *helicase* early promoter (CGTGC) has been affected by the deletion being too close to the promoter and thus preventing the binding of key protein(s) involved in DNA transcription. Also there is some doubt about the authenticity of *orf97* since this orf only encodes a 55 aa protein with a predicated mass of

6.5kDa. Related viruses such as BmNPV or RoNPV lack this orf, which may suggest it is non functional and simply an artifact of the original bioinformatic analysis (Ayres *et al.*, 1994). *Helicase* is one of the core baculovirus genes and deletion of this gene is lethal for virus replication. Fang *et al.* (2009) also demonstrated that a similar deletion of *odv-e28* was non viable due to the flanking genes being interrupted, and was not a consequence of the changes to the target gene itself. However, they continued their work using insertion of a zeocin cassette into *odv-e28* to delete it and showed that this had no effect on viral replication in cell culture but the Δ *odv-e28* virus was unable to infect *Trichoplusia ni* larvae orally. These results suggest that *odv-e28* encodes a new *per os* infectivity factor (Fang *et al.*, 2009). They also supported the idea of deleting the gene from AcMNPV expression vectors to minimise both the size of the virus genome and decrease transcription/translation load very late in virus infection.

Ideally, when designing virus gene deletion experiments it would be advisable to have a thorough knowledge of gene transcription and termination in the regions flanking the target to avoid bystander effects on neighbouring sequences. Primer extension could be used to map transcription start sites, although the more modern technique of 5' RACE analysis could also be used. For transcription termination studies, simply sequencing the 3' ends of mRNAs via cDNA synthesis and cloning would be efficient.

4.5.4 Analysis of the deletion mutant virus; **Ac Δ orf79**

The deletion of *orf79* from AcMNPV to produce Δ *orf79* yielded similar results to the deletion of *odv-e28*: **Ac Δ orf79** wasn't viable and rescue of *orf79* at the *polh* locus didn't restore viability to the Δ *orf79* virus, whereas rescue at its own locus did restore viability. The flanking genes of *orf79* are *orf78* and *gp41* (Figure 4.14). It is apparent that the late promoter of *orf78* could have been disrupted by the deletion of *orf79*. The *orf78* may be an essential gene as homologues are found in all lepidopteran NPVs and GVs. However, the Δ *orf79* virus remained non-viable after the insertion of *orf78* at the *polh* locus in **Ac Δ orf79**. This suggests that both *orf78* and *orf79* are required by the virus to replicate and produce viral progeny. This could be tested by constructing a transfer vector to insert both *orf78* and *orf79* into the Δ *orf79* virus at the *polh* locus. This rescue virus would confirm whether or not both *orf78* and *orf79* are indeed essential genes. It would also rule out that the expression of *gp41* had been interrupted, which could cause the loss of infectivity seen in Δ *orf79* as *gp41* is an essential gene required for the transport of nucleocapsids from the nucleus (Olszewski and Miller, 1997).

4.5.5 Conclusion

In this chapter several deletion mutant viruses were constructed and three of them were analysed further, namely *AcΔorf79*, *AcΔodv-e28* and *AcΔodv-ec43*, which were non-infectious in insect cell culture. The results from this work demonstrated the possibility that *orf79*, *orf78* and *odv-ec43* are all essential genes. However, it also indicated that *odv-ec43* most likely does not play a role in viral DNA replication or translation of the viral genome but in processing of the BV particle. The *odv-e28* was initially believed to be essential but the results confirmed this was incorrect and suggested that an essential neighboring gene had been interrupted instead. Overall, the results show that deleting genes from a virus genome such as AcMNPV, where ORFs and promoters overlap, can cause unseen problems even when such factors are taken into account. A better strategy for analyzing virus gene function might be first to delete the coding region of interest by insertion of a marker such as kanamycin selectable in *E. coli* essentially as was done in this study. If this modification proved lethal for virus replication, a gene rescue could be attempted using a modified version of the target sequences in which the putative translation initiation codon was mutated to a non functional triplet. Such an approach would overcome bystander effects on flanking genes unless the ATG sequence itself was involved in a regulatory role for upstream or downstream genes.

Chapter 5
**Characterisation of *Ac*Δ*odv-e66*,
*Ac*Δ*cg30* and *Ac*Δ*odv-e56***

5.1 Introduction

The Red/ET recombination system was successfully used to generate eight recombinant viruses with deletions in specific genes. Three of these viruses, *AcΔorf79*, *AcΔodv-ec43* and *AcΔodv-e28*, which did not appear to replicate in insect cells have already been discussed in Chapter 4, section 5. Those deletion mutant viruses that did appear to replicate in insect cells and were not classified as *pifs* at the start of this project are further investigated in this chapter. Each of the targets; *odv-e66*, *cg30* and *odv-e56* will be briefly introduced along with information on the deletion of each gene (More information for each of the targets can be found in Chapter 3). Then experimental work to elucidate the roles of these selected proteins within the baculovirus replication cycle with specific regard to ODV production and packaging into the OB will be discussed.

5.2 Characterisation of *odv-e66*, *cg30* and *odv-e56*

5.2.1 *odv-e66*

The *odv-e66* is 2112 bp gene that encodes a predicted ~79 kDa protein and is found in all lepidopteran baculoviruses. ODV-E66 is bound at the highly hydrophobic N-terminal to the ODV envelope and experiments have shown that ODV-E66 interacts with another viral envelope protein ODV-E25, at their exposed C-terminal regions (Braunagel *et al.*, 1999).

5.2.2 *cg30*

The *cg30* is 792 bp gene that encodes a predicted ~30.1 kDa protein and is only found NPV. Interestingly, all *cg30* homologues are located downstream and in the same direction as *vp39*, which encodes the major capsid protein. CG30 contains two DNA binding motifs, zinc ring finger motif (C3HC4) and leucine zipper motif at the C-terminal and N-terminal, respectively (Thiem and Miller, 1989). This suggests that CG30 is located to the inside of the nucleocapsids bound to the viral genome.

5.2.3 *odv-e56*

The *odv-e56* is 1128 bp gene that encodes a predicted ~40.9 kDa protein. ODV-E56 is bound at the C-terminal to the ODV envelope, which is unlike most other ODV envelope

proteins that are bound at their N-terminal (Braunagel *et al.*, 1996; Theilmann *et al.*, 1996).

5.3 Amplification of deletion mutant viruses for analysis

The Red/ET recombination system was successfully used to produce deletion mutant bacmids ($\Delta odv-e66$, $\Delta cg30$ and $\Delta odv-e56$) in which the majority of the coding region of each of the target genes was removed and replaced with a kanamycin resistance gene (Figure 5.1). For a more detailed explanation of the method used to create these deletion mutant bacmids; Red/ET recombination system and methods used to confirm the deletions see Chapter 4. As also described in Chapter 4, the bacmid DNA was used to transfect Sf9 cells to recover infectious budded virus and the virus recovered from these infections was designated $Ac\Delta odv-e66$, $Ac\Delta cg30$ and $Ac\Delta odv-e56$, to distinguish them from the bacmid DNAs.

Each recombinant virus and the parental control virus $AcBAC\Delta chitinase$ was amplified to a working stock in Sf9 cells and was titrated by plaque-assay so that the experiments described in the later sections of this chapter could be carried out using known multiplicities of infection (MOI). The deletion mutant viruses amplified to titres of 4.2×10^7 ($Ac\Delta cg30$), 3.5×10^7 ($Ac\Delta odv-e66$) and 2.8×10^7 pfu/ml ($Ac\Delta odv-e56$) whereas $AcBAC\Delta chitinase$ amplified to titre of 8.3×10^7 pfu/ml.

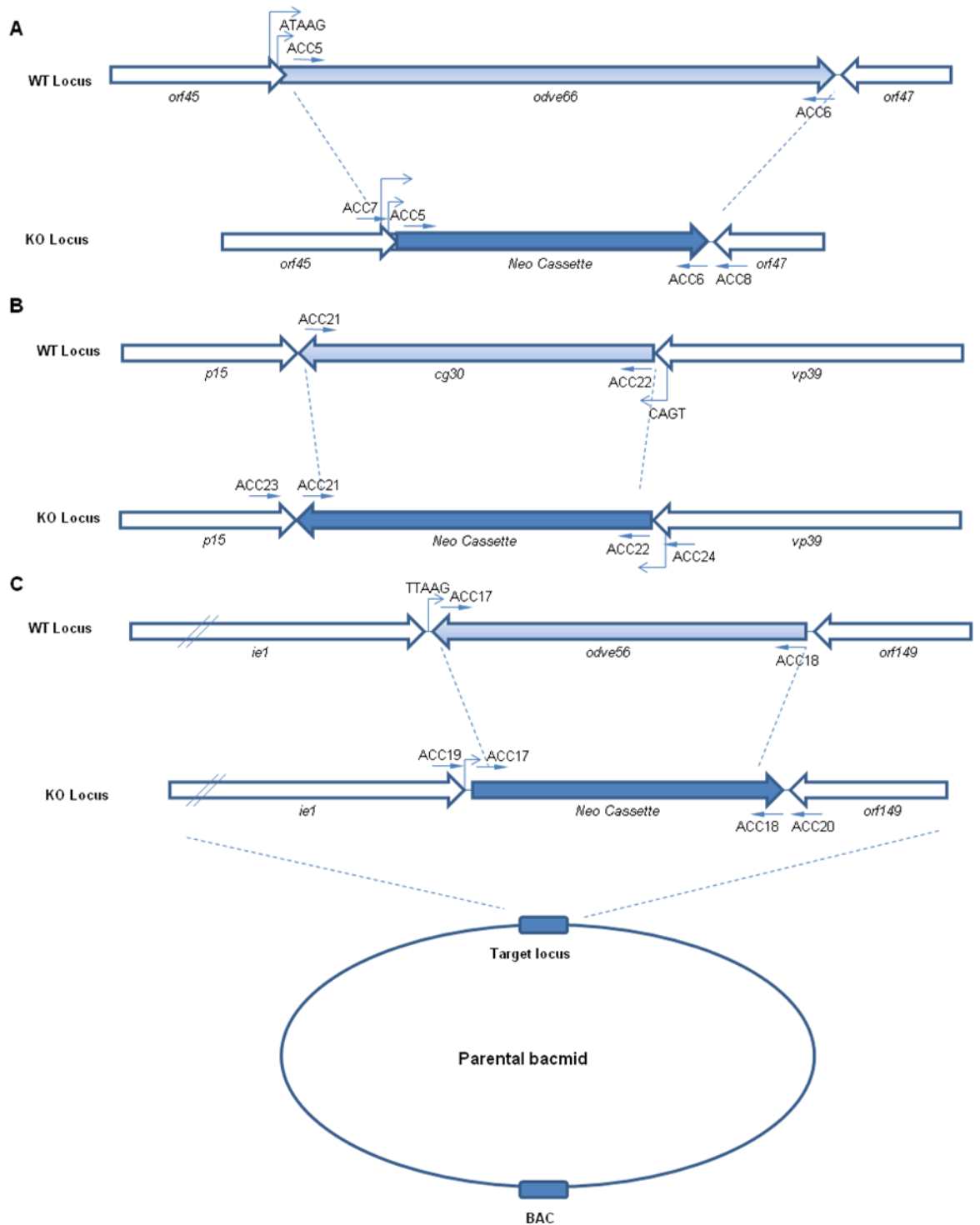


Figure 5.1 Schematic of the construction of $\Delta odv-e66$, $\Delta cg30$ and $\Delta odv-e56$ bacmids.

The *odv-e66* (A), *cg30* (B) and *odv-e56* (C) ORFs were almost completely deleted by the insertion of a DNA fragment containing a kanamycin resistance gene between nucleotides 36734-38830 (A), 74737-75529 (B) and 129008-130136 (C) relative to the AcMNPV genome via homologous recombination in *E. coli* using the Red/ET recombination system as described in Chapter 4.

5.4 Temporal analysis of virus replication in *Ac* Δ *odv-e66*, *Ac* Δ *cg30*, *Ac* Δ *odv-e56* and *AcBAC* Δ *chitinase*-infected Sf9 cells.

5.4.1 Cell Viability

Triplicate Sf9 suspension cultures were infected (MOI = 5 pfu/cell) with *AcBAC* Δ *chitinase*, *Ac* Δ *odv-e66*, *Ac* Δ *cg30* or *Ac* Δ *odv-e56* and incubated for 120 hours. Over this period, mock-infected cells remained >90% viable as judged by trypan blue staining. Up to 24hpi, the viability of all the virus-infected cells remained comparable (about 95%) to the mock-infected Sf9 cultures, except for the initial reading (73% viable) for *Ac* Δ *odv-e66* at 0hpi (Figure 5.2). By 48hpi, the viability of all the virus-infected cells had declined compared to the control cells with *AcBAC* Δ *chitinase*-infected cells showing the greatest decrease. However, a two-tailed student t-test showed no significant difference ($P>0.05$) between the cell viabilities of the deletion mutant viruses-infected cells compared to that of *AcBAC* Δ *chitinase*-infected cells at this time point. The decrease in all the virus-infected cell viabilities continued until the last sample was taken at 120hpi.

At 120hpi, the viability of *AcBAC* Δ *chitinase*-infected Sf9 cells had decreased to approximately 19%. The viabilities of *Ac* Δ *odv-e66*-, *Ac* Δ *cg30*- and *Ac* Δ *odv-e56*-infected cells had decreased to 27%, 24% and 36%, respectively, by the end of the experiment (Figure 5.2). A two-tailed student t-test showed a significant difference ($P<0.05$) in the virus-infected cell viability at 120hpi between the parental virus, *AcBAC* Δ *chitinase*, and the two deletion mutant viruses, *Ac* Δ *odv-e66* and *Ac* Δ *odv-e56*. However, there was no significant difference ($P>0.05$) between the cell viabilities at 120hpi for *AcBAC* Δ *chitinase* and *Ac* Δ *cg30* using the same statistical test. However, despite these temporal differences, Analysis of variance (Anova) statistical analysis demonstrated that there was no significant difference between any of the virus infected cell viabilities across the time course study ($P>0.05$).

5.4.2 Budded Virus Production

The experiment to determine virus-infected cell viability described above (5.4.1) was accompanied by a study of budded virus production by *AcBAC* Δ *chitinase*, *Ac* Δ *odv-e66*, *Ac* Δ *cg30* or *Ac* Δ *odv-e56* over the same 120 hour time course (Figure 5.3). The infectious virus titres for each time point were obtained using the plaque assay method (methods section 2.3.4a). All the viruses displayed a typical eclipse phase decrease in titre between 0hpi and 12hpi. By 24hpi, however, all viruses had produced greater than background levels of budded virus, although the increase for *Ac* Δ *odv-e56* was modest (3.5×10^6

pfu/ml). In subsequent time points, the parental AcBAC Δ chitinase exceeded infectious virus production by the three virus gene mutants, which attained lower rates of increase, although all mutants amplified to titres in excess of 10^7 pfu/ml. The final budded virus titres at 120hpi were: AcBAC Δ chitinase (7.15×10^7 pfu/ml), Ac Δ odv-e66 (1.87×10^7 pfu/ml), Ac Δ cg30 (2.97×10^7 pfu/ml) and Ac Δ odv-e56 (1.52×10^7 pfu/ml). A two-tailed student t-test showed significant differences ($P < 0.05$) between these titres for the parental virus, compared to the three deletion mutant viruses, suggesting that budded virus production had been compromised in each of the virus mutants. Anova statistical analysis further demonstrated that there was a significant difference ($P < 0.05$) between Ac Δ odv-e56 BV production kinetics and that of AcBAC Δ chitinase, which was not shown for the other two deletion mutant viruses (Ac Δ cg30 or Ac Δ odv-e66, $P > 0.05$).

The final virus titres in this time course study were similar to those obtained when the viruses were amplified using a low moi 0.1 to produce working stocks (Section 5.3; Ac Δ odv-e66 (3.5×10^7 pfu/ml), Ac Δ cg30 (4.2×10^7 pfu/ml) and Ac Δ odv-e56 (2.8×10^7 pfu/ml)). Therefore, confirming the earlier indication that BV production had been affected in all three of these deletion mutant viruses.

Earlier work on AcMNPV with a deletion in CG30 demonstrated an increase in budded virus production when compared to its parental virus (Passarelli and Miller, 1994). However, the results reported in Figure 5.3 showed that Ac Δ cg30 was deficient in budded virus production compared to the unmodified virus. Since *vp39* neighbours *cg30* (Figure 5.1), it is possible that the modifications made in the current study disrupted normal VP39 production. This was tested by analysing VP39 steady state levels in virus-infected cells (section 5.5).

5.5 Western blot analysis of VP39 production in Ac Δ cg30-infected Sf9 cells

To investigate whether or not VP39 expression had been compromised in Ac Δ cg30-infected cells, Western blots were used to analyse the production of the protein at various times after infection in mutant, parental and wild-type AcMNPV-infected cells.

Triplicate 35mm dishes containing 2×10^6 Sf9 cells were infected with, AcMNPV, AcBAC Δ chitinase or Ac Δ cg30 using an MOI of 5 pfu/cell. Dishes were harvested every 24hpi until 96hpi and the protein content of each cell lysate was determined using Quabrit (Qiagen). Protein samples (15 μ g) were fractionated using 12% SDS PAGE and transferred to nitrocellulose membranes using electroblotting. Western blot analysis (see method section 2.7.2) was then performed using antibody to VP39 (Figure 5.4).

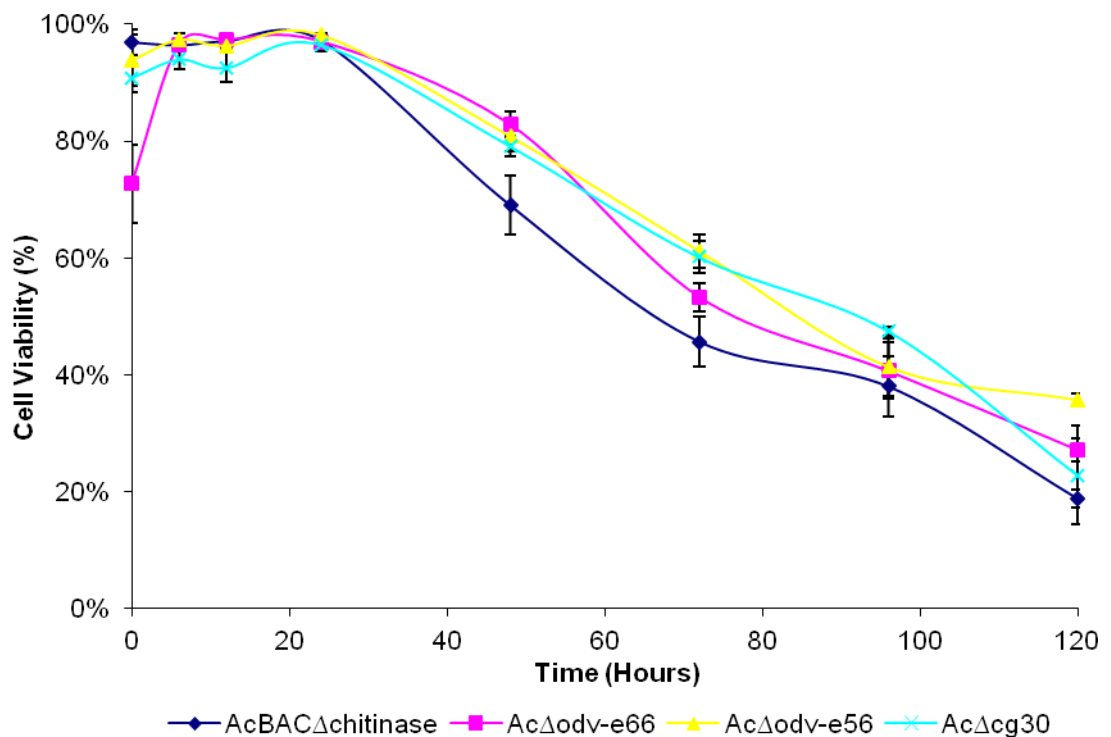


Figure 5.2 Cell viability of *AcΔodv-e66*, *AcΔcg30* or *AcΔodv-e56*-infected Sf9 cells.

The viability of triplicate cultures of *AcBACΔchitinase*-, *AcΔodv-e66*-, *AcΔcg30*- or *AcΔodv-e56*-infected Sf9 cells (MOI = 5 pfu/cell) were assessed over 120 hours. Cell viability was determined by trypan blue staining as described in methods (section 2.3.5). Standard error bars are shown. N=3.

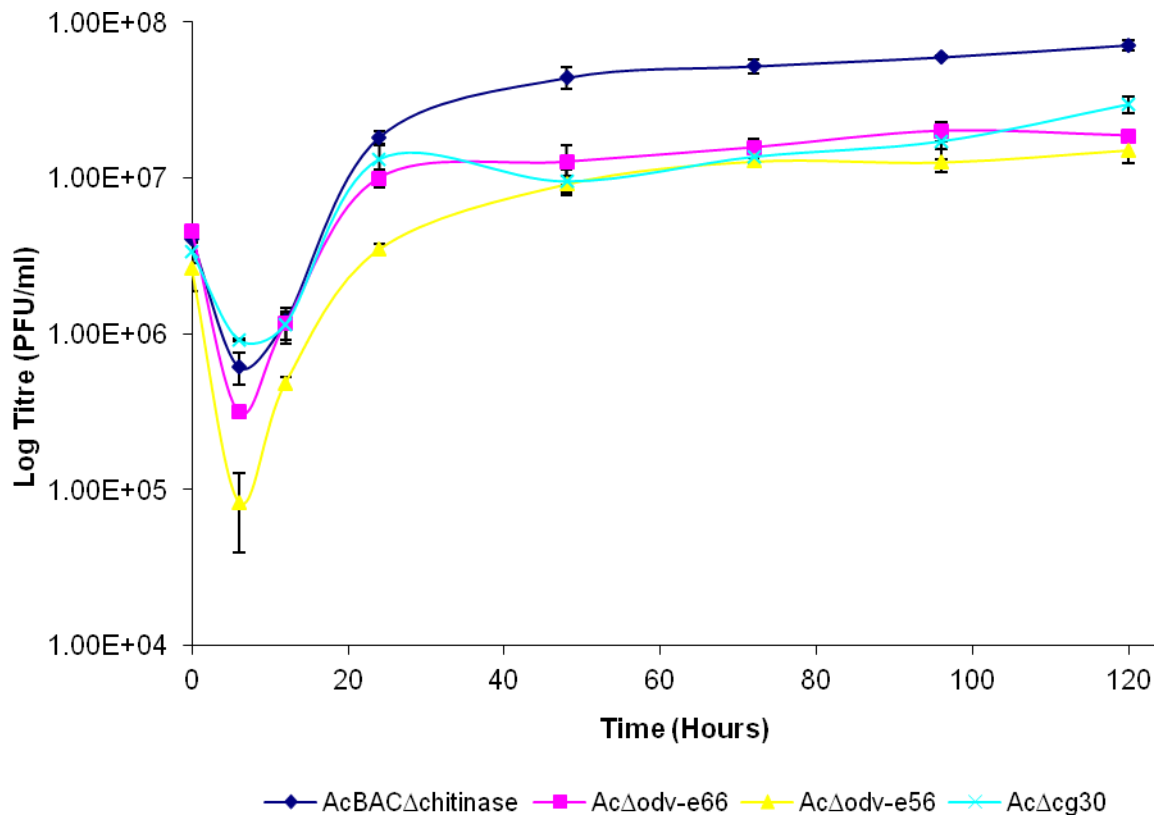


Figure 5.3 Kinetics of budded virus production for *Ac Δ odv-e66*, *Ac Δ cg30* or *Ac Δ odv-e56*.

Culture medium from the Sf9 cell cultures infected with AcBAC Δ chitinase, Ac Δ odv-e66, Ac Δ cg30 or Ac Δ odv-e56 (as described in Figure 5.2) were assayed using plaque titration to determine their budded virus content. Standard error bars are shown for each time point of the 120 hour time course. N=3.

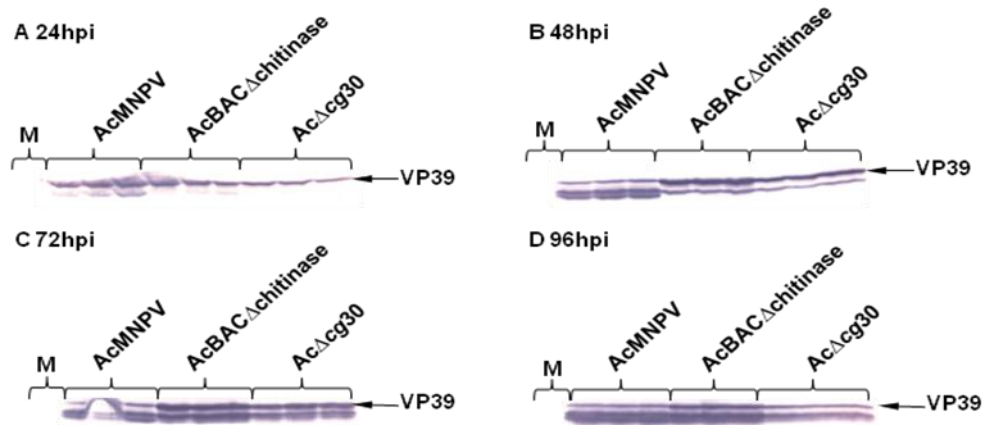


Figure 5.4 Western blot analysis of AcMNPV, AcBAC Δ chitinase and Ac Δ cg30 infected Sf9 cells

Triplicate total cell lysates from Sf9 cells infected with AcMNPV, AcBAC Δ chitinase, or Ac Δ cg30 (MOI = 5 pfu/cell) were collected throughout a time course and 15 μ g of protein was fractionated using 12% SDS PAGE, transferred to a nitrocellulose membrane and probed with antibody to VP39 as described in methods. A: 24hpi, B: 48hpi, C: 72hpi D: 96hpi. Arrow indicates the predicted band for VP39 and M indicates mock infected cell lysate samples.

This demonstrated that a protein of the predicted size (38.9 kDa) was present in cells infected with each virus at 24, 48, 72 and 96hpi. However, there were some important differences between the samples. The temporal expression of VP39 by Ac Δ cg30 closely matched that of its parental virus (AcBAC Δ chitinase). Interestingly, the expression of VP39 by AcMNPV differed to that of Ac Δ cg30 and AcBAC Δ chitinase, with production of two VP39-specific protein bands with estimated molecular weights of 36 and 34 kDa. These were more prominent in AcMNPV-infected cells at 48hpi than in cells infected with the other two viruses. By 72hpi, AcBAC Δ chitinase and Ac Δ cg30-infected cells had approximately equal ratios of full length and lower molecular weight VP39. At 96hpi, the final time point analysed, all three virus-infected cell samples contained more of the lower molecular weight proteins. Overall, Ac Δ cg30-infected cells also appeared to have lower levels of VP39 than the other two viruses at 96hpi in each of the triplicate samples.

Comparing the relative amounts of VP39 bands on the Western blots was not very accurate due to the unevenness in running of the SDS PAGE. For example, AcBAC Δ chitinase VP39 bands in all the Western blot images shown in Figure 5.4 seem darker but this could be solely due to compression of these bands and not the amount of VP39 present. To obtain a more accurate and quantitative estimate for the expression of VP39 for each of these viruses at the chosen time points, a programme from Syngene known as Gene tool was used to semi-quantify the VP39 bands. Briefly, Gene tool

analyses the Western blot images by comparing band intensity and volume to each other, after this a value of 100 was given to the highest intensity band to allow an easier comparison between bands. In this case, the third AcBAC Δ chitinase sample at 48hpi (Figure 5.4 B) was the highest intensity and all the other bands were compared to this band and given a value. The second AcMNPV sample at 72hpi (Figure 5.4 C) was excluded from this analysis due to the miss formation of the band This process was repeated three times and the mean value for each time point was determined (Figure 5.5).

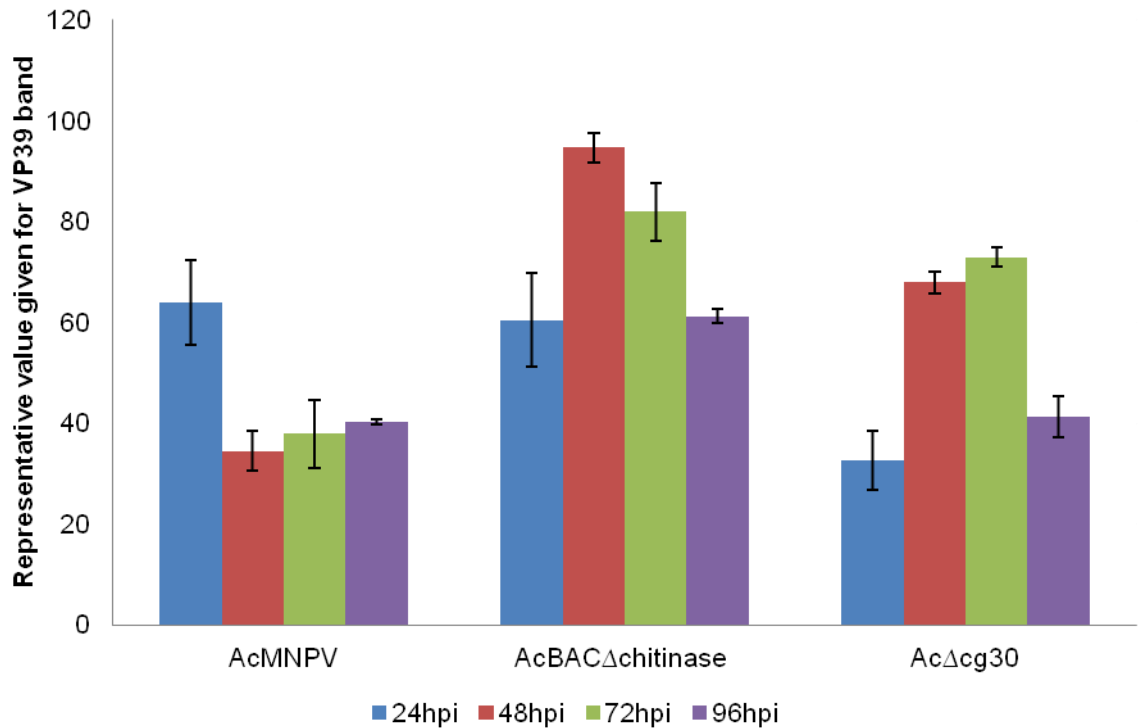


Figure 5.5 Semi-quantification of VP39 production in AcMNPV-, AcBAC Δ chitinase- and Ac Δ cg30-infected Sf9 cells

The Western blot images in Figure 5.4 were analysed using Gene tools to determine relative VP39 levels for each of the viruses at a given time point with standard error bars, grouped by viruses. All values are relative to the third AcBAC Δ chitinase 48 hour time-point band in Figure 5.4 panel B, which was arbitrarily set at 100.

The AcMNPV relative VP39 expression profile differs to that seen for AcBAC Δ chitinase and Ac Δ cg30 after 24hpi, most likely due to the earlier prominence of the other two VP39-specific protein bands seen for AcMNPV (Figure 5.4). The Kruskal-Wallis test was used to compare the AcBAC Δ chitinase values given for each time point to those of AcMNPV and significant difference was seen ($P < 0.05$), suggesting the deletion of *chitinase* effected the expression profile of VP39.

When the *AcΔcg30* relative VP39 expression profile was compared to that of *AcBACΔchitinase*, a decrease in VP39 level was seen at all time points tested here. However, Anova statistical analysis demonstrated no significant difference ($P>0.05$) when *AcΔcg30* values were compared to those of *AcBACΔchitinase*. Therefore, the statistical analysis confirmed that there were no significant differences between the levels of VP39 in the parental or *cg30* deletion mutant virus at the time points examined here and thus this cannot account for the differences in BV titres observed between these viruses (Figure 5.3).

The effects of the *cg30* deletion on virus replication in insect cell culture will be discussed in the final sections of this chapter. The next part of this chapter focuses on the effects the deletion mutant viruses could potentially have on ODV production and occlusion into polyhedra. However, this work required the polyhedrin gene to be restored to these viruses to allow the occlusion of ODV.

5.6 Restoration of *polh* into *AcBACΔchitinase*, *AcΔodv-e66*, *AcΔcg30* and *AcΔodv-e56*

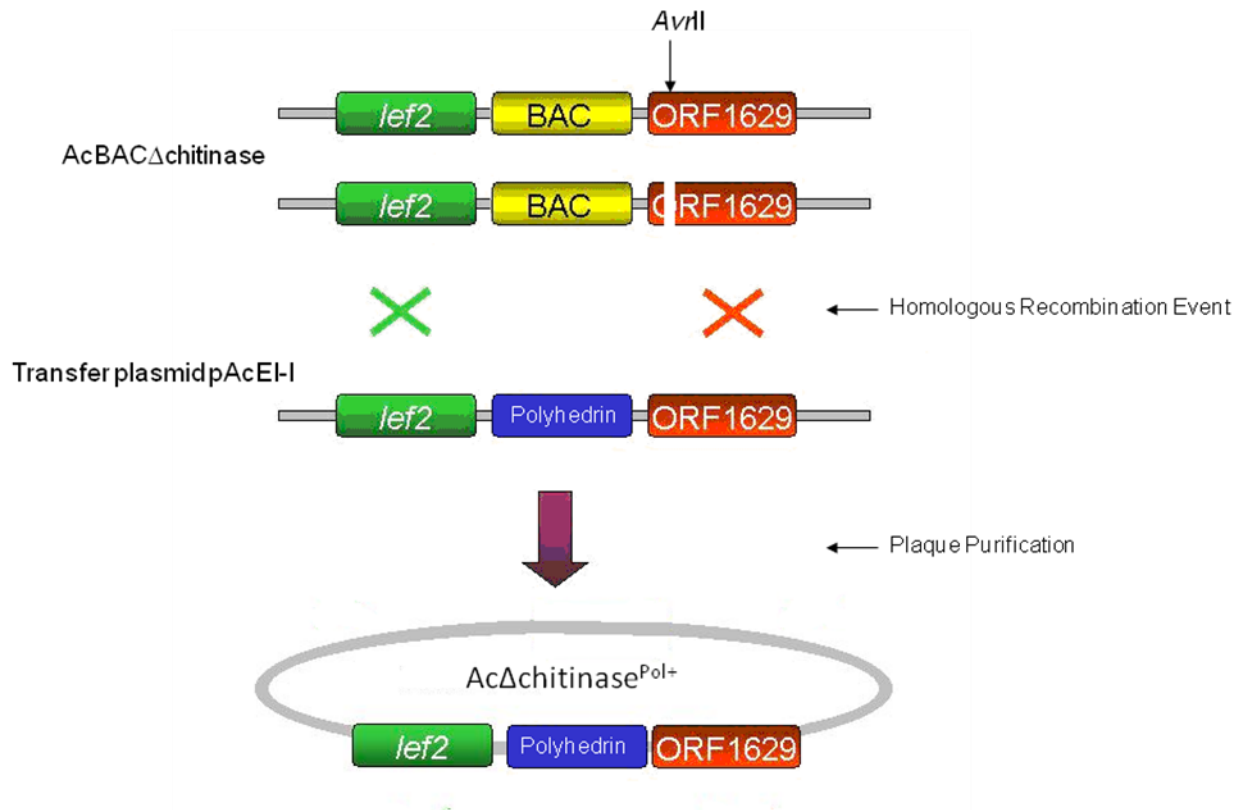
The reinsertion of *polh* was carried out by cotransfecting insect Sf9 cells with a transfer plasmid containing the *EcoRI* I fragment of the *AcMNPV* that includes the polyhedrin orf (obtained from Prof R Possee) and bacmid DNA from each of the four mutants that had been purified from *E.coli* and linearised by restriction digestion with *AvrII*. Each of the virus deletion mutants and *AcBACΔchitinase* contain a single *AvrII* site located within the essential gene *orf1629*. This produces a selection marker in which only those viruses that are rescued with a transfer plasmid that restores the whole of *orf1629* will be viable in insect cells. A double cross-over recombination event between any of these bacmids and pAcEI-I should remove the BAC and result in a virus with a restored polyhedrin gene in place of the BAC (Figure 5.6).

The resulting viruses were plaque-purified for several rounds until only polyhedrin-positive plaques were generated, as observed using a microscope (data not shown). The viruses were amplified to titres comparable to the original polyhedrin-negative viruses, suggesting that they were replicating normally in insect cells (See Figure 5.6 for virus names and titres). The next stage was to purify the OB from these polyhedrin-positive viruses to allow further experimental work to be carried on ODV.

The BV produced by each of these polyhedrin-positive viruses was injected into the hemocoels of separate groups of 50 fourth instar *T. ni* larvae. Each larva received 1×10^5 BVs to ensure 100% mortality for *AcΔchitinase*^{Pol+}. The three viruses, *AcΔodv-e66*^{Pol+},

AcΔcg30^{Pol+} and *AcΔodv-e56^{Pol+}* all produced similar levels of mortality to that of *AcBACΔchitinase* (data not shown). The OBs were then purified from the larvae using two different methods involving sucrose gradients. The first method purified OB from individual larvae, which were treated with no SDS for electron microscopy (EM) imaging (methods section 2.3.9a). The second method purified OB from approximately 40 larvae using SDS and high speed centrifugation for bioassays (methods section 2.3.9).

A



B

Target	Virus name	Short form virus name	Short form for polyhedrin positive virus	Virus titre (pfu/ml)
Parental	<i>AcBACΔchitinase</i>	<i>AcBACΔchitinase</i>	<i>AcΔchitinase^{Pol+}</i>	7.9×10^7
ODV-E66	<i>AcBACΔchitinase/odv-e66</i>	<i>AcΔcg30</i>	<i>AcΔcg30^{Pol+}</i>	4.5×10^7
CG30	<i>AcBACΔchitinase/cg30</i>	<i>AcΔodv-e56</i>	<i>AcΔodv-e56^{Pol+}</i>	3.5×10^7
ODV-E56	<i>AcBACΔchitinase/odv-e56</i>	<i>AcΔodv-e66</i>	<i>AcΔodv-e66^{Pol+}</i>	3.7×10^7

Figure 5.6 The restoration of the polyhedrin gene in *AcBACΔchitinase Δodv-e66*, *Δcg30* and *Δodv-e56* bacmids.

The BAC was completely deleted from *AcBACΔchitinase* and the deletion mutant viruses by the insertion of the polyhedrin gene via homologous recombination in Sf9 insect cells between pAcEI-I and virus genomes (A). (B) Table showing summary of deletion mutant viruses with updated abbreviated names for polyhedrin-positive viruses and the titres obtained when these viruses were amplified in Sf9 cells.

5.7 Bioassays for $Ac\Delta chitinase^{Pol+}$, $Ac\Delta odv-e66^{Pol+}$, $Ac\Delta cg30^{Pol+}$ and $Ac\Delta odv-e56^{Pol+}$

To examine the effect of $Ac\Delta odv-e66^{Pol+}$, $Ac\Delta cg30^{Pol+}$ and $Ac\Delta odv-e56^{Pol+}$ on viral infection *in vivo*, OBs from the deletion mutant viruses and $Ac\Delta chitinase^{Pol+}$ were purified from infected larvae and counted using a haemocytometer. They were assayed by oral infection in third instar *T. ni* larvae at a range of doses to determine their LD₅₀, LD₉₀ and survival time for each virus. Duplicate bioassays were set up as described in methods section 2.3.11 and the results are summarised in Table 5.1.

Table 5.1 Infectivity of $Ac\Delta odv-e66^{Pol+}$, $Ac\Delta cg30^{Pol+}$ and $Ac\Delta odv-e56^{Pol+}$ occlusion bodies

Virus	Lethal dose (OB/larva)							
	Experiment 1			Experiment 2			Survival Time	
	LD ₅₀	LD ₉₀	P	LD ₅₀	LD ₉₀	P	hpi±SE	P
AcMNPV	33.5	1137.2		48.2	1704.2		167.3±7.6	
$Ac\Delta chitinase^{Pol+}$	30.2	1289.8	0.3947	48.5	1823.2	0.3879	166.4±5.9	0.931
$Ac\Delta odv-e66^{Pol+}$	415.3	78276.1	0.0062	195	4764.3	0.0001	155.1±8.5	0.267
$Ac\Delta cg30^{Pol+}$	7.5	939.1	0.0393	7.5	539.9	0.0005	160.8±3.6	0.423
$Ac\Delta odv-e56^{Pol+}$	2.6×10^{10}	8.9×10^{18}	0.0060				164.5±6.5	0.875

The lethal dose (LD₅₀ and LD₉₀) values in Table 5.1 were determined by linear regression analysis; values above 10,000 OBs were extrapolated. Chi-square analysis was used to determine the P value for $Ac\Delta chitinase^{Pol+}$ compared to AcMNPV. In both bioassays no significant difference was seen between the infectivity of OBs from these two viruses. However, when each of the deletion mutant viruses were compared to $Ac\Delta chitinase^{Pol+}$ using the same chi-square analysis, a statistically significant difference was seen between the infectivity of OBs produced from larva infected with $Ac\Delta chitinase^{Pol+}$ compared to $Ac\Delta odv-e66^{Pol+}$, $Ac\Delta cg30^{Pol+}$ and $Ac\Delta odv-e56^{Pol+}$ OBs. This significant difference was seen in both of the bioassays for $Ac\Delta odv-e66^{Pol+}$ and $Ac\Delta cg30^{Pol+}$.

The oral infectivity of these viruses was also compared using Probit analysis (PoloPlus, LeOra Software). This further confirmed the results above suggesting the three deletion mutant viruses oral infectivity was significantly different to that of $Ac\Delta chitinase^{Pol+}$. However, the Probit analysis did suggest that the relative potency of $Ac\Delta chitinase^{Pol+}$ and $Ac\Delta cg30^{Pol+}$ OBs were the same.

The survival times in hpi was only carried out in the first bioassay. A student t-test was used to compare survival times between viruses to determine their P values. The survival times for $Ac\Delta chitinase^{Pol+}$ were compared to those for AcMNPV and demonstrated no significant difference between these two viruses. The survival times for $Ac\Delta chitinase^{Pol+}$

were then compared to each of the survival times from the deletion mutant viruses using the student t-test and no significant difference was determined. This observation is confirmed by Figure 5.7 that demonstrates the majority of virus infected larva at the top dose (10^4 OBs/larva) died in a narrow window between 5.5-9.5 days post infection for all of the viruses even for *Ac Δ odv-e66^{Pol+}* (61%), and *Ac Δ odv-e56^{Pol+}* (21%), which didn't cause 100% mortality at their top dose.

The effects of these deletions on oral infection was investigated and differences have been observed compared to the parental virus; *Ac Δ chitinase^{Pol+}*. These differences suggest that deletion of either *odv-e66* or *odv-e56* has a negative effect on oral infectivity of OBs, whereas the deletion of *cg30* seems to increase oral infectivity of OBs. However, none of the deletions effected the replication of the virus within the host shown by no differences between the survival times of the deletion mutant viruses compared to their parental virus. The next stage was to determine whether or not these effects could have been caused by defects in ODV production or occlusion by examining purified OBs under EM.

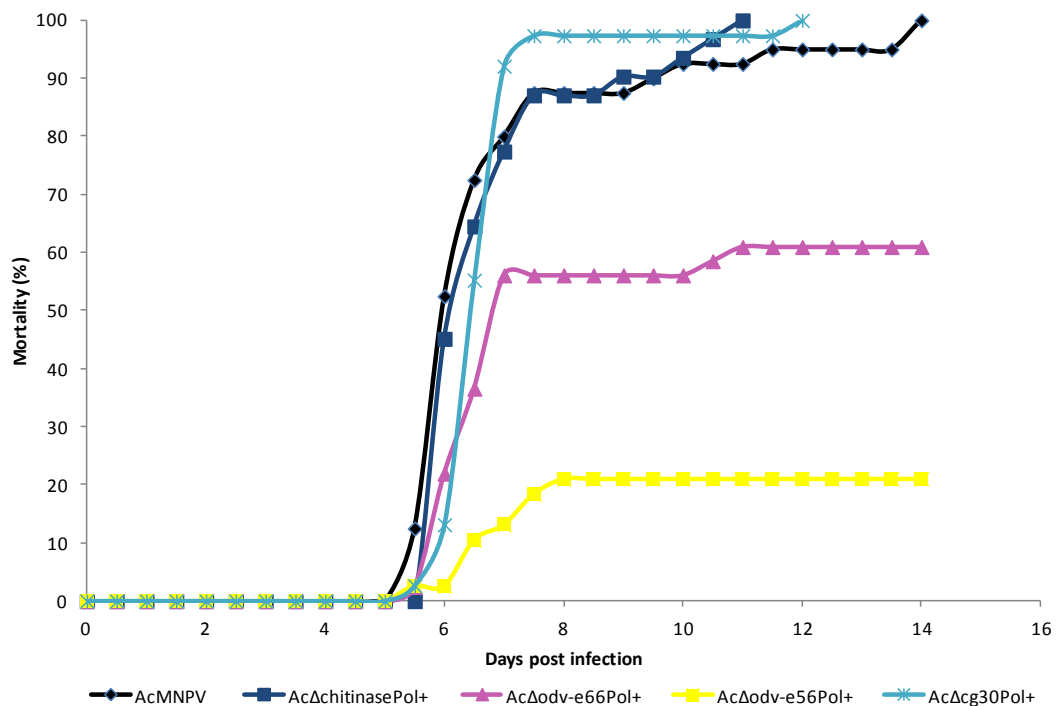


Figure 5.7 Mortality of *AcMNPV*, *Ac Δ chitinase^{Pol+}*, *Ac Δ odv-e66^{Pol+}*, *Ac Δ cg30^{Pol+}* and *Ac Δ odv-e56^{Pol+}* infected larvae

The mortality rate of *AcMNPV*, *Ac Δ chitinase^{Pol+}*, *Ac Δ odv-e66^{Pol+}*, *Ac Δ cg30^{Pol+}* and *Ac Δ odv-e56^{Pol+}* infected larvae at the top dose (10^4 OBs/larva) were assessed until all larvae had succumb to viral infection or pupated.

5.8 Electron microscopic analysis of *Ac* Δ chitinase^{Pol+}, *Ac* Δ odv-e66^{Pol+}, *Ac* Δ cg30^{Pol+} and *Ac* Δ odv-e56^{Pol+} OBs

The OBs purified from *Ac* Δ chitinase^{Pol+}, *Ac* Δ odv-e66^{Pol+}, *Ac* Δ cg30^{Pol+} and *Ac* Δ odv-e56^{Pol+} infected larvae were then prepared for EM imaging. This involved the samples being fixed, stained, dehydrated and then embedded in resin. Once the resin had set, ultrathin sections were produced using a microtome and these sections were then restained to increase imaging detail (methods section 2.4.2). The OB images taken on the EM (Hitachi H7650) for the deletion mutant viruses and *Ac* Δ chitinase^{Pol+} are shown in Figure 5.8.

The sections through *Ac* Δ chitinase^{Pol+} polyhedra show that the ODVs contain multiple nucleocapsids and are embedded in polyhedrin with each OB surrounded by the polyhedron envelope (PE), which is evident as a dark outline (Figure 5.8, panel A). The OB sections from *Ac* Δ odv-e66^{Pol+} appear structurally similar to those from *Ac* Δ chitinase^{Pol+} suggesting no differences in ODV production or occlusion that can be seen by EM (Figure 5.8, panel B).

However, the OBs from *Ac* Δ cg30^{Pol+} show the loss of the PE, as indicated by red arrows in Figure 5.8, panel C. These OBs also seem to have started to degrade and release ODV, as indicated by the 'empty pockets' left behind. The OBs from *Ac* Δ odv-e56^{Pol+} also look structurally similar to those from *Ac* Δ chitinase^{Pol+} suggesting no difference in the ODV production or occlusion that can be seen by EM. However, these OBs appear to be associated with another, unidentified, protein even after the purification process. This protein appears to be wrapped around the *Ac* Δ odv-e56^{Pol+} OBs and is indicated by blue arrows in Figure 5.8, panel D. In the last image (Figure 5.8, panel D4), two *Ac* Δ odv-e56^{Pol+} OBs are clearly linked together by this protein. A possible candidate for this protein is P10 as it is known to associate with polyhedra during their formation (Lee *et al.*, 1996; Patmanidi *et al.*, 2003; Carpentier *et al.*, 2008).

Chapter 5

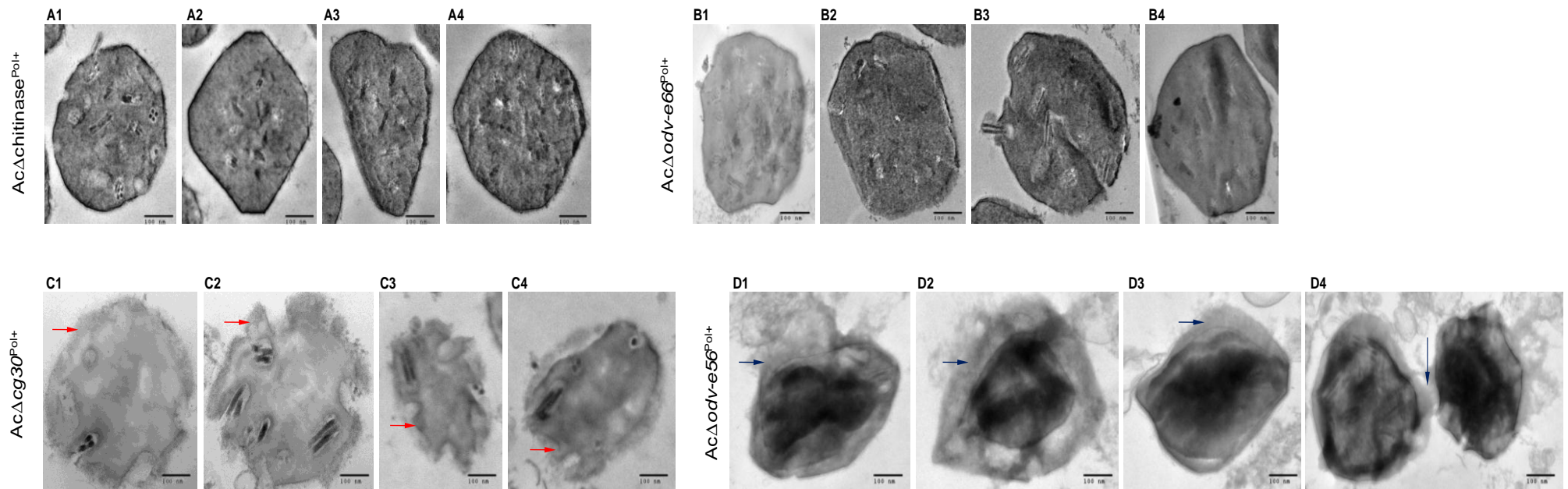


Figure 5.8 Electron microscopy of purified OBs from *AcΔchitinase^{Pol+}*, *AcΔodv-e66^{Pol+}*, *AcΔcg30^{Pol+}* and *AcΔodv-e56^{Pol+}* infected larva.

A selection of EM images which are representative of those obtained after fixing, staining and sectioning OBs from each of the deletion mutant viruses and *AcΔchitinase^{Pol+}* are shown. Red arrows in *AcΔcg30^{Pol+}* images (C1-C4) indicate loss of the polyhedral envelope protein and blue arrows in *AcΔodv-e56^{Pol+}* images (D1-D4) indicate an unidentified protein wrapped around *AcΔodv-e56^{Pol+}* OBs. Scale bars represent 100 nm.

5.9 Discussion

In this chapter three viruses, *AcΔodv-e66*, *AcΔcg30* and *AcΔodv-e56*, which were able to replicate in insect cell culture but not initially classified as part of the *pif* family, were examined, particularly with regard to any effect on ODV production or packaging into the OB.

5.9.1 *AcΔodv-e66*

The effect of *odv-e66* deletion on BV production and cell viability in Sf9 cells was examined in a time course experiment. These results showed that both the viability of the *AcΔodv-e66*-infected cells (27%) and BV titre (1.87×10^7 pfu/ml) were significantly different to those of *AcBACΔchitinase* at 120hpi (19% and 7.15×10^7 pfu/ml). This suggests that the deletion of *odv-e66* has affected both these aspects of viral replication. It is likely that the improvement in virus-infected cell viability at 120hpi is a consequence of the decrease in BV production by *AcΔodv-e66*. It would be interesting to continue the sampling of virus-infected cell cultures to later time points to determine if BV production reaches the levels seen for the parental virus and if virus-infected cell viability also decreases further.

This result conflicts with a current publication on deletion mutant of *odv-e66* that demonstrated no effect on BV production (Xiang *et al.*, 2011). In their study, BV production kinetics were analysed after the transfection of Sf9 cells with bacmid DNA instead of a virus stocks that had been accurately titrated prior to the experiment, as was carried out in this thesis. Transfection of insect cells with baculovirus DNA (e.g., bacmids) rarely produces a synchronous infection. This has the result that there will be multiple rounds of virus replication as cells initially escaping transfection with DNA become infected with virus in secondary rounds of replication.

It was demonstrated that the deletion of *odv-e66* affected *per os* infectivity of OBs fed to third instar *T. ni* larvae. However, different results were seen in two independent bioassays. In the first bioassay there was approximately a 14-fold increase in LD₅₀ (415 OBs per larva) when compared to *AcΔchitinase*^{Pol+} (30 OBs per larvae). In the second bioassay, the increase in LD₅₀ (195 OBs per larva) was approximately only four-fold when compared to *AcΔchitinase*^{Pol+} (48 OBs per larva) in the second bioassay. This gives an average nine-fold increase of LD₅₀ for the *AcΔodv-e66*^{Pol+} that is similar to the 10-fold increase reported by Xiang *et al.* (2011) for their *odv-e66* deletion mutant virus. However, there was a statistically very significant difference seen between the infectivity of OBs produced from larva infected with *AcΔchitinase*^{Pol+} compared to *AcΔodv-e66*^{Pol+}. Therefore

both bioassays suggest that *odv-e66* plays a role in oral infection. When BV from $\text{Ac}\Delta\text{odv-e66}^{\text{Pol}^+}$ infected cells was injected into the hemocoels of fourth instar *T. ni* larvae, 100% mortality was seen. There was no significant difference between $\text{Ac}\Delta\text{odv-e66}^{\text{Pol}^+}$ and $\text{Ac}\Delta\text{chitinase}^{\text{Pol}^+}$ survival times at the top dose of 10,000 OBs/larva, which suggests there is no difference between the replication efficiencies of the two viruses in the host larva. This information strongly suggests that *odv-e66* plays a role in oral infection but that this role may not be as critical as the involvement of the *pif* family. It is not suggested that *odv-e66* should be considered a member of this protein family.

It could be argued that the decrease in *per os* infectivity of $\text{Ac}\Delta\text{odv-e66}^{\text{Pol}^+}$ OBs is a consequence of impaired ODV packaging within polyhedra. However, electron microscopy imaging of $\text{Ac}\Delta\text{odv-e66}^{\text{Pol}^+}$ OBs revealed no apparent difference in structure or ODV packaging when compared to images of $\text{Ac}\Delta\text{chitinase}^{\text{Pol}^+}$ OBs. This confirms the electron microscopic analysis of deletion mutant virus ($\Delta\text{odv-e66}$) OB previously published (Xiang *et al.*, 2011). This suggests the observed affects seen on oral infection of $\text{Ac}\Delta\text{odv-e66}^{\text{Pol}^+}$ OBs is due to the actual function of *odv-e66* and not some structural defect caused by the deletion of *odv-e66*. These results also strengthen the view that ODV-E66 is a protein bound at the N-terminal to the ODV envelope facing outwards and not inwards. This contradicts evidence suggesting that ODV-E66, together with another viral protein ODV-E25, are involved in ODV capsid envelopment (Russell *et al.*, 1997).

It might be interesting to extract ODVs from $\text{Ac}\Delta\text{odv-e66}^{\text{Pol}^+}$ OBs and compare their *per os* infectivity with parental viruses. This experiment would disassociate the dissolving of OBs in the insect mid gut from the initial stages of virus infection. It might also be possible to go one stage further and strip the ODV envelopes from the particles and then mediate infection of insect cells *in vivo* or *in vitro* by using liposomes as carriers. This was done to study rotavirus entry to host cells (Bass *et al.*, 1992). The advantage of studying the infectivity of artificially enveloped ODVs is that it might be possible to determine if there is an inherent difference in particle structure if ODV-E66 is withheld during maturation.

5.9.2 $\text{Ac}\Delta\text{cg30}$

Using the same approach described for $\text{Ac}\Delta\text{odv-e66}$, BV production and virus-infected cell viability was assessed during a time course of replication for $\text{Ac}\Delta\text{cg30}$. These results showed that there was no significant difference between the cell viability of $\text{Ac}\Delta\text{cg30}$ -infected cells (24%) and $\text{AcBAC}\Delta\text{chitinase}$ infected cells (19%) at 120hpi. However, there was a significant difference between the BV titres of infectivity for $\text{Ac}\Delta\text{cg30}$ (2.97×10^7 pfu/ml) and $\text{AcBAC}\Delta\text{chitinase}$ (7.15×10^7 pfu/ml) at 120hpi, suggesting that the deletion of

cg30 had impacted on BV production. This 2.4-fold difference contradicts work already done on a *cg30* deletion mutant virus that showed it produced slightly more BV than the parental virus (Passarelli and Miller, 1994). Therefore, in this study it was investigated whether or not the deletion of *cg30* had affected the major capsid protein VP39 expression, since the two genes are neighbours in the AcMNPV genome. However, the results from this experiment showed no significant difference between the expression of VP39 in Ac Δ *cg30*- and that observed in AcBAC Δ chitinase-infected cells. However, this analysis did highlight some interesting observations on the size of VP39 that accumulated throughout virus infection. In AcMNPV-infected cells two proteins smaller than the predicted mass of VP39 were present from 24hpi but accounted for the majority of immune-reactive material by 48hpi. In both AcBAC Δ chitinase- and Ac Δ *cg30*-infected cells, however, these two smaller bands were in the minority until 72hpi. It is conceivable that these differences may be accounted for by the lack of the *chiA* in both viruses. The baculovirus chitinase is reported to serve as a chaperone in the maturation of active virus-encoded cathepsin (Hom *et al.*, 2002; Hodgson *et al.*, 2011). The appearance of lower molecular weight species of VP39 in AcMNPV-infected cells may be a consequence of cathepsin-mediated processing of protein that is not sequestered within virus particles. A definitive test of this hypothesis would be to examine VP39 accumulation in mutants of AcMNPV lacking *cath*. The *chiA* could also be restored to AcBAC Δ chitinase to determine if VP39 processing kinetics could be returned to the wild-type profile. While these differences in VP39 may be of little consequence to the study of *cg30* function, they highlight that caution should be exercised in the selection of a parental virus genome for making further deletions. It is better to employ a baculovirus genome that only has a modified *polh*, since this encodes a very late protein that should have no effect on earlier events in virus replication.

The apparent decrease in VP39 levels at 96hpi may be indicative of events in the Ac Δ *cg30*-infected cells that differ from the parental- or wild type-infected cells. Coupled with the apparent sharp increase in BV titre of Ac Δ *cg30* by 120hpi this indicates that further studies of virus replication in the very late stages are merited. It is feasible that BV titres of Ac Δ *cg30* could rise further to near those of AcBAC Δ chitinase.

It was also demonstrated that the deletion of *cg30* affected *per os* infectivity of OBs fed to third instar *T. ni* larvae. This effect was positive as shown by an approximate four-fold and seven-fold decrease in LD₅₀ when compared to Ac Δ chitinase^{Pol+} LD₅₀ in two different bioassays. Passarelli and Miller (1994) observed a two-fold decrease in LD₅₀ with their *cg30* deletion mutant virus in first instar *T. ni* larvae. However, they suggested this effect was conferred by the presence of *lacZ* within their virus, which could be altering the

polyhedron envelope structure. The data collected here suggests that this interpretation was incorrect and the decrease in LD₅₀ could have been caused by deletion of *cg30* and not the presences of *lacZ* within the virus. There was a very statistically significant difference seen between the infectivity of OBs produced from larva infected with *AcΔchitinase*^{P_{ol}+} compared to *AcΔcg30*^{P_{ol}+}. However, there was no significant difference between *AcΔcg30*^{P_{ol}+} and *AcΔchitinase*^{P_{ol}+} survival times at the top dose of 10,000 OBs. This suggests there is no difference between the replication speeds of the two viruses in the host larva. This correlates with observations seen before for *cg30* deletion mutant virus (Passarelli and Miller, 1994). Therefore the *AcΔcg30*^{P_{ol}+} decrease in LD₅₀ is most likely caused by increase in the efficiency of midgut infection of *AcΔcg30*^{P_{ol}+} ODVs.

Electron microscopy imaging of *AcΔcg30*^{P_{ol}+} OBs showed that the polyhedron envelope (PE) was deformed and the OBs seem to be degrading due to the loss of the PE. This was not seen in the OB images of *AcΔchitinase*^{P_{ol}+}. This could suggest that the loss of *cg30* caused the OB to become unstable and during oral infection of fresh *AcΔcg30*^{P_{ol}+} OBs. This degradation allows the release of ODV more easily in the midgut of the larva during oral infection. Interestingly, deletion of the PE gene also results in unstable OBs that have an uneven surface, which are prone to losing ODVs (Russell and Rohrmann, 1990; Russell *et al.*, 1991). The assembly of the PE on mature OB during the late stages of infection has been demonstrated to involve P10 (Gross *et al.*, 1994; Lee *et al.*, 1996). Therefore, investigation of the relationship between CG30, P10 and PE during viral replication could give insights into the formation of the PE.

It would be interesting to examine whether or not the increase in oral infection has a cost for the *AcΔcg30*^{P_{ol}+} survivability in the long term due to the weakened OB structure. Although an increase in polyhedra infectivity would be very advantageous in biocontrol programmes, a decrease in product shelf life would negate this.

5.9.3 *AcΔodv-e56*

The results from a time course to examine cell viability of *AcΔodv-e56*-infected cells (36%) and the resultant BV titre (1.52×10^7 pfu/ml) were significantly different to those of *AcBACΔchitinase* at 120hpi (19% and 7.15×10^7 pfu/ml). This does suggest that the deletion of *odv-e56* has affected both these aspects of the viral replication. However, as was the case with the *odv-e66* deletion, if the time course had continued past 120hpi most likely the titre for *AcΔodv-e56* might have continued to increase due to the cell viability of the *AcΔodv-e56* infected cell still being so high at 120hpi. Work currently done on ODV-E56 suggests its absence has no effect on BV production. However, all of these studies

used a disrupted *odv-e56* by insertion of *lacZ* rather than a deletion strategy (Braunagel *et al.*, 1996; Harrison *et al.*, 2010; Spark *et al.*, 2011a). Attempts to generate a complete *odv-e56* deletion mutant virus have been unsuccessful in other studies (Braunagel and Summers, 2007).

It was demonstrated here that the deletion of *odv-e56* did affect the *per os* infectivity of OBs in third instar *T. ni* larvae, having an extrapolated LD₅₀ of 2.6x10¹⁰ OBs per larva. This indicates that *odv-e56* is essential for oral infection because when BV from AcΔ*odv-e56*^{P^{ol+}} infected cells was injected into the hemocoels of fourth instar *T. ni* larvae, 100% mortality was seen. Interestingly, the larva that did die in the top dose of 10,000 AcΔ*odv-e56*^{P^{ol+}} OBs on average had a survival time that was not significantly different to AcΔ*chitinase*^{P^{ol+}} average survival times at the same dose. This degree of impairment of oral infectivity observed here for AcΔ*odv-e56*^{P^{ol+}} is in agreement with previous studies carried out with *H. virescens* larva (Harrison *et al.*, 2010; Sparks *et al.*, 2011a).

Electron microscopy imaging of AcΔ*odv-e56*^{P^{ol+}} OBs showed no apparent difference in structure or ODV packaging when compared to images of OBs from AcΔ*chitinase*^{P^{ol+}}. However, the AcΔ*odv-e56*^{P^{ol+}} OBs did seem to be surrounded by another protein structure. This was only observed in AcΔ*odv-e56*^{P^{ol+}} OBs images and not in those from AcΔ*chitinase*^{P^{ol+}} or the other two deletion mutant viruses, suggesting that this structure has been altered in AcΔ*odv-e56*^{P^{ol+}} and has survived the purification process. This unidentified protein structure is most likely comprised of P10 that has been shown to be involved in cell lysis and interacts with host cell microtubules to form a cage like structure around OBs inside the nuclei of the infected cells to aid release of the OBs (Patmanidi *et al.*, 2003; Carpentier *et al.*, 2008). However, another explanation for this protein structure could be due to malformation of the polyhedron envelope, which has allowed other non-specific proteins to be incorporated into it causing an expansion of the polyhedron envelope. Electron microscopy analysis carried out by Harrison *et al.* (2010), on deletion mutant *odv-e56* OBs in infected insect cells, showed no obvious differences in structure or ODV packaging as shown in Figure 5.8, panel D1-D4. However, these images were of unpurified OBs in infected cells and therefore the protein structure observed in Figure 5.8, panel D1-D4 wouldn't have been detected. The presence of this structure still surrounding AcΔ*odv-e56*^{P^{ol+}} OBs could have affected the breakdown of the OB in the larva midgut stopping the release of ODVs and may help explain the results seen in the bioassay. This is further confirmed by Sparks *et al.* (2011a) that demonstrated that ODV purified from deletion mutant *odv-e56* OBs increased oral infectivity from the five orders of magnitude less infectious seen comparing OBs from AcMNPV to two orders of magnitude less infectious when compared against AcMNPV ODV. It would be interesting to isolate OBs

from *AcΔodv-e56^{P^{ol+}}*-infected insect after injection with BV and determine how dissolution of polyhedra in the presence of alkaline solutions is affected by this newly observed structure. It would also be possible to use immunoblotting to confirm the hypothesis that it comprises P10.

5.9.4 Conclusion

For all three virus gene deletion mutants the results obtained from the time course observing BV production kinetics seems to conflict with the current literature. Repetition of the experiments to ensure reproducibility would be advisable as would deriving further recombinant viruses where each gene target has been rescued at the *polh* locus. The rescue viruses are more easily obtainable now due to the polyhedrin-positive forms having a marker to indicate insertion of the rescue gene fragment at the polyhedrin locus. The derivation of baculovirus mutants is now relatively facile given the availability of the Red-ET system in *E. coli*, but this method is accompanied by the risk of random mutations elsewhere in the virus genome.

It is possible that the deformed PE observed with *AcΔcg30^{P^{ol+}}* OBs is a consequence of other mutations in the virus genomes of *AcΔcg30* or *AcΔcg30^{P^{ol+}}* affecting PE envelope protein production. Western blot analysis using antibody for PE to demonstrate the temporal expression of PE could show if the expression profile for *AcΔcg30^{P^{ol+}}* throughout a time course closely matched its parental virus profile; *AcΔchitinase^{P^{ol+}}*. DNA sequencing across the *PE* locus could indicate whether or not any mutations at the DNA level have occurred that could cause the observed effect of deformed PE either through change in amino acid sequence or the expression of PE. If the affect is pin pointed to the *cg30* deletion then studies could be directed to the survivability of these degraded OBs to different environmental factors such as temperature and UV and the affects these could have on oral infectivity of larva. Studies could also be directed towards the reason for the deletion of *cg30* to cause this loss of PE. CG30 does contain two DNA binding motifs, comprising a zinc ring finger motif (C3HC4) and a leucine zipper motif at the C-terminus and N-terminus, respectively (Thiem and Miller, 1989). This could suggest that CG30 directly or indirectly affects PE expression by binding to specific DNA sequences; however an indication of this would be given by the western blot analysis and DNA sequencing of PE suggested earlier.

The unidentified protein structure surrounding *AcΔodv-e56^{P^{ol+}}* OBs shown by the election microscopy analysis could be further investigated, and either confirmed or denied as P10 as suggested here by using election microscopy analysis with immunostaining to see if

the P10 antibody binds the unidentified protein structure. If it was confirmed as P10 and there was no indication of mutation to the p10 sequence in *AcΔodv-e56^{P^{ol+}}* then a double deletion mutant virus could be constructed in which both *p10* and *odv-e56* had been deleted (*AcΔp10/odv-e56^{P^{ol+}}*). Election microscopy analysis could be used to observe the *AcΔp10/odv-e56^{P^{ol+}}* OBs structure and bioassay could be used to test the oral infectivity of these OBs compared to parental and single deletion mutant viruses. However, it has been suggested that ODV-E56 plays a role in ODV morphogenesis that could suggest that the removal of *p10* maybe not fully restore the oral infectivity of *AcΔodv-e56^{P^{ol+}}* (Braunagel and Summers, 2007).

Chapter 6
Characterisation of *Ac* Δ *pif2* and
Ac* Δ *pif3

6.1 Introduction

The final two viruses generated using the Red/ET recombination system had deletions in *pif2* and *pif3*, respectively, to yield *AcΔpif2* and *AcΔpif3*. The baculovirus *pif2* and *pif3* have already been characterised as members of the *pif* family of genes, which have an important role in facilitating *per os* infectivity of ODV. This chapter will provide a brief introduction to *pif2* and *pif3* and then focus on experimental work to investigate the possible effects these two deletions could have on recombinant protein expression.

The *AcΔpif2* virus contains the reporter gene *lacZ* at the *polh* locus allowing expression tests to be carried out to observe any effects the *pif2* deletion has on recombinant protein expression under the control of the *polh* promoter. However, the *AcΔpif3* virus contains no reporter gene and requires insertion of such genes at the *polh* locus using classical techniques, using the *AvrII* site to linearise *AcΔpif3* at the essential gene *orf1629* prior to cotransfection with a plasmid transfer vector containing the foreign coding region.

6.1.1 *per os* infectivity factor (PIF) family

The *per os* infectivity factor (PIF) family contains proteins that are non-essential for viral replication but are essential for oral infection of the host lepidopteran larvae by AcMNPV and other baculoviruses. To date, the PIF family consists of PIF0 (P74; Faulkner *et al.*, 1997), PIF1 (ORF119; Kikhno *et al.*, 2002), PIF2 (ORF22; Pijlman *et al.*, 2003), PIF3 (ORF115; Ohkawa *et al.*, 2005), PIF4 (ODV-E28; Fang *et al.*, 2009) and PIF5 (ODV-E56; (Sparks *et al.*, 2011a)) that are all core genes conserved among all sequenced baculoviruses. Homologues of the PIF family are also found in nudiviruses, which are double-stranded DNA viruses that infect insects and are related to the *Baculoviridae* (Wang *et al.*, 2007). The two proteins of interest in this study were PIF2 (Pijlman *et al.*, 2003) and PIF3 (Ohkawa *et al.*, 2005) that have already been demonstrated to be members of the PIF family.

6.1.2 PIF2

PIF2 was first characterized in *Spodoptera exigua* multiple nucleopolyhedrovirus (SeMNPV) as ORF35 (Pijlman *et al.*, 2003). The *pif2* is found in all sequenced alphabaculoviruses and betabaculoviruses; alignments of *pif2* homologues can be seen in Chapter 3. The AcMNPV homologue for *pif2* is ORF22 that produces a 44 kDa protein

that contains highly conserved hydrophobic N-terminal transmembrane motif, which is used to anchor PIF2 to the ODV envelope (Braunagel *et al.*, 2003).

PIF2 is believed to be involved in mediating specific binding of ODV to the primary midgut cells in oral infection of larva (Pijlman *et al.*, 2003; Ohkawa *et al.*, 2005). It has been more recently demonstrated that PIF2 along with three other conserved PIF proteins, P74, PIF1 and PIF3, form a stable complex on the surface of the ODV, which is essential for the early stages of baculovirus oral infection (Peng *et al.*, 2010).

6.1.3 PIF3

The AcMNPV *pif3* (ORF115) produces a 23 kDa protein and is found in all sequenced alphabaculoviruses and betabaculoviruses. PIF3, like most other ODV envelope proteins contains an N-terminal transmembrane domain, which most likely anchors the protein to the ODV envelope (Ohkawa *et al.*, 2005). However, PIF3 was not located to the ODV envelope during a protein composition analysis of AcMNPV ODV (Braunagel *et al.*, 2003). Peng *et al.* (2010) further demonstrated this by electron microscopy analysis that localized PIF2 to the surface of the ODV with a scattered distribution but was unable to detect PIF3 on the ODV surface or the nucleocapsid; therefore the localization of PIF3 on the ODV is still inconclusive. However, Peng *et al.* (2010) did demonstrate PIF3 to be part of a stable protein complex along with other PIF proteins on the surface of the ODV.

Unlike the other PIF proteins, PIF3 deletion mutant viruses showed similar ODV binding levels as wild-type virus, during binding and fusion assays. Therefore, this protein must be involved in a critical event in early primary infection such as translocation of the ODV capsids along the microvillus of the midgut cells or interacting with cytoskeletal elements aiding transport of the ODV, if it is located to the inside of the ODV envelope (Ohkawa *et al.*, 2005; Slack and Arif, 2007).

6.2 Characterization of Ac Δ *pif2* and Ac Δ *pif3*

The Red/ET recombination system was successfully used to produce deletion mutant bacmids Δ *pif2* and Δ *pif3*. In Δ *pif2*, the majority of the *pif2* coding region was removed and replaced with a kanamycin resistance gene, leaving 50bp of *pif2* at the 5' end to ensure that the *orf21* promoter was unaffected by the deletion (Figure 6.1, panel A). In the case of Δ *pif3*, only part of the *pif3* coding region was removed and replaced with a kanamycin

Chapter 6

resistance gene, leaving 159 bp of at the 5' end to ensure that the *orf114* promoter was unaffected by the deletion (Figure 6.1, panel B). Chapter 4 provides a more detailed explanation of the method used to create these deletion mutant bacmids using the Red/ET recombination system and the methods used to confirm the deletions.

AcΔpif2 and *AcΔpif3* were obtained by transfection of Sf9 cells with bacmid DNA and recovery of budded virus (as described in Chapter 4). The BV was amplified further in Sf9 cells to provide working stocks of titrated virus for further study. *AcΔpif2* amplified to 7.4×10^7 pfu/ml and *AcΔpif3* amplified to 5.0×10^6 pfu/ml.

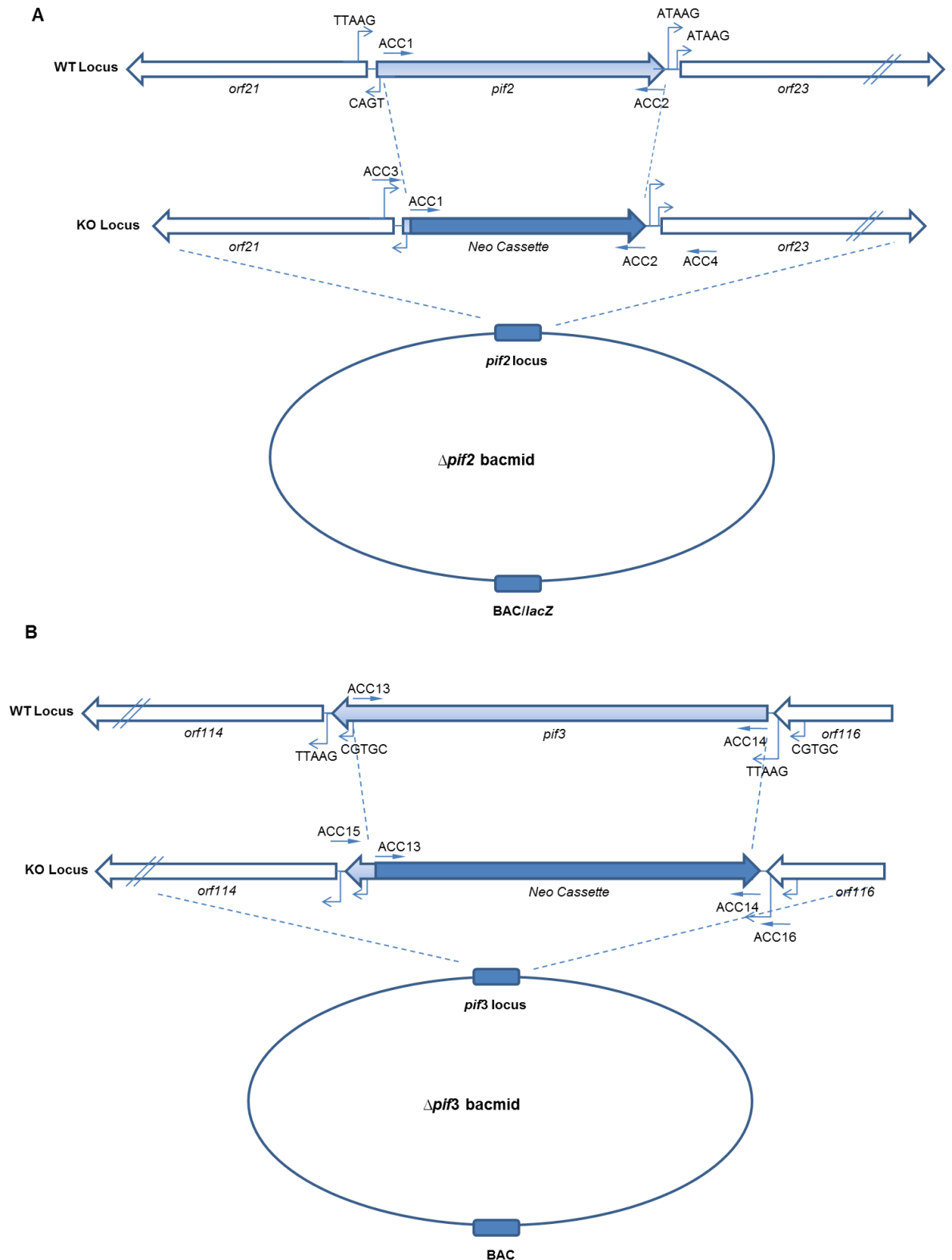


Figure 6.1 Schematic of the construction of $\Delta pif2$ (A) and $\Delta pif3$ (B) bacmids

The *pif2* and *pif3* ORFs were partially deleted by the insertion of a DNA fragment encoding a kanamycin resistance cassette between 17351-18449 (A) and 99341-99796 (B) bp positions respectively on the AcMNPV genome via homologous recombination in *E. coli* using the Red/ET recombination system.

6.3 Temporal analysis of virus replication in *AcΔpif2*- and *AcBacPAK5/lacZ/BAC^{pol}*-infected Sf9 cells.

A time course study was carried out and samples were taken over 120 hours from triplicate Sf9 cultures either mock-infected or infected with *AcΔpif2* or *AcBacPAK5/lacZ/BAC^{pol}* at a moi of 5 pfu/cell. These samples were analysed to determine any effects that the *pif2* deletion could have on the expression of the recombinant protein β -galactosidase, cell viability and BV production kinetics.

6.3.1 Virus-infected cell viability

Cell viability analysis showed that mock-infected cells remained >96% viable until the end of the experiment at 96hpi. The viability of the virus-infected cells began to differ from the mock-infected from 24hpi. After this point there was a continuous decrease in cell viability, which followed the same trend for both viruses until 72hpi. At the 72hpi and 96hpi sampling points, *AcBacPAK5/lacZ/BAC^{pol}* infected cells had decreased to approximately 9% and 5% viability, respectively. The *AcΔpif2* infected cells decreased to approximately 17% and 9% at these time points (Figure 6.2). The cell viability readings were not taken at 120hpi due to the reading for 96hpi being so close to zero for both viruses. Anova statistical analysis demonstrated that there was no significant difference between *AcBacPAK5/lacZ/BAC^{pol}* and *AcΔpif2* infected cell viabilities ($P>0.05$).

6.3.2 Budded virus production

The *AcBacPAK5/lacZ/BAC^{pol}* and *AcΔpif2* infectious virus titres for each time point were obtained using the plaque assay method (See methods section 2.3.4a; Figure 6.3). A decrease in titre between 0hpi and 12hpi was observed for both viruses. The *AcBacPAK5/lacZ/BAC^{pol}* titre increased sharply between 12hpi and 48hpi from 1.00×10^5 pfu/ml to 9.88×10^6 pfu/ml. This increase continued to 120hpi, where a final BV titre of 1.57×10^7 pfu/ml was reached. The *AcΔpif2* BV production kinetics differed from those of *AcBacPAK5/lacZ/BAC^{pol}* in that after an initial lag phase until 12hpi, the subsequent exponential period of infectious virus release was not as rapid (Figure 6.3). Between 12hpi and 48hpi BV titres increased from 2.08×10^5 pfu/ml to 1.24×10^7 pfu/ml. By 96hpi, the titres of both viruses were almost identical and by 120 hpi *AcΔpif2* attained a titre of 1.58×10^7 pfu/ml. Despite these temporal differences, Anova statistical analysis demonstrated that there was no significant difference between *AcBacPAK5/lacZ/BAC^{pol}* and *AcΔpif2* BV production kinetics ($P>0.05$). A two-tailed student t-test performed on individual time points showed no significant difference ($P>0.05$) between *AcBacPAK5/lacZ/BAC^{pol}* and *AcΔpif2* titres, confirming these slight differences in BV production kinetics were not significant even at individual time points.

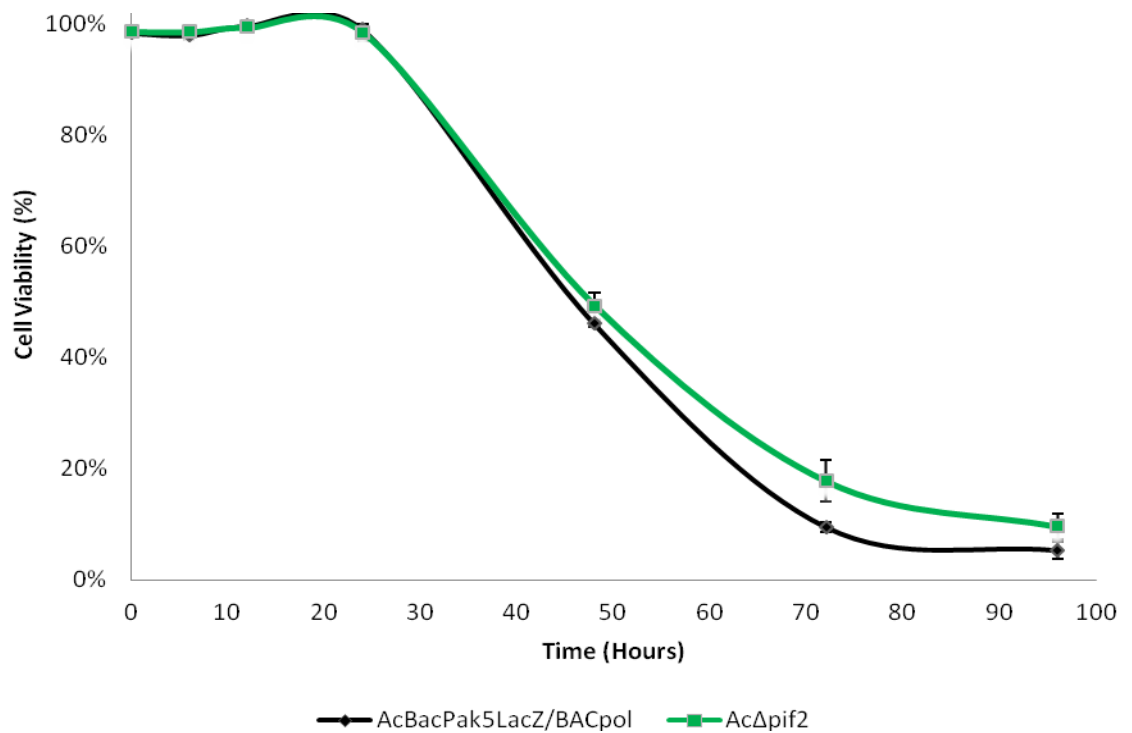


Figure 6.2 Cell viability of AcBacPAK5/lacZ/BAC^{pol} or AcΔpif2-infected Sf9 cells.

Cultures of Sf9 cells were infected with AcBacPAK5lacZ/BAC^{pol} or AcΔpif2 (MOI = 5 pfu/cell) and cell viability was assessed at the indicated time points. The experiment was terminated before the final time point at 120hpi owing to the very low cell viability. Standard error bars are shown. N = 3.

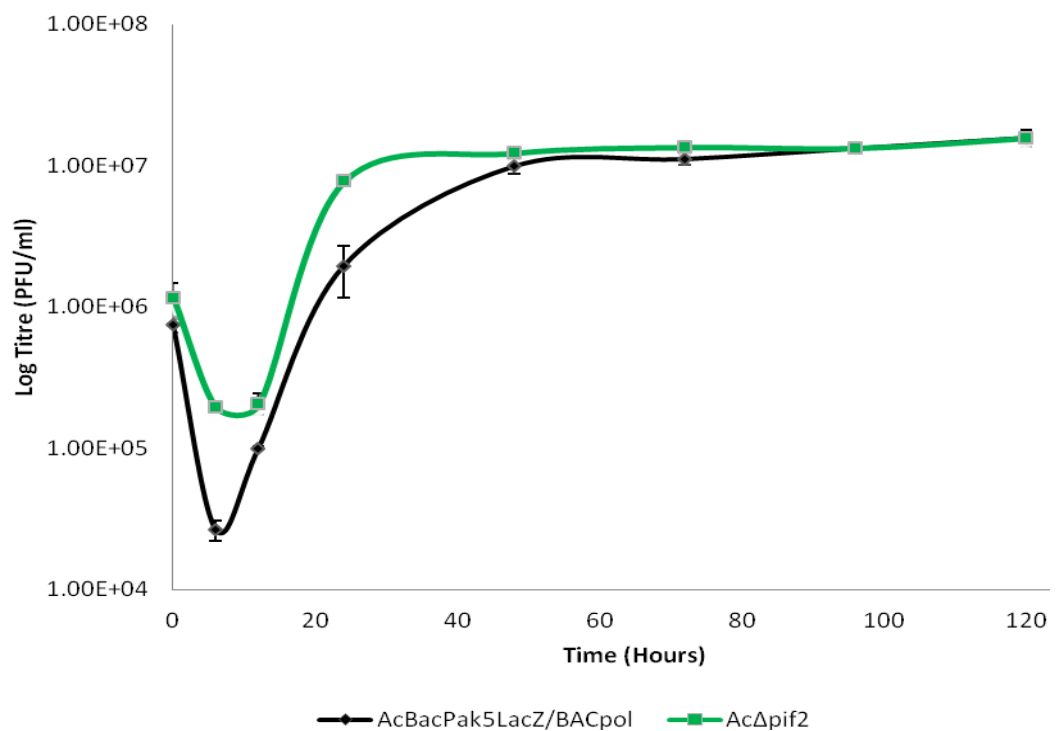


Figure 6.3 Kinetics of budded virus production by AcΔpif2

Budded virus production by AcBacPak5LacZ/Bac^{pol} and AcΔpif2, The Sf9 cells were infected as described in Figure 6.2. Standard error bars are shown. N = 3.

6.3.3 β -galactosidase production

The production of β -galactosidase was also measured during the virus-infected cell time course (see method section 2.7.3a). Both the virus-infected cell culture medium and cell pellets were assayed (Figure 6.4). In the β -galactosidase assay on virus-infected cell pellets, there was no detectable enzyme activity until 24hpi for either virus. The AcBacPAK5/*lacZ*/BAC^{pol}-infected cell pellet β -galactosidase activity increased sharply after 24hpi reaching a peak of 10.62 u/10⁶ cells at 48hpi. Thereafter, enzyme activity levels in virus-infected cells decreased to 1.68 u/10⁶ cells at 120hpi. The activity of β -galactosidase in Ac Δ *pif2*-infected cell pellets also increased rapidly between 24hpi and 48hpi reaching 4.78 u/10⁶ cells at the latter time point. However, the peak activity of β -galactosidase was reached at 72 hpi with 5.14 u/10⁶ cells before decreasing to 0.54 u/10⁶ cells at 120 hpi. Despite these temporal differences, Anova statistical analysis demonstrated that there was no significant difference between AcBacPAK5/*lacZ*/BAC^{pol}- and Ac Δ *pif2* cell pellets β -galactosidase activities ($P > 0.05$). However, the two-tailed student t-test did show a significant difference ($P < 0.05$) between the β -galactosidase activity of AcBacPAK5/*lacZ*/BAC^{pol}- and Ac Δ *pif2*-infected cell pellets at 48hpi.

The levels of β -galactosidase activity in culture medium from virus-infected cells remained below those introduced by the virus inocula (less than 0.52 u/10⁶ cells) until 48hpi. The levels of β -galactosidase in AcBacPAK5/*lacZ*/BAC^{pol}-infected cells increased sharply from 24hpi until 72hpi reaching 1.70 u/10⁶ cells. After this time point, the β -galactosidase activity in the medium continued to increase but at a lower rate, reaching a final activity of 2.14 u/10⁶ cells at 120hpi. In Ac Δ *pif2*-infected cells, β -galactosidase activity increased sharply from 24hpi to 48hpi reaching 1.58 u/10⁶ cells, before dropping to 0.92 u/10⁶ cells at 72hpi and remaining at a similar level until 120hpi. Anova statistical analysis demonstrated that there was no significant difference between the β -galactosidase activity in media from AcBacPAK5/*lacZ*/BAC^{pol}- and Ac Δ *pif2*-infected cell cultures ($P > 0.05$). However, a two-tailed student t-test did show a significant difference ($P < 0.05$) between the β -galactosidase activity in media from AcBacPAK5/*lacZ*/BAC^{pol}- and Ac Δ *pif2*-infected cell cultures between 48hpi and 120hpi.

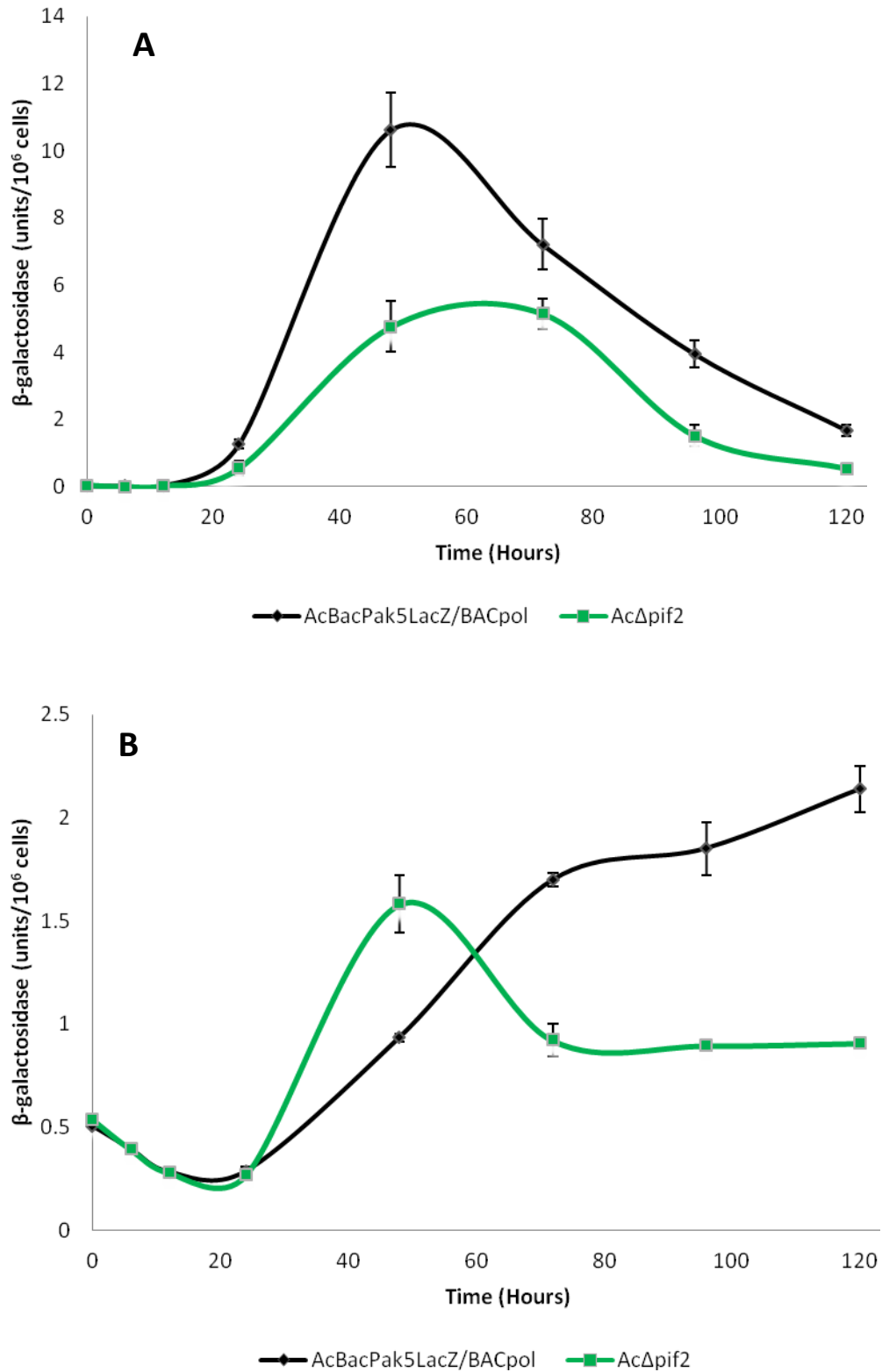


Figure 6.4 β-galactosidase activities in virus-infected cell cultures

β-galactosidase activity in Sf9 cells infected with AcBacPak5LacZ/Bac^{pol} or AcΔpif2 (MOI = 5 pfu/cell). Cell pellets (A) and virus-infected cell culture media (B). Standard error bars are shown for the 120 hour time course. N = 3.

6.4 Construction of recombinant viruses for urokinase synthesis

The *AcΔpif2* described in the previous section had demonstrated a significant increase in the release of β -galactosidase from virus-infected cells at 48hpi compared to *AcBacPAK5/lacZ/BAC^{pol}*. To investigate this observation further, both *AcΔpif2* and *AcBacPAK5/lacZ/BAC^{pol}* viruses were modified to express the secreted protein urokinase, in place of β -galactosidase. Urokinase was chosen due to the availability of an easy to use activity assay kit (Millipore) and a baculovirus transfer vector, which already contained urokinase under the *polh* promoter.

This modification was carried out by cotransfection of Sf9 cells with a baculovirus transfer vector containing urokinase (pBacPAK8-urokinase; R. B. Hitchman, personal communication) and either *AcΔpif2* or *AcBacPAK5/lacZ/BAC^{pol}* DNA, which had been linearized by restriction enzyme digestion with *Bsu361*. Both of these virus genomes contain a single *Bsu361* site within *lacZ* at the *polh* locus. Recombination between these viruses and pBacPAK8-urokinase should remove *lacZ/BAC* at the *polh* locus and replace it with urokinase. The resulting recombinant viruses were plaque-purified three times, to generate genetically homogeneous *lacZ*-negative plaques (plaques that did not turn blue when stained with X-gal; data not shown). Each of the plaque-purified viruses amplified to titres of $\sim 9 \times 10^7$ pfu/ml and virus-infected cells did not turn blue in the presence of X-gal (data not shown) suggesting an absence of parental virus. The viruses were designated *AcBacPAK5urokinase^{pol}* and *AcBacPAK5urokinase^{pol}Δpif2* (*AcUKΔpif2*).

To determine if *AcBacPAK5urokinase^{pol}* and *AcUKΔpif2* were producing urokinase, Sf9 cells were infected with either of these viruses or with a positive control virus known to express urokinase (*flashBAC-UK*; R. B. Hitchman, personal communication) at an MOI of 5 pfu/cell and cell pellets and culture medium were harvested at 48hpi. The protein content for each of the cell lysates was determined using Quabrit (Quigen). Samples (15 μ g) were fractionated by SDS PAGE and either stained with Coomassie blue or blotted onto a nitrocellulose membrane (See method section 2.7.1). Western blot analysis was then performed by using antibody to urokinase (See method section 2.7.2; Figure 6.5). This showed that both *AcBacPAK5urokinase^{pol}* and *AcUKΔpif2*-infected Sf9 cells were expressing urokinase from the *polyhedrin* promoter, demonstrated by the accumulation of urokinase at 48hpi. Therefore, confirming that the *urokinase* had successfully been inserted into these two viruses. The next stage was to examine the expression profile of urokinase by these two viruses along with the production of BV throughout the replication cycle of infected Sf9 cells.

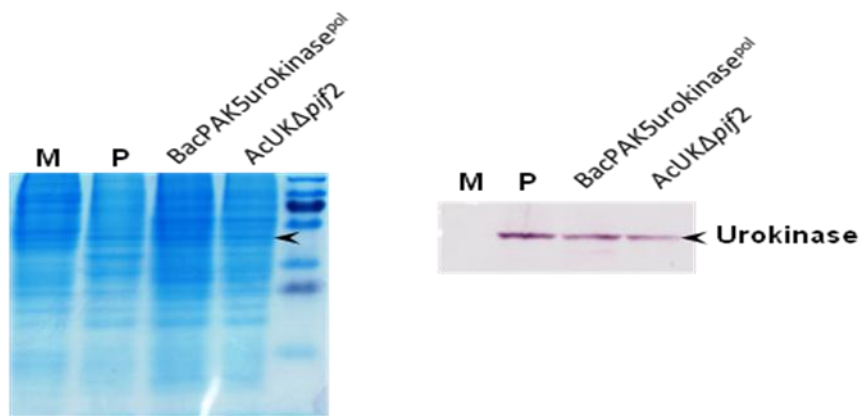


Figure 6.5 Coomassie blue and western blot analyses of AcBacPAK5urokinase^{pol} and AcUKΔpif2-infected Sf9 cells

Cell lysates from Sf9 cells infected with either *flashBAC-UK* (P), AcBacPAK5urokinase^{pol} or AcUKΔpif2 were collected at 48 hpi and 15 μg of protein from each lysate was fractionated using 12% SDS-PAGE before staining with Coomassie blue or transfer to filters for probing with antibody to urokinase. M indicates mock-infected cells. Arrow indicates the predicted band for urokinase in both images.

6.5 Temporal analysis of virus replication in AcBacPAK5urokinase^{pol} and AcUKΔ*pif2* infected Sf9 cells.

Triplicate Sf9 cultures were infected with either AcBacPAK5urokinase^{pol} or AcUKΔ*pif2* at a moi 5 and cell viability, BV production and urokinase synthesis were analysed over 120 hours to determine any effects of the *pif2* deletion on these processes

6.5.1 Cell viability

Cell viability analysis showed that mock-infected cells remained >94% viable until the end of the experiment at 120hpi. The viability of the virus-infected cells differed from mock-infected cells after 24hpi (Figure 6.6). After this point there was a continuous decrease in cell viability that followed the same trend for both viruses. However, AcBacPAK5urokinase^{pol} infected cells were approximately 5% less viable (48%, 15% and 6%, respectively) than AcUKΔ*pif2* infected cells at each time point after 24hpi (Figure 6.6). However, these slight differences between BacPAK5urokinase^{pol} and AcUKΔ*pif2* infected cells were shown not to be significantly different ($P>0.05$) when Anova statistical analysis was performed on the data.

6.5.2 Budded virus production

The AcBacPAK5urokinase^{pol} and AcUKΔ*pif2* titres for each time point were obtained using the plaque assay method (See methods section 2.3.4a; Figure 6.7). Neither virus showed an increase in BV until after 12hpi. The AcBacPAK5urokinase^{pol} titre increased sharply between 12hpi and 24hpi from 3.5×10^5 to 1.77×10^8 pfu/ml and reached a final titre of 3.43×10^8 pfu/ml at 120hpi. The AcUKΔ*pif2* BV production kinetics were similar to that of AcBacPAK5urokinase^{pol} with a rapid increase between 12hpi and 24hpi from 3.07×10^4 to 1.8×10^8 pfu/ml and reaching a final titre of 2.67×10^8 pfu/ml at 120hpi. The BV production kinetics of AcUKΔ*pif2* slightly differed from that of AcBacPAK5urokinase^{pol}. However, Anova statistical analysis demonstrated that there was no significant difference between AcBacPAK5urokinase^{pol} and AcΔ*pif2* BV production kinetics ($P>0.05$).

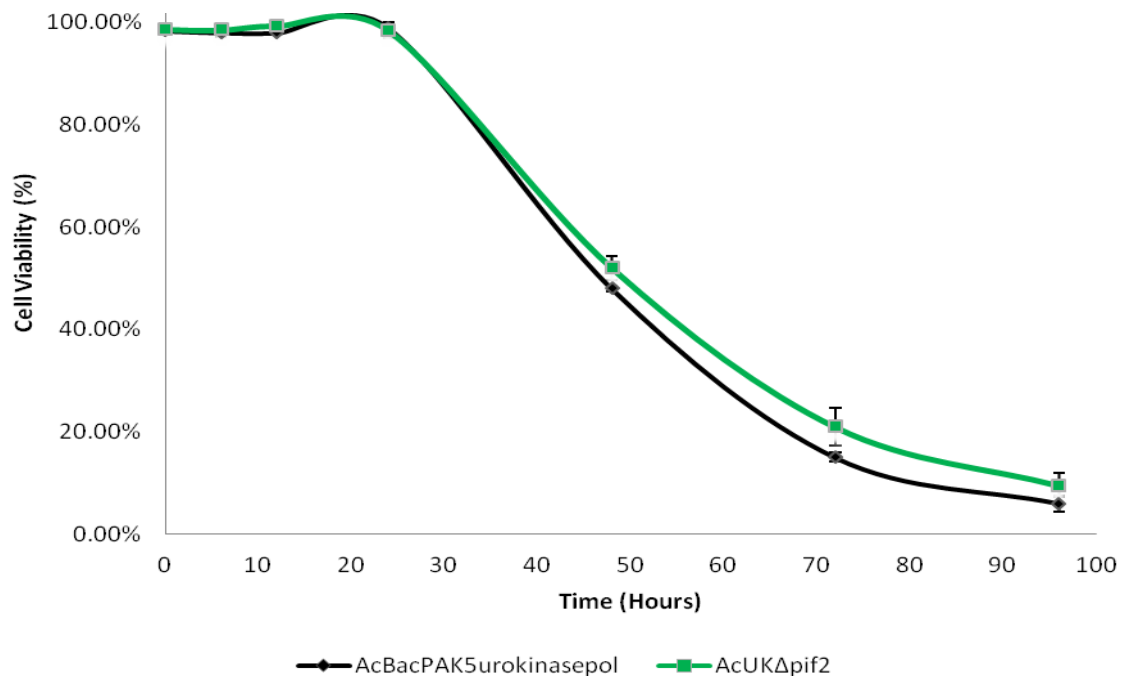


Figure 6.6 Cell viability of AcBacPAK5urokinase^{pol} and AcUKΔpif2-infected Sf9 cells.

Cultures of Sf9 cells were infected with AcBacPAK5urokinase^{pol} and AcUKΔpif2 (MOI = 5 pfu/cell) and cell viability was assessed at the indicated time points. The experiment was terminated before the final time point at 120hpi owing to the very low cell viability. Standard error bars are shown. N = 3.

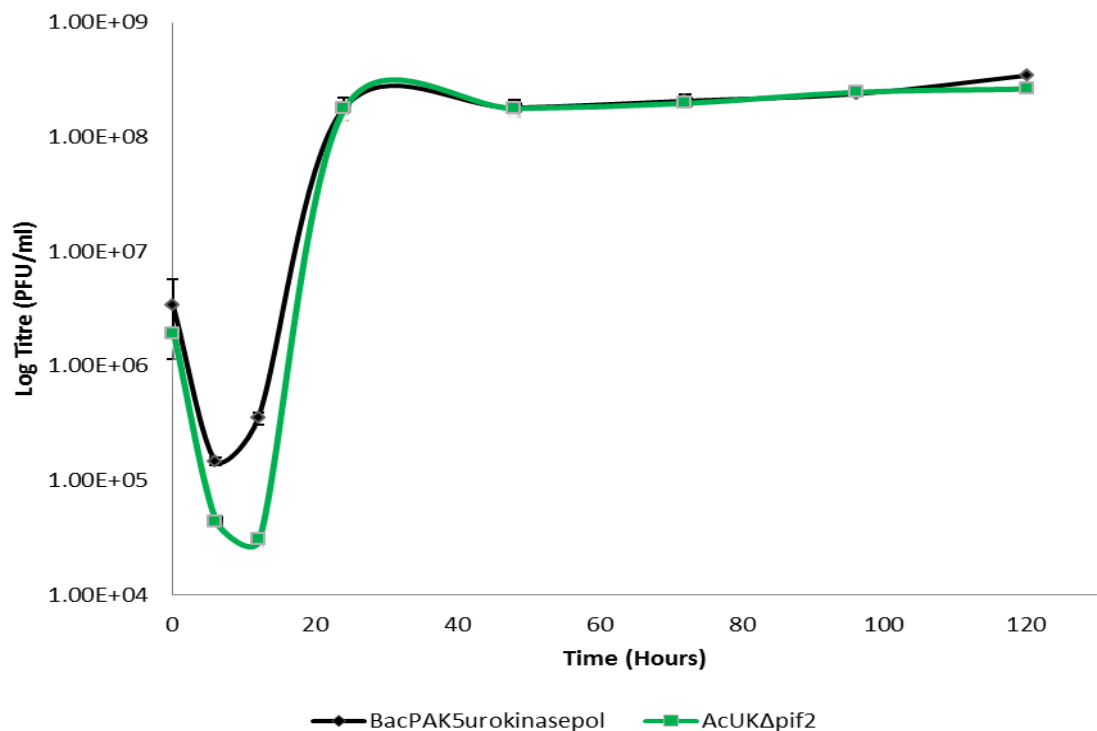


Figure 6.7 Kinetics of budded virus production by AcBacPAK5urokinase^{pol} and AcUKΔpif2

Budded virus production by AcBacPAK5urokinase^{pol} and AcUKΔpif2, The Sf9 cells were infected as described in Figure 6.6. Standard error bars are shown during 120 hour time course. N = 3.

6.5.3 Urokinase production

The production of urokinase was measured during this time course study using a standard urokinase assay method (See method section 2.7.3b; Millipore). Measurements were taken from both the virus-infected cell culture medium and cell pellets (Figure 6.8).

The activity of urokinase in AcBacPAK5urokinase^{pol} infected cell pellets increased rapidly from 0hpi and reached a peak concentration of 139 units/ml at 48hpi (Figure 6.8 A). After this point the activity of urokinase declined to 66 units/ml at 120hpi. In AcUKΔ*pif2* infected cell pellets, urokinase activity followed the same trend as AcBacPAK5urokinase^{pol}. However, the peak urokinase activity at 48hpi was only 85 units/ml and 46 units/ml at 120 hpi. Despite these temporal differences, Anova statistical analysis demonstrated that there was no significant difference between AcBacPAK5urokinase^{pol} and AcUKΔ*pif2* cell pellets urokinase activities ($P>0.05$). However, a two-tailed student t-test performed on individual time points did show a significant difference ($P<0.05$) between 48 hpi to 120 hpi.

The urokinase activities in the cell culture medium samples from both AcBacPAK5urokinase^{pol} and AcUKΔ*pif2*-infected Sf9 cultures were about 25-fold higher than in the corresponding cell pellets described above (Figure 6.8 B). The peak urokinase activity was approximately 3480 units/ml at 48 hpi for both viruses. This decreased to 2982 units/ml for AcBacPAK5urokinase^{pol} and to 2671 units/ml for AcUKΔ*pif2* at 120 hpi. Anova statistical analysis demonstrated that there was no significant difference between the urokinase activity in media from AcBacPAK5urokinase^{pol} and AcUKΔ*pif2*-infected Sf9 cultures ($P>0.05$). However, the two-tailed student t-test showed a significant difference ($P<0.05$) between the urokinase activity in AcBacPAK5urokinase^{pol} and AcUKΔ*pif2* infected cell culture medium samples at 72 hpi and the two subsequent time points.

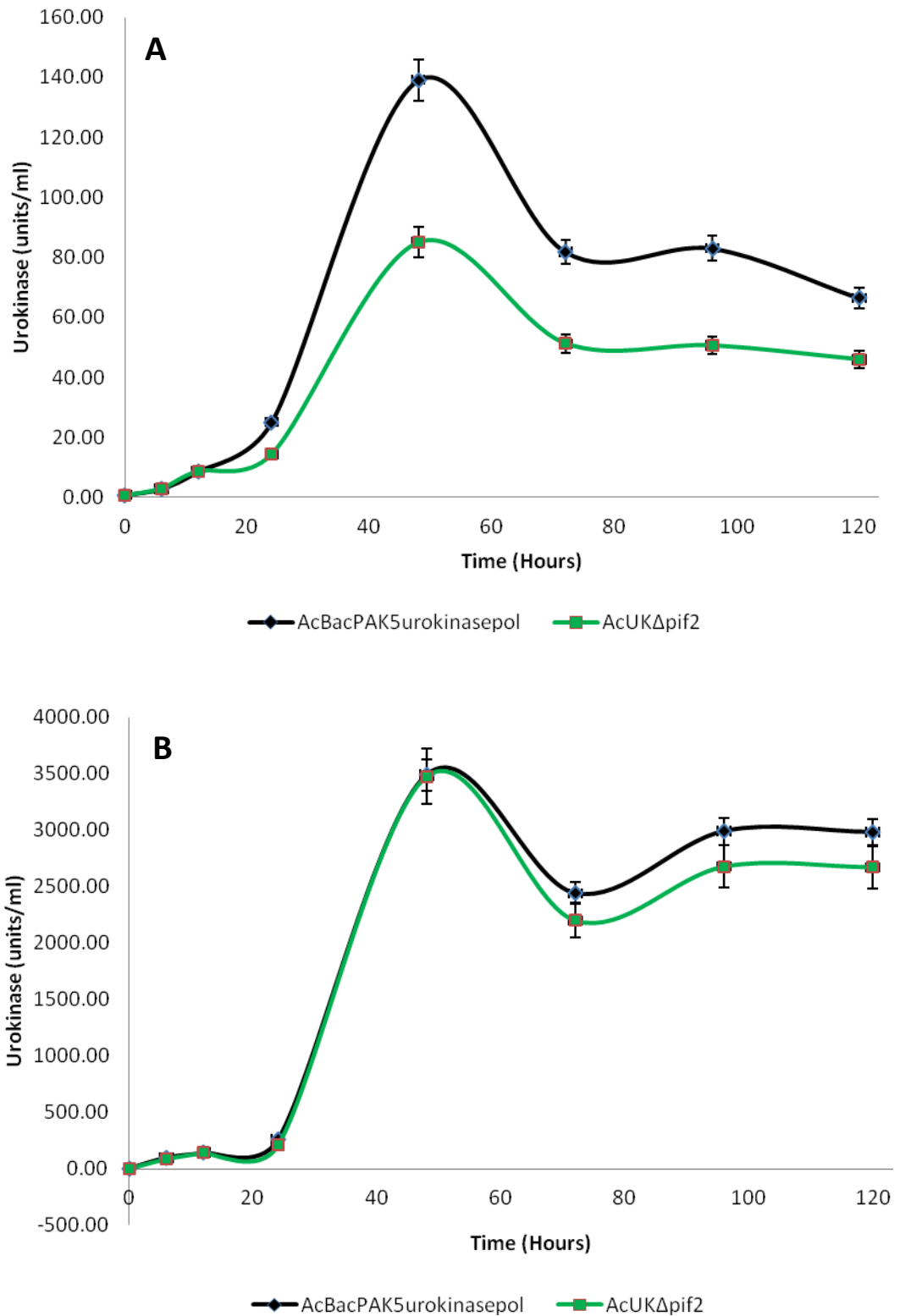


Figure 6.8 Graphical presentation of Urokinase expression against time for AcUKΔpif2 Time Course.

Urokinase activity in Sf9 cells infected with AcBacPAK5urokinase^{pol} or AcUKΔpif2 (MOI = 5 pfu/cell). Cell pellets (A) and virus-infected cell culture media (B). Standard error bars are shown for the 120 hour time course. N = 3.

6.6 *AcΔpif3*

The results described in Chapter 4 (section 4.5) demonstrated that *AcΔpif3* was infectious when Sf9 cells were transfected with $\Delta pif3$ DNA. Firstly, the cells showed signs of a virus-induced cytopathic effect. Secondly, virus DNA could be purified from the medium supporting the growth of Sf9 cells transfected with the $\Delta pif3$ bacmid, which suggested that BV had been produced. However, subsequent amplification of the *AcΔpif3* BV showed that this virus was unable to produce high titre stocks. Typically, *AcΔpif3* attained titres of only 5×10^6 pfu/ml, whereas other viruses had infectious titres at least 10-fold higher. The low titres of *AcΔpif3* rendered it unsuitable for determining the effect of this gene deletion in recombinant protein production. Therefore, the next sections of this chapter describe experiments to resolve whether or not the reduction in BV production was due to the deletion of *pif3* or a bystander effect on a neighbouring gene.

6.6.1 Rescue of *pif3*

In this study, the region of the AcMNPV genome deleted to remove *pif3* (ORF115) encompassed nucleotides 99132 – 99796, leaving ORFs 114 and 116 intact. However, when the strategy used by Ohkawa *et al.* (2005) to delete *pif3* was compared with the one described in Chapter 4, it was noted that the deletion made to the 3' end of *pif3* extended to within 40 bp of a potential early promoter (CGTGC) for ORF114. The deletion made by Ohkawa *et al.* (2005) extended to within 64 bp of this sequence. The region deleted at the other end of *pif3* was very similar in both studies.

Therefore, to investigate if this 24 bp difference was responsible for the defect in *AcΔpif3* BV production, an intact *orf114* was restored to the polyhedrin locus of *AcΔpif3*. In an additional experiment, *orf116* was also inserted at the polyhedrin locus in *AcΔpif3* to ensure that it too hadn't been affected by the *pif3* deletion. Finally, the *pif3* was also restored and rescued at the polyhedrin locus of *AcΔpif3*; to determine if the loss of *pif3* was the cause of the abnormal BV production.

The *orf114*, *pif3* and *orf116* coding regions and their predicted promoters were amplified using specific primers with AcMNPV DNA as a template and a proof reading polymerase (Expand, Roche). The amplified gene fragments were then inserted into a Topo vector and sequenced. The gene fragments were removed from the vector and ligated into a modified pBAC1 (pBAC1 Δ PP) to allow insertion of each gene at the *polh* locus. The modification of pBAC1 involved the removal of the *polh* promoter to allow the selected genes to be expressed by only their own promoters. The modified region of pBAC1 Δ PP

was sequenced. Figure 6.9 describes the cloning strategy used with protocols described in methods (section 2.6). All constructs were confirmed by RE mapping (data not shown).

Insect Sf9 cells were cotransfected with one of pBAC1 Δ PP-*orf114*, pBAC1 Δ PP-*pif3* or pBAC1 Δ PP-*orf116* and Δ *pif3* bacmid DNA purified from *E. coli* and linearised by restriction enzyme digestion with *AvrII*. The Δ *pif3* contains a single *AvrII* site located within the essential gene *orf1629*. These cotransfections rescued the target gene at the *polh* locus. For the rescue to occur at the *pif3* locus, the deletion mutant bacmid DNA purified from *E. coli* was linearised by restriction enzyme digestion with *SrfI* and cotransfected with the Topo vector containing *pif3*. The deletion mutant bacmids all contain two *SrfI* sites flanking the kanamycin insert.

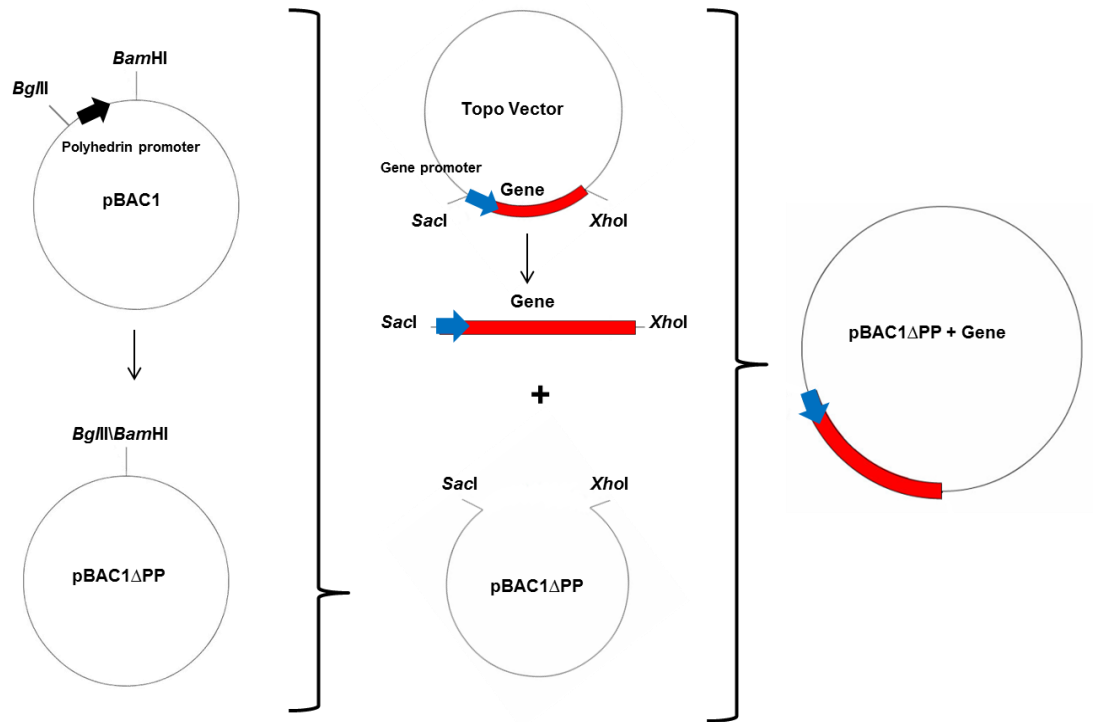
The cell culture medium from each cotransfection was titrated using a plaque assay to determine if viable recombinant virus was produced. The results demonstrated that *Ac* Δ *pif3* was only rescued by insertion of *pif3* at its own or the *polh* locus. The cotransfections between *Ac* Δ *pif3* and pBAC1 Δ PP-*orf114* or pBAC1 Δ PP-*orf116* failed to rescue the parental virus. Interestingly, the cell culture medium from Sf9 cells transfected with linearised Δ *pif3* bacmid DNA failed to produce plaques in the subsequent assay, suggesting that the residual circular DNA was unable to initiate an infection. Further attempts to rescue *orf114* or *orf116* at the polyhedrin locus of the Δ *pif3* yielded the same results. Only the rescue of *pif3* function could restore infectivity to linearised Δ *pif3* bacmid DNA. Therefore it was decided to continue further analyses with the two viruses rescued with *pif3* at the polyhedrin locus (*Ac* Δ *pif3*-R*pif3*^{pol}) or its native locus (*Ac*-*pif3*).

Figure 6.9 Insertion of baculovirus genes into pBAC1

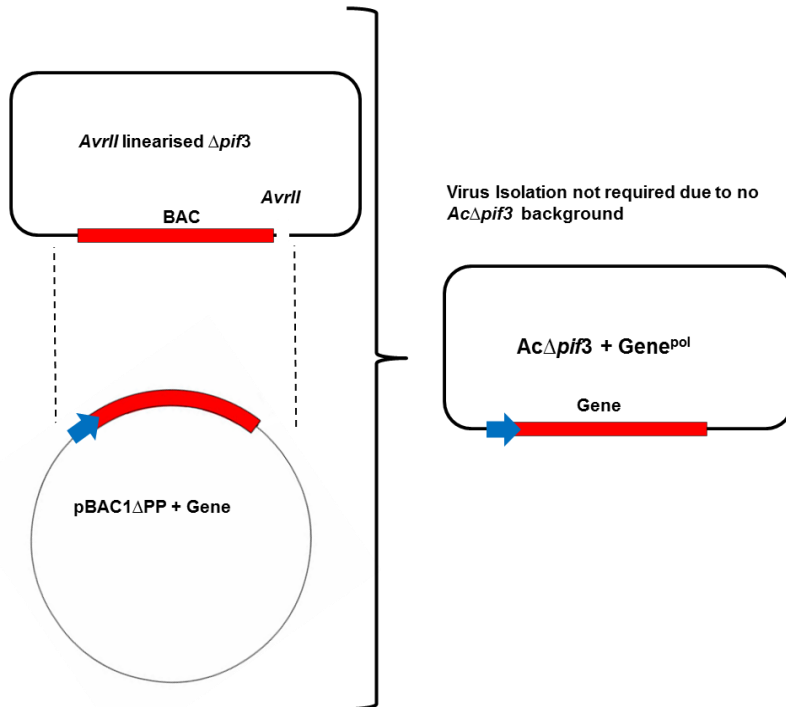
(A) The baculovirus transfer vectors were constructed using standard classical cloning techniques. The target genes were amplified by PCR using Expand DNA polymerase and inserted into the Invitrogen Topo vector, where their sequences were confirmed. The target genes were subcloned from the Topo vector into the *SacI* and *XhoI* sites of the modified pBAC1 (pBAC1 Δ PP). These baculovirus transfer vectors permitted insertion of the target gene under the control of its own promoter into the baculovirus genome at the *polh* locus via homologous recombination in insect cells.

(B) Sf9 Cells co-transfected with pBAC1 Δ PP+Gene and *AvrII* linearised Δ *pif3* bacmid DNA, to form Ac Δ *pif3*+Gene^{Pol} bacmid DNA.

A



B



6.6.2 Infectivity of *Ac*Δ*pif3* and rescued viruses *Ac*Δ*pif3-Rpif3*^{pol} and *Ac-pif3*^f

The next step was to investigate whether or not these *pif3*-rescued viruses could reach normal levels of BV infectivity when amplified in Sf9 cells. Briefly, 500μl of medium from each transfection that produced *Ac*Δ*pif3-Rpif3*^{pol} and *Ac-pif3*^f were added to 50ml of Sf9 shake cell cultures (2×10^6 cells/ml) and incubated at 28°C for 5 days to produce p1 stocks. The infectivity of each stock was determined by plaque assay. These data allowed P2 stocks in Sf9 cells to be produced by using an moi of 0.1 pfu/cell. This process was repeated to produce p3 virus stocks. The results of the plaque assay titrations for each virus stock are summarized in Table 6.1. Similar results were obtained with replicate viruses for each genotype. These results clearly show that *Ac*Δ*pif3* is unable to achieve titres as high as those for either *Ac*BACΔ*chitinase* or *Ac*Δ*pif3-Rpif3*^{pol} and *Ac-pif3*^f. Both *pif3* rescue viruses achieved similar titres to *Ac*BACΔ*chitinase* at all passages examined, which suggests the cause of the low titres observed in *Ac*Δ*pif3* is due to the deletion of *pif3* and not another mutation that could have occurred in the virus during the deletion process with the Red/ET recombination system.

Table 6.1 Budded virus titres for *Ac*Δ*pif3*, *Ac-pif3* and *Ac*Δ*pif3-Rpif3*^{pol} stocks

Virus	Titre (pfu/ml)		
	P1 stock	P2 stock	P3 stock
<i>Ac</i> BACΔ <i>chitinase</i>	1.4×10^8	3.2×10^8	2.6×10^8
<i>Ac</i> BACΔ <i>chitinase</i>	1.2×10^8	2.8×10^8	2.3×10^8
<i>Ac</i> Δ <i>pif3</i>	1.7×10^6	1.9×10^6	1.4×10^6
<i>Ac</i> Δ <i>pif3</i>	1.0×10^7	2.6×10^6	1.7×10^6
<i>Ac-pif3</i> ^f	1.6×10^8	5.9×10^8	2.4×10^8
<i>Ac-pif3</i> ^f	2.2×10^8	3.5×10^8	2.9×10^8
<i>Ac</i> Δ <i>pif3-Rpif3</i> ^{pol}	1.1×10^8	3.4×10^8	3.1×10^8
<i>Ac</i> Δ <i>pif3-Rpif3</i> ^{pol}	1.2×10^8	3.0×10^8	2.8×10^8

To confirm the identities of the *Ac*Δ*pif3*, *Ac-pif3*^f and *Ac*Δ*pif3-Rpif3*^{pol} P3 stocks, DNA was purified from virus-infected cells at 48hpi and the *pif3* locus in each virus amplified using specific primers external and internal to the target locus (Figure 6.10).

The external primers were specific to a region 96 bp upstream and 123 bp downstream of the *pif3* locus. The insertion of the kanamycin resistance cassette *in lieu* of *pif3* was predicted to result in the amplification of a 1210 bp fragment with this primer set. If the original gene was still present, a fragment of 833 bp was predicted. For *Ac*BACΔ*chitinase* (Figure 6.10, lane 3) and *Ac**pif3*^f (Figure 6.10, lanes 8 and 9), a fragment of approximately

800 bp was produced in the PCR. For *AcΔpif3* and *AcΔpif3-Rpif3^{pol}* (Fig. 6.10, lanes 4-5 and 6-7, respectively) a fragment of approximately 1200 bp was amplified. The primers internal to *pif3* amplified a 295 bp DNA fragment in *AcBACΔchitinase*, *AcΔpif3-Rpif3^{pol}* and *Ac-pif3^f* (Figure 6.10, lanes 3, 6-7 and 8-9, respectively). A *pif3*-specific DNA fragment was not amplified in *AcΔpif3* (Figure 6.10, lanes 4-5). These results confirmed the identities of *AcΔpif3*, *Ac-pif3* and *AcΔpif3-Rpif3^{pol}*.

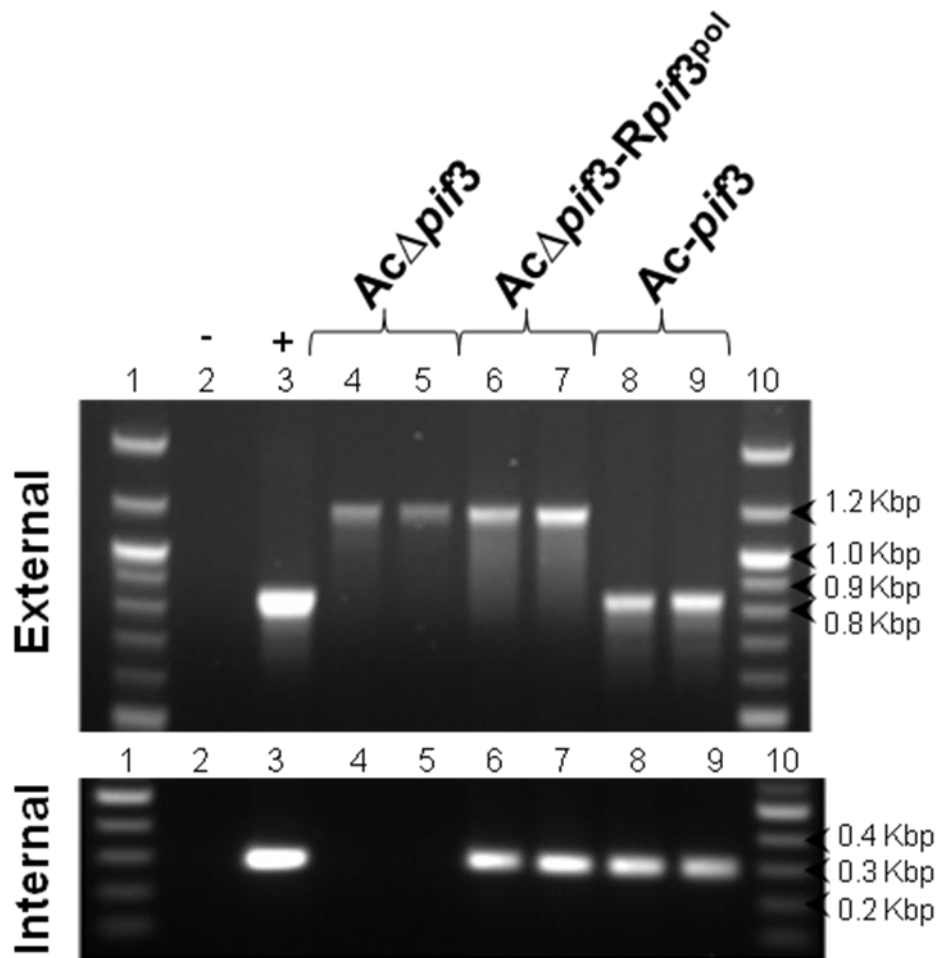


Figure 6.10 PCR analyses of *AcΔpif3*, *Ac-pif3^f* and *AcΔpif3-Rpif3^{pol}* DNA

Template DNA for *AcΔpif3* (lanes 4-5), *AcΔpif3-Rpif3^{pol}* (lanes 6-7) and *Ac-pif3^f* (lanes 8-9) was isolated from virus-infected cells and analysed by PCR using primers external (ACC15/16; upper panel) and internal (ACC39/40; lower panel) to *pif3*. Lanes 1 and 10, NEB log2 Markers; lane 2, negative control; lane 3, *AcBACΔchitinase*.

6.6.3 Construction of 6xHis-tagged *pif3* virus (Ac-his*pif3*)

To investigate further the role of PIF3 in viral replication, a rescue of $\Delta pif3$ bacmid DNA with 3' polyhistidine-tagged (6xHis-tag) *pif3* was performed to allow localisation of the protein during viral infection to be observed using confocal microscopy. This was necessary because an antibody to PIF3 was not available.

The virus deletion mutant Ac $\Delta pif3$ was modified by inserting a 6xHis-tagged *pif3* at the native locus to generate Ac-his*pif3*. The his peptide was added to the C-terminus of PIF3 as the N-terminus contains a transmembrane domain, which might have prevented detection of the his-tag in later experiments.

A DNA fragment encoding *pif3* with his tag sequences at the 3' end of the gene was generated in two rounds of PCR (Figure 6.11). The first round used specific primers (his*pif3*-1F and his*pif3*-1R) and AcMNPV template DNA to add the sequence encoding the C-terminus 6xHis-tag to *pif3*. In the second round of PCR, the primers added 40 bp of sequence homologous to regions flanking *pif3*. This DNA fragment containing the modified *pif3* was inserted into a Topo vector prior to sequencing to confirm the fidelity of the construction (pTOPO-his*pif3*) (Figure 6.11).

Insect Sf9 cells were cotransfected with pTOPO-his*pif3* and $\Delta pif3$ bacmid DNA from *E. coli* that had been linearised by restriction enzyme digestion with *SrfI*. The Ac $\Delta pif3$ contains two *SrfI* sites flanking the kanamycin insert at the *pif3* locus. Recombination between the homologous sequences in pTOPO-his*pif3* and the native locus for the gene target in Ac $\Delta pif3$ resulted in insertion of the modified version of *pif3*. The virus produced, Ac-his*pif3*, was plaque purified for three rounds to ensure the removal of parental Ac $\Delta pif3$ and amplified to a high titre working stock (2.3×10^8 pfu/ml) in Sf9 cells, suggesting the 6xHis-tag of *pif3* had not affected the replication of the virus.

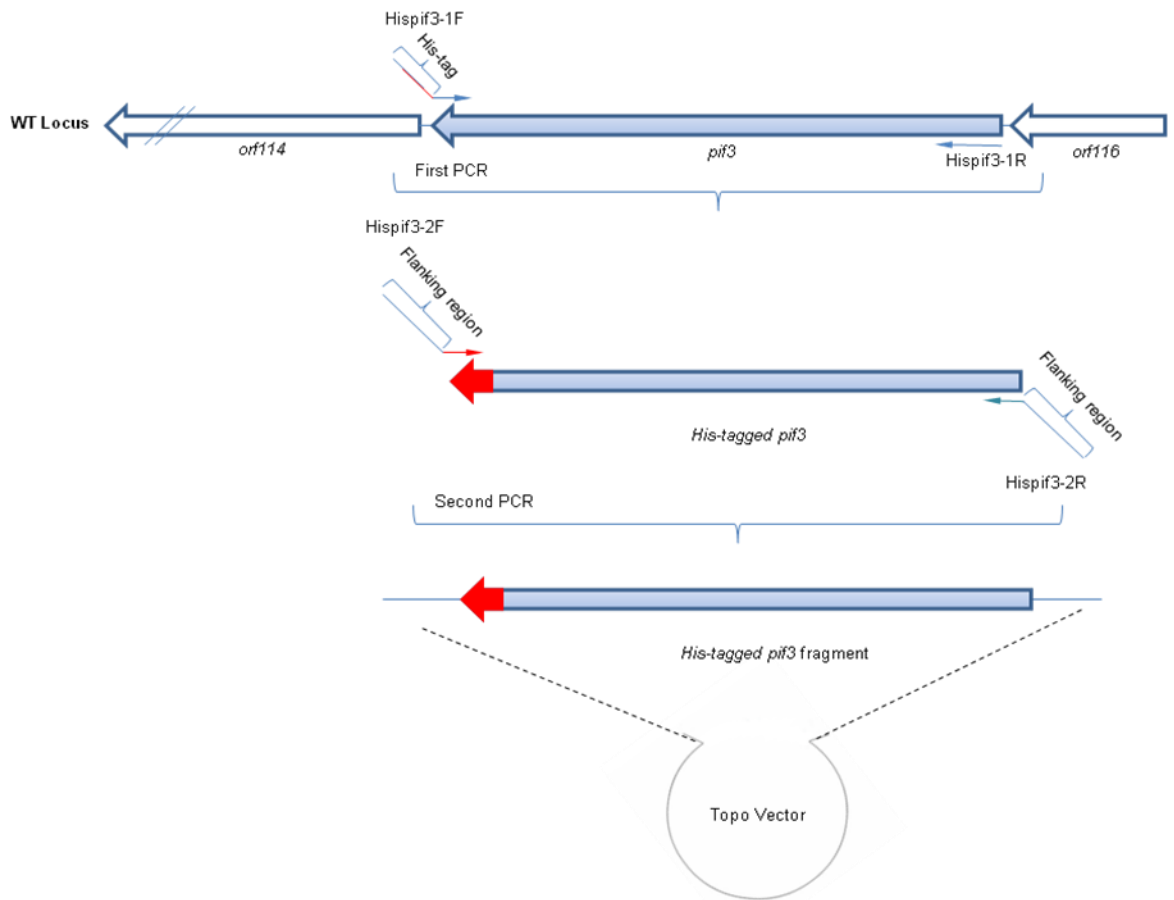


Figure 6.11. Schematic showing the construction of 6xHis-tagged *pif3* fragment and insertion into Topo vector.

The *pif3* was amplified twice by PCR using Expand DNA polymerase; in the first PCR 6xHis-tag coding sequence was added to the gene using primers Hispif3-1F and Hispif3-1R. In the second PCR homologous arms were added using primers Hispif3-2F and Hispif3-2R. The 6xHis-tagged *pif3* fragment was inserted into the Invitrogen Topo vector to derive pTOPO-his*pif3* prior to sequencing and cotransfection with *AcΔpif3* to derive *Ac-hispif3*.

6.6.4 Immunoblotting analysis of *Ac-hispif3* PIF3 expression

To determine if the C-terminus 6xHis-tag coding region added to PIF3 resulted in the production of the anticipated protein, *Ac-hispif3* was used to infect Sf9 cells prior to analysis of the virus-induced polypeptides using immunoblotting. Successful his-tagging of PIF3 would then allow the temporal expression of *pif3* to be examined in more detail.

Nine 35mm dishes, each containing 2×10^6 Sf9 cells were infected with *Ac-hispif3* at an MOI of 5. Triplicate dishes were harvested at 12, 24 and 48hpi. and the protein content of each cell lysate was determined using Quabrit (Quigen). Fifteen μg of protein were then fractionated by SDS PAGE and blotted onto nitrocellulose membrane. Western blot analysis was then performed by using antibody to the 6xHis-tag (See method section 2.7.2; Figure 6.12).

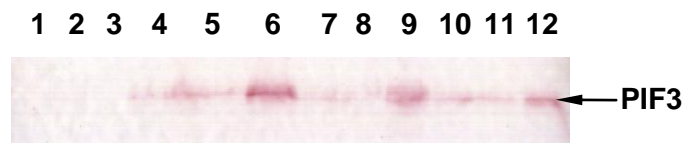


Figure 6.12. Western blot analysis of *Ac-hispif3* infected Sf9 cells

Triplicate Sf9 cell cultures infected with *Ac-hispif3* (MOI, 5 pfu/cell) were harvested at 12 (lanes 4, 7 and 10), 24 (lanes 5, 8 and 11), and 72 (lanes 6, 9 and 12) hpi, lysed and $5\mu\text{g}$ of protein fractionated using a 12% SDS-PAGE. The proteins were transferred to nitrocellulose and probed with antibody to 6xHis-tag. Lanes 1-3 contain mock-infected cells harvested at 12, 24 and 48hpi, respectively. An arrow indicates the predicted band for the C-terminus 6xHis-tagged PIF3.

The western blot analysis of *Ac-hispif3*-infected Sf9 cells using anti-his antibody demonstrated that the 6xHis-tag was exposed and detectable between 12 and 48hpi. The protein band detected migrated with an apparent molecular mass of 28 kDa, which was slightly larger than the predicted 23 kDa for PIF3. This suggested that PIF3 may undergo post-translational modification. The three replicate *Ac-hispif3* infections for each time point demonstrated similar temporal expression of PIF3. His-tagged PIF3 levels at 12 and 24hpi were low but by 48hpi had increased significantly, indicating a possible burst of expression between 24hpi and 48hpi, most likely from the late promoter (TTAAG) indicated in Figure 6.1.

6.6.5 Sub cellular localisation of PIF3 during baculovirus infection

The western blot analysis described in the previous section confirmed that the 6xHis-tag had been successfully fused with PIF3 and was detectable. Therefore, immunofluorescence confocal microscopy with a commercial antibody to the 6xHis-tag was used to investigate the localisation of PIF3 during *Ac-hispi3* infection of TN-368 cells (Method section 2.4.1). The TN-368 cells were chosen due to them being an adherent cell line with a fibroblast-like morphology, which allows them to survive the repeated washing stages of this procedure.

In this experiment PIF3 localisation within virus-infected TN-368 cells was determined between 12 and 48hpi. The TN-368 cells were infected at moi 5 pfu/cell with AcMNPV, *Ac-hispi3* or were mocked-infected with media and fixed at various times post-infection to allow analysis by immunofluorescence staining and confocal microscopy (Figure 6.13). The expression of PIF3 was undetectable at any time point for mock-infected and AcMNPV-infected cells, as expected. PIF3 expression by *Ac-hispi3* was undetectable by immunofluorescence until 18hpi and was localised to the nuclei of cells. At 24hpi, 36hpi and 48hpi PIF3 remained localised to the nucleus but increased in concentration over this period.

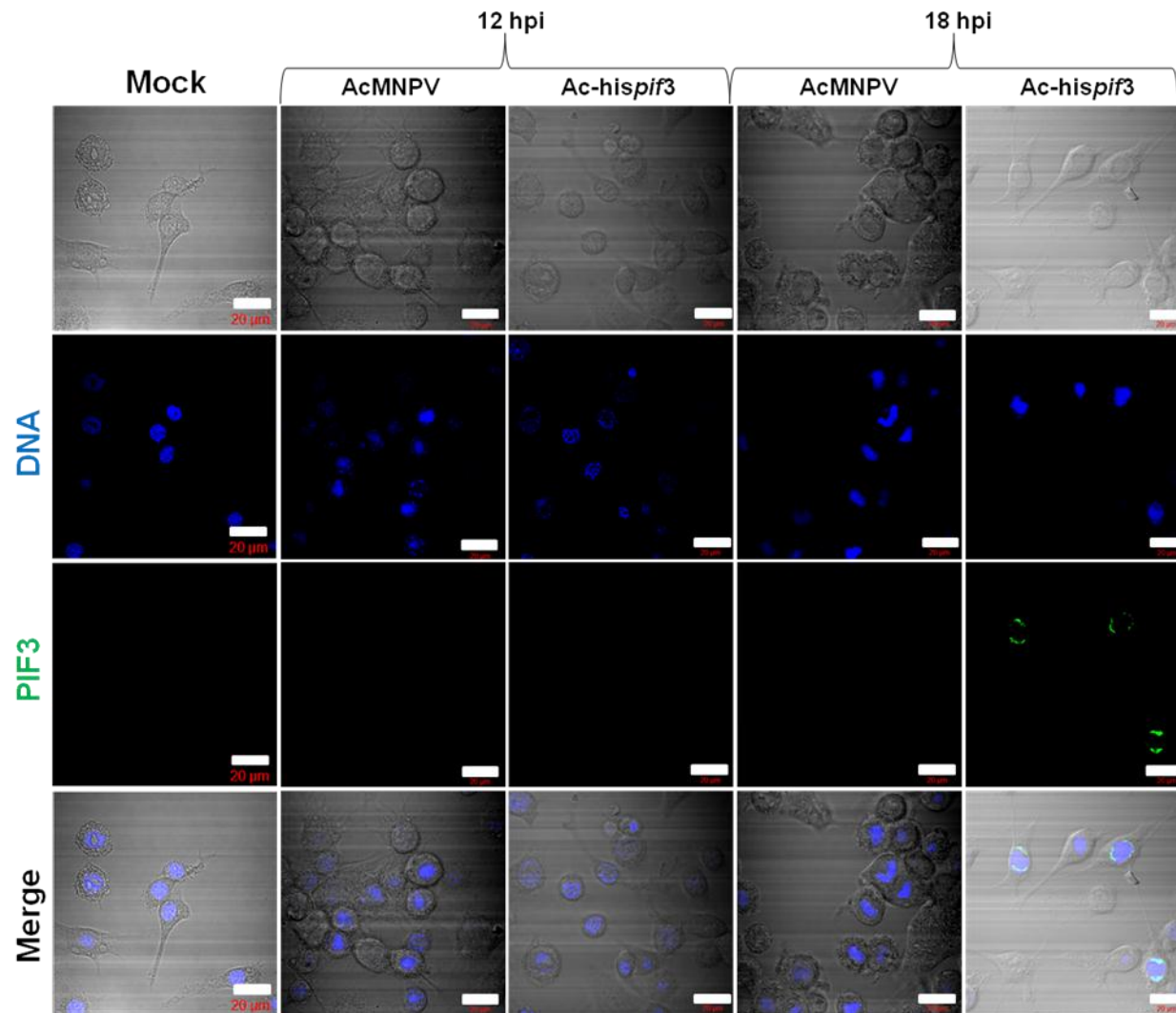
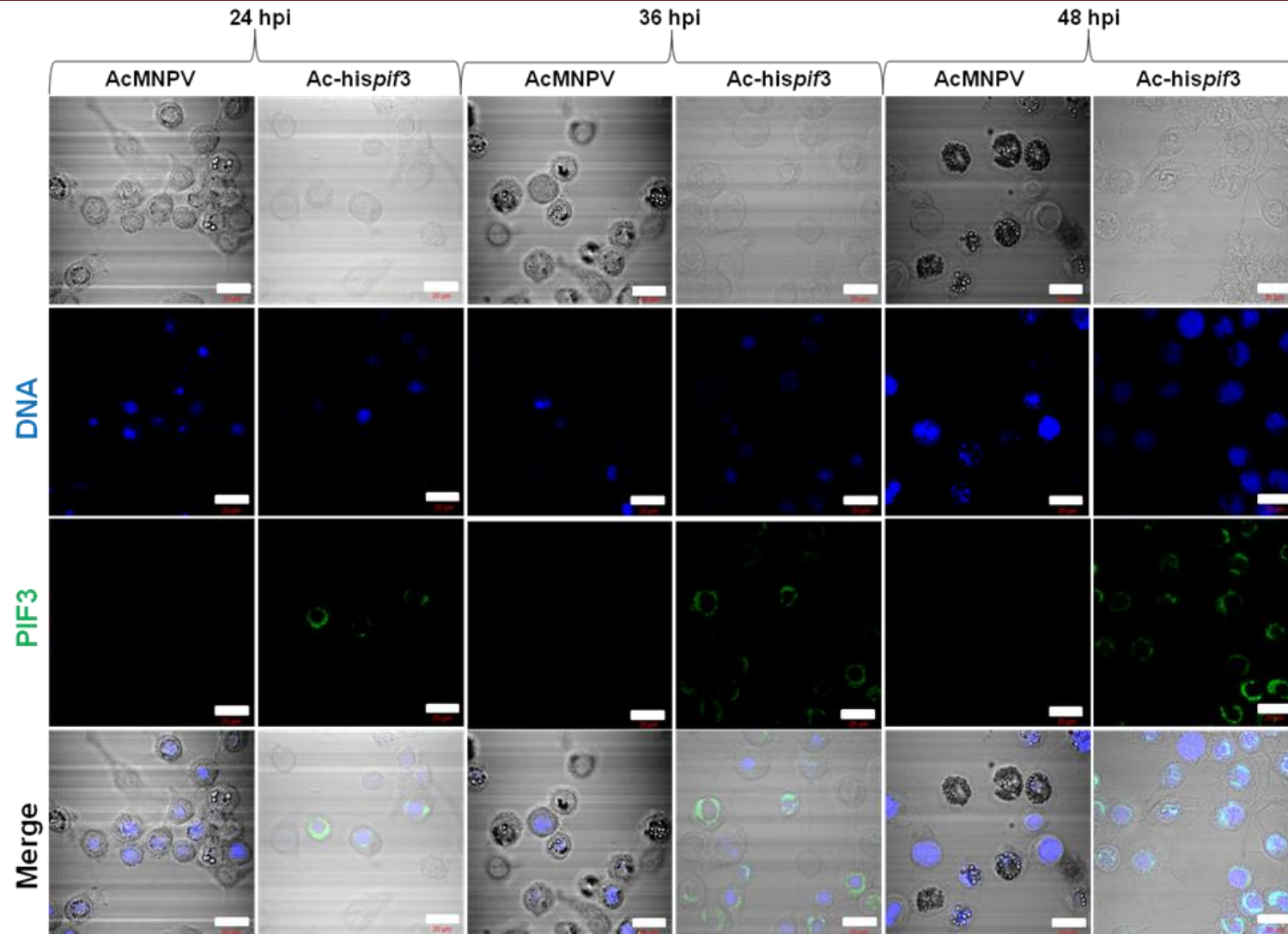


Figure 6.13 Time course of PIF3 localisation in *Ac-hispiF3* infected TN-368 cells

Confocal microscopy optical sections of TN-368 cells infected at an MOI 5 with AcMNPV or *Ac-hispiF3* and fixed at various times post infection. The cells shown are representative of the majority of infected cells. Mock-infected cells were treated with an inoculum lacking virus and fixed at 48hpi. DNA stained with DAPI is shown in blue and 6xHis-tag fused with PIF3 was detected by a commercial 6xHis-tag antibody and visualised by a secondary antibody conjugated to FITC shown in green to visualise PIF3. Differential interference contrast is also shown for each section. Scale bars represent 20 μm.



6.7 Discussion

In this chapter the two viruses modified using the Red/ET recombination system, which contained deletions in *pif* genes (*AcΔpif2* and *AcΔpif3*) were characterised initially with regard to their effect on recombinant protein expression. However, this was only possible for the *pif2* deletion due to an unpredicted reduction in BV production in cells infected with *AcΔpif3*. Therefore, the investigation on *AcΔpif3* focused on attempting to explain this observation, particularly since a previous study had shown no effect on BV formation after deletion of *pif3* (Ohkawa *et al.*, 2005; Song *et al.*, 2012).

6.7.1 Analysis *AcΔpif2*-infected cell viability and BV production

During the two time course experiments conducted cell viability and virus titres were recorded for the *pif2* deletion mutant viruses (*AcΔpif2* or *AcUKΔpif2*) and their parental viruses; *AcBacPAK5/acZ/BAC^{pol}* or *AcBacPAK5urokinase^{pol}*, respectively. Despite any temporal differences during these time course studies, Anova statistical analysis demonstrated that there was no significant difference in cell viability or BV production ($P > 0.05$) between the parental virus and the *pif2* deletion mutant virus. A two-tailed student t-test was also performed on the time course studies data for infected cell viability and BV production to identify any significant differences at individual times points between the parental virus and the *pif2* deletion mutant virus. However, no significant difference ($P > 0.05$) was observed for any individual time point for either time course study. The differences in virus-infected cell viability and BV production for each virus between the two time course studies could be due to the variation in passage number and health of the Sf9 cells used in each study. Therefore the deletion of *pif2* has not affected BV production, which is in agreement with the literature (Pijlman *et al.*, 2003; Ohkawa *et al.*, 2005). These results also demonstrated that the deletion of *pif2* had no effect on the rate of decline in virus-infected cell viability.

The effect of deleting *pif2* on recombinant protein production in insect cells was examined using β -galactosidase and urokinase as reporter targets. These proteins were chosen as they allowed easy monitoring of intracellular and extracellular, secreted products through activity assays.

6.7.1a Analysis of *AcΔpif2* β-galactosidase activity

Anova statistical analysis was used on the data obtained from the β-galactosidase activity assays, which were carried out on *AcBacPAK5/lacZ/BAC^{pol}* and *AcΔpif2* samples from the time course study. This analysis demonstrated that there was no significant difference ($P > 0.05$) between *AcBacPAK5/lacZ/BAC^{pol}* and *AcΔpif2* β-galactosidase activities during the course of infection, for either cell pellets or medium samples from virus-infected cells. However, this was misleading due to a clear difference between *AcBacPAK5/lacZ/BAC^{pol}* and *AcΔpif2* infected cell pellet and medium β-galactosidase activities at 48hpi, which was obscured in the Anova statistical analysis due to the similarity of β-galactosidase activity at the remaining time points. Also when analysing the β-galactosidase activity during this time course, the nature of the *polh* promoter should be taken into account, which has been demonstrated to cause a burst in recombinant protein expression during very late phase of infection (~48hpi) (Ooi *et al.*, 1989). Therefore, single analysis of the 48hpi β-galactosidase activities would give better indication of any effect the deletion of *pif2* is having on recombinant protein expression from the *polh* promoter.

This was confirmed by a two-tailed student t-test, which showed a significant difference ($P < 0.05$) between the β-galactosidase activity at 48hpi for either cell pellet or medium when these two viruses were compared. Even though *AcΔpif2* showed a significant increase (1.7 fold higher, $1.58 \text{ u}/10^6 \text{ cells}$) in the release of β-galactosidase at 48hpi compared to that of *AcBacPAK5/lacZ/BAC^{pol}* ($0.94 \text{ u}/10^6 \text{ cells}$). Overall the deletion of *pif2* had a negative effect on the peak expression of β-galactosidase, being 1.8 fold lower ($6.34 \text{ u}/10^6 \text{ cells}$) than that of *AcBacPAK5/lacZ/BAC^{pol}* ($11.55 \text{ u}/10^6 \text{ cells}$).

The increase in β-galactosidase activity at 48hpi in the medium sample from *AcΔpif2* infected cells could be considered abnormally high due to significant difference shown when compared to *AcBacPAK5/lacZ/BAC^{pol}* using two-tailed student t-test. Therefore the result could have occurred due to an error during either the time course study or activity assay. Interestingly, when β-galactosidase is expressed from the *polh* promoter, the peak β-galactosidase activity for the infected cell pellet would be expected at 48hpi (Hitchman *et al.*, 2010a). However, the peak β-galactosidase activity in *AcΔpif2* infected cells was shifted from 48hpi ($4.78 \text{ u}/10^6 \text{ cells}$) to 72hpi ($5.14 \text{ u}/10^6 \text{ cells}$), which could have been caused by the increased release of β-galactosidase from these cells at 48hpi. The *AcΔpif2* infected cell viability at 48hpi was not significantly different to that of *AcBacPAK5/lacZ/BAC^{pol}* infected cells. This suggests the release of β-galactosidase was not caused by a decline in cell viability at this time point, which normally would be associated with such an increase in activity in the medium sample as the intracellular

protein is lost from the dying cells. To further investigate this observation, the time course study should be repeated to ensure this initial observation is reproducible and wasn't due to abnormality during this time course study. Also SDS PAGEs could be used to further confirm the results seen in the activity assay.

After the peak β -galactosidase activity for all three virus-infected cell samples, there was a rapid decrease in their β -galactosidase activities. This decrease in β -galactosidase activity does coincide with a decline in cell viability and increase of β -galactosidase activity within the medium samples of each virus infected cell culture. This activity increase in the medium sample is due to the decline in cell viability, as intracellular β -galactosidase is lost from the dying cells. However, the overall loss of β -galactosidase activity from the infected cell pellet samples isn't seen as an increase in β -galactosidase activity for the medium samples, for any of the virus infected cultures examined here. This could suggest that β -galactosidase is being degraded from either a combination of the culture conditions, the accumulation of β -galactosidase or proteases from lysed cells.

6.7.1b Analysis of AcUK Δ *pif2* urokinase activity

Anova statistical analysis was used on the data obtained from the urokinase activity assays, which were carried out on AcBacPAK5urokinase^{pol} and AcUK Δ *pif2* samples from the time course study. This analysis demonstrated that there was no significant difference ($P>0.05$) between AcBacPAK5*lacZ*/BAC^{pol} and Ac Δ *pif2* β -galactosidase activities during this time course study, for either cell pellet or medium from virus-infected cells. However, as previously discussed the Anova statistical analysis could be misleading due to the very late expression from the *polh* promoter. Therefore, a two-tailed student t-test was performed on individual time points to compare the urokinase activities in virus infected cell pellets, it showed a significant difference ($P<0.05$) between 48 hpi to 120 hpi. Therefore, the deletion of *pif2* had a negative effect on the expression of urokinase in the infected cell pellet when compared to its parental virus. However, urokinase is an extracellular protein and when considering recombinant protein expression this would not be important due to an average 25 fold increase between the infected cell pellet urokinase activities and those obtained in the media samples. Also when a two-tailed student t-test was performed on individual time points to compare the urokinase activities in samples of media from each virus-infected cell culture it showed a significant difference ($P<0.05$) between 72 hpi to 120 hpi. These time points were after the peak urokinase activity observed at 48hpi for both viruses (~3480 units/ml), which was not considered significant different when compared using the two-tailed student t-test. This suggests that the

deletion of *pif2* does not have a negative effect on the peak expression of urokinase when compared to its parental virus.

It has been demonstrated here that the deletion of *pif2* could have a strongly negative impact on intracellular recombinant protein expression but this observation was not seen for extracellular recombinant protein. It would be interesting to repeat the time course studies to ensure these initial findings can be reproduced and also investigate the effect of the *pif2* deletion on the expression of different intracellular and extracellular recombinant proteins. The effect of the *pif2* deletion on recombinant proteins expressed from different viral promoters such as the late *p6.9* promoter could also be investigated to observe the effects on recombinant protein expression from different time points.

6.7.2 Analysis of the deletion mutant virus *AcΔpif3*

The observed effect of the *pif3* deletion on BV production was unexpected due to publications providing evidence that it is a member of the PIF family (Ohkawa *et al.*, 2005; Song *et al.*, 2012) and demonstrating that it is non-essential for virus propagation in cell culture. However, the reduced BV production of *AcΔpif3* could only be restored with the replacement of *pif3* at either its own locus or the *polh* locus. Concerns that the *pif3* deletion might have affected function of ORF114 or ORF116 were largely answered by attempting to rescue *AcΔpif3* at the *polh* locus with copies of either gene. Several attempts to place either of these genes at the *polh* locus and generate viable virus were unsuccessful. Interestingly, *AvrII* or *SrfI* linearised *AcΔpif3* produced no detectable viral growth when Sf9 cells were transfected with these viruses or when attempts were made to amplify them after the transfection stage. It is unusual for a baculovirus not to produce any background parental progeny from its non linearised virus, suggesting that the impact on BV production prevents the remaining non linearised *AcΔpif3* establishing a viral infection.

Overall this provides evidence to suggest that only the rescue of *pif3* can restore normal levels of BV production for *AcΔpif3* and neither of the neighboring genes had been affected by the deletion of *pif3*. Furthermore the literature suggests that *orf114* and *orf116* are most likely nonessential for viral replication. The deletion of the homologues to *orf114* in BmNPV demonstrated that it was nonessential for viral infectivity as the deletion mutant virus appeared to replicate normally in insect cells (Rohrmann, 2011). Homologues to *orf116* are only found in two other Type I alphabaculoviruses; RoNPV and PlxyNPV, which could suggest that like *orf114*, *orf116* is nonessential for viral infection.

However, future work could be directed towards further confirming that the deletion of *pif3* does not have an effect on *orf114* and/or *orf116* transcription. One method could involve using qPCR to analysis transcription rates from these two genes via cDNA synthesis and compared with transcription rates observed for *AcBAC Δ chitinase*

The localization of PIF3 was also investigated by fusion with a 6xHis-tag and immunofluorescence confocal microscopy, which demonstrated that PIF3 was localised to the nucleus of the infected TN-368 cells from 18hpi. This was as expected due to PIF3 containing an inner nuclear membrane sorting motif, which is involved in targeting proteins to the ODV envelope and therefore back to the nucleus of the cell. Song *et al.* (2012) have also demonstrated that *Helicoverpa armigera* nucleopolyhedrovirus PIF3 is localised to the nuclear ring zone of infected cells using immunofluorescence assays. Western blot analysis of 6xHis-tag PIF3 did detect it earlier at 12hpi, unfortunately samples before 12hpi were not analyzed and therefore no evidence was collected to suggest whether the predicted early promoter (CGTGC) for *pif3* is active or not. Therefore, future work could be directed towards investigating whether the early promoter of *pif3* is active, either by using the western blot analysis described here for earlier time points or by mapping of transcription start sites using 5' RACE analysis on cDNA. If the early promoter of *pif3* is found to be active this could suggest that PIF3 does play a role in earlier stages of viral infection such as those involved in BV production. However, the conclusion that *Ac Δ pif3* is defective for BV production means that this gene is not suitable for deletion from the AcMNPV genome to enhance its attributes as an expression vector. It was removed from further work plans in this project.

6.7.3 Conclusion

In this chapter the two deletion mutant viruses containing deletions from the PIF family, *Ac Δ pif2* and *Ac Δ pif3*, were analysed further. The results from this work demonstrated the possibility that the deletion of *pif2* negatively affects intracellular recombinant protein production but did not impact the expression of extracellular recombinant proteins, when expressed from the *polh* promoter. Unfortunately, the effects of the *pif3* deletion on recombinant protein expression could not be observed here due to *Ac Δ pif3* BV production being reduced. However, further investigation into this suggested that the cause of this reduced BV production was the deletion of *pif3* itself. Clearly, the deletion of *pif3* from AcMNPV reduces BV production significantly, but the modified virus was still capable of replication and in forming plaques in titrations of infectivity. Therefore, PIF3 may have another function that is yet to be fully characterized.

Chapter 7

Characterisation of *Ac* Δ *orf118/pif1*

7.1 Introduction

The Red/ET recombination system was successfully used to generate eight deletion mutant viruses, which were discussed in the previous chapters. In this chapter, a ninth deletion mutant virus constructed using the Red/ET recombination system is presented for the first time. This deletion mutant virus was not discussed in any of the previous chapters as it represents a double deletion of two adjacent genes, *orf118* and *pif1*.

The role of the predicted ORF118 product in baculovirus infection is unknown. However, in earlier studies the deletion of *orf118* from AcMNPV demonstrated that it was nonessential for viral infectivity as the deletion mutant virus appeared to replicate normally in insect cells (R.D. Possee, personal communication). Homologues of *orf118* are only found in two other Type I alphabaculoviruses; RoNPV and PlxyNPV (Rohrmann, 2011). In contrast, the role of PIF1 (ORF119) in the baculovirus infection is better defined as it has been demonstrated to be essential for oral infection of larvae (Kikhno *et al.*, 2002). The deletion of *pif1* from the virus genome does not affect baculovirus infection in insect cell culture (Kikhno *et al.*, 2002; Ohkawa *et al.*, 2005). PIF1 is believed to be involved in mediating specific binding of ODV to the primary midgut cells in oral infection of larva and has been localised to the ODV envelope, forming a stable complex with P74, PIF2 and PIF3 (Ohkawa *et al.*, 2005; Peng *et al.*, 2010). Since neither ORF118 nor PIF1 have been reported to affect virus replication in cell culture, it will be interesting to determine if deletion of these genes has any effect on protein production in recombinant virus infect cells.

The *pif1* is found in all sequenced alphabaculoviruses and betabaculoviruses and is also present in nudivirus genomes (Rohrmann, 2011). A closer inspection of AcMNPV PIF1 peptide sequence shows that it contains two RGD motifs, which were originally identified to mediate cell attachment in fibronectin (D'Souza *et al.*, 1991). Figure 7.1 presents alignments of the PIF1 peptide sequence with its homologues in alphabaculovirus Type I, which shows that PIF1 is highly conserved and all of the homologues apart from EppoNPV PIF1 contain at least one RGD motif. Since the discovery of RGD motifs a number of other proteins involved in cell adhesion have been found to contain this motif, supporting its role in cell attachment (D'Souza *et al.*, 1991). However, RGD motifs are also found in viral envelope proteins and disruption of this motif in a number of different viruses can cause reduced infectivity. The role of the RGD motif in viral infection can involve viral attachment, internalisation and escape of viral particles from the endosome (van der Most *et al.*, 1999; Shayakhmetov *et al.*, 2005; Rothwangl and Rong, 2009). Therefore, to investigate whether or not the PIF1 RGD motifs are functionally important, the arginine of

Chapter 7

these motifs was chosen for mutation. It has been shown in the literature that this positively charged amino acid plays a vital role in other protein RGD motifs and active sites (van der Most *et al.*, 1999; Shayakhmetov *et al.*, 2005; Rothwangl and Rong, 2009). It's also known to be important for binding to negatively charged groups such as those found on the plasma membrane of cells (Futaki *et al.*, 2001).

The aim of this chapter was first to characterise the deletion of *orf118* and *pif1* specifically in relation to recombinant protein expression and secondly to use mutagenesis to investigate the possible role of the PIF1 RGD motifs in oral infection of larvae.

Chapter 7

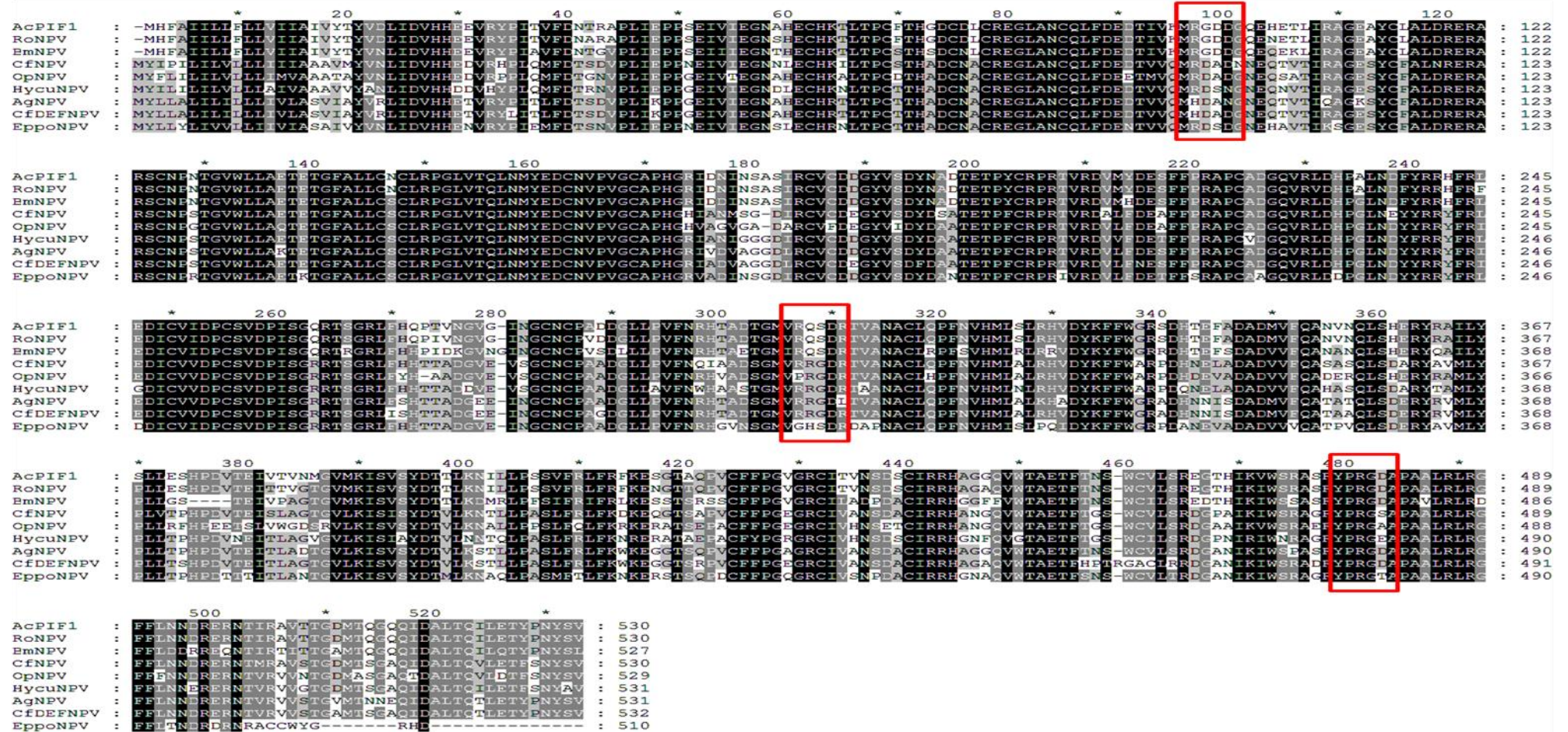


Figure 7.1 Sequence alignments of Type I PIF1 Sequences

The sequence alignments of type I alphaculoviruses PIF1 sequences were shaded using the GeneDoc software package to highlight the conserved amino acid sequences;

7.2 Construction of a deletion mutant: AcBAC Δ *orf118/pif1*

The deletion of *orf118* and *pif1* was carried out in a different bacmid (AcBAC Δ chitinase/cathepsin) to the one used to construct the deletions described in chapter 4. This bacmid contained a copy of the AcMNPV genome minus chitinase and cathepsin genes. These genes are non-essential for viral replication in cell culture and both play a role in host insect liquefaction (Slack *et al.*, 1995; Hawtin *et al.*, 1997). The AcBAC Δ chitinase/cathepsin bacmid also contains a 42bp deletion at the 5' end of the essential gene *orf1629*. This deletion removes the requirement for a selection process such as a plaque assay to be carried out after insect cells are transfected with the bacmid and a transfer plasmid since no parental virus background is produced (R.D Possee, personal communication), and is the basis for the commercial *flashBAC* expression system (Possee *et al.*, 2008; Hitchman *et al.*, 2010a; Hitchman *et al.*, 2010b). This is the underlying reason why AcBAC Δ chitinase/cathepsin bacmid was chosen for this deletion work, as it allows rapid generation of recombinant viruses that do not require any selection from non-recombinant parental virus.

In order to delete *orf118* and *pif1* from the AcBAC Δ chitinase/cathepsin bacmid, it was necessary to construct a kanamycin resistance gene cassette flanked by *orf118* and *pif1*-specific sequences. The kanamycin resistance gene fragment was generated by primers that contained these flanking regions: NeoORF118 primer (AAAAAAATTGTGTATAAATAA AATACCAAATTTTATTATATCATTTTGTT**neo-F*) and NeoORF119 primer (CGTTCGCGAT CGTTGTTTCAGAAAGAAGCCGCGCAATCTTAACGCTGCAGG**neo-R*), see Figure 7.2 for kanamycin-specific sequences *neo-F/neo-R*. The flanking regions were designed to remove the whole coding region of *orf118* and the majority of the *pif1* coding region with the insertion of a kanamycin resistance gene, leaving ~150bp of *pif1* at the 3' end to ensure that putative *orf120* promoters were unaffected by the deletion (Figure 7.2). The modified kanamycin resistance gene fragment was electroporated into Red/ET recombination competent *E. coli* containing the AcBAC Δ chitinase/cathepsin bacmid. Kanamycin-resistant colonies were picked and the deletion mutant bacmids were analysed by PCR and restriction digests to verify that the required sequences had been deleted.

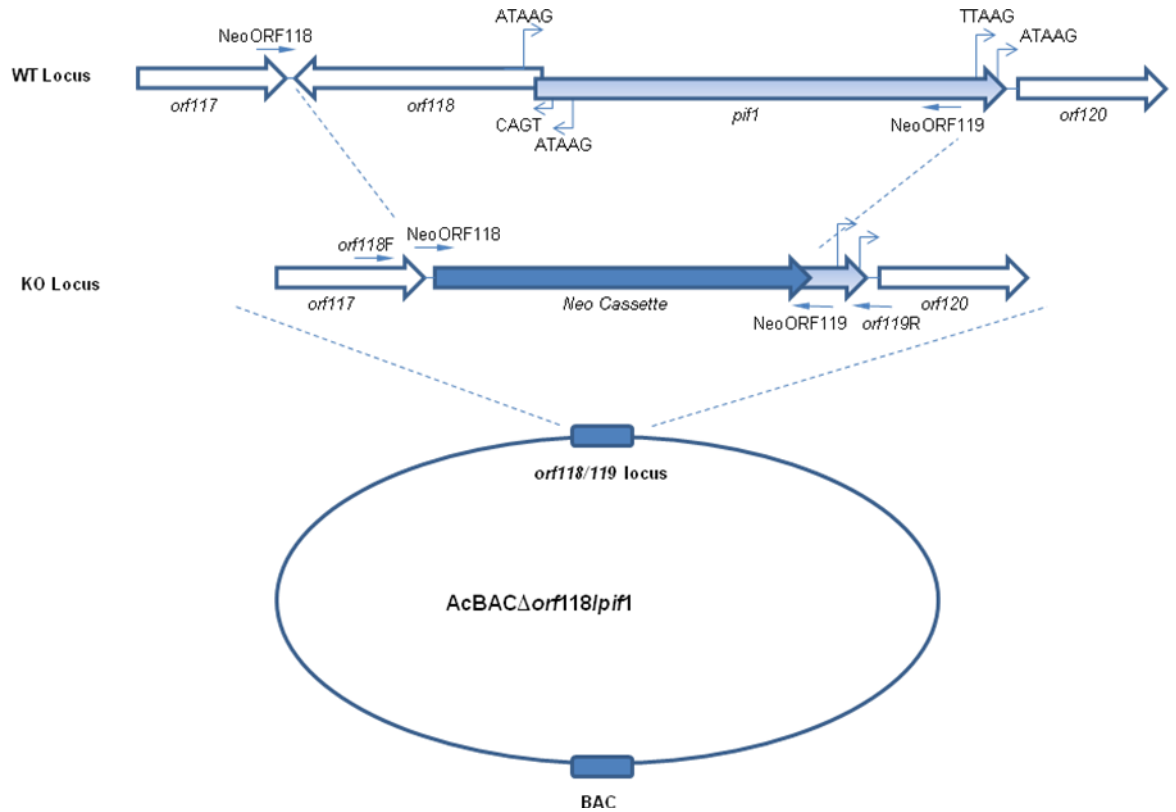


Figure 7.2 Schematic of the construction of *AcBAC Δ orf118/pif1* bacmid.

The *orf118* and *orf119* were mostly deleted by the insertion of kanamycin resistance gene between 100181 and 102141 bp on the AcMNPV genome via homologous recombination in *E. coli* using the Red/ET recombination system. The kanamycin resistance gene fragment was generated using NeoORF118 (AAAAAAATTGTGTATAAATAAAATACCAAATTTTATTATATCATTGTTTGGACAG CAAGCGAACCGGAATTGC) and NeoORF119 (CGTTCGCGATCGTTGTTTCAGAAAGAAGCCGC GCAATCTTAACGCTGCAGGTCAGAAGAACTCGTCAAGAAGGCG; sequences in red are kanamycin-specific) primers.

7.2.1 PCR Analysis of AcBAC Δ *orf118/pif1*

The target genes, *orf118* and *pif1* were successfully deleted from the AcBAC Δ chitinase/cathepsin bacmid and the resultant deletion bacmid was designated AcBAC Δ *orf118/pif1*. This deletion was confirmed using external primers designed to 99 bp upstream and 70 bp downstream of the target locus, which were used in PCR with Taq DNA polymerase to amplify the region containing the kanamycin cassette. The insertion of the kanamycin coding region into the target locus was predicted to result in the amplification of a 1294bp fragment, whereas the product from AcMNPV was 2319bp. The first set of external primers designed for this purpose did not amplify any bands, therefore a second set of external primers were designed and these were also paired with opposite primers from the first set of external primers (Figure 7.3 A). This proved successful and generated the DNA fragments described in Figure 7.3, B-C. A negative control (H₂O) in the PCR did not amplify a product (Figure 7.3 B, lane 2). The original *orf118* and *pif1* genes were not detected in any of the AcBAC Δ *orf118/pif1* samples tested. Therefore, the PCR analysis of the AcBAC Δ *orf118/pif1* clones produced only one DNA fragment with each primer pair with a size consistent with the presence of the kanamycin insert. However, one of the primer sets did not amplify any band for clone one (Figure 7.3 B, lane 3). The integrity of these deletion mutants was further characterised by restriction enzyme digestion.

7.2.2 Restriction Enzyme Analysis of AcBAC Δ *orf118/pif1*

Restriction enzyme analysis of bacmid DNA (Figure 7.4) was used to confirm the successful recombination events: (1) the insertion of the kanamycin resistance gene at the target gene locus and (2) that the rest of the virus genome was not affected by the recombination process, as judged by restriction enzyme analysis. The *HindIII* restriction fragment pattern of the deletion mutant bacmid was compared to the pattern of the parental bacmid. The expected alteration in the fragment pattern was a 976 bp decrease in fragment A. This alteration matched the profiles obtained for all of the deletion mutant bacmids apart from those in lanes 7 and 10 in Figure 7.4. This suggested that *orf118* and *pif1* were still present in those samples. The gel electrophoresis image in Figure 7.4 also showed that the rest of the deletion mutant bacmid profiles matched that of the parental bacmid's genome as expected, and that no random mutations had occurred that could be detected using this restriction enzyme.

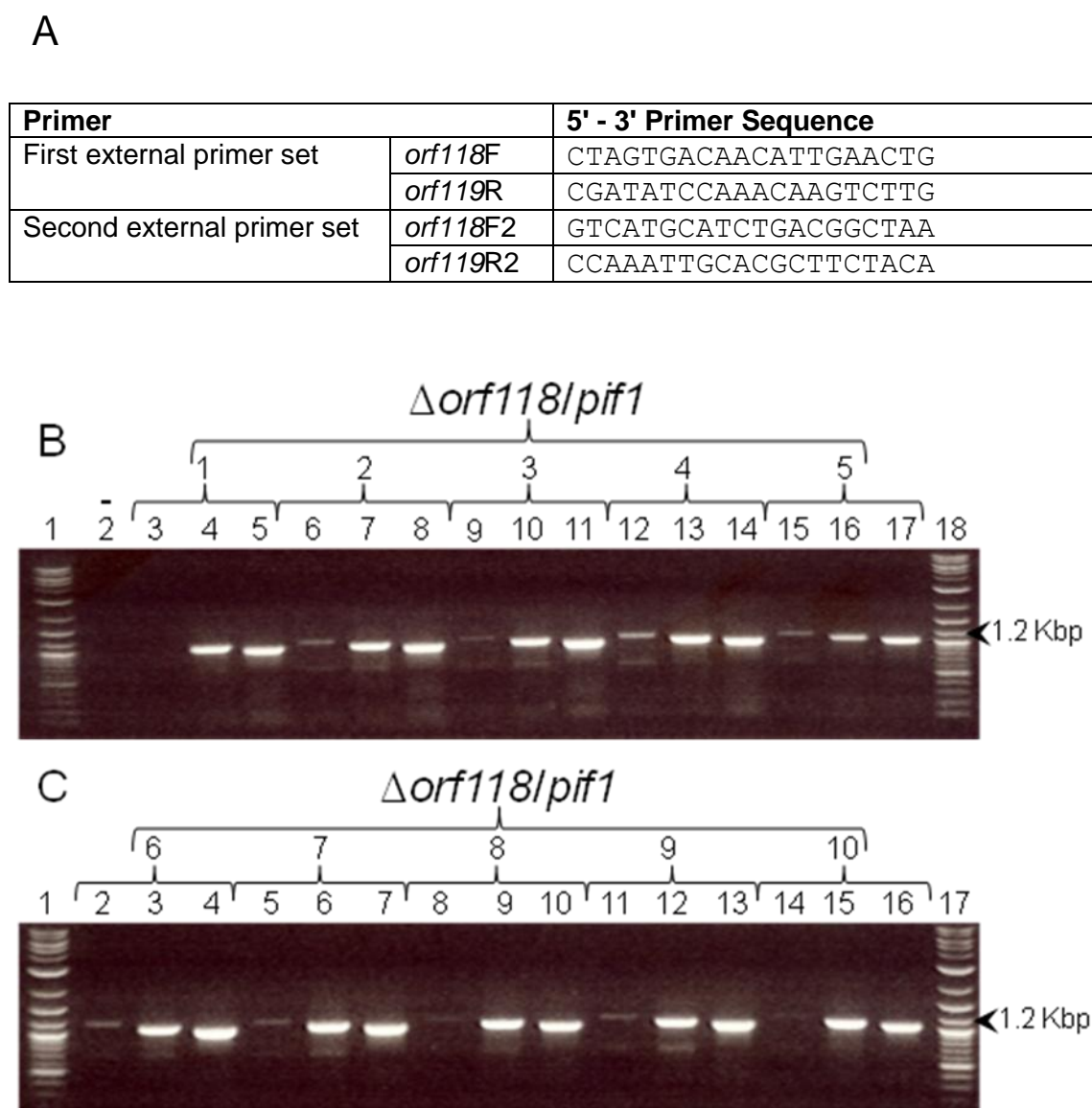


Figure 7.3 PCR analysis of *AcBAC $\Delta orf118/pif1$* DNA

Panel A contains a table displaying the external primers used to confirm *orf118* and *pif1* deletion from *AcBAC $\Delta orf118/pif1$* , with the label given to each primer along with the sequence for each primer

Panel B and C. DNA was isolated from colonies containing putative *AcBAC $\Delta orf118/pif1$* and analysed by PCR using primers 99 bp upstream and 70 bp downstream of the target locus and Taq DNA polymerase (B lanes 3-17 and C lanes 2-16). PCR results from the ten *AcBAC $\Delta orf118/pif1$* clones using *orf118F/orf119R2*, *orf118F2/orf119R* and *orf118F2/orf119R2* external primers are shown in this order for each clone. A negative (water-only) control is shown in A lane 2 and NEB log2 Marker (Kbp) shown in A lanes 1/18 and B lanes 1/17 with arrows indicating 1.2 Kbp size.

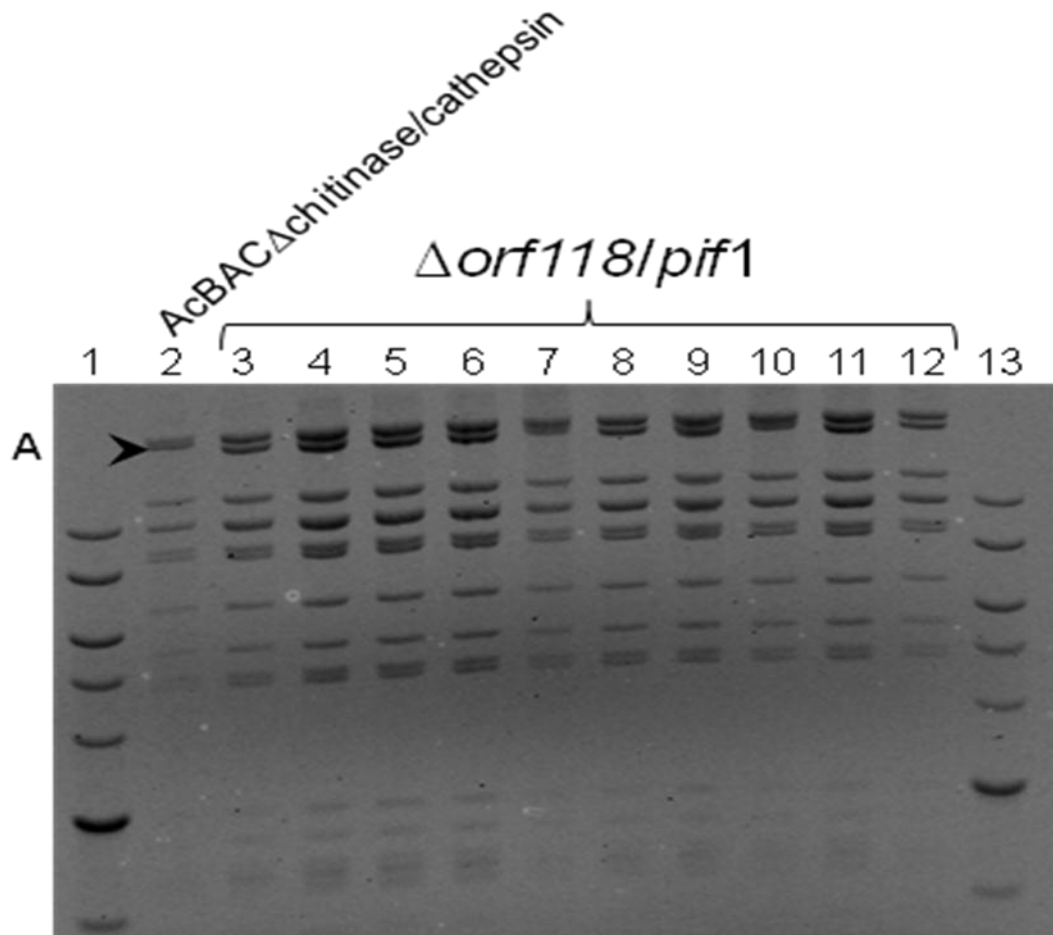


Figure 7.4 *Hind*III restriction enzyme analyses of deletion mutant bacmids

DNA was isolated from *E. coli* containing AcBACΔ*orf118/pif1* and validated by restriction enzyme (*Hind*III) analysis in a 0.6% agarose gel. Lanes 1 and 13 NEB log2 marker; lane 2, AcBACΔchitinase/cathepsin and lanes 3-12, AcBACΔ*orf118/pif1* clones 1-10.

7.3 Construction of *AcIacZ Δ orf118/pif1*

The *AcIacZ Δ orf118/pif1* was constructed to provide a virus to allow an investigation of the possible effects these two deletions (*orf118* and *pif1*) might have on recombinant protein expression. To aid this study, *lacZ* under the control of the *polh* promoter was introduced into the *AcBAC Δ orf118/pif1* genome. The next sections detail the construction and purification of *AcIacZ Δ orf118/pif1*.

Insect Sf9 cells were cotransfected with pBacPAK8-*lacZ* and bacmid DNA purified from *E. coli* containing *AcBAC Δ orf118/pif1*. The *AcBAC Δ orf118/pif1* contains a small deletion in the essential gene *orf1629*. This produces a selection marker in which only those viruses that are rescued with a transfer plasmid that restores the whole of *orf1629* will be viable in insect cells (R.D Possee, personal communication). Recombination between *AcBAC Δ orf118/pif1* and pBacPAK8-*lacZ* should knock-out the BAC at the *polh* locus and replace it with *lacZ* from the baculovirus transfer vector (Figure 7.5).

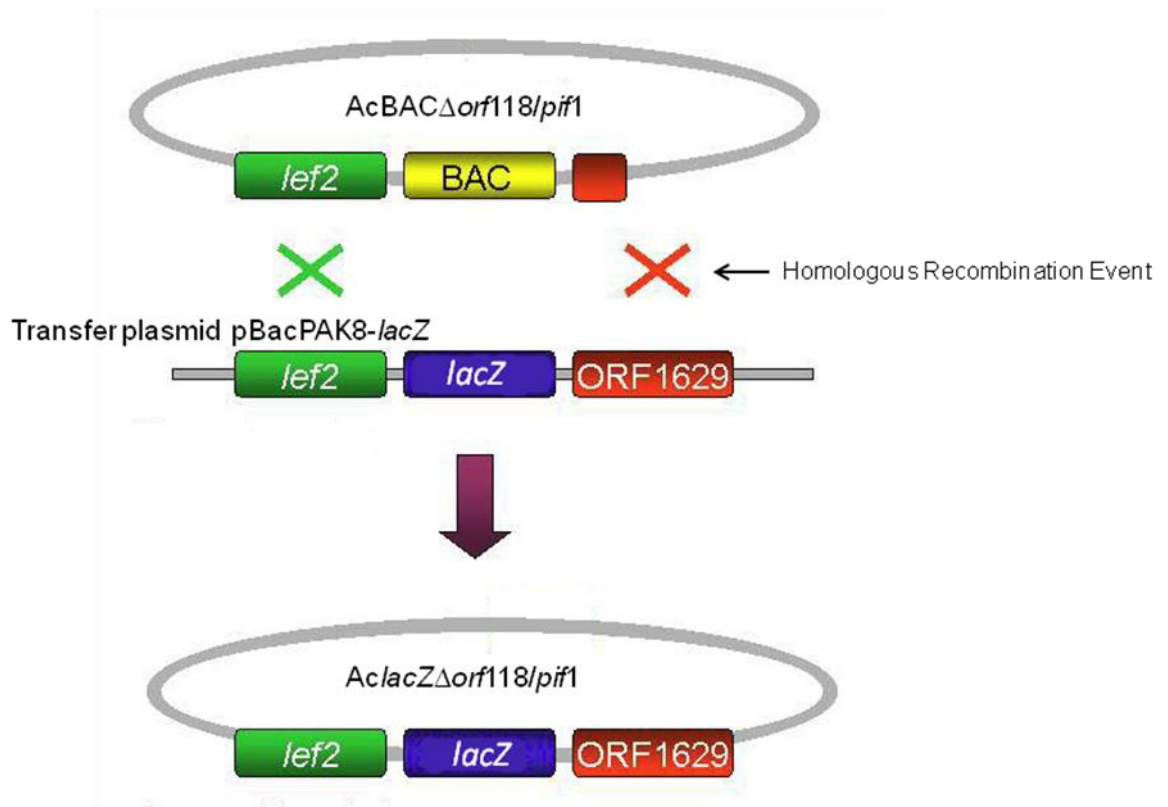


Figure 7.5 Schematic showing the insertion of *lacZ* at *polh* locus for *AcBAC Δ orf118/pif1*

The BAC was completely deleted from *AcBAC Δ orf118/pif1* by the insertion of *lacZ* at *polh* locus via homologous recombination in Sf9 insect cells between pBacPAK8-*lacZ* and bacmid genome.

Chapter 7

The resulting recombinant virus *AclacZΔorf118/pif1* was plaque-purified for one round to confirm that beta-galactosidase was synthesised by staining in the presence of X-gal (data not shown). The virus selected amplified to titres of 5×10^7 pfu/ml and infected cells turned blue in the presence of X-gal (data not shown) suggesting that the virus was replicating normally in insect cells. This confirmed that the *lacZ* had been correctly inserted into the *polh* locus of *AclacZΔorf118/pif1*.

7.4 Temporal analysis of virus replication in *AclacZ* Δ *orf118/pif1* and *AclacZ* Δ *chitinase/cathepsin* infected Sf9 cells.

Two control viruses were used in this time course study: AcBacPAK6 and *AclacZ* Δ *chitinase/cathepsin*. AcBacPAK6 is a wild-type control virus; its only difference from AcMNPV being the presence of *lacZ* in place of the *polh*. *AclacZ* Δ *chitinase/cathepsin* is the parental virus of *AclacZ* Δ *orf118/pif1*; the only difference between these two viruses is the deletion of *orf118* and *pif1*. Therefore, any statistically significant difference seen between *AclacZ* Δ *chitinase/cathepsin* and *AclacZ* Δ *orf118/pif1* during this time course study, could suggest an effect of *orf118* and *pif1* deletion. Any differences observed between AcBacPAK6 and *AclacZ* Δ *chitinase/cathepsin* is likely to be attributed to the chitinase and cathepsin genes.

A time course study was carried out and samples were taken over 96 hours from triplicate shaking cultures of Sf9 cells (2×10^6 cells/ml) either mock-infected or infected (AcBacPAK6, *AclacZ* Δ *orf118/pif1* or *AclacZ* Δ *chitinase/cathepsin*) at a moi of 5 pfu/cell. These samples were analysed to determine any affects that the *orf118* and *pif1* deletion could have on the expression of the recombinant protein β -galactosidase, cell viability and BV production kinetics.

7.4.1 Cell Viability

The viability of virus-infected Sf9 cells was assessed over a time course between 0-96 hpi., as described above. Figure 7.6 shows that all virus-infected cells had a viability greater than 97% until 24hpi, at which point the cell viability decreased for all of the viruses. AcBacPAK6 infected cells showed the highest cell viability through the last three time points, dropping from 84% (48hpi) to 31% (96hpi). The viability of *AclacZ* Δ *orf118/pif1*-infected cells showed the lowest cell viability, dropping from 58% (48hpi) to 8% (96hpi). The *AclacZ* Δ *chitinase/cathepsin* infected cell viability dropped to a value between AcBacPAK6 and *AclacZ* Δ *orf118/pif1* for the 48hpi and 72hpi time points, but decreased to 5% at 96hpi.

A two-tailed student t-test showed a significant difference ($P < 0.05$) in the virus-infected cell viability at 48hpi between *AclacZ* Δ *orf118/pif1* and the two control viruses, *AclacZ* Δ *chitinase/cathepsin* and AcBacPAK6. A two-tailed student t-test also showed a significant difference ($P < 0.05$) in the virus-infected cell viability at 72hpi between all three of the viruses. However, despite these temporal differences, Anova statistical analysis demonstrated that there was no significant difference between any of the virus infected cell viabilities across the time course study ($P > 0.05$).

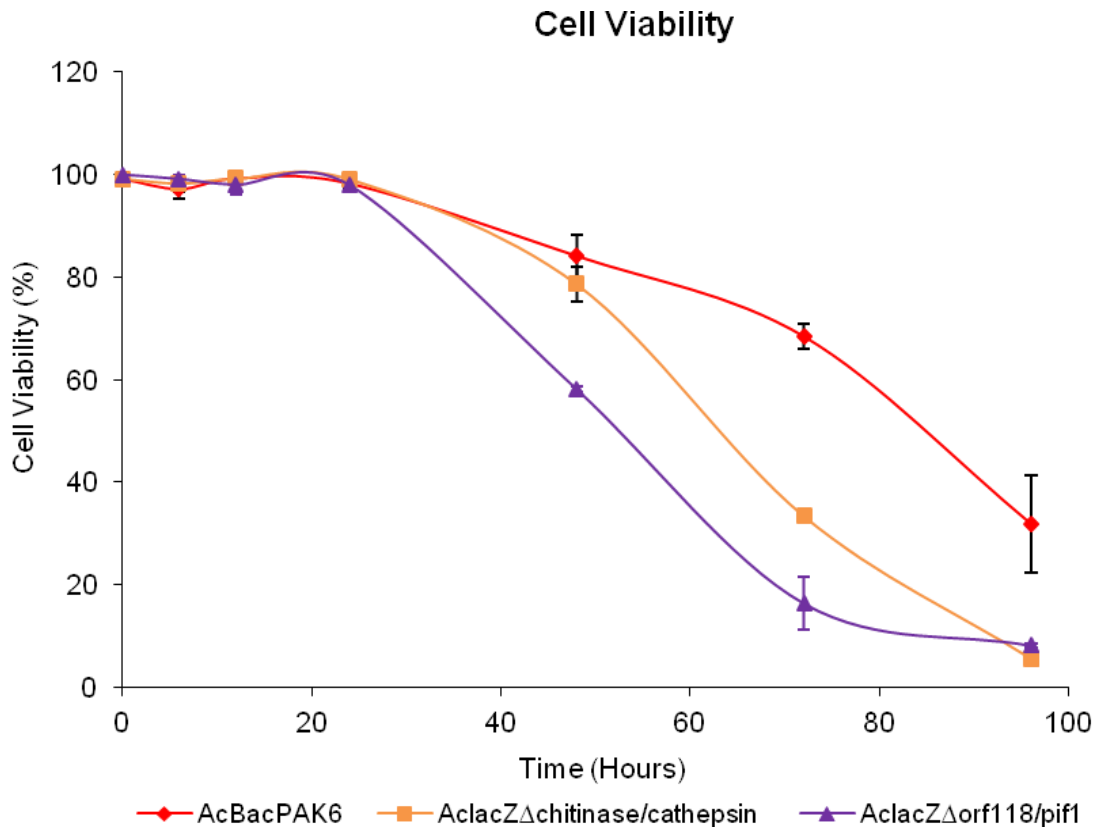


Figure 7.6 Virus-infected cell viabilities.

Cell viability results for AcBacPAK6-, AclacZ Δ orf118/pif1- and AclacZ Δ chitinase/cathepsin-infected Sf9 cells (MOI = 5 pfu/cell), were obtained using trypan blue stain to visualise dead cells. Standard error bars are shown during 96 hour time course. N=3

7.4.2 Budded Virus Production

The virus-infected cell culture medium collected at each time point in the above experiment (7.4.1) was titrated using *baculoQUANT*[™], a qPCR-based system (Hitchman *et al.*, 2007b) as described in methods section 2.3.4 (Figure 7.7). The DNA for qPCR was obtained from the samples using the High Pure Viral Nucleic Acid Kit from Roche Applied Science. The 0hpi titre values for all three viruses were approximately 2.21×10^6 pfu/ml due to residual virus from the initial inocula used to infect the shake cultures. Significant BV production for any virus was not evident until after 12hpi. Both AcAcBacPAK6 and AclacZ Δ chitinase/cathepsin titres increased rapidly after 12hpi, reaching approximately 2.6×10^7 pfu/ml at 24hpi. After this time point the virus titres did not increase significantly,

reaching 4.54×10^7 pfu/ml and 4.96×10^7 pfu/ml at 72hpi, respectively. Between 12 and 24hpi, the titre of *AclacZ Δ orf118/pif1* didn't increase as rapidly as the other two viruses. By 24hpi, the *AclacZ Δ orf118/pif1* had reached 6.65×10^6 pfu/ml. However, by 72 hpi its titre was 4.29×10^7 pfu/ml, indicating a delay in BV production rather than an inability to attain normal levels. Despite the temporal difference seen at 24hpi for *AclacZ Δ orf118/pif1*, Anova statistical analysis demonstrated that there was no significant difference between any of the BV production kinetics ($P > 0.05$).

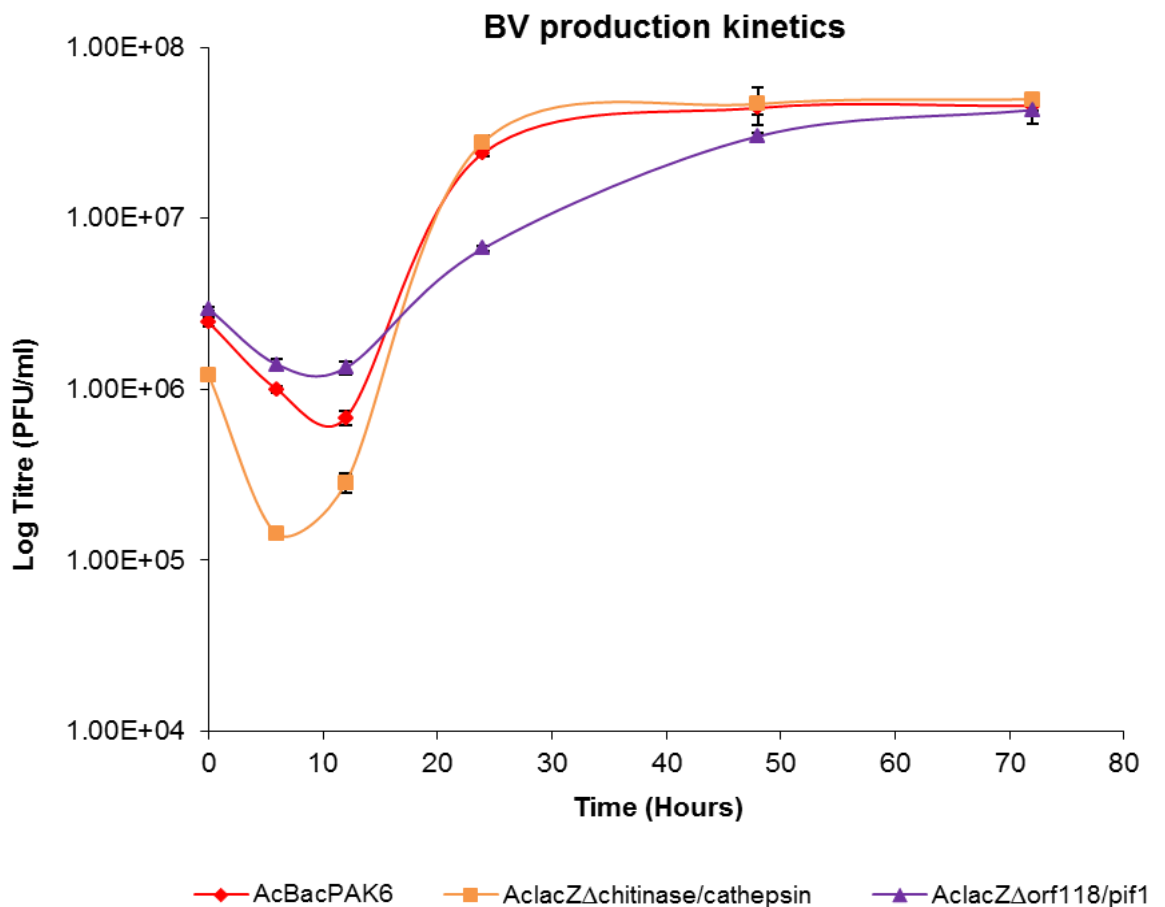


Figure 7.7 Kinetics of budded virus production for *AclacZ Δ orf118/pif1*

Budded virus production by values *AcBacPAK6*-, *AclacZ Δ orf118/pif1*- and *AclacZ Δ chitinase/cathepsin*-infected Sf9 cells (MOI = 5 pfu/cell), were obtained using a qPCR-based system (Hitchman *et al.*, 2007b). Standard error bars are shown during the 72 hour time course. N=3

7.4.3 β -galactosidase production

The production of β -galactosidase for each of the viruses was measured over time using a standard β -galactosidase assay method as described in methods section 2.7.3a. Measurements were taken from both the harvested medium and cell pellets described above (Figure 7.8). In the cell pellets, β -galactosidase was not detectable until after 12hpi for any of the viruses. After 12hpi, all three of the viruses followed the same trend, showing a sharp increase in β -galactosidase activity and reaching a peak at 48hpi. After this time point the β -galactosidase activity declined to very low levels at 72hpi and 96hpi. Although the viruses followed the same trend, the peak activity of β -galactosidase at 48hpi varied between them. The activity (in arbitrary units/ 10^6 cells) was maximum at 48hpi and ranged from 13.75 u/ 10^6 cells (AcBacPAK6), to 24.48 u/ 10^6 cells (*AclacZ Δ orf118/pif1*) and 41.80 u/ 10^6 cells (*AclacZ Δ chitinase/cathepsin*). Anova statistical analysis demonstrated that there was no significant difference between any of the viruses cell pellet β -galactosidase activities ($P > 0.05$). However, a two-tailed student t-test showed a significant difference ($P < 0.05$) between the β -galactosidase activity produced at 48hpi when comparing any two of the virus infected cells at this time point.

The samples of medium from all virus infections had different initial activity levels of β -galactosidase, which is most likely from the initial viral inoculum used to infect the Sf9 shake cultures. These initial β -galactosidase activities were approximately 0.5 u/ 10^6 cells for all three of the viruses. The β -galactosidase activity of AcBacPAK6 medium didn't increase past its initial activity until after 48hpi, whereas both *AclacZ Δ chitinase/cathepsin* and *AclacZ Δ orf118/pif1* mediums increased past their initial β -galactosidase activities after 24 hpi. The AcBacPAK6 medium β -galactosidase activity increased at a steady rate from 48hpi to 96hpi reaching 1.84 u/ 10^6 cells at this time point. Both *AclacZ Δ chitinase/cathepsin* and *AclacZ Δ orf118/pif1* increased at a steady rate from 24hpi to 96hpi reaching approximately 2.60 u/ 10^6 cells for *AclacZ Δ chitinase/cathepsin* and 3.00 u/ 10^6 cells for *AclacZ Δ orf118/pif1*. Despite these temporal differences, Anova statistical analysis demonstrated that there was no significant difference between any of the virus β -galactosidase activities in the culture medium ($P > 0.05$). However, a two-tailed student t-test showed a significant difference ($P < 0.05$) when comparing either AcBacPAK6 or *AclacZ Δ orf118/pif1* with *AclacZ Δ chitinase/cathepsin* β -galactosidase activity between 0 and 24hpi.

In summary despite some slight temporal differences, the deletion of *orf118* and *pif1* in *AclacZ Δ orf118/pif1* did not significantly affect either BV production or infected-cell viability during this time course study. However, the deletion did negatively affect β -galactosidase production when it was compared to its parental virus; *AclacZ Δ chitinase/cathepsin*.

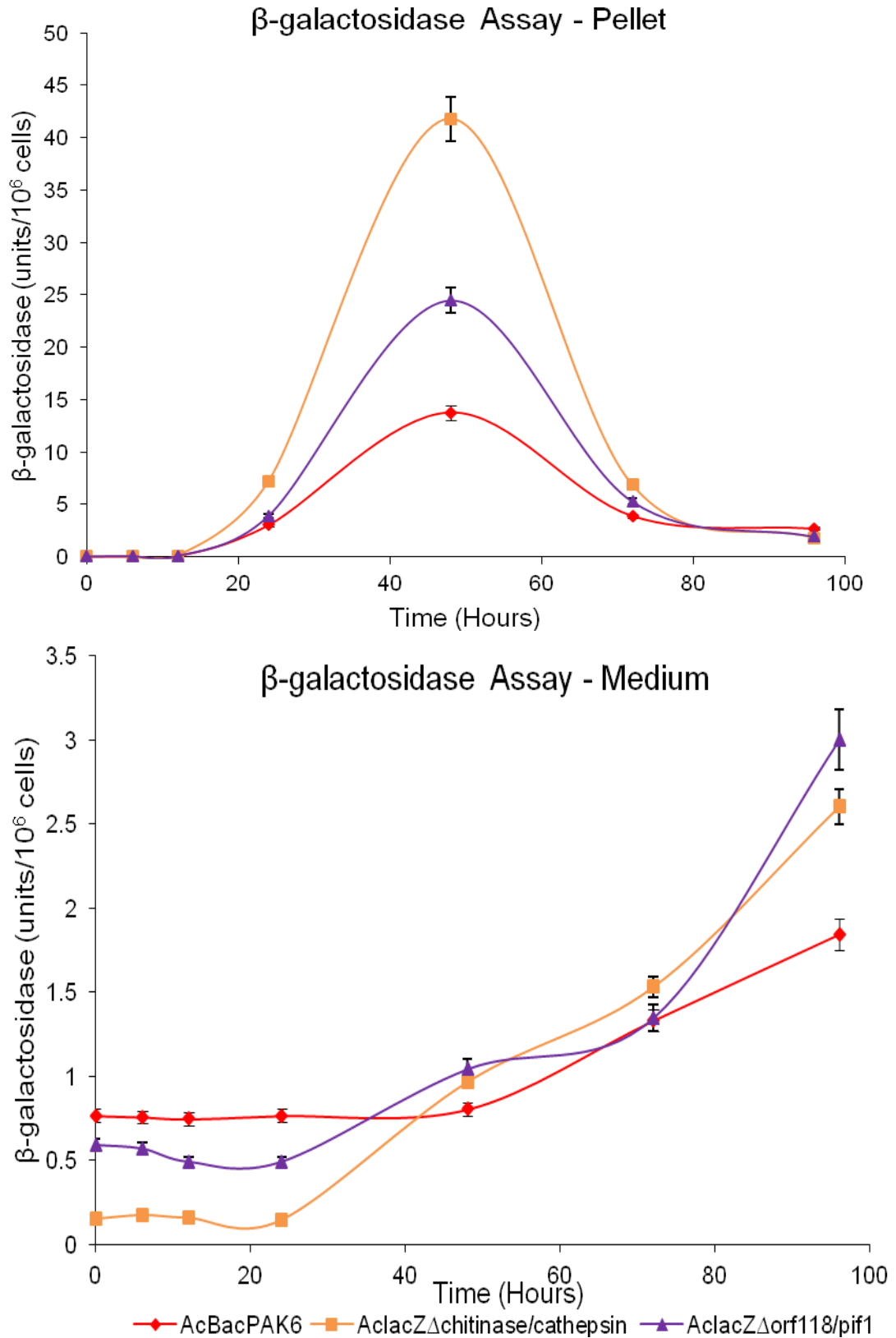


Figure 7.8 β -galactosidase productions by recombinant baculoviruses.

β -galactosidase activities in the cell pellets and medium for AcBacPAK6, AclacZ Δ orf118/pif1 and AclacZ Δ chitinase/cathepsin, obtained using a β -galactosidase assay. Standard error bars are shown during 96 hour time course. N=3

7.5 Construction of recombinant viruses with PIF1 RGD motif mutations.

To investigate a potential role for PIF1 RGD motifs in the fusion between the ODV and the larva midgut, viruses were constructed that contained single or double mutations within the *pif1* coding sequence (Figure 7.9). These mutations resulted in an arginine to alanine change within each RGD motifs. For economy, complete copies of *pif1* with modified RGD motifs were not synthesized. Instead, the region between 100934-102188 in the AcMNPV genome was modified to contain the mutated RGD motifs. The mutations inserted into the virus genome are summarized in Table 7.1.

Table 7.1: Summary of *pif1* mutant viruses.

Name	Virus description	Titres
<i>AcΔpif1</i> ^{Pol+}	Control virus that contains the deletion of <i>pif1</i> , with restored polyhedrin production using pAcUW21 that contained no <i>pif1</i>	8.2 x10 ⁷ pfu/ml
<i>Ac</i> <i>pif1</i> ^{Pol+}	Control virus that contains a restored wild type <i>pif1</i> at the <i>polh</i> locus	9.3x10 ⁷ pfu/ml
<i>Ac</i> <i>pif1</i> ^{Arg96AlaPol+}	Test virus with restored <i>pif1</i> function at the <i>polh</i> locus, which contains amino acid change at position 96 going from arginine to alanine	8.7x10 ⁷ pfu/ml
<i>Ac</i> <i>pif1</i> ^{Arg478AlaPol+}	Test virus with restored <i>pif1</i> , which contains amino acid change at position 478 going from arginine to alanine	9.4x10 ⁷ pfu/ml
<i>Ac</i> <i>pif1</i> ^{Arg96/478AlaPol+}	Test virus that contains both the above amino acids changes to its restored <i>pif1</i> .	8.6x10 ⁷ pfu/ml

For these modified *pif1* sequences to be inserted into the AcMNPV genome, a parental virus was required that was missing the wild-type gene. Such a parental virus would allow reliable homologous recombination between the mutant fragments and the virus genome, and ensure no further mutations would be introduced through the slippage of the homologous arms during recombination between the plasmid transfer vector and the virus genome.

The initial method (Figure 7.10) and parental virus chosen for this was *AcΔpif1*^{lacZ}, which comprises a copy of the AcMNPV genome with *lacZ* inserted into the *XhoI* site (AcMNPV genome 101806-101811 bp) of *pif1* (R.D Possee, personal communication). However, this virus still contained the complete *pif1* coding region, which would have meant that homologous recombination between plasmid and virus might have resulted in retention of the original RGD motifs. Therefore, *AcΔpif1*^{lacZ} was modified in insect cells by replacing the *lacZ* and the majority of the *pif1* coding region with a kanamycin resistance gene fragment (Figure 7.10). The *AcΔpif1*^{lacZ} DNA was linearized by restriction enzyme

digestion with *Bsu361*, which contains a single *Bsu361* site within *lacZ*. Insect Sf9 cells were then cotransfected with the linearized *AcΔpif1^{lacZ}* DNA and PCR generated kanamycin resistance gene cassette flanked by *pif1* sequences. The resulting recombinant virus (*AcΔpif1^{Neo}*) was plaque-purified until only *lacZ*-negative plaques were generated (plaques that did not turn blue when stained with X-gal) (data not shown).

The next stage was to construct the *pif1* mutant viruses using *AcΔpif1^{Neo}* and the pBS^{Arg96Ala; Arg478Ala; Arg96/478Ala} plasmids (Figure 7.10) by cotransfection of Sf9 cell. The progeny virus was titrated using a plaque assay and well-isolated plaques were picked and used to infect a single well within a 24 well plate containing 5×10^5 Sf9 cells. After 72hpi, DNA from the BV was extracted using the High Pure Viral Nucleic Acid Kit (Roche Applied Science) and used in PCR with primers external to the *pif1* locus. However, despite several attempts this method didn't produce a single isolate indicating the presence of modified *pif1*. All of the viruses isolated and subsequently sequenced retained the original RGD motif coding regions. Therefore, a second method was designed and is described in the following section.

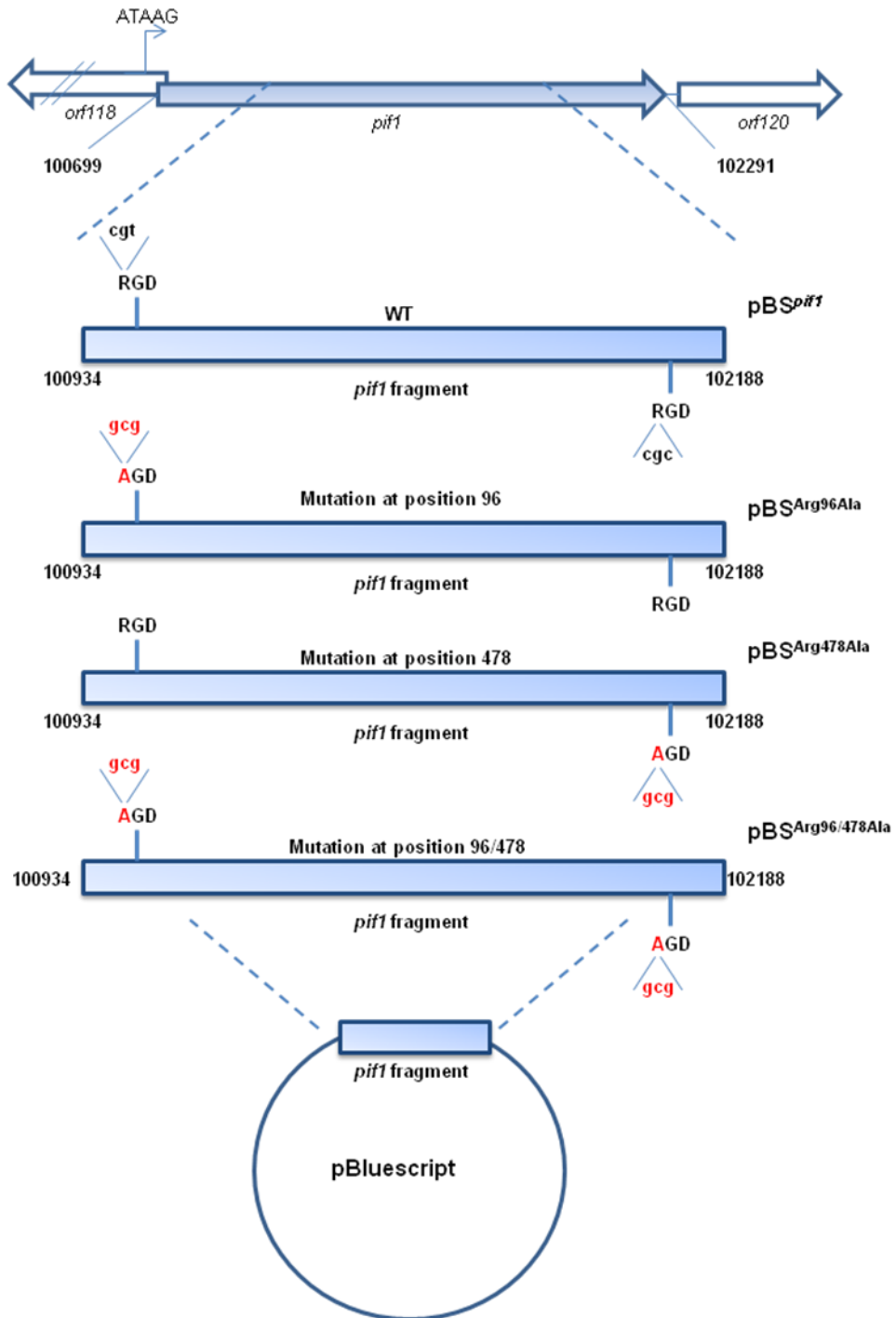


Figure 7.9 Schematic of the *pif1* mutations

Mutations were introduced into the *pif1* sequence to derive pBS variants containing mutations to the RGD motif as indicated, resulting in either or both amino acids 96 and 478 to be changed from arginine to alanine. Mutations were synthesized by Advantagen.

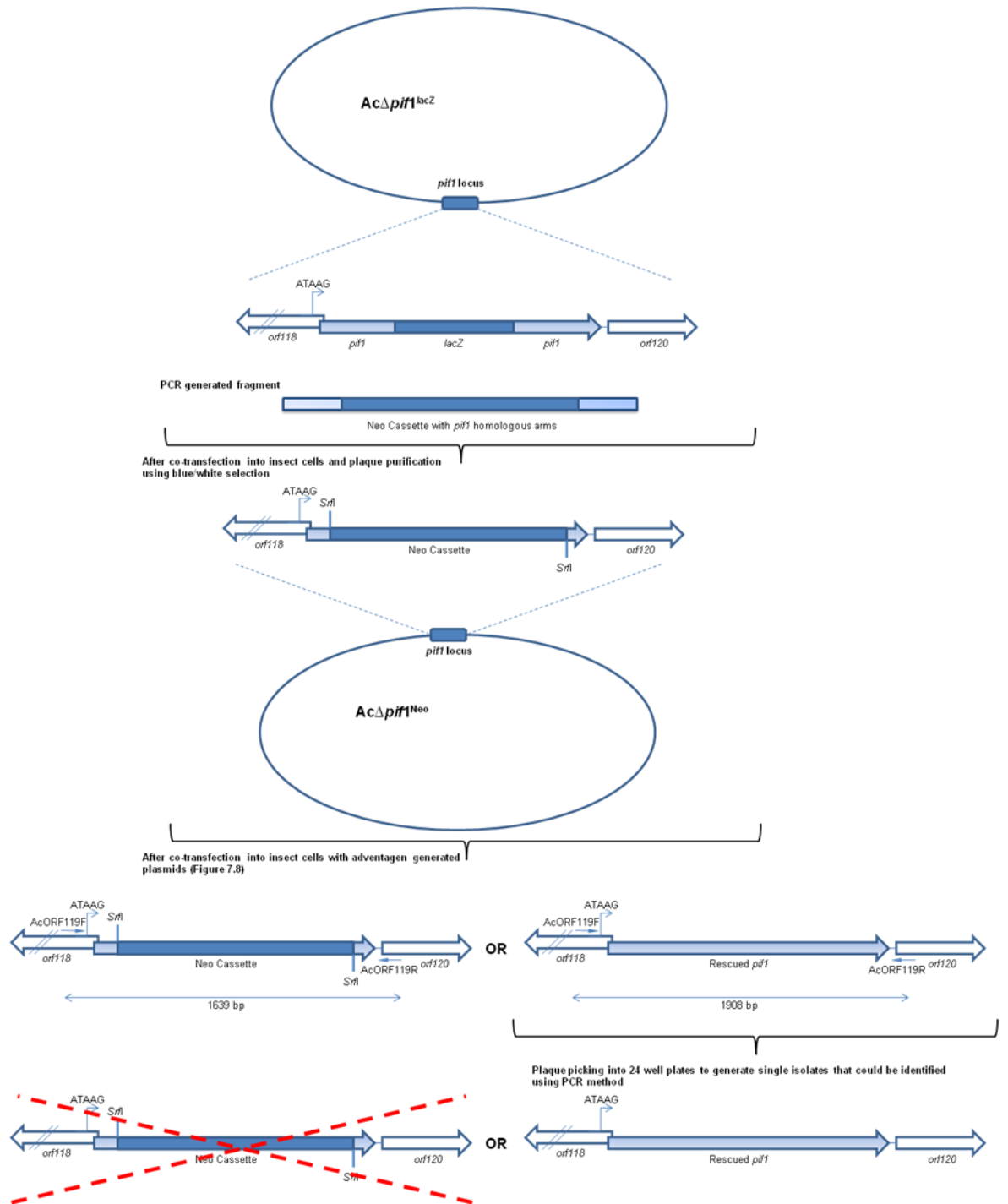


Figure 7.10 Schematic of the initial method used to construct *pif1* mutant viruses

The *pif1* was mostly deleted by the insertion of the kanamycin resistance gene between 100934 and 102188 bp on the AcMNPV genome via homologous recombination in insect cells. Attempts to rescue *pif1* with the fragments were then undertaken. The rescued viruses could then be isolated using plaque purification and identified using PCR with AcORF119F (AGGATCCGCAATTGTTTTT GCGATATC)/AcORF119R(AGGATCCAAACAAGTCTTGCCCC) primers.

7.5.1 AcBAC Δ *pif1*

The parental virus for the construction of AcBAC Δ *pif1* was AcBAC¹⁶²⁹ Δ chitinase, which is a copy of the AcMNPV genome minus *chitinase* and 42bp of the essential gene *orf1629*. The small deletion of *orf1629* removes the need for a selection process to be carried out after insect cells are transfected with the bacmid and a transfer plasmid as no parental virus background is produced (R.D Possee, personal communication). First, the Red/ET recombination system was used to modify AcBAC¹⁶²⁹ Δ chitinase by replacing *pif1* with a kanamycin resistance cassette to derive AcBAC Δ *pif1* (Figure 7.11).

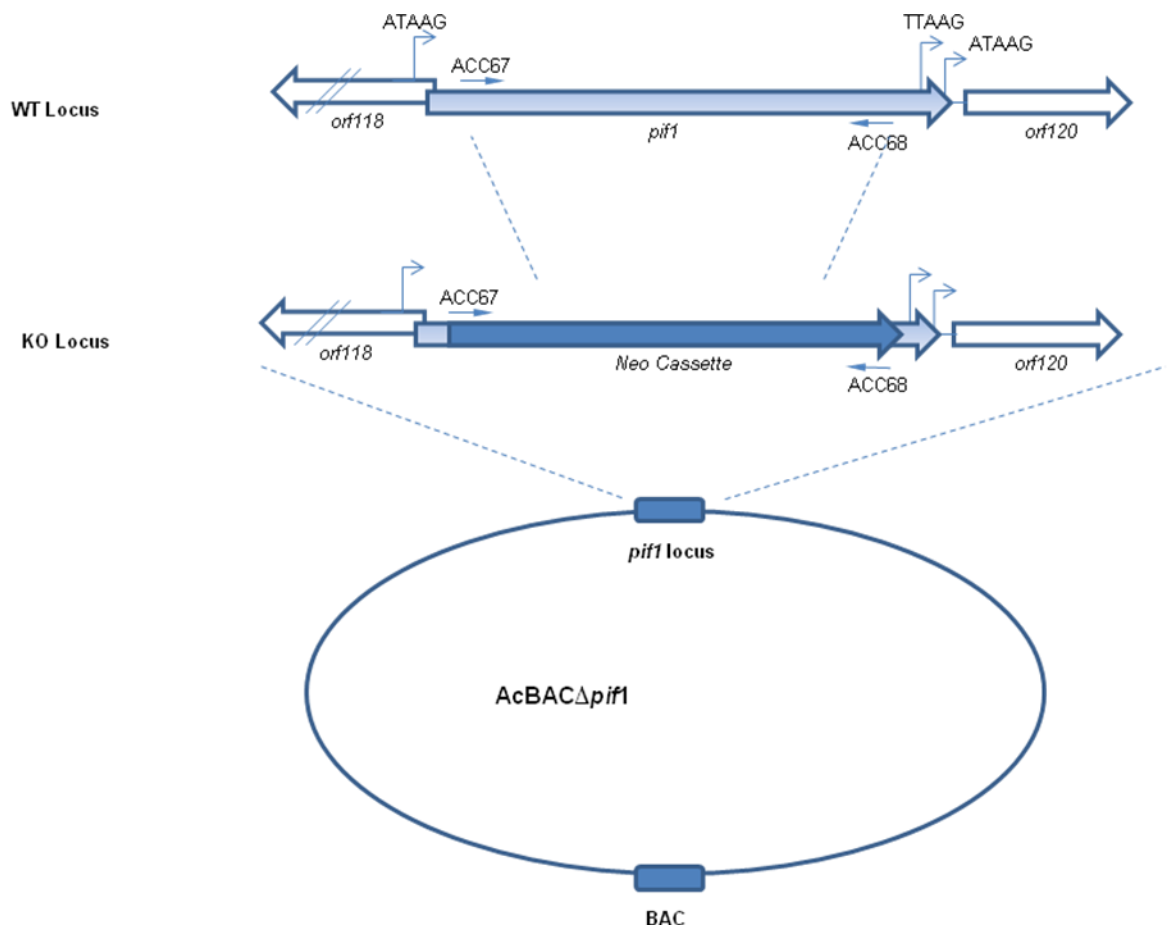


Figure 7.11 Schematic of the construction of AcBAC Δ *pif1* bacmid

The *pif1* was mostly deleted using a kanamycin resistance gene fragment generated using ACC67(AAGGATTAGCCAAGTCCAGTTGTTTGACGAAGATACAATAGTCAAGATGGCCCGGCTGGACAGCAAGCGAACC~~CGGAATTGC~~)/ACC68(TTCGCGATCGTTGTTTCAGAAAGAAGCCGCGCATCTTAACGCTGCAGGCGCGCCCGGGCTCAGAAGA~~ACTCGTCAAGAAGGCG~~); sequences in red are kanamycin-specific primers that could be inserted into the AcMNPV genome between 100934 and 102188 bp via homologous recombination in *E. coli* using the Red/ET recombination system.

This *pif1* deletion mutant (AcBAC Δ *pif1*) became the parental virus into which modified versions of *pif1* could be inserted at the *polh* locus. However, since the *pif1* RGD mutants were contained within an incomplete copy of the coding region (Figure 7.9), it was first necessary to restore the sequences omitted from the 5' and 3' ends of the gene and place them within a transfer vector suitable for subsequent insertion into the virus genome (Figure 7.12). PCR was used to synthesize two DNA fragments that contained the two ends of the *pif1* coding region. These were then mixed with each vector containing the RGD mutants and cross over PCR used to produce the complete *pif1* coding region. The amplified gene fragments were then inserted into a pGEM-T vector (Promega) and sequenced to confirm the fidelity of the amplification process.

The gene fragments were then removed from pGEM-T and inserted into a modified pAcUW21 (Lopez-Ferber *et al.*, 1995). This vector contains a copy of the *p10* promoter inserted upstream and in the opposite orientation to *polh*. It was modified by removal of the *p10* promoter with *Xba*I and *Eco*RI and replacing it with a synthetic multiple cloning site containing *Apa*I and *Sac*I sites to produce pAcUW21 Δ *p10* (Figure 7.12). Three derivatives of this vector, containing either single or double RGD mutations within *pif1* were produced. All constructs were confirmed by RE mapping (data not shown). These plasmids could then be used to insert *pif1* under the control of its own promoter upstream of the AcMNPV polyhedrin gene.

Insect Sf9 cells were then cotransfected with one of three modified pAcUW21 vectors (pAcUW21 Δ *p10*.Arg96Ala; Arg478Ala; Arg96/478Ala) and viral DNA purified from *E. coli* containing AcBAC Δ *pif1*, which on its own is non-infectious. Recombination between AcBAC Δ *pif1* and each transfer vector was predicted to remove the BAC while replacing *polh*, restoring orf1629 to functionality and inserting a RGD-mutated *pif1*. A summary of the recombinant viruses constructed in this section, along with their abbreviations used subsequently in this thesis, is shown in Table 7.1.

The resulting recombinant viruses amplified to titres indicated in Table 7.1. Virus-infected cells contained polyhedra that were visible under the microscope (data not shown). Viral DNA was isolated from infected cells and PCR was used to confirm the successful recombination event with insertion of *pif1* fragments. Figure 7.13 shows that Ac Δ *pif1*^{Pol+} sample contained only one DNA fragment at 1639 bp, which indicates the presence of the kanamycin fragment at the *pif1* locus. All of the recombinant viruses also contained this fragment as expected, with the addition of a second DNA fragment at 1908 bp suggesting the presence of the *pif1* coding region.

Chapter 7

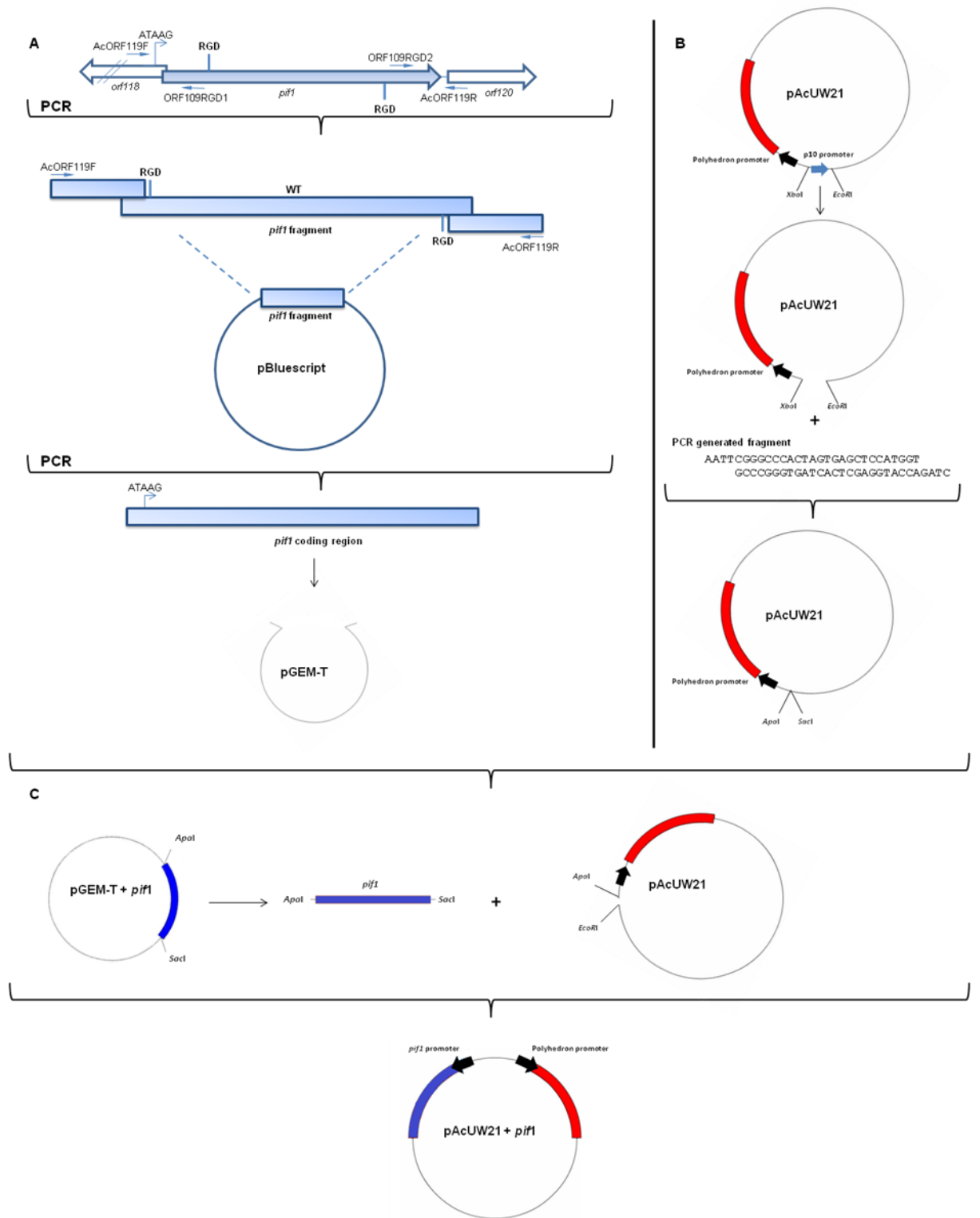
The next stage was to amplify the OB from these now polyhedrin positive viruses to allow further experimental work to be carried on ODV.

Figure 7.12 Insertion of *pif1* coding regions into modified pAcUW21

A, The whole *pif1* coding region was constructed by PCR using Expand DNA polymerase with fragments generated using AcORF119F (see Figure 7.10)/ORF109RGD1 (CATCTTGACTATTGTATCTTCGTC) primers and ORF109RGD2 (GCGCCTGCAGCGTTAAGATTGCGC)/AcORF119R (see Figure 7.10) primers. These fragments were then used in the cross over PCR with the fragments containing mutated RGD coding regions and AcORF119F/AcORF119R primers to generate the complete *pif1*, which was then inserted into pGEM-T vector and sequenced.

B, The pAcUW21 baculovirus transfer vector was modified using standard techniques to remove the *p10* promoter and replace it with primer generated fragment that contained the restriction sites required for the later insertion of the *pif1* coding region.

C, The *pif1* coding regions were subcloned from the pGEM-T vector into the *Apal* and *SacI* sites of the modified pAcUW21^{Δp10}. This baculovirus transfer vector would restore polyhedrin production and allow the insertion of *pif1* under the control of its own promoter into the baculovirus genome at the *polh* locus through homologous recombination in insect cells.



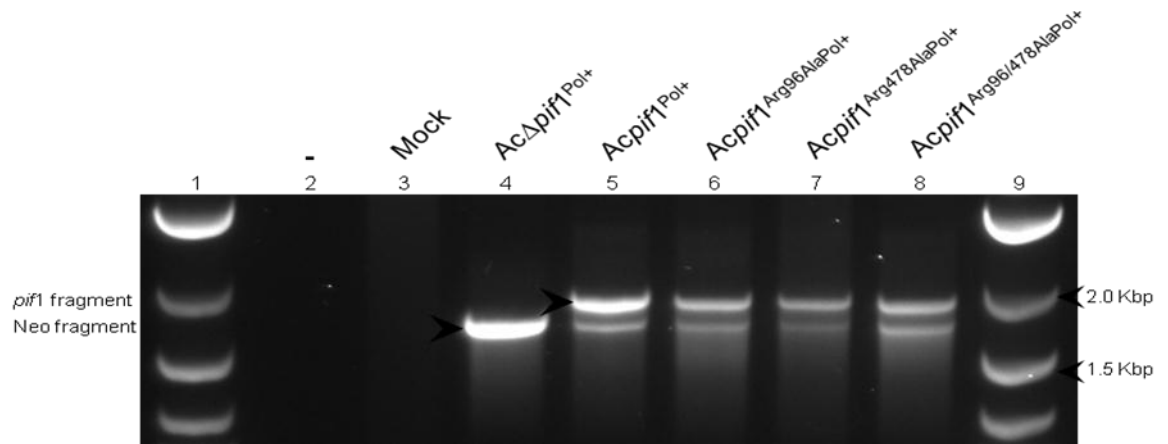


Figure 7.13 PCR analysis of recombinant virus DNA from *pif1* mutants

DNA was isolated from virus-infected cells and analysed by PCR using primers AcORF119F/AcORF119R. Lanes 1 and 9, NEB log2 Marker (Kbp); lane 2, water only negative control; lane 3, mock infected cells control; lane 4, positive control virus *AcΔpif1*^{Pol+}; lanes 5-8, recombinant viruses *Acpif1*^{Pol+}, *Acpif1*^{Arg96AlaPol+}, *Acpif1*^{Arg478AlaPol+} and *Acpif1*^{Arg96/478AlaPol+} respectively.

7.6 Bioassays for *Acpiif1*^{Arg96AlaPol+}, *Acpiif1*^{Arg478AlaPol+} and *Acpiif1*^{Arg96/478AlaPol+}

The BV produced by each polyhedrin positive virus (Table 7.2) was injected into the haemocoel of groups of 50 fourth instar *T. ni* larvae, with each larva receiving 1×10^5 pfu to ensure 100% mortality. The OBs were then purified from the larvae using centrifugation (see methods sections 2.3.9). They were counted using a haemocytometer and assayed by oral infection in third instar *T. ni* larvae at a range of doses to enable calculation of their LD₅₀, LD₉₀ and survival time for each virus (Table 7.2).

Table 7.2 Infectivity of *Acpiif1*^{Arg96AlaPol+}, *Acpiif1*^{Arg478AlaPol+} and *Acpiif1*^{Arg96/478AlaPol+} occlusion bodies

Virus	Lethal dose (OB/larva)			Survival Time	
	LD ₅₀	LD ₉₀	<i>P</i>	hpi±SE	<i>P</i>
AcMNPV	41.2	1085.8		173.5±2.3	
AcΔchitinase ^{Pol+}	46.5	1248.6	0.9885	172.2±2.9	0.7236
<i>Acpiif1</i> ^{Pol+}	32.3	971.9	0.7993	165.0±4.2	0.1479
AcΔ <i>pif1</i> ^{Pol+}	N/A	N/A	N/A	N/A	N/A
<i>Acpiif1</i> ^{Pol+}	32.3	971.9		165.0±4.2	
<i>Acpiif1</i> ^{Arg96AlaPol+}	120.0	2722.8	0.0001	170.2±2.7	0.3029
<i>Acpiif1</i> ^{Arg478AlaPol+}	79.9	2270.4	0.0033	176.9±3.9	0.0402
<i>Acpiif1</i> ^{Arg96/478AlaPol+}	24.3	880.4	0.2259	159.9±4.1	0.3883

Notes: AcΔ*pif1*^{Pol+} values could not be reliably calculated from linear regression due to low mortality rates of larvae orally infected with its OBs.

The lethal dose (LD₅₀ and LD₉₀) values seen in Table 7.2 for each of the viruses tested were determined by linear regression. Chi-square analysis was used to determine the *P* value for AcΔchitinase^{Pol+} compared to AcMNPV and no significant difference was seen between the infectivity of OBs from these two viruses. The same statistical method showed no significant difference between the infectivity of OBs from *Acpiif1*^{Pol+} compared to that of AcΔchitinase^{Pol+}.

However, when the three *pif1* mutant viruses were compared to *Acpiif1*^{Pol+} using the same chi-square analysis a very statistically significant difference was seen between the infectivity of OBs produced from larva infected with *Acpiif1*^{Pol+} compared to *Acpiif1*^{Arg96AlaPol+} and *Acpiif1*^{Arg478AlaPol+} OBs. There was no significant difference seen for *Acpiif1*^{Arg96/478AlaPol+} OBs during this comparison with *Acpiif1*^{Pol+}. The infectivity of these viruses was also compared using Probit analysis (PoloPlus, LeOra Software). This further confirmed the results above suggesting that *Acpiif1*^{Arg96AlaPol+} and *Acpiif1*^{Arg478AlaPol+} oral infectivity was

significantly different to that of *Acpif1*^{Pol+}. However, the Probit analysis did suggest that the relative potency of both *Acpif1*^{Arg96AlaPol+} and *Acpif1*^{Arg478AlaPol+} was the same as *Acpif1*^{Pol+}. Interestingly, this analysis also confirmed there was no significant difference between *Acpif1*^{Arg96/478AlaPol+} and *Acpif1*^{Pol+} oral infectivity.

The survival times in hpi were recorded during this bioassay and student t-test was used to compare survival times between viruses to determine P values. The survival times for *Ac*Δchitinase^{Pol+} were compared to that of *Ac*MNPV and the student t-test showed no significant difference between these two viruses. The survival time for *Ac*Δchitinase^{Pol+} was then compared to *Acpif1*^{Pol+} survival time using the student t-test, which showed no significant difference between the two viruses. Then the survival time for *Acpif1*^{Pol+} was compared to the survival times of the test *pif1* viruses and no significant difference was demonstrated using the student t-test between *Acpif1*^{Pol+} and *Acpif1*^{Arg96AlaPol+} or *Acpif1*^{Arg96/478AlaPol+}. However, a significant difference was shown by the student t-test for *Acpif1*^{Arg478AlaPol+} when compared to *Acpif1*^{Pol+} survival time. Interestingly, when the other two control viruses' survival times were compared to that of the test *pif1* viruses using the student t-test, some differences were observed to those seen using *Acpif1*^{Pol+}. For both *Ac*MNPV and *Ac*Δchitinase^{Pol+} there was no significant difference (P>0.05) seen when compared to *Acpif1*^{Arg478AlaPol+}.

The difference observed for *Acpif1*^{Arg478AlaPol+} survival times could be due to slight increase in mortality rate for *Acpif1*^{Pol+} infected larvae shown in Figure 7.14. This slight increase in mortality rate was also seen for *Acpif1*^{Arg96/478AlaPol+} infected larvae, whereas the other viruses' infected larvae demonstrated mortality rates similar to those seen for *Acpif1*^{Arg478AlaPol+} infected larvae. Therefore, the differences seen in survival times could be due to variation in the bioassay method itself. However, the majority of virus infected larva at the top dose (10⁴ OBs/larva) still died in a narrow window between 5.5-8 days post infection for all of the viruses. Also all viruses caused 100% mortality at their top dose in this bioassay.

In summary, the bioassay suggests that mutating the PIF1 RGD motifs does not affect the replication efficiency of the virus in the host larva. However, single mutations to either PIF1 RGD motifs (*Acpif1*^{Arg96AlaPol+} and *Acpif1*^{Arg478AlaPol+}) did seem to decrease oral infectivity rates of OBs but mutations to both of the PIF1 RGD motifs (*Acpif1*^{Arg96/478AlaPol+}) seem to negate this decrease in oral infectivity.

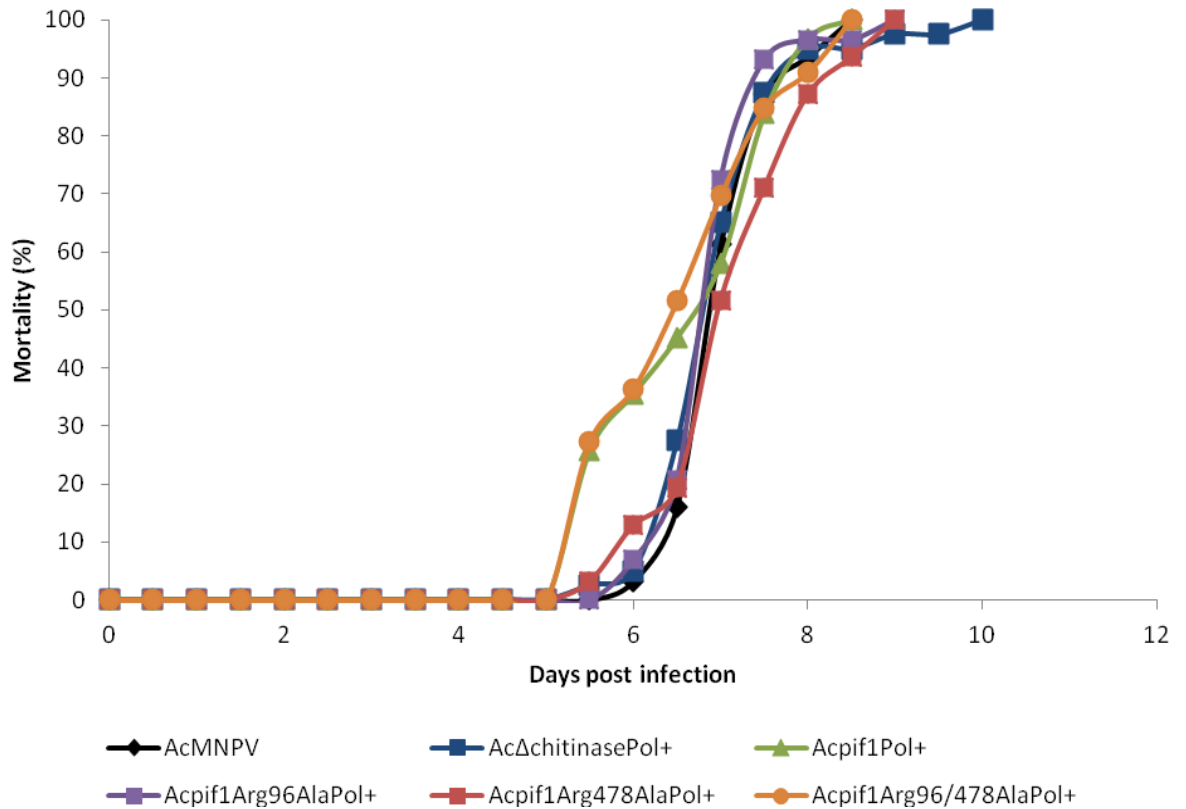


Figure 7.14 Mortality of AcMNPV, AcΔchitinase^{Pol+}, Acpif1^{Pol+}, AcΔpif1^{Pol+}, Acpif1^{Arg96AlaPol+}, Acpif1^{Arg478AlaPol+} and Acpif1^{Arg96/478AlaPol+} infected larvae

The mortality rate of AcMNPV, AcΔchitinase^{Pol+}, Acpif1^{Pol+}, AcΔpif1^{Pol+}, Acpif1^{Arg96AlaPol+}, Acpif1^{Arg478AlaPol+} and Acpif1^{Arg96/478AlaPol+} infected larvae at the top dose (10⁴ OBS/larva) were assessed until all larvae had succumb to viral infection or pupated.

7.7 Discussion

In this chapter the Red/ET recombination system was successfully used to create an *orf118* and *pif1* deletion mutant virus (*AclacZΔorf118/pif1*). This deletion mutant virus was then characterised, with a focus towards any effect the deletion could have on recombinant protein (β -galactosidase) expression. This chapter also contains investigations towards the possible role of the PIF1 RGD motifs in oral infection of larvae, through the use of mutagenesis that resulted in an arginine to alanine change within each RGD motifs (Figure 7.9).

7.7.1 Analysis of the deletion mutant virus; *AclacZΔorf118/pif1*

The deletion of *orf118* and *pif1* in *AclacZΔorf118/pif1* did not significantly affect either BV production or virus infected-cell viability during a time course study. Despite any slight temporal differences between *AclacZΔorf118/pif1* and the two control viruses (parental virus; *AclacZΔchitinase/cathepsin* and wild-type virus; AcBacPAK6), Anova statistical analysis demonstrated that there was no significant difference ($P>0.05$) between these viruses for either BV production or virus infected cell viabilities.

Although, no significant difference was seen when virus infected-cell viabilities were compared during this time course study, there was decrease in *AclacZΔorf118/pif1* infected-cell viability when compared to that of the two control viruses between 24-96hpi, which was not observed for *pif1* deletion mutant virus in a previous study (Gutierrez *et al.*, 2005). This suggests that the decrease in infected-cell viability could be caused by the deletion of *orf118* in *AclacZΔorf118/pif1*.

However, the temporal analysis of virus infection did show a delay in *AclacZΔorf118/pif1* BV production at 24hpi, which wasn't seen for either control virus. When a two-tailed student t-test was used to analyse the 24hpi time point, it demonstrated a significant difference ($P<0.05$) between *AclacZΔorf118/pif1* and *AclacZΔchitinase/cathepsin* titres at this time point. This suggested that the deletion of *orf118*, *pif1* or both altered the BV production kinetics of *AclacZΔorf118/pif1*, but not affected the virus's ability to reach normal titres. Therefore, this observation does not conflict with the literature that shows neither ORF118 nor PIF1 affect virus replication in cell culture (Kikhno *et al.*, 2002; Ohkawa *et al.*, 2005; R.D. Possee, personal communication). However, a delay in BV production was observed with a *pif1* deletion mutant virus and not with an *orf118* deletion mutant virus (R.D. Possee, personal communication), which suggests the *pif1* deletion is the cause of the observed affect here with the double deletion virus.

The effect of deleting *orf118* and *pif1* on recombinant protein production in insect cells was examined using β -galactosidase as a reporter target. This protein was chosen as it allowed easy monitoring of an intracellular protein through activity assays.

Anova statistical analysis was used on the data obtained from the β -galactosidase activity assays, which were carried out on AcBacPAK6, *AdlacZ Δ orf118/pif1* and *AclacZ Δ chitinase/cathepsin* samples from the time course study. This analysis demonstrated that there was no significant difference between any of the viruses total β -galactosidase activities during this time course ($P > 0.05$). However, this is misleading due to a clear difference between all three viruses infected cells β -galactosidase activities at 48hpi, which is being obscured in the Anova statistical analysis due to the similarity of β -galactosidase activity at the remaining time points for all three viruses. Also 48hpi time point will hold more significance than the other time points due to the nature of the *polh* promoter, which has been demonstrated to cause a burst in recombinant protein expression during very late phase of infection (~48hpi) (Ooi *et al.*, 1989). Therefore, single analysis of the 48hpi β -galactosidase activities would give better indication of any effect the deletion of *orf118/pif1* is having on recombinant protein expression from the *polh* promoter.

Therefore, a two-tailed student t-test was used, which showed a significant difference ($P < 0.05$) between the β -galactosidase activity produced at 48hpi when any of the two virus-infected cell pellet values were compared. This demonstrates that the deletion of *orf118* and *pif1* had an overall negative effect on the peak β -galactosidase expression from infected insect cells compared to the parental virus, which was 1.7-fold higher (41.80 u/10⁶ cells). Interestingly, the positive impact of chitinase and cathepsin deletion on recombinant protein expression production was not totally abolished by the deletion of *orf118* and *pif1*, as *AclacZ Δ orf118/pif1* (24.48 u/10⁶ cells) peak β -galactosidase activity was 1.8-fold higher than that observed for AcBacPAK6 (13.75 u/10⁶ cells) during this time course study. This negative effect on the peak β -galactosidase expression caused by the deletion of *orf118* and *pif1* could be due to the deletion of *orf118*. Since a previous study had shown that deletion of *pif1* caused a two-fold increase in chloramphenicol acetyltransferase expression from the polyhedrin promoter when compared to its parental virus (Gutierrez *et al.*, 2005).

After the peak β -galactosidase activity at 48hpi for all three virus-infected cell samples, there was a rapid decrease in their β -galactosidase activities. This decrease in β -galactosidase activity does coincide with a decline in cell viability and increase of β -galactosidase activity within the medium samples of each virus infected cell culture. This activity increase in the medium sample is due to the decline in cell viability, as intracellular

β -galactosidase is lost from the dying cells. However, the overall loss of β -galactosidase activity from the infected cell pellet samples isn't seen as an increase in β -galactosidase activity for the medium samples, for any of the virus infected cultures examined here. This could suggest that β -galactosidase is being degraded from either a combination of the culture conditions, the accumulation of β -galactosidase or proteases from lysed cells.

It would be interesting to investigate the effect of *orf118* and *pif1* deletion on recombinant proteins expressed from different viral promoters such as the late *p6.9* promoter, to observe any effect this deletion could have on recombinant protein expression from different time points. The effect of *orf118* and *pif1* deletion on extracellular recombinant protein expression could also be investigated to observe any differences there could be between the expression of intracellular and extracellular recombinant proteins.

7.7.2 Characterisation summary for *pif1* mutant viruses

The initial strategy to construct the *pif1* mutant viruses proved unsuccessful. However, the *pif1* mutant viruses were constructed using an alternative strategy involving the bacmid *AcBAC Δ pif1*, which is non-infectious in insect cells. *AcBAC Δ pif1* was rescued in insect cells with a transfer vector containing RGD-mutated *pif1* and polyhedrin, which resulted in viruses containing the different RGD-mutated *pif1* that did not require plaque-purification from parental virus. OBs for the RGD-mutated *pif1* viruses and several control viruses were obtained by injecting fourth instar *T. ni* larvae in the haemocoel with 1×10^5 pfu and then purifying the resulting OBs for use in the bioassay. The bioassay suggested that none of the RGD-mutated *pif1* viruses affected the replication efficiency of the virus in the host larva when compared to the control viruses. Both *Acpif1*^{Arg96AlaPol+} and *Acpif1*^{Arg478AlaPol+} OBs seemed to have decreased oral infectivity rates when compared to their parental virus; *Acpif1*^{Pol+}. However, *Acpif1*^{Arg96/478AlaPol+} OBs oral infectivity seems unaffected, which suggests that the negative effect seen with the single PIF1 RGD motif mutates is negated when both PIF1 RGD motifs are mutated.

7.7.3 Analysis of the PIF1 RGD motif mutant viruses

It was demonstrated that individual mutations of PIF1 RGD motifs affected *per os* infectivity of OBs fed to third instar *T. ni* larvae. The bioassay showed an approximate 4-fold increase in LD₅₀ when *Acpif1*^{Arg96AlaPol+} (120 OBs per larva) was compared to *Acpif1*^{Pol+} (32 OBs per larvae). For *Acpif1*^{Arg478AlaPol+} there was only a 2.5-fold increase in LD₅₀ (80 OBs per larva) when compared to *Acpif1*^{Pol+} (32 OBs per larvae). However, chi-square

analysis demonstrated these differences in oral infectivity to be very statistically significant when either *Acpif1*^{Arg96AlaPol+} or *Acpif1*^{Arg478AlaPol+} was compared to their parental virus; *Acpif1*^{Pol+}. Therefore, these results suggest that mutation of either PIF1 RGD motifs impacts the function of PIF1 during oral infection, but not to the similar extent of a *pif1* deletion mutant virus that only killed approximately 7% of the larvae at the top dose of 10,000 OBs/larva in the bioassay carried out here.

Interestingly, *Acpif1*^{Arg96/478AlaPol+} LD₅₀ (23 OBs per larvae) was very similar to that of *Acpif1*^{Pol+} (32 OBs per larvae) and the chi-square analysis demonstrated no statistically significant difference when these two viruses were compared. This suggests that mutation of both PIF1 RGD motifs counteracts the negative impact on oral infectivity seen in the viruses containing single mutant PIF1 RGD motif.

There was no significant difference between *Acpif1*^{Arg96AlaPol+} or *Acpif1*^{Arg96/478AlaPol+} and *Acpif1*^{Pol+} survival times at the top dose of 10,000 OBs/larva, which suggests that neither mutated PIF1 has affected the replication efficiency of the virus in the host larva. However, a slight significant difference ($p=0.0402$) between *Acpif1*^{Arg478AlaPol+} and *Acpif1*^{Pol+} survival times was seen, but no significant difference ($p=0.4553$) was demonstrated between *Acpif1*^{Arg478AlaPol+} and AcMNPV survival times. Therefore, *Acpif1*^{Arg478AlaPol+} replication efficiency in the host larva is most likely unaffected by the mutation in the PIF1 RGD motif.

The bioassay data collected does indicate an effect on PIF1 function when either PIF1 RGD motif was disrupted. However, disruption of both PIF1 RGD motifs seems to be slightly beneficial for the virus lowering both its LD₅₀, LD₉₀ and larva survival time. However, further investigation is required to confirm these initial findings on PIF1 RGD motifs and their involvement with PIF1 function and oral infection of larvae. This could involve repeating this bioassay to confirm the initial findings and labelling the ODVs with self-quenching fluorescent probe octadecyl rhodamine B chloride (R-18) to allow binding, fusion and competition assays to be carried out, which will identify any effects the mutant PIF1 RGD motifs have on direct binding and fusion with the larva midgut cells. These assays were done to study other *per os* infectivity proteins (Haas-Stapleton *et al.*, 2004; Ohkawa *et al.*, 2005).

7.7.4 Conclusion

In this chapter the *orf118* and *pif1* deletion mutant virus was constructed and analysed with a focus on recombinant protein production. The results from this work demonstrated

that the deletion of *orf118* and *pif1* caused some temporal differences in cell viability and BV production kinetics when compared to its parental virus. However, these differences were not considered significantly different according to statistical analysis. The deletion of *orf118* and *pif1* did have a negative effect on intracellular recombinant protein production from the *polh* promoter; it would be interesting to see if this deletion or single deletions did affect the native polyhedrin production.

This chapter also investigated through mutagenesis the possible role of the PIF1 RGD motifs in oral infection of larvae. The initial findings suggest that the PIF1 RGD motifs functional role is not very clear, due to disruption of a single PIF1 RGD motif impacts oral infection whereas disruption of both PIF1 RGD motif made the virus slightly more orally infectious. The role of RGD motif in other viruses is also uncertain. The transmembrane glycoprotein E2 from Hepatitis C virus (HCV) contains highly conserved RGD motif and mutagenesis of the E2 RGD motif resulted in greatly reduced HCV infectivity. However, the mutants E2 were still able to bind to the target receptor suggesting that the role of RGD motif does not involve integrin binding (Rothwangl and Rong, 2009). Therefore, PIF1 RGD motifs could mediate other interactions during viral entry and like that of HCV not be involved in integrin binding, which would explain why none of the viruses containing mutations of PIF1 RGD motifs displayed similar characteristics to a *pif1* deletion mutant virus.

Chapter 8

Final Discussion and Future work

8.1 Summary of Thesis

The aims of this PhD were to understand the mechanisms involved in the production of ODV and determine whether the deletion of ODV-specific genes could improve the baculovirus expression vector system (BEVs). To achieve these goals included identifying genes encoding structural components of the ODV that were not associated with BV and which theoretically could be removed from the AcMNPV genome without affecting virus infectivity (Chapter 3). The selected targets (*odv-e66*, *orf79*, *cg30*, *odv-e28*, *pif3*, *odv-e56*, *pif2* and *odv-ec43*) were deleted from the AcMNPV genome using the Red/ET recombination system. Those deletions that unexpectedly prevented virus replication in insect cell culture were characterised further (Chapter 4, *orf79*, *odv-e28*, and *odv-ec43*). The remaining modified viruses with deletions in *odv-e66*, *cg30*, and *odv-e56*, which were viable in insect cell culture and did not contain a deletion of a known *per os* infectivity factor, were investigated for any effect on ODV production and occlusion into the OBs using bioassays and electron microscopy imaging (Chapter 5). Those viruses with deletions of known *pifs* (*pif3* and *pif2*) were analysed for any effect on recombinant protein production. Unexpectedly, the *pif3* deletion mutant virus was defective in BV production and so the cause of this was investigated (Chapter 6). The Red/ET recombination system was also used to construct a ninth deletion mutant virus lacking both auxiliary genes; *orf118* and *pif1*. The effect of this deletion on recombinant protein production was investigated. In addition, the RGD motifs of PIF1 were investigated for any possible role they might have in the functional aspect of PIF1 during oral infection of larva (Chapter 7). While the mechanism involved in the production of ODV was not elucidated, a number of interesting observations have been made about the targeted structural components of the ODV.

The deletion mutant viruses (*AcΔorf79*, *AcΔodv-e28* and *AcΔodv-ec43*) characterised in chapter 4 were non-infectious in insect cell culture. Further analysis demonstrated that *orf78*, *orf79* and *odv-ec43* most likely comprise essential genes. During this investigation no further information on the roles of *orf78* or *orf79* were uncovered. However, data was obtained indicating that *odv-ec43* most likely plays a role in the processing of the BV particle. The non-viability of *AcΔodv-e28* in insect cell culture was the result of interruption to an essential neighboring gene (*helicase*) and not the deletion of *odv-e28*. Overall these results demonstrated that deleting genes from AcMNPV genome, which contains overlapping ORFs and promoters, can cause unforeseen problems. The results also highlight that structural components of the ODV such as *orf79* and *odv-ec43* could play a role in

multiple processes during viral replication, and thus both be essential for viral replication and located to the ODV.

The deletion mutant viruses, *AcΔodv-e66*, *AcΔcg30* and *AcΔodv-e56* were characterized in chapter 5, which demonstrated that all three deletion mutant viruses had slightly decreased BV production compared to their parental virus. Interestingly, the deletion of *odv-e56* altered the overall BV production kinetics of the virus during a time course study. This further suggests that structural components of the ODV are not just involved in ODV production during viral replication. Bioassays and electron microscopy imaging were used to analyse ODV production and occlusion into the OBs for each of the deletion mutant viruses. Both the deletions of *odv-e66* and *odv-e56* negatively affected oral infectivity of OBs, furthermore *AcΔodv-e56* OBs seemed wrapped in an unidentified protein, which is most likely the polyhedra associated protein P10 (Lee *et al.*, 1996; Patmanidi *et al.*, 2003; Carpentier *et al.*, 2008), whereas *AcΔodv-e66* OBs seemed normal under electron microscopy. The deletion of *cg30* increased the oral infectivity of OBs while electron microscopy imaging of *AcΔcg30* OBs suggested that the PE had not formed correctly causing the OBs to be deformed and degraded. Alternatively, the aberrant OB structure might have affected application of the PE their outer surface. These results suggest that both ODV-E56 and CG30 effect on oral infectivity could be due to abnormalities of the OBs and possibly to the ODV, whereas ODV-E66 effect on oral infectivity could be due to abnormalities isolated to the ODV.

Some investigations towards the effect of *pif2* and *orf118/pif1* deletions on recombinant protein yield were undertaken in chapters 6 and 7, respectively. Both of these deletions were demonstrated to have a negative effect on intracellular recombinant protein (β -galactosidase) expression from the *polh* promoter, whereas the *pif2* deletion was shown not to impact the expression of extracellular recombinant protein (urokinase). Interestingly, the deletion of *orf118/pif1* altered the viruses BV production kinetics at 24hpi but did not affect the virus's ability to attain normal titres at the end of a time course. The cause of this observation was most likely due to the deletion of *pif1*, as this altered BV production kinetics has been demonstrated previously with a *pif1* deletion mutant virus (R.D. Possee, personal communication). The *AcΔpif3* was observed to have low titres due to reduced BV production and further analysis carried out in chapter 6 suggests the most likely cause of this observation to be the deletion of *pif3* itself. Chapter 7 investigated through mutagenesis the possible role of the PIF1 RGD motifs in oral infection of larvae. However, this investigation did not clearly elucidate the functional role of PIF1 RGD motifs but did indicate the motifs were most likely not involved in integrin binding and further

experimental work is required to understand the role(s) these PIF1 RGD motifs could play during oral infection of larvae.

8.2 Discussion of thesis results and future work

It is apparent from the studies described in this thesis that they do not support the hypothesis that all genes encoding structural proteins of the ODV can be deleted from AcMNPV without affecting BV production kinetics. Furthermore, those deletion mutant viruses that were tested for recombinant protein expression did not have an advantage for recombinant protein production. From a virus evolution perspective this may be explained if the genes encoding structural proteins of the ODV were acquired prior to the development of this virion phenotype and thus had functional roles involving earlier stages of baculovirus replication. Therefore, there may not be a population of genes involved in ODV formation within the AcMNPV genome that can be readily deleted without affecting BV production.

8.2.1 Construction of deletion mutant viruses

Construction and analysis of AcMNPV gene deletion mutants is problematic due to the closely packed nature of the ORFs with over-lapping promoters (Figure 8.1). Therefore, deletion sites have to be carefully selected to avoid affecting neighbouring genes. It would be ideal to have a thorough knowledge of gene transcription and termination in the regions flanking the deletion site to prevent this, but in many cases this information isn't available. However, due to more modern techniques such as 5' RACE analysis mapping transcription start sites along with simple sequencing of the 3' ends of mRNAs via cDNA synthesis and cloning, this information can be obtained relatively easy before performing any deletions on the AcMNPV genome.

Once this information is obtained the target site for deletion can be selected and deleted using similar strategies to the ones performed in this thesis. This involves a different Red/ET recombination system that contains a counter-selection marker (Counter Selection BAC Modification Kit, Gene Bridge). This system is essentially the same as the one used in this study to construct the deletion mutant viruses. However, the coding region of interest is deleted by the insertion of a kanamycin gene fragment with the addition of the *rpsL* gene. The *rpsL* gene expresses wild type S12 ribosomal protein, which causes streptomycin resistant *E. coli* strains that contain mutant *rpsL* genes to become streptomycin sensitive. This allows a secondary recombination stage, which is used to replace the whole kanamycin insert with a different DNA fragment. The insertion

of the new DNA fragment causes the loss of the *rpsL* gene within the bacmid allowing the *E. coli* containing these recombinant bacmids to be isolated by streptomycin resistance. Therefore, if the deletion of the target region proves to be lethal for virus replication, a gene rescue using this system could be attempted applying a modified version of the target sequences in which the putative translation initiation codon was mutated to a non functional triplet.

This strategy would overcome the problem seen with deletions such as *AcΔorf79* or *AcΔodv-e28* that affected the neighbouring gene(s) and ensure the removal of the target protein expression from the virus-infected cells. However, care would have to be taken with the mutation of the ATG to ensure any involvement it could have in regulatory role for upstream or downstream genes was not affected, for example if it coincided with a promoter motif. Another target for mutation could be the transcription start site(s) of the gene of interest but the same precautions would have to be taken as with the ATG mutation not to affect neighbouring genes regulation or amino acid sequence as most promoters are within neighbouring genes mRNA sequence.

Figure 8.1 Circular map of the AcMNPV genome.

Schematic representation of the AcMNPV genome, demonstrating the over-lapping nature of genes contain within the AcMNPV genome (Ayres *et al.*, 1994).

8.2.2 Construction of Synthetic virus

A different strategy involving the construction of a synthetic virus could be taken to elucidate the transition from BV to polyhedra production. Synthetic biology has advanced since the first synthetic virus was constructed by Cello *et al.* (2002), allowing synthesis of an entire bacterial genome (Gibson *et al.*, 2008). Therefore, this technology along with the availability of yeast and bacteria vectors for maintaining large circular plasmids in these hosts, would allow construction of a synthetic baculovirus genome. However, a literature review would be required first to identify all of the known essential baculovirus genes for viral replication in insect cell culture. These would be used to construct the core of the initial synthetic virus and rather than making gene deletions, instead gene additions would be used to create a viable virus. The viability of the viruses could be easily accessed by the production of plaques during plaque assays. Once a functional virus was constructed, examination of its genome compared to AcMNPV could be undertaken to identify any key genes involved in ODV production and occlusion.

8.2.3 Construction of Insect expression vector

The BEVs is widely used for the production of recombinant proteins in insect cell culture. However, the system cannot provide long term expression of recombinant proteins from a single culture due to the lytic properties of the virus. Therefore, an alternative system that could allow long term expression from insect culture using the strong *polh* promoter would be ideal. One strategy might be the construction of a stable expression vector, which contained all of baculovirus genes that encoded the machinery necessary to express the *polh* promoter. The stable expression vector could be constructed using similar techniques to those described in section 8.2.2. However, this stable expression vector would be rather large and most likely unstable in the insect cells. For example, a standard stable expression vector (~6.3 kbp) that contained just the family of late expression factor genes alone would be roughly 19 kbp.

Therefore, using the same principle as before, a second strategy would attempt to integrate the viral sequences into the insect cell genome using transposons. The insect cell transposons are capable of integrating sequences to and from baculovirus genome and thus this strategy could work using plasmids containing viral sequences in between two transposons recognised by the insect cell (Wang and Fraser, 1993; Fraser *et al.*, 1996)). This would reduce the size of the stable expression vector that could just contain the recombinant protein under the control of the *polh* promoter. The modified insect cell

line could then be used to express a number of recombinant proteins using different stable expression vectors. The stable expression vector could be further modified to contain transcriptional regulator, which would allow the timing of recombinant protein expression from the insect cell culture to be controlled. This transcriptional regulator could be similar to the operon used in the pRedET plasmid.

8.2.4 Analysis of AcMNPV to other occluded viruses

The evolution of an occlusion viral particle that allows delayed transmission has appeared in two other insect-infecting virus taxa: the Entomopoxvirinae subfamily of the Poxviridae and the Cypovirus genus of the *Reoviridae* family (Rohrmann, 1986; Adams and Bonami, 1991). Therefore, the literature review and bioinformatic analysis that was performed in Chapter 3 on genes associated with the AcMNPV ODV could be expanded to compare the AcMNPV genome with that of Entomopoxvirinae and Cypovirus members. This could identify key proteins involved in either BV production or ODV production/occlusion due to none of the other occluded insect virus families containing two virion phenotypes, which is unique to the Baculoviridae family.

The literature contains information on baculoviruses, whose replication seem confined to the midgut like that of the cypoviruses. These include NPVs of Diptera, Hymenoptera, and certain types of GVs (Federici and Stern, 1990; Moser *et al.*, 2001), which causes the OBs to be excreted in the insects faeces (Federici, 1997). Therefore, comparing the AcMNPV genome with these baculoviruses could also highlight key proteins involved in either BV production or ODV production/occlusion due to the undeveloped BV form. Any key targets identified for ODV production or occlusion during these two comparisons could then be investigated using the experimental methods out line in this thesis.

8.3 Concluding remarks

After over three decades of research into baculoviruses at the molecular level the major transition from BV to ODV production during the baculovirus infection has still not been resolved. The understanding of this transition is hindered due the number of baculovirus proteins whose roles are still not fully understood, due the complexity of the baculovirus replication cycle and multifunctional role of many of these proteins. This study highlights the possible multifunctional role of viral proteins due to the deletion of structural components of the ODV affecting the viruses BV production kinetics. It strongly suggests that the production of BV and ODV could be closely linked and any transition that exists

could be due to slight changes in both virus and cellular components during viral replication. Furthermore the studies on this transition are difficult due to the uniqueness of these two virion phenotypes in one virus, meaning there is no other insect infecting virus to compare with baculovirus that may allow the identification of key genes that could be involved in this process.

A deeper understanding of the virogenic stroma where viral transcription (Passarelli and Guarino, 2007), DNA replication (Carstens, 2009), and progeny nucleocapsid assembly (Volkman, 1988) occur, could give insight into this transition. However, studies of the virogenic stroma are difficult due to it being essential for viral replication. Therefore, the mechanisms involving the assembly, DNA packaging, and egress of progeny nucleocapsids are not well defined.

Interestingly, two deletion mutant viruses; $\Delta vp80$ (Marek *et al.*, 2011) and $\Delta orf66$ (Ke *et al.*, 2008), which interact with the cellular filamentous-actin (F-actin) cytoskeleton demonstrated a defect in both BV and ODV production due to failure in nucleocapsid transport within the nucleus. It has been demonstrated that the F-actin cytoskeleton forms a highly organized three-dimensional network connecting the virogenic stroma physically with the nuclear envelope. This interaction is virus driven and required for the transport of nucleocapsids to the periphery of the nucleus where they are directed towards the plasma membrane for BV production or in later stages of infection held in the periphery of the nucleus to form ODV (Ohkawa and Volkman, 1999; Marek *et al.*, 2011). Therefore, a study that monitored the interaction of the insect cells cytoskeleton with virogenic stroma could give insights into the changes occurring during viral replication, which could cause the transition from BV to ODV production. If the transition was caused by rearrangement of the insect cells cytoskeleton either within the nucleus or the cytoplasm, further investigations using standard molecular techniques would then be required in attempts to identify the viral protein(s) causing this rearrangement.

Until a deeper understanding of the molecular workings of the baculovirus replication cycle is obtained, the transition of BV to ODV production will remain a mystery. It is a subject deserving of future study.

References

- Abbas, M. and Boucias, D. G. (1984). Interaction between nuclear polyhedrosis virus-infected *Anticarsia gemmatalis* (Lepidoptera: *Noctuidae*) larvae and predator *Podisus maculiventris* (Say) (Hemiptera: *Pentatomidae*). *Environ. Entomol* 13 (2), pp.599-602.
- Ackermann, H. W. and Smirnov, W. A. (1983). A morphological investigation of 23 baculoviruses. *Journal of Invertebrate Pathology* 41 (3), pp.269-280.
- Adam, J. R. and McClintock, J. T. (1991). *Baculoviridae*, nuclear *poluhedrosis* viruses Part 1. Nuclear polyhedrosis viruses of insects. In "Atlas of Invertebrate Viruses" (J. R. Adams and J. R. Bonami, eds), Chapter 6, pp. 87-180. CRC Press, Boca Raton
- Adams, J. R. and Bonami, J. R. (1991). Atlas of invertebrate viruses. In "Atlas of Invertebrate Viruses" (J. R. Adams and J. R. Bonami, eds.). CRC Press, Boca Raton.
- Alber, F., Dokudovskaya, S., Veenhoff, L. M., Zhang, W., Kipper, J., Devos, D., Suprpto, A., Karni-Schmidt, O., Williams, R., Chait, B. T., Rout, M. P. and Sali, A. (2007). Determining the architectures of macromolecular assemblies. *Nature* 450 (7170), pp.683-694.
- Andreadis, T. G., Becnel, J. J. and White, S. E. (2003). Infectivity and pathogenicity of a novel baculovirus, CuniNPV from *Culex nigripalpus* (Diptera: *Culicidae*) for thirteen species and four genera of mosquitoes. *J Med Entomol* 40 (4), pp.512-517.
- Aravind, L., Walker, D. R. and Koonin, E. V. (1999). Conserved domains in DNA repair proteins and evolution of repair systems. *Nucleic Acids Res* 27 (5), pp.1223-1242.
- Ashida, H., Mimuro, H., Ogawa, M., Kobayashi, T., Sanada, T., Kim, M. and Sasakawa, C. (2011). Cell death and infection: a double-edged sword for host and pathogen survival. *J Cell Biol* 195 (6), pp.931-942.
- Ayres, M. D., Howard, S. C., Kuzio, J., Lopez-Ferber, M. and Possee, R. D. (1994). The complete DNA sequence of *Autographa californica* nuclear polyhedrosis virus. *Virology* 202 (2), pp.586-605.
- Bao, Y., Federhen, S., Leipe, D., Pham, V., Resenchuk, S., Rozanov, M., Tatusov, R. and Tatusova, T. (2004). National center for biotechnology information viral genomes project. *J Virol* 78 (14), pp.7291-7298.
- Barbehenn, R. V. and Martin, M. M. (1995). Peritrophic envelope permeability in herbivorous insects. *Journal of Insect Physiology* 41 (4), pp.303-311.
- Bass, D. M., Baylor, M. R., Chen, C., Mackow, E. M., Bremont, M. and Greenberg, H. B. (1992). Liposome-mediated transfection of intact viral particles reveals that plasma membrane penetration determines permissivity of tissue culture cells to rotavirus. *J Clin Invest* 90 (6), pp.2313-2320.
- Belyavskiy, M., Braunagel, S. C. and Summers, M. D. (1998). The structural protein ODV-EC27 of *Autographa californica* nucleopolyhedrovirus is a multifunctional viral cyclin. *Proc Natl Acad Sci U S A* 95 (19), pp.11205-11210.
- Bergold, G. H. (1953). Insect viruses. *Advances in Virus Research* 1, pp.91-139.
- Bergold, G. H. (1963). The nature of nuclear polyhedrosis viruses. In "Insect Pathology: An Advance Treatise" (E. A. Steinhaus, ed.), pp. 413-455. Academic Press, New York.
- Bilimoria, S. L. (1991). The biology of nuclear polyhedrosis viruses. In "Viruses of Invertebrates" (E. Kurstak, ed.), pp. 1-60. Marcel Dekker Inc., New York. .
- Blissard, G. W., Quant-Russell, R. L., Rohrmann, G. F. and Beaudreau, G. S. (1989). Nucleotide sequence, transcriptional mapping, and temporal expression of the gene encoding p39, a major structural protein of the multicapsid nuclear polyhedrosis virus of *Orgyia pseudotsugata*. *Virology* 168 (2), pp.354-362.
- Blissard, G. W. and Rohrmann, G. F. (1989). Location, sequence, transcriptional mapping, and temporal expression of the gp64 envelope glycoprotein gene of the *Orgyia pseudotsugata* multicapsid nuclear polyhedrosis virus. *Virology* 170 (2), pp.537-555.

-
- Bonning, B. C. and Hammock, B. D. (1992). Development and potential of genetically engineered viral insecticides. *Biotechnol Genet Eng Rev* 10, pp.455-489.
- Boucias, D. G. and Pendland, J. C. (1998). Baculoviruses. In "Principles of Insect Pathology," pp. 111-146. Kluwer Academic Publishers, Norwell.
- Boutell, C. and Everett, R. D. (2003). The herpes simplex virus type 1 (HSV-1) regulatory protein ICP0 interacts with and Ubiquitinates p53. *J Biol Chem* 278 (38), pp.36596-36602.
- Boyce, F. M. and Bucher, N. L. (1996). Baculovirus-mediated gene transfer into mammalian cells. *Proc Natl Acad Sci U S A* 93 (6), pp.2348-2352.
- Braunagel, S. C., Burks, J. K., Rosas-Acosta, G., Harrison, R. L., Ma, H. and Summers, M. D. (1999). Mutations within the *Autographa californica* nucleopolyhedrovirus FP25K gene decrease the accumulation of ODV-E66 and alter its intranuclear transport. *J Virol* 73 (10), pp.8559-8570.
- Braunagel, S. C., Elton, D. M., Ma, H. and Summers, M. D. (1996). Identification and analysis of an *Autographa californica* nuclear polyhedrosis virus structural protein of the occlusion-derived virus envelope: ODV-E56. *Virology* 217 (1), pp.97-110.
- Braunagel, S. C., Guidry, P. A., Rosas-Acosta, G., Engelking, L. and Summers, M. D. (2001). Identification of BV/ODV-C42, an *Autographa californica* nucleopolyhedrovirus orf101-encoded structural protein detected in infected-cell complexes with ODV-EC27 and p78/83. *J Virol* 75 (24), pp.12331-12338.
- Braunagel, S. C., Russell, W. K., Rosas-Acosta, G., Russell, D. H. and Summers, M. D. (2003). Determination of the protein composition of the occlusion-derived virus of *Autographa californica* nucleopolyhedrovirus. *Proc Natl Acad Sci U S A* 100 (17), pp.9797-9802.
- Braunagel, S. C. and Summers, M. D. (1994). *Autographa californica* nuclear polyhedrosis virus, PDV, and ECV viral envelopes and nucleocapsids: structural proteins, antigens, lipid and fatty acid profiles. *Virology* 202 (1), pp.315-328.
- Braunagel, S. C. and Summers, M. D. (2007). Molecular biology of the baculovirus occlusion-derived virus envelope. *Curr Drug Targets* 8 (10), pp.1084-1095.
- Braunagel, S. C., Williamson, S. T., Saksena, S., Zhong, Z., Russell, W. K., Russell, D. H. and Summers, M. D. (2004). Trafficking of ODV-E66 is mediated via a sorting motif and other viral proteins: facilitated trafficking to the inner nuclear membrane. *Proc Natl Acad Sci U S A* 101 (22), pp.8372-8377.
- Brown, M., Crawford, A. M. and Faulkner, P. (1979). Genetic Analysis of a Baculovirus, *Autographa californica* Nuclear Polyhedrosis Virus I. Isolation of Temperature-Sensitive Mutants and Assortment into Complementation Groups. *J Virol* 31 (1), pp.190-198.
- Bull, J. C., Godfray, H. C. and O'Reilly, D. R. (2001). Persistence of an occlusion-negative recombinant nucleopolyhedrovirus in *Trichoplusia ni* indicates high multiplicity of cellular infection. *Appl Environ Microbiol* 67 (11), pp.5204-5209.
- Burks, J. K., Summers, M. D. and Braunagel, S. C. (2007). BV/ODV-E26: a palmitoylated, multifunctional structural protein of *Autographa californica* nucleopolyhedrovirus. *Virology* 361 (1), pp.194-203.
- Carbonell, L. F., Klowden, M. J. and Miller, L. K. (1985). Baculovirus-mediated expression of bacterial genes in dipteran and mammalian cells. *J Virol* 56 (1), pp.153-160.
- Carpentier, D. and King, L. A. (2009). The long road to understanding the baculovirus P10 protein. *Virologica Sinica* 24, pp.227-242.
- Carpentier, D. C., Griffiths, C. M. and King, L. A. (2008). The baculovirus P10 protein of *Autographa californica* nucleopolyhedrovirus forms two distinct cytoskeletal-like structures and associates with polyhedral occlusion bodies during infection. *Virology* 371 (2), pp.278-291.
- Carstens, E. (2009). AcMNPV as a model for baculovirus DNA replication. *Virologica Sinica* 24 (4), pp.243-267.
- Carstens, E. B., Chan, H., Yu, H., Williams, G. V. and Casselman, R. (1994). Genetic analyses of temperature-sensitive mutations in baculovirus late expression factors.

-
- Virology* 204 (1), pp.323-337.
- Carstens, E. B., Williams, G. V., Faulkner, P. and Partington, S. (1992). Analysis of polyhedra morphology mutants of *Autographa californica* nuclear polyhedrosis virus: molecular and ultrastructural features. *J Gen Virol* 73 (Pt 6), pp.1471-1479.
- Cass, L. G. and Wilcox, G. (1988). Novel activation of *araC* expression and a DNA site required for *araC* autoregulation in *Escherichia coli* B/r. *J Bacteriol* 170 (9), pp.4174-4180.
- Cello, J., Paul, A. V. and Wimmer, E. (2002). Chemical synthesis of poliovirus cDNA: generation of infectious virus in the absence of natural template. *Science* 297 (5583), pp.1016-1018.
- Chang, M. J. and Blissard, G. W. (1997). Baculovirus *gp64* gene expression: negative regulation by a minicistron. *J Virol* 71 (10), pp.7448-7460.
- Charlton, C. A. and Volkman, L. E. (1991). Sequential rearrangement and nuclear polymerization of actin in baculovirus-infected *Spodoptera frugiperda* cells. *J Virol* 65 (3), pp.1219-1227.
- Chartrand, P., Wilkie, N. M. and Timbury, M. C. (1981). Physical mapping of temperature-sensitive mutations of herpes simplex virus type 2 by marker rescue. *J Gen Virol* 52 (Pt 1), pp.121-133.
- Chisholm, G. E. and Henner, D. J. (1988). Multiple early transcripts and splicing of the *Autographa californica* nuclear polyhedrosis virus IE-1 gene. *J Virol* 62 (9), pp.3193-3200.
- Clavijo, G., Williams, T., Munoz, D., Caballero, P. and Lopez-Ferber, M. (2010). Mixed genotype transmission bodies and virions contribute to the maintenance of diversity in an insect virus. *Proc Biol Sci* 277 (1683), pp.943-951.
- Clavijo, G., Williams, T., Simon, O., Munoz, D., Cerutti, M., Lopez-Ferber, M. and Caballero, P. (2009). Mixtures of complete and *pif1*- and *pif2*-deficient genotypes are required for increased potency of an insect nucleopolyhedrovirus. *J Virol* 83 (10), pp.5127-5136.
- Clem, R. J. (2007). Baculoviruses and apoptosis: a diversity of genes and responses. *Curr Drug Targets* 8 (10), pp.1069-1074.
- Clem, R. J., Fechheimer, M. and Miller, L. K. (1991). Prevention of apoptosis by a baculovirus gene during infection of insect cells. *Science* 254 (5036), pp.1388-1390.
- Clem, R. J. and Miller, L. K. (1994). Control of programmed cell death by the baculovirus genes *p35* and *iap*. *Mol Cell Biol* 14 (8), pp.5212-5222.
- Collot-Teixeira, S., Bass, J., Denis, F. and Ranger-Rogez, S. (2004). Human tumor suppressor *p53* and DNA viruses. *Rev Med Virol* 14 (5), pp.301-319.
- Condreay, J. P. and Kost, T. A. (2007). Baculovirus expression vectors for insect and mammalian cells. *Curr Drug Targets* 8 (10), pp.1126-1131.
- Cook, S. P., Webb, R. E., Podgwaite, J. D. and Reardon, R. C. (2003). Increased mortality of gypsy moth *Lymantria dispar* (L.) (Lepidoptera: *Lymantriidae*) exposed to gypsy moth nuclear polyhedrosis virus in combination with the phenolic glycoside salicin. *J Econ Entomol* 96 (6), pp.1662-1667.
- Cory, J. S., Green, B. M., Paul, R. K. and Hunter-Fujita, F. (2005). Genotypic and phenotypic diversity of a baculovirus population within an individual insect host. *J Invertebr Pathol* 89 (2), pp.101-111.
- D'Souza, S. E., Ginsberg, M. H. and Plow, E. F. (1991). Arginyl-glycyl-aspartic acid (RGD): a cell adhesion motif. *Trends in Biochemical Sciences* 16 (0), pp.246-250.
- Danquah, J. O., Botchway, S., Jeshtadi, A. and King, L. A. (2012). Direct interaction of baculovirus capsid proteins VP39 and EXON0 with kinesin-1 in insect cells determined by fluorescence resonance energy transfer-fluorescence lifetime imaging microscopy. *J Virol* 86 (2), pp.844-853.
- Dong, S., Wang, M., Qiu, Z., Deng, F., Vlak, J. M., Hu, Z. and Wang, H. (2010). *Autographa californica* multicapsid nucleopolyhedrovirus efficiently infects Sf9 cells and transduces mammalian cells via direct fusion with the plasma membrane at

-
- low pH. *J Virol* 84 (10), pp.5351-5359.
- Dornan, S., Jackson, A. P. and Gay, N. J. (1997). Alpha-adaptin, a marker for endocytosis, is expressed in complex patterns during *Drosophila* development. *Mol Biol Cell* 8 (8), pp.1391-1403.
- Eckelman, B. P., Salvesen, G. S. and Scott, F. L. (2006). Human inhibitor of apoptosis proteins: why XIAP is the black sheep of the family. *EMBO Rep* 7 (10), pp.988-994.
- Engelhard, E. K., Kam-Morgan, L. N., Washburn, J. O. and Volkman, L. E. (1994). The insect tracheal system: a conduit for the systemic spread of *Autographa californica* M nuclear polyhedrosis virus. *Proc Natl Acad Sci U S A* 91 (8), pp.3224-3227.
- Engelhard, E. K. and Volkman, L. E. (1995). Developmental resistance in fourth instar *Trichoplusia ni* orally inoculated with *Autographa californica* M nuclear polyhedrosis virus. *Virology* 209 (2), pp.384-389.
- Escribano, A., Williams, T., Goulson, D., Cave, R. D., Chapman, J. W. and Caballero, P. (1999). Selection of a nucleopolyhedrovirus for control of *Spodoptera frugiperda* (Lepidoptera: Noctuidae): structural, genetic, and biological comparison of four isolates from the Americas. *J Econ Entomol* 92 (5), pp.1079-1085.
- Falcon, L. A. and Hess, R. T. (1985). Electron microscope observations of multiple occluded virions in the granulosis virus of the codling moth, *Cydia pomonella*. *Journal of Invertebrate Pathology* 45 (3), pp.356-359.
- Fang, M., Nie, Y., Harris, S., Erlandson, M. A. and Theilmann, D. A. (2009). *Autographa californica* multiple nucleopolyhedrovirus core gene ac96 encodes a per Os infectivity factor (PIF-4). *J Virol* 83 (23), pp.12569-12578.
- Fang, M., Wang, H., Wang, H., Yuan, L., Chen, X., Vlak, J. M. and Hu, Z. (2003). Open reading frame 94 of *Helicoverpa armigera* single nucleocapsid nucleopolyhedrovirus encodes a novel conserved occlusion-derived virion protein, ODV-EC43. *J Gen Virol* 84 (Pt 11), pp.3021-3027.
- Faulkner, P., Kuzio, J., Williams, G. V. and Wilson, J. A. (1997). Analysis of p74, a PDV envelope protein of *Autographa californica* nucleopolyhedrovirus required for occlusion body infectivity in vivo. *J Gen Virol* 78 (Pt 12), pp.3091-3100.
- Federici, B. A. (1997). Baculovirus Pathogenesis (L. K. Miller, eds) . In "The Baculoviruses" , Chapter 3, pp. 33-56. Plenum Press, New York.
- Federici, B. A. and Stern, V. M. (1990). Replication and occlusion of a granulosis virus in larval and adult midgut epithelium of the western grapeleaf skeletonizer, *Harrisina brillians*. *Journal of Invertebrate Pathology* 56 (3), pp.401-414.
- Fornwald, J. A., Lu, Q., Wang, D. and Ames, R. S. (2007). Gene expression in mammalian cells using BacMam, a modified baculovirus system. *Methods Mol Biol* 388, pp.95-114.
- Fraiser, M. J. (1986). Ultrastructural observations of virion maturation in *Autographica californica* nuclear polyhedra virus infected *Spodoptera frugiperda* cull cultures. *Journal of Ultrastructure, Molecular Structure Research* 95, pp.189-195.
- Fraser, M. J., Ciszczon, T., Elick, T. and Bauser, C. (1996). Precise excision of TTAA-specific lepidopteran transposons piggyBac (IFP2) and tagalong (TFP3) from the baculovirus genome in cell lines from two species of Lepidoptera. *Insect Mol Biol* 5 (2), pp.141-151.
- Friesen, P. D. and Miller, L. K. (2001). Insect Viruses (B. N. Fields, D. M. Knipe, P. M. Howley, and D E Griffin, eds) . In "Fields Virology 4th edition" , Chapter 21, Vol 1. pp. 707-736. Williams and Wilkins, Lippincott
- Fuchs, Y. and Steller, H. (2011). Programmed Cell Death in Animal Development and Disease. *Cell* 147 (4), pp.742-758.
- Funk, C. J., Braunagel, S. C. and Rohrmann, G. F. (1997). Baculovirus Structure (L. K. Miller, eds) . In "The Baculoviruses" , Chapter 2, pp. 7-27. Plenum Press, New York
- Funk, C. J. and Consigli, R. A. (1993). Phosphate cycling on the basic protein of *Plodia interpunctella* granulosis virus. *Virology* 193 (1), pp.396-402.

- Futaki, S., Suzuki, T., Ohashi, W., Yagami, T., Tanaka, S., Ueda, K. and Sugiura, Y. (2001). Arginine-rich peptides. An abundant source of membrane-permeable peptides having potential as carriers for intracellular protein delivery. *The Journal of biological chemistry* 276 (8), pp.5836-5840.
- Gibson, D. G., Benders, G. A., Andrews-Pfannkoch, C., Denisova, E. A., Baden-Tillson, H., Zaveri, J., Stockwell, T. B., Brownley, A., Thomas, D. W., Algire, M. A., Merryman, C., Young, L., Noskov, V. N., Glass, J. I., Venter, J. C., Hutchison, I. C. A. and Smith, H. O. (2008). Complete chemical synthesis, assembly, and cloning of a *Mycoplasma genitalium* genome. *Science* 319 (5867), pp.1215-1220.
- Gomi, S., Zhou, C. E., Yih, W., Majima, K. and Maeda, S. (1997). Deletion analysis of four of eighteen late gene expression factor gene homologues of the baculovirus, BmNPV. *Virology* 230 (1), pp.35-47.
- Graham, R. I., Tyne, W. I., Possee, R. D., Sait, S. M. and Hails, R. S. (2004). Genetically variable nucleopolyhedroviruses isolated from spatially separate populations of the winter moth *Operophtera brumata* (Lepidoptera: Geometridae) in Orkney. *J Invertebr Pathol* 87 (1), pp.29-38.
- Granados, R. R. (1978). Early events in the infection of *Hiliothis zea* midgut cells by a baculovirus. *Virology* 90 (1), pp.170-174.
- Granados, R. R. and Federici, B. A. (1986). *Introduction: Historical perspective* (G. A. Benz eds) . In "*The Biology of baculoviruses*" , Chapter 1. Boca Raton, Fla.: CRC Press.
- Granados, R. R. and Lawler, K. A. (1981). *In vivo* pathway of *Autographa californica* baculovirus invasion and infection. *Virology* 108 (2), pp.297-308.
- Gross, C. H., Russell, R. L. and Rohrmann, G. F. (1994). *Orgyia pseudotsugata* baculovirus p10 and polyhedron envelope protein genes: analysis of their relative expression levels and role in polyhedron structure. *J Gen Virol* 75 (Pt 5), pp.1115-1123.
- Gross, C. H., Wolgamot, G. M., Russell, R. L., Pearson, M. N. and Rohrmann, G. F. (1993). A baculovirus encoded 16-kDa glycoprotein localizes near the nuclear membrane of infected cells. *Virology* 192 (1), pp.386-390.
- Guarino, L. A., Dong, W., Xu, B., Broussard, D. R., Davis, R. W. and Jarvis, D. L. (1992). Baculovirus phosphoprotein pp31 is associated with virogenic stroma. *J Virol* 66 (12), pp.7113-7120.
- Gutierrez, S., Mutuel, D., Grard, N., Cerutti, M. and Lopez-Ferber, M. (2005). The deletion of the pif gene improves the biosafety of the baculovirus-based technologies. *J Biotechnol* 116 (2), pp.135-143.
- Haas-Stapleton, E. J., Washburn, J. O. and Volkman, L. E. (2004). P74 mediates specific binding of *Autographa californica* M nucleopolyhedrovirus occlusion-derived virus to primary cellular targets in the midgut epithelia of *Heliothis virescens* Larvae. *J Virol* 78 (13), pp.6786-6791.
- Hall, C. V., Jacob, P. E., Ringold, G. M. and Lee, F. (1983). Expression and regulation of *Escherichia coli* lacZ gene fusions in mammalian cells. *J Mol Appl Genet* 2 (1), pp.101-109.
- Harrison, R. and Hoover, K. (2012). Baculoviruses and Other Occluded Insect Viruses. In "Insect Pathology Second Edition" (F. E. Vega and H. K. Kaya, ed.), pp. 74-110. Academic Press, London. .
- Harrison, R. L., Sparks, W. O. and Bonning, B. C. (2010). *Autographa californica* multiple nucleopolyhedrovirus ODV-E56 envelope protein is required for oral infectivity and can be substituted functionally by *Rachiplusia* ou multiple nucleopolyhedrovirus ODV-E56. *J Gen Virol* 91 (Pt 5), pp.1173-1182.
- Hawtin, R. E., Arnold, K., Ayres, M. D., Zanutto, P. M., Howard, S. C., Gooday, G. W., Chappell, L. H., Kitts, P. A., King, L. A. and Possee, R. D. (1995). Identification and preliminary characterization of a chitinase gene in the *Autographa californica* nuclear polyhedrosis virus genome. *Virology* 212 (2), pp.673-685.
- Hawtin, R. E., Zarkowska, T., Arnold, K., Thomas, C. J., Gooday, G. W., King, L. A., Kuzio,

-
- J. A. and Possee, R. D. (1997). Liquefaction of *Autographa californica* nucleopolyhedrovirus-infected insects is dependent on the integrity of virus-encoded chitinase and cathepsin genes. *Virology* 238 (2), pp.243-253.
- Hefferon, K. L., Oomens, A. G., Monsma, S. A., Finnerty, C. M. and Blissard, G. W. (1999). Host cell receptor binding by baculovirus GP64 and kinetics of virion entry. *Virology* 258 (2), pp.455-468.
- Hegedus, D., Erlandson, M., Gillott, C. and Toprak, U. (2009). New insights into peritrophic matrix synthesis, architecture, and function. *Annu Rev Entomol* 54, pp.285-302.
- Heikura, T., Nieminen, T., Roschier, M. M., Karvinen, H., Kaikkonen, M. U., Mahonen, A. J., Lesch, H. P., Rissanen, T. T., Laitinen, O. H., Airene, K. J. and Yla-Herttuala, S. (2012). Baculovirus-mediated vascular endothelial growth factor-D(DeltaNDeltaC) gene transfer induces angiogenesis in rabbit skeletal muscle. *J Gene Med* 14 (1), pp.35-43.
- Herniou, E. A., Luque, T., Chen, X., Vlak, J. M., Winstanley, D., Cory, J. S. and O'Reilly, D. R. (2001). Use of whole genome sequence data to infer baculovirus phylogeny. *J Virol* 75 (17), pp.8117-8126.
- Herniou, E. A., Olszewski, J. A., Cory, J. S. and O'Reilly, D. R. (2003). The genome sequence and evolution of baculoviruses. *Annu Rev Entomol* 48, pp.211-234.
- Hershberger, P. A., Dickson, J. A. and Friesen, P. D. (1992). Site-specific mutagenesis of the 35-kilodalton protein gene encoded by *Autographa californica* nuclear polyhedrosis virus: cell line-specific effects on virus replication. *J Virol* 66 (9), pp.5525-5533.
- Hiscock, D. and Upton, C. (2000). Viral Genome DataBase: storing and analyzing genes and proteins from complete viral genomes. *Bioinformatics* 16 (5), pp.484-485.
- Hitchman, R. B., Hodgson, D. J., King, L. A., Hails, R. S., Cory, J. S. and Possee, R. D. (2007a). Host mediated selection of pathogen genotypes as a mechanism for the maintenance of baculovirus diversity in the field. *J Invertebr Pathol* 94 (3), pp.153-162.
- Hitchman, R. B., Locanto, E., Possee, R. D. and King, L. A. (2011). Optimizing the baculovirus expression vector system. *Methods* 55 (1), pp.52-57.
- Hitchman, R. B., Possee, R. D., Crombie, A. T., Chambers, A., Ho, K., Siaterli, E., Lissina, O., Sternard, H., Novy, R., Loomis, K., Bird, L. E., Owens, R. J. and King, L. A. (2010a). Genetic modification of a baculovirus vector for increased expression in insect cells. *Cell Biol Toxicol* 26 (1), pp.57-68.
- Hitchman, R. B., Possee, R. D. and King, L. A. (2012). High-throughput baculovirus expression in insect cells. *Methods Mol Biol* 824, pp.609-627.
- Hitchman, R. B., Possee, R. D., Siaterli, E., Richards, K. S., Clayton, A. J., Bird, L. E., Owens, R. J., Carpentier, D. C., King, F. L., Danquah, J. O., Spink, K. G. and King, L. A. (2010b). Improved expression of secreted and membrane-targeted proteins in insect cells. *Biotechnol Appl Biochem* 56 (3), pp.85-93.
- Hitchman, R. B., Siaterli, E. A., Nixon, C. P. and King, L. A. (2007b). Quantitative real-time PCR for rapid and accurate titration of recombinant baculovirus particles. *Biotechnol Bioeng* 96 (4), pp.810-814.
- Ho Je, Y., Hee Chang, J., Young Choi, J., Yul Roh, J., Rae Jin, B., O'Reilly, D. R. and Kwon Kang, S. (2001). A defective viral genome maintained in *Escherichia coli* for the generation of baculovirus expression vectors. *Biotechnology Letters* 23 (8), pp.575-582.
- Hodgson, J. J., Arif, B. M. and Krell, P. J. (2011). Interaction of *Autographa californica* multiple nucleopolyhedrovirus cathepsin protease progenitor (proV-CATH) with insect baculovirus chitinase as a mechanism for proV-CATH cellular retention. *J Virol* 85 (8), pp.3918-3929.
- Hofmann, C., Sandig, V., Jennings, G., Rudolph, M., Schlag, P. and Strauss, M. (1995). Efficient gene transfer into human hepatocytes by baculovirus vectors. *Proc Natl Acad Sci U S A* 92 (22), pp.10099-10103.
- Hofmann, K. and Stoffel, W. (1993). TMBASE - a database of membrane spanning protein

-
- segments. *Biol Chem HoppeSeyler*, 374(374), p.166.
- Hom, L. G., Ohkawa, T., Trudeau, D. and Volkman, L. E. (2002). *Autographa californica* M nucleopolyhedrovirus ProV-CATH is activated during infected cell death. *Virology* 296 (2), pp.212-218.
- Hong, T., Braunagel, S. C. and Summers, M. D. (1994). Transcription, Translation, and Cellular Localization of PDV-E66: A Structural Protein of the PDV Envelope of *Autographa californica* Nuclear Polyhedrosis Virus. *Virology* 204 (1), pp.210-222.
- Hong, T., Summers, M. D. and Braunagel, S. C. (1997). N-terminal sequences from *Autographa californica* nuclear polyhedrosis virus envelope proteins ODV-E66 and ODV-E25 are sufficient to direct reporter proteins to the nuclear envelope, intranuclear microvesicles and the envelope of occlusion derived virus. *Proc Natl Acad Sci U S A* 94 (8), pp.4050-4055.
- Hoover, K., Grove, M., Gardner, M., Hughes, D. P., McNeil, J. and Slavicek, J. (2011). A gene for an extended phenotype. *Science* 333 (6048), p.1401.
- Horton, H. M. and Burand, J. P. (1993). Saturable attachment sites for polyhedron-derived baculovirus on insect cells and evidence for entry via direct membrane fusion. *J Virol* 67 (4), pp.1860-1868.
- Hughes, K. M. and Addison, R. B. (1970). Two nuclear polyhedrosis viruses of the Douglas-fir tussock moth. *Journal of Invertebrate Pathology* 16 (2), pp.196-204.
- Hunter, F. R., Crook, N. E. and Entwistle, P. F. (1984). Viruses as pathogens for the control of insects. In *Microbial Methods for Environmental Biotechnology*, pp. 323-347. Edited by J. M. Grainger & J. M. Lynch. New York & London: Academic Press.
- Imai, N., Matsuda, N., Tanaka, K., Nakano, A., Matsumoto, S. and Kang, W. (2003). Ubiquitin ligase activities of *Bombyx mori* nucleopolyhedrovirus RING finger proteins. *J Virol* 77 (2), pp.923-930.
- Jarvis, D. L., Bohlmeier, D. A. and Garcia, A., Jr. (1991). Requirements for nuclear localization and supramolecular assembly of a baculovirus polyhedrin protein. *Virology* 185 (2), pp.795-810.
- Jehle, J. A. (2009). "André Paillot (1885–1944): His work lives on." *Journal of Invertebrate Pathology* 101(3): 162-168.
- Jehle, J. A., Lange, M., Wang, H., Hu, Z., Wang, Y. and Hauschild, R. (2006). Molecular identification and phylogenetic analysis of baculoviruses from Lepidoptera. *Virology* 346 (1), pp.180-193.
- Jiang, Y., Deng, F., Rayner, S., Wang, H. and Hu, Z. (2009). Evidence of a major role of GP64 in group I alphabaculovirus evolution. *Virus Res* 142 (1-2), pp.85-91.
- Kamita, S. G., Nagasaka, K., Chua, J. W., Shimada, T., Mita, K., Kobayashi, M., Maeda, S. and Hammock, B. D. (2005). A baculovirus-encoded protein tyrosine phosphatase gene induces enhanced locomotory activity in a lepidopteran host. *Proc Natl Acad Sci U S A* 102 (7), pp.2584-2589.
- Kawasaki, Y., Matsumoto, S. and Nagamine, T. (2004). Analysis of baculovirus IE1 in living cells: dynamics and spatial relationships to viral structural proteins. *J Gen Virol* 85 (Pt 12), pp.3575-3583.
- Ke, J., Wang, J., Deng, R. and Wang, X. (2008). *Autographa californica* multiple nucleopolyhedrovirus ac66 is required for the efficient egress of nucleocapsids from the nucleus, general synthesis of preoccluded virions and occlusion body formation. *Virology* 374 (2), pp.421-431.
- Keddie, B. A., Aponte, G. W. and Volkman, L. E. (1989). The pathway of infection of *Autographa californica* nuclear polyhedrosis virus in an insect host. *Science* 243 (4899), pp.1728-1730.
- Kikhno, I., Gutierrez, S., Croizier, L., Croizier, G. and Ferber, M. L. (2002). Characterization of *pif*, a gene required for the *per os* infectivity of *Spodoptera littoralis* nucleopolyhedrovirus. *J Gen Virol* 83 (Pt 12), pp.3013-3022.
- Kim, U. J., Shizuya, H., Kang, H. L., Choi, S. S., Garrett, C. L., Smink, L. J., Birren, B. W., Korenberg, J. R., Dunham, I. and Simon, M. I. (1996). A bacterial artificial chromosome-based framework contig map of human chromosome 22q. *Proc Natl*

-
- Acad Sci U S A* 93 (13), pp.6297-6301.
- King, L. A. and Possee, R. D. (1992). *The baculovirus expression system : a laboratory guide*. London; New York, N.Y.: Chapman & Hall.
- Kitts, P. A., Ayres, M. D. and Possee, R. D. (1990). Linearization of baculovirus DNA enhances the recovery of recombinant virus expression vectors. *Nucleic Acids Res* 18 (19), pp.5667-5672.
- Kitts, P. A. and Possee, R. D. (1993). A method for producing recombinant baculovirus expression vectors at high frequency. *Biotechniques* 14 (5), pp.810-817.
- Kost, T. A., Condreay, J. P., Ames, R. S., Rees, S. and Romanos, M. A. (2007). Implementation of BacMam virus gene delivery technology in a drug discovery setting. *Drug Discov Today* 12 (9-10), pp.396-403.
- Kost, T. A., Condreay, J. P. and Jarvis, D. L. (2005). Baculovirus as versatile vectors for protein expression in insect and mammalian cells. *Nat Biotechnol* 23 (5), pp.567-575.
- Kukan, B. (1999). Vertical transmission of nucleopolyhedrovirus in insects. *J Invertebr Pathol* 74 (2), pp.103-111.
- Lapointe, R., Popham, H. J., Straschil, U., Goulding, D., O'Reilly, D. R. and Olszewski, J. A. (2004). Characterization of two *Autographa californica* nucleopolyhedrovirus proteins, Ac145 and Ac150, which affect oral infectivity in a host-dependent manner. *J Virol* 78 (12), pp.6439-6448.
- Lee, S. Y., Poloumienko, A., Belfry, S., Qu, X., Chen, W., MacAfee, N., Morin, B., Lucarotti, C. and Krause, M. (1996). A common pathway for p10 and calyx proteins in progressive stages of polyhedron envelope assembly in AcMNPV-infected *Spodoptera frugiperda* larvae. *Arch Virol* 141 (7), pp.1247-1258.
- Lehane, M. J. (1997). Peritrophic matrix structure and function. *Annu Rev Entomol* 42, pp.525-550.
- Lepore, L. S., Roelvink, P. R. and Granados, R. R. (1996). Enhancin, the granulosis virus protein that facilitates nucleopolyhedrovirus (NPV) infections, is a metalloprotease. *J Invertebr Pathol* 68 (2), pp.131-140.
- Lewin, A., Mayer, M., Chusainow, J., Jacob, D. and Appel, B. (2005). Viral promoters can initiate expression of toxin genes introduced into *Escherichia coli*. *BMC Biotechnology* 5 (19).
- Li, Z., Pan, L., Yu, H., Li, S., Zhang, G. and Pang, Y. (2006). Identification and characterization of odv-e25 of *Spodoptera litura* multicapsid nucleopolyhedrovirus. *Virus Genes* 32 (1), pp.13-19.
- Lin, J. J., Phillips, A. M., Hearst, J. E. and Sancar, A. (1992). Active site of (A)BC excinuclease. II. Binding, bending, and catalysis mutants of UvrB reveal a direct role in 3' and an indirect role in 5' incision. *J Biol Chem* 267 (25), pp.17693-17700.
- Lin, J. J. and Sancar, A. (1992). Active site of (A)BC excinuclease. I. Evidence for 5' incision by UvrC through a catalytic site involving Asp399, Asp438, Asp466, and His538 residues. *J Biol Chem* 267 (25), pp.17688-17692.
- Lin, L., Wang, J., Deng, R., Ke, J., Wu, H. and Wang, X. (2009). ac109 is required for the nucleocapsid assembly of *Autographa californica* multiple nucleopolyhedrovirus. *Virus Res* 144 (1-2), pp.130-135.
- Long, G., Pan, X., Kormelink, R. and Vlak, J. M. (2006). Functional entry of baculovirus into insect and mammalian cells is dependent on clathrin-mediated endocytosis. *J Virol* 80 (17), pp.8830-8833.
- Lopez-Ferber, M., Sisk, W. P. and Possee, R. D. (1995). Baculovirus transfer vectors. *Methods Mol Biol* 39, pp.25-63.
- Lu, M. and Iatrou, K. (1996). The genes encoding the P39 and CG30 proteins of *Bombyx mori* nuclear polyhedrosis virus. *J Gen Virol* 77 (Pt 12), pp.3135-3143.
- Lu, S., Ge, G. and Qi, Y. (2004). Ha-VP39 binding to actin and the influence of F-actin on assembly of progeny virions. *Arch Virol* 149 (11), pp.2187-2198.
- Luckow, V. A., Lee, S. C., Barry, G. F. and Olins, P. O. (1993). Efficient generation of infectious recombinant baculoviruses by site-specific transposon-mediated

-
- insertion of foreign genes into a baculovirus genome propagated in *Escherichia coli*. *J Virol* 67 (8), pp.4566-4579.
- Luo, W. Y., Shih, Y. S., Lo, W. H., Chen, H. R., Wang, S. C., Wang, C. H., Chien, C. H., Chiang, C. S., Chuang, Y. J. and Hu, Y. C. (2011). Baculovirus vectors for antiangiogenesis-based cancer gene therapy. *Cancer Gene Ther* 18 (9), pp.637-645.
- Mackett, M., Smith, G. L. and Moss, B. (1982). Vaccinia virus: a selectable eukaryotic cloning and expression vector. *Proc Natl Acad Sci U S A* 79 (23), pp.7415-7419.
- Manji, G. A. and Friesen, P. D. (2001). Apoptosis in motion. An apical, P35-insensitive caspase mediates programmed cell death in insect cells. *J Biol Chem* 276 (20), pp.16704-16710.
- Marek, M., Merten, O. W., Galibert, L., Vlak, J. M. and van Oers, M. M. (2011). Baculovirus VP80 protein and the F-actin cytoskeleton interact and connect the viral replication factory with the nuclear periphery. *J Virol* 85 (11), pp.5350-5362.
- McCarthy, C. B., Dai, X., Donly, C. and Theilmann, D. A. (2008). Autographa californica multiple nucleopolyhedrovirus ac142, a core gene that is essential for BV production and ODV envelopment. *Virology* 372 (2), pp.325-339.
- McCarthy, C. B. and Theilmann, D. A. (2008). AcMNPV ac143 (odv-e18) is essential for mediating budded virus production and is the 30th baculovirus core gene. *Virology* 375 (1), pp.277-291.
- Mikhailov, V. S., Vanarsdall, A. L. and Rohrmann, G. F. (2008). Isolation and characterization of the DNA-binding protein (DBP) of the *Autographa californica* multiple nucleopolyhedrovirus. *Virology* 370 (2), pp.415-429.
- Miller, L. K. (1997). Introduction to the Baculoviruses (L. K. Miller eds) . In "The Baculoviruses" , Chapter 1, pp. 1-6. Plenum Press, New York.
- Monsma, S. A., Oomens, A. G. and Blissard, G. W. (1996). The GP64 envelope fusion protein is an essential baculovirus protein required for cell-to-cell transmission of infection. *J Virol* 70 (7), pp.4607-4616.
- Moscardi, F. (1999). Assessment of the application of baculoviruses for control of Lepidoptera. *Annu Rev Entomol* 44, pp.257-289.
- Moser, B., Becnel, J., White, S., Afonso, C., Kutish, G., Shanker, S. and Almira, E. (2001). Morphological and molecular evidence that *Culex nigripalpus* baculovirus is an unusual member of the family *Baculoviridae*. *J Gen Virol* 82 (Pt 2), pp.283-297.
- Munoz, D., Murillo, R., Krell, P. J., Vlak, J. M. and Caballero, P. (1999). Four genotypic variants of a *Spodoptera exigua* Nucleopolyhedrovirus (Se-SP2) are distinguishable by a hypervariable genomic region. *Virus Res* 59 (1), pp.61-74.
- Murphy, F. A., Fauquet, C. M., Bishop, D. H. L., Ghabrial, S. A., Jarvis, A. W., Martelli, G. P., Mayo, M. A. and Summers, M. D. (1995). Virus Taxonomy – The Classification and Nomenclature of viruses: Sixth Report of the International Committee on Taxonomy of Viruses. Springer-Verlag, New York.
- Muyrers, J. P., Zhang, Y., Buchholz, F. and Stewart, A. F. (2000). RecE/RecT and Redalpha/Redbeta initiate double-stranded break repair by specifically interacting with their respective partners. *Genes Dev* 14 (15), pp.1971-1982.
- Muyrers, J. P., Zhang, Y., Testa, G. and Stewart, A. F. (1999). Rapid modification of bacterial artificial chromosomes by ET-recombination. *Nucleic Acids Res* 27 (6), pp.1555-1557.
- Nicholas, K. B., Nicholas, H. B. J. and Deerfield, D. I. (1997). GeneDoc: Analysis and Visualization of Genetic Variation. *EMBNEW.NEWS*, 4, 14.
- Ohkawa, T. (1997). Identification and characterization of genes of the baculovirus *Bombyx mori* nucleopolyhedrovirus (BmNPV) involved in viral pathogenesis. Ph.D. thesis. University of California, Davis, Calif.
- Ohkawa, T. and Volkman, L. E. (1999). Nuclear F-actin is required for AcMNPV nucleocapsid morphogenesis. *Virology* 264 (1), pp.1-4.
- Ohkawa, T., Volkman, L. E. and Welch, M. D. (2010). Actin-based motility drives baculovirus transit to the nucleus and cell surface. *J Cell Biol* 190 (2), pp.187-195.

-
- Ohkawa, T., Washburn, J. O., Sitapara, R., Sid, E. and Volkman, L. E. (2005). Specific binding of *Autographa californica* M nucleopolyhedrovirus occlusion-derived virus to midgut cells of *Heliothis virescens* larvae is mediated by products of pif genes Ac119 and Ac022 but not by Ac115. *J Virol* 79 (24), pp.15258-15264.
- Olszewski, J. and Miller, L. K. (1997). A role for baculovirus GP41 in budded virus production. *Virology* 233 (2), pp.292-301.
- Ooi, B. G., Rankin, C. and Miller, L. K. (1989). Downstream sequences augment transcription from the essential initiation site of a baculovirus polyhedrin gene. *J Mol Biol* 210 (4), pp.721-736.
- Passarelli, A. L. and Guarino, L. A. (2007). Baculovirus late and very late gene regulation. *Curr Drug Targets* 8 (10), pp.1103-1115.
- Passarelli, A. L. and Miller, L. K. (1994). *In vivo* and *in vitro* analyses of recombinant baculoviruses lacking a functional cg30 gene. *J Virol* 68 (2), pp.1186-1190.
- Patel, G., Nasmyth, K. and Jones, N. (1992). A new method for the isolation of recombinant baculovirus. *Nucleic Acids Res* 20 (1), pp.97-104.
- Patmanidi, A. L., Possee, R. D. and King, L. A. (2003). Formation of P10 tubular structures during AcMNPV infection depends on the integrity of host-cell microtubules. *Virology* 317 (2), pp.308-320.
- Paul, A., Binsalamah, Z. M., Khan, A. A., Abbasia, S., Elias, C. B., Shum-Tim, D. and Prakash, S. (2011). A nanobiohybrid complex of recombinant baculovirus and Tat/DNA nanoparticles for delivery of Ang-1 transgene in myocardial infarction therapy. *Biomaterials* 32 (32), pp.8304-8318.
- Pearson, M. N., Groten, C. and Rohrmann, G. F. (2000). Identification of the *lymantria dispar* nucleopolyhedrovirus envelope fusion protein provides evidence for a phylogenetic division of the *Baculoviridae*. *J Virol* 74 (13), pp.6126-6131.
- Pearson, M. N., Russell, R. L. and Rohrmann, G. F. (2001). Characterization of a baculovirus-encoded protein that is associated with infected-cell membranes and budded virions. *Virology* 291 (1), pp.22-31.
- Peng, J., Zhong, J. and R, R. G. (1999). A baculovirus enhancin alters the permeability of a mucosal midgut peritrophic matrix from lepidopteran larvae. *J Insect Physiol* 45 (2), pp.159-166.
- Peng, K., van Oers, M. M., Hu, Z., van Lent, J. W. and Vlak, J. M. (2010). Baculovirus *per os* infectivity factors form a complex on the surface of occlusion-derived virus. *J Virol* 84 (18), pp.9497-9504.
- Pennock, G. D., Shoemaker, C. and Miller, L. K. (1984). Strong and regulated expression of *Escherichia coli* beta-galactosidase in insect cells with a baculovirus vector. *Mol Cell Biol* 4 (3), pp.399-406.
- Pijlman, G. P., Pruijssers, A. J. and Vlak, J. M. (2003). Identification of *pif-2*, a third conserved baculovirus gene required for *per os* infection of insects. *J Gen Virol* 84 (Pt 8), pp.2041-2049.
- Possee, R. D. (1986). Cell-surface expression of influenza virus haemagglutinin in insect cells using a baculovirus vector. *Virus Res* 5 (1), pp.43-59.
- Possee, R. D., Hitchman, R. B., Richards, K. S., Mann, S. G., Siaterli, E., Nixon, C. P., Irving, H., Assenberg, R., Alderton, D., Owens, R. J. and King, L. A. (2008). Generation of baculovirus vectors for the high-throughput production of proteins in insect cells. *Biotechnol Bioeng*.
- Prikhod'ko, G. G., Wang, Y., Freulich, E., Prives, C. and Miller, L. K. (1999). Baculovirus p33 binds human p53 and enhances p53-mediated apoptosis. *J Virol* 73 (2), pp.1227-1234.
- Rashidan, K. K., Nassoury, N., Giannopoulos, P. N. and Guertin, C. (2002). Identification and characterization of a conserved baculoviral structural protein ODVP-6E/ODV-E56 from *Choristoneura fumiferana* granulovirus. *J Biochem Mol Biol* 35 (6), pp.595-603.
- Raymond, B., Hartley, S. E., Cory, J. S. and Hails, R. S. (2005). The role of food plant and pathogen-induced behaviour in the persistence of a nucleopolyhedrovirus. *J*

-
- Invertebr Pathol* 88 (1), pp.49-57.
- Rivera-Gonzalez, G. C., Swift, S. L., Dussupt, V., Georgopoulos, L. J. and Maitland, N. J. (2011). Baculoviruses as gene therapy vectors for human prostate cancer. *Journal of Invertebrate Pathology* 107, Supplement (0), pp.S59-S70.
- Rohrmann, G. F. (1986). Evolution of occluded baculoviruses. In "The Biology of Baculoviruses" (R. R. Granados and B. A. Federici, eds.), Vol. 1, pp. 203–315. CRC Press, Boca Raton, FL 2 vols.
- Rohrmann, G. F. (2011). Baculovirus Molecular Biology. [e-book] Bethesda (MD): National Center for Biotechnology Information (US): NCBI <<http://www.ncbi.nlm.nih.gov/books/NBK49500/>> (Accessed 2011).
- Rohrmann, G. F., Pearson, M. N., Bailey, T. J., Becker, R. R. and Beaudreau, G. S. (1981). N-Terminal polyhedrin sequences and occluded Baculovirus evolution. *J Mol Evol* 17 (6), pp.329-333.
- Rosas-Acosta, G., Braunagel, S. C. and Summers, M. D. (2001). Effects of deletion and overexpression of the *Autographa californica* nuclear polyhedrosis virus FP25K gene on synthesis of two occlusion-derived virus envelope proteins and their transport into virus-induced intranuclear membranes. *J Virol* 75 (22), pp.10829-10842.
- Rothwangl, K. B. and Rong, L. (2009). Analysis of a conserved RGE/RGD motif in HCV E2 in mediating entry. *Viol. J. Virology Journal* 6.
- Roux, L., Simon, A. E. and Holland, J. J. (1991). Effects of defective interfering viruses on virus replication and pathogenesis *in vitro* and *in vivo*. *Adv Virus Res* 40, pp.181-211.
- Rubinstein, R. and Polson, A. (1983). Midgut and viral associated proteases of *Heliothis armigera*. *Intervirology* 19 (1), pp.16-25.
- Russell, R. L., Funk, C. J. and Rohrmann, G. F. (1997). Association of a baculovirus-encoded protein with the capsid basal region. *Virology* 227 (1), pp.142-152.
- Russell, R. L., Pearson, M. N. and Rohrmann, G. F. (1991). Immunoelectron microscopic examination of *Orgyia pseudotsugata* multicapsid nuclear polyhedrosis virus-infected *Lymantria dispar* cells: time course and localization of major polyhedron-associated proteins. *J Gen Virol* 72 (Pt 2), pp.275-283.
- Russell, R. L. and Rohrmann, G. F. (1990). A baculovirus polyhedron envelope protein: immunogold localization in infected cells and mature polyhedra. *Virology* 174 (1), pp.177-184.
- Russell, R. L. Q. and Rohrmann, G. F. (1997). Characterization of P91, a Protein Associated with Virions of an *Orgyia pseudotsugata* Baculovirus. *Virology* 233 (1), pp.210-223.
- Sambrook, J. and Russell, D. W. (2001). *Molecular cloning : a laboratory manual*. Cold Spring Harbor, N.Y. Cold Spring Harbor Laboratory Press.
- Schultz, K. L. and Friesen, P. D. (2009). Baculovirus DNA replication-specific expression factors trigger apoptosis and shutoff of host protein synthesis during infection. *J Virol* 83 (21), pp.11123-11132.
- Shayakhmetov, D. M., Eberly, A. M., Li, Z. Y. and Lieber, A. (2005). Deletion of penton RGD motifs affects the efficiency of both the internalization and the endosome escape of viral particles containing adenovirus serotype 5 or 35 fiber knobs. *Journal of virology* 79 (2), pp.1053-1061.
- Shikata, M., Sano, Y., Hashimoto, Y. and Matsumoto, T. (1998). Isolation and characterization of a temperature-sensitive mutant of *Bombyx mori* nucleopolyhedrovirus for a putative RNA polymerase gene. *J Gen Virol* 79 (Pt 8), pp.2071-2078.
- Shizuya, H., Birren, B., Kim, U. J., Mancino, V., Slepak, T., Tachiiri, Y. and Simon, M. (1992). Cloning and stable maintenance of 300-kilobase-pair fragments of human DNA in *Escherichia coli* using an F-factor-based vector. *Proc Natl Acad Sci U S A* 89 (18), pp.8794-8797.
- Simon, O., Palma, L., Bepere, I., Munoz, D., Lopez-Ferber, M., Caballero, P. and

-
- Williams, T. (2011). Sequence comparison between three geographically distinct *Spodoptera frugiperda* multiple nucleopolyhedrovirus isolates: Detecting positively selected genes. *J Invertebr Pathol* 107 (1), pp.33-42.
- Simon, O., Williams, T., Caballero, P. and Lopez-Ferber, M. (2006). Dynamics of deletion genotypes in an experimental insect virus population. *Proc Biol Sci* 273 (1588), pp.783-790.
- Simon, O., Williams, T., Lopez-Ferber, M. and Caballero, P. (2004). Genetic structure of a *Spodoptera frugiperda* nucleopolyhedrovirus population: high prevalence of deletion genotypes. *Appl Environ Microbiol* 70 (9), pp.5579-5588.
- Slack, J. and Arif, B. M. (2007). The baculoviruses occlusion-derived virus: virion structure and function. *Adv Virus Res* 69, pp.99-165.
- Slack, J. M., Kuzio, J. and Faulkner, P. (1995). Characterization of v-cath, a cathepsin L-like proteinase expressed by the baculovirus *Autographa californica* multiple nuclear polyhedrosis virus. *J Gen Virol* 76 (Pt 5), pp.1091-1098.
- Smith, G. E., Summers, M. D. and Fraser, M. J. (1983a). Production of human beta interferon in insect cells infected with a baculovirus expression vector. *Mol Cell Biol* 3 (12), pp.2156-2165.
- Smith, G. L., Mackett, M. and Moss, B. (1983b). Infectious vaccinia virus recombinants that express hepatitis B virus surface antigen. *Nature* 302 (5908), pp.490-495.
- Smith, G. L., Murphy, B. R. and Moss, B. (1983c). Construction and characterization of an infectious vaccinia virus recombinant that expresses the influenza hemagglutinin gene and induces resistance to influenza virus infection in hamsters. *Proc Natl Acad Sci U S A* 80 (23), pp.7155-7159.
- Soeda, E., Maruyama, T., Arrand, J. R. and Griffin, B. E. (1980). Host-dependent evolution of three papova viruses. *Nature* 285 (5761), pp.165-167.
- Song, J., Wang, M., Huang, H., Luo, X., Deng, F., Wang, H. and Hu, Z. (2012). Functional studies of *per os* infectivity factor 3 of *Helicoverpa armigera* nucleopolyhedrovirus. *J Gen Virol* 93 (Pt 2), pp.374-382.
- Sparks, W. O., Harrison, R. L. and Bonning, B. C. (2011a). *Autographa californica* multiple nucleopolyhedrovirus ODV-E56 is a *per os* infectivity factor, but is not essential for binding and fusion of occlusion-derived virus to the host midgut. *Virology* 409 (1), pp.69-76.
- Sparks, W. O., Rohlfing, A. and Bonning, B. C. (2011b). A peptide with similarity to baculovirus ODV-E66 binds the gut epithelium of *Heliothis virescens* and impedes infection with *Autographa californica* multiple nucleopolyhedrovirus. *J Gen Virol* 92 (Pt 5), pp.1051-1060.
- Steinhaus, E. A. (1975). *Disease in a minor chord*. Columbus, Ohio: Ohio State Univ. Press.
- Stow, N. D., Subak-Sharpe, J. H. and Wilkie, N. M. (1978). Physical mapping of herpes simplex virus type 1 mutations by marker rescue. *J Virol* 28 (1), pp.182-192.
- Sugiura, N., Setoyama, Y., Chiba, M., Kimata, K. and Watanabe, H. (2011). Baculovirus envelope protein ODV-E66 is a novel chondroitinase with distinct substrate specificity. *J Biol Chem* 286 (33), pp.29026-29034.
- Summers, M. D. (1971). Electron microscopic observations on granulosis virus entry, uncoating and replication processes during infection of the midgut cells of *Trichoplusia ni*. *J Ultrastruct Res* 35 (5), pp.606-625.
- Summers, M. D. (2006). Milestones leading to the genetic engineering of baculoviruses as expression vector systems and viral pesticides. *Adv Virus Res* 68, pp.3-73.
- Tanada, Y. and Kaya, H. K. (1993). *Insect pathology*. San Diego: Academic Press.
- Tani, H., Nishijima, M., Ushijima, H., Miyamura, T. and Matsuura, Y. (2001). Characterization of cell-surface determinants important for baculovirus infection. *Virology* 279 (1), pp.343-353.
- Terra, W. R. and Ferreira, C. (1994). Insect digestive enzymes: properties, compartmentalization and function *Comparative Biochemistry and Physiology Part B: Biochemistry and Molecular Biology* 109 (1), pp.1-62

-
- Theilmann, D. A., Chantler, J. K., Stewart, S., Flipsen, H. T., Vlak, J. M. and Crook, N. E. (1996). Characterization of a highly conserved baculovirus structural protein that is specific for occlusion-derived virions. *Virology* 218 (1), pp.148-158.
- Thiem, S. M. and Chejanovsky, N. (2004). The role of baculovirus apoptotic suppressors in AcMNPV-mediated translation arrest in Ld652Y cells. *Virology* 319 (2), pp.292-305.
- Thiem, S. M. and Miller, L. K. (1989). A baculovirus gene with a novel transcription pattern encodes a polypeptide with a zinc finger and a leucine zipper. *J Virol* 63 (11), pp.4489-4497.
- Thornberry, N. A., Bull, H. G., Calaycay, J. R., Chapman, K. T., Howard, A. D., Kostura, M. J., Miller, D. K., Molineaux, S. M., Weidner, J. R., Aunins, J. and et al. (1992). A novel heterodimeric cysteine protease is required for interleukin-1 beta processing in monocytes. *Nature* 356 (6372), pp.768-774.
- Timbury, M. C. (1971). Temperature-sensitive mutants of herpes simplex virus type 2. *J Gen Virol* 13 (2), pp.373-376.
- Uwo, M. F., Ui-Tei, K., Park, P. and Takeda, M. (2002). Replacement of midgut epithelium in the greater wax moth, *Galleria mellonella*, during larval-pupal moult. *Cell Tissue Res* 308 (2), pp.319-331.
- Vago, C., Aizawa, K., Ignoffo, C., Martignoni, M. E., Tarasevitch, L. and Tinsley, T. W. (1974). Editorial: Present status of the nomenclature and classification of invertebrate viruses. *J Invertebr Pathol* 23 (2), pp.133-134.
- Vail, P. V., Jay, D. L. and Hunter, D. K. (1973). Infectivity of a nuclear polyhedrosis virus from the alfalfa looper, *Autographa californica*, after passage through alternate hosts. *Journal of Invertebrate Pathology* 21 (1), pp.16-20.
- van der Most, R. G., Corver, J. and Strauss, J. H. (1999). Mutagenesis of the RGD Motif in the Yellow Fever Virus 17D Envelope Protein. *Virology* 265 (1), pp.83-95.
- van Loo, N. D., Fortunati, E., Ehlert, E., Rabelink, M., Grosveld, F. and Scholte, B. J. (2001). Baculovirus infection of nondividing mammalian cells: mechanisms of entry and nuclear transport of capsids. *J Virol* 75 (2), pp.961-970.
- van Oers, M. M. (2011). Opportunities and challenges for the baculovirus expression system. *J Invertebr Pathol* 107 Suppl, pp.S3-15.
- Vanarsdall, A. L., Mikhailov, V. S. and Rohrmann, G. F. (2007). Characterization of a baculovirus lacking the DBP (DNA-binding protein) gene. *Virology* 364 (2), pp.475-485.
- Vaux, D. L. and Silke, J. (2005). IAPs, RINGs and ubiquitylation. *Nat Rev Mol Cell Biol* 6 (4), pp.287-297.
- Volkman, L. E. (1988). *Autographa californica* MNPV nucleocapsid assembly: inhibition by cytochalasin D. *Virology* 163 (2), pp.547-553.
- Volkman, L. E. and Goldsmith, P. A. (1985). Mechanism of neutralization of budded *Autographa californica* nuclear polyhedrosis virus by a monoclonal antibody: Inhibition of entry by adsorptive endocytosis. *Virology* 143 (1), pp.185-195.
- Volkman, L. E., Goldsmith, P. A., Hess, R. T. and Faulkner, P. (1984). Neutralization of budded *Autographa californica* NPV by a monoclonal antibody: identification of the target antigen. *Virology* 133 (2), pp.354-362.
- Volkman, L. E. and Zaal, K. J. (1990). *Autographa californica* M nuclear polyhedrosis virus: microtubules and replication. *Virology* 175 (1), pp.292-302.
- Wang, D. and Zhang, C. X. (2006). HearSNPV orf83 encodes a late, nonstructural protein with an active chitin-binding domain. *Virus Res* 117 (2), pp.237-243.
- Wang, H. G. and Fraser, M. J. (1993). TTAA serves as the target site for TFP3 lepidopteran transposon insertions in both nuclear polyhedrosis virus and *Trichoplusia ni* genomes. *Insect Mol Biol* 1 (3), pp.109-116.
- Wang, P. and Granados, R. R. (1997). An intestinal mucin is the target substrate for a baculovirus enhancer. *Proc Natl Acad Sci U S A* 94 (13), pp.6977-6982.
- Washburn, J. O., Chan, E. Y., Volkman, L. E., Aumiller, J. J. and Jarvis, D. L. (2003a). Early synthesis of budded virus envelope fusion protein GP64 enhances

-
- Autographa californica* multicapsid nucleopolyhedrovirus virulence in orally infected *Heliothis virescens*. *J Virol* 77 (1), pp.280-290.
- Washburn, J. O., Kirkpatrick, B. A. and Volkman, L. E. (1995). Comparative pathogenesis of *Autographa californica* M nuclear polyhedrosis virus in larvae of *Trichoplusia ni* and *Heliothis virescens*. *Virology* 209 (2), pp.561-568.
- Washburn, J. O., Lyons, E. H., Haas-Stapleton, E. J. and Volkman, L. E. (1999). Multiple nucleocapsid packaging of *Autographa californica* nucleopolyhedrovirus accelerates the onset of systemic infection in *Trichoplusia ni*. *J Virol* 73 (1), pp.411-416.
- Washburn, J. O., Trudeau, D., Wong, J. F. and Volkman, L. E. (2003b). Early pathogenesis of *Autographa californica* multiple nucleopolyhedrovirus and *Helicoverpa zea* single nucleopolyhedrovirus in *Heliothis virescens*: a comparison of the 'M' and 'S' strategies for establishing fatal infection. *J Gen Virol* 84 (Pt 2), pp.343-351.
- Weger, S., Hammer, E. and Heilbronn, R. (2002). Topors, a p53 and topoisomerase I binding protein, interacts with the adeno-associated virus (AAV-2) Rep78/68 proteins and enhances AAV-2 gene expression. *J Gen Virol* 83 (Pt 3), pp.511-516.
- Westenberg, M., Wang, H., WF, I. J., Goldbach, R. W., Vlak, J. M. and Zuidema, D. (2002). Furin is involved in baculovirus envelope fusion protein activation. *J Virol* 76 (1), pp.178-184.
- Whitford, M., Stewart, S., Kuzio, J. and Faulkner, P. (1989). Identification and sequence analysis of a gene encoding gp67, an abundant envelope glycoprotein of the baculovirus *Autographa californica* nuclear polyhedrosis virus. *J Virol* 63 (3), pp.1393-1399.
- Whitt, M. A. and Manning, J. S. (1988). A phosphorylated 34-kDa protein and a subpopulation of polyhedrin are thiol linked to the carbohydrate layer surrounding a baculovirus occlusion body. *Virology* 163 (1), pp.33-42.
- Williams, G. V. and Faulkner, P. (1997). Cytological changes and viral morphogenesis during Baculovirus infection. In "The Baculoviruses" (L. K. Miller, ed.) pp. 61-108.
- Wilson, M. E. and Consigli, R. A. (1985). Functions of a protein kinase activity associated with purified capsids of the granulosis virus infecting *Plodia interpunctella*. *Virology* 143 (2), pp.526-535.
- Wu, D., Deng, F., Sun, X., Wang, H., Yuan, L., Vlak, J. M. and Hu, Z. (2005). Functional analysis of FP25K of *Helicoverpa armigera* single nucleocapsid nucleopolyhedrovirus. *J Gen Virol* 86 (Pt 9), pp.2439-2444.
- Xiang, X., Chen, L., Guo, A., Yu, S., Yang, R. and Wu, X. (2011). The *Bombyx mori* nucleopolyhedrovirus (BmNPV) ODV-E56 envelope protein is also a *per os* infectivity factor. *Virus Research* 155 (1), pp.69-75.
- Xu, H. J., Yang, Z. N., Wang, F. and Zhang, C. X. (2006). *Bombyx mori* nucleopolyhedrovirus ORF79 encodes a 28-kDa structural protein of the ODV envelope. *Arch Virol* 151 (4), pp.681-695.
- Xu, H. J., Yang, Z. N., Zhao, J. F., Tian, C. H., Ge, J. Q., Tang, X. D., Bao, Y. Y. and Zhang, C. X. (2008). *Bombyx mori* nucleopolyhedrovirus ORF56 encodes an occlusion-derived virus protein and is not essential for budded virus production. *J Gen Virol* 89 (Pt 5), pp.1212-1219.
- Yamagishi, J., Burnett, E. D., Harwood, S. H. and Blissard, G. W. (2007). The AcMNPV pp31 gene is not essential for productive AcMNPV replication or late gene transcription but appears to increase levels of most viral transcripts. *Virology* 365 (1), pp.34-47.
- Young, J. C., MacKinnon, E. A. and Faulkner, P. (1993). The Architecture of the Virogenic Stroma in Isolated Nuclei of *Spodoptera frugiperda* Cells *in Vitro* Infected by *Autographa californica* Nuclear Polyhedrosis Virus *Journal of Structural Biology* 110 (2), pp.141-153.
- Zanotto, P. M., Kessing, B. D. and Maruniak, J. E. (1993). Phylogenetic interrelationships among baculoviruses: evolutionary rates and host associations. *J Invertebr Pathol*

-
- 62 (2), pp.147-164.
- Zhang, G. (1994). Research, development and application of *Heliothis* viral pesticide in China. *Resour. Environ. Yangze Balley* (3), pp.1-6.
- Zhang, J. H., Ohkawa, T., Washburn, J. O. and Volkman, L. E. (2005). Effects of Ac150 on virulence and pathogenesis of *Autographa californica* multiple nucleopolyhedrovirus in noctuid hosts. *J Gen Virol* 86 (Pt 6), pp.1619-1627.
- Zhang, J. H., Washburn, J. O., Jarvis, D. L. and Volkman, L. E. (2004). *Autographa californica* M nucleopolyhedrovirus early GP64 synthesis mitigates developmental resistance in orally infected noctuid hosts. *J Gen Virol* 85 (Pt 4), pp.833-842.
- Zhang, Y., Buchholz, F., Muyrers, J. P. and Stewart, A. F. (1998). A new logic for DNA engineering using recombination in *Escherichia coli*. *Nat Genet* 20 (2), pp.123-128.